SHORELINE DYNAMICS IN RESPONSE TO RIVER SEDIMENT: A CASE STUDY

Thesis

Submitted in partial fulfillment of the requirements for the degree of

DOCTOR OF PHILOSOPHY

By

ARUNKUMAR YADAV

Under the guidance of

Dr. B. M. Dodamani   **Dr. G. S. Dwarakish**

Professor   Professor

DEPARTMENT OF APPLIED MECHANICS AND HYDRAULICS

NATIONAL INSTITUTE OF TECHNOLOGY KARNATAKA

SURATHKAL, MANGALORE – 575025

JUNE, 2020

DECLARATION

I hereby declare that the Research Thesis entitled **"Shoreline Dynamics In Response To River Sediment: A Case Study"** which is being submitted to the **National Institute of Technology Karnataka, Surathkal** in partial fulfillment of the requirements for the award of the Degree of **Doctor of Philosophy** in **Department of Applied Mechanics and Hydraulics** is a *bonafide report of the research work carried out by me*. The material contained in this Research Thesis has not been submitted to any other Universities or Institutes for the award of any degree.

Register Number: **155092AM15F03**

Name of the Research Scholar: **ARUNKUMAR YADAV**

Signature of the Research Scholar:

Department of Applied Mechanics and Hydraulics

Place: NITK-Surathkal

Date:

CERTIFICATE

This is to certify that the Research Thesis entitled **"Shoreline Dynamics In Response To River Sediment: A Case Study" submitted** by **Mr. ARUNKUMAR YADAV. (Register Number: 155092AM15F03)** as the record of the research work carried out by him, *is accepted as the Research Thesis submission* in partial fulfillment of the requirements for the award of the Degree of **Doctor of Philosophy.**

Dr. B. M. Dodamani

Professor

Dr. G. S. Dwarakish

Professor

Chairman-DRPC

(Signature with Date and Seal)

Date:

ACKNOWLEDGMENTS

ABSTRACT

The coastal zone of Karwar is acquiring increasing importance due to its rich ocean resources and favorable conditions for the development of port-based industries, defense activity, tourism, fisheries, and small scale industries.

Rivers and its networks are the major sources of the sediments, which supplies to the coast. These sediments are responsible for beach nourishment and shoreline configuration.

The present study is carried out with a view to study the long-term shoreline configuration with the response to pre-construction dam and post-construction of the dam, to study the seasonal variation on shoreline configuration, to investigate the change in Kali estuary to assess the impact of the dam on sediment yield, To understand the sediment dynamics of beach face sand using granulometric method and To quantify the seasonal coastal process in terms of beach sand volume. These objectives are addressed using various conventional data, related tools, and freely available satellite data. Kali river basin, Aghanashini river basin, Karwar coast and Aghanashini coast along the west coast of India is the study area.

There are five dams constructed across the Kali river basin for hydel power purposes. The presence of these reservoirs regulates stream flow and thus sediment load in the basin. However, the free flow of water across the catchment of the Aghanashini river leads to the unobstructed or natural passage of sediments and sediment budget to the downstream and the river mouth, as the catchment is not disturbed by the reservoir.

Survey of India toposheet was used to prepare the base map. A conceptual, continuous-time and semi-distributed, SWAT2012 (Soil and Water Assessment Tool) model was selected for the sediment yield analysis. Dam location and dam discharge data were one of the major inputs for the model to estimate the sediment yield. Simulated and observed values of runoff are compared, and calibration and validation were done for the basins using SWAT CUP. The long-term shoreline configuration was carried out using LANDSAT satellite products only. The predominant direction of sediment transport was determined by drawing sediment trend matrices based on the statistical

parameters of beach face sediments. To understand the change in Kali estuary a portion of Devabag beach, satellite data were used for the duration from 1975 to 2018. The Total Station survey was carried for Ravindranath Tagore beach and Devabagh beach of Karwar coast, including a seasonal wise profile survey and cross-section survey during 2017.

Based on the present analysis of sediment yield, it is concluded that the Sediment yield obtained at the catchment outlet was 1.39t/ha/year and 4.58t/ha/year for the Kali river and Aghanasini river basins respectively. It was observed that the decline in sediment load in the Kali river basin compared to the Aghanashini river basin indicates that the influence of reservoir operation on streamflow and sediment yield.

The analysis to study the long-term shoreline configuration with the response to the pre-construction dam and post-construction of the dam, shows that shoreline of the Karwar coast was having accretion and later, it is turned in to erosion zone due to post-construction of the dam. It shows the importance of natural river flow. Shoreline change analysis on the Aghanashini coast shows the accretion zone due to the natural flow of the Aghanashini river to the coast.

The study estuary change shows that for the period of 1975 to 2018 northern part of the estuary has lost area and construction of seawall was revealed from ground truth data.

Beach profile studies by total station on Ravindranath Tagore beach reveals that beach profile changes according to the season. The volume of sand is decreased during the pre-monsoon season and increased during the post-monsoon season.

The accuracy of all the results can be increased by an increase in a number of inputs in the case of SWAT tool, the accuracy of results obtained from the satellite can be increased by higher resolution data. From the study, it is concluded that the river and its network are the major sources for the sediment supply to the coast. Sediment is one of the major factors for beach nourishment. Dam influences the flow of the river and its network and reduces sediment supply to the coast. A natural flow of the river and natural supply of river sediment enhances the beach nourishment and maintains the equilibrium of sediment budget to the coast.

TABLE OF CONTENTS

LIST OF TABLES

LIST OF FIGURES

LIST OF ABBREVIATIONS

Abbreviations	Description
ASTER	Advanced Spaceborne Thermal Emission and Reflection Radiometer
CN	Curve Number
CWC	Central Water Commission
DEM	Digital Elevation Model
DSAS	Digital Shoreline Analysis System
EPR	End Point Rate
ERDAS	Earth Resource Development Assessment System
ESRI	Environmental Systems Research Institute
ET	Actual Evapotranspiration
ETM+	Enhanced Thematic Mapper Plus
FAO	Food and Agricultural Organization
FCC	False Color Composition
GCP	Ground Control Points
GIS	Geographic Information System
GPS	Global Positioning System
HRU	Hydrological Response Unit
HWL	High Water Lines
IRS	Indian Remote Sensing
IWRM	Integrated Water Resources Management
Landsat	Land Remote-Sensing Satellite (System)
LISS	Linear Imaging Self Scanner
LRR	Linear Regression Rate
LU/LC	Land use/land cover
MSS	Multispectral Scanner

MUSLE	Modified Universal Soil Loss Equation
NASA	National Aeronautics and Space Administration
OLI/TIRS	The Operational Land Imager (OLI) and Thermal Infrared Sensor (TIRS)
PBIAS	Percent bias
PET	Potential Evapotranspiration
R^2	Coefficient of determination
RGB	Red, Green and Blue
RMSE	Root Mean Square Error
RS	Remote Sensing
SCS	Soil Conservation Service
SD	Standard Deviation
SED	Sediment Yield
SSY	Specific Sediment Yield
SUFI-2	Sequential Uncertainty Fitting
SWAT	Soil and Water Assessment Tool
SWAT–CUP	Soil and Water Assessment Tool – Calibration and Uncertainty Program
TM	Thematic Mapper
USDA	United States Department of Agriculture
USGS	United States Geological Survey
USLE	Universal Soil Loss Equation
UTM	Universal Transverse Mercator
WLR	Weighted Linear Regression Rate

CHAPTER 1

1 INTRODUCTION

1.1 General

Coastal zones are considered as the most important geomorphologic features of a maritime state. Nearly 70% of the world population lives within a narrow belt directly landward from the ocean edge, and many of them depend on the resources of the sea for their income. They are the great economic importance both for recreational use and as a barrier zone to protect land and other properties on it from wave attack. They also provide a unique habitat for a variety of plants and animals.

In southern Asia, India is found to be an emerging and developing country (EDC). There are so many sources that help national development and economy. The generation of electricity through hydropower is one of the factors which boosts the economy and development of the country. To generate the hydropower, the dam are constructed across the river. Due to the construction of hydraulic structures across the river, the sediments are trapped behind the dams, and also dam alters the natural flow of the river to the downstream. Sediment supply from the river is the source of beach nourishment. The sediment trapped behind the dams is responsible for the decline in the supply of sediment to the coast. If the decline in sediment supply increases, it will affect to sediment conveyor belt and the beach nourishment.

1.2 Shoreline

The shoreline is a boundary between land and sea. Many developmental activities are being carried out near shoreline and considerable population living there. The shoreline is dynamic in nature (Boak and Turner 2005, Dolan et al., 1980). The shoreline is shaped by various geographical protests, for example, sediment silt discharge of rivers and seas, distinctive climate and ocean conditions, and additionally, the general human social and financial exercises (Boak and Turner 2005). Due to dynamic environmental conditions, it keeps on changing its profile and position regularly. Sea-level rise, Waves, tides, winds, irregular storms, and the geomorphic processes of erosion and accumulation are the primary causes of the shoreline change (Salghuna and Bharthvaj,

2015). The International Geographic Data Committee (IGDC) recognized the shoreline position as one of the 27 Geoindicators (Berger and Iams, 1996). Figure 1.1 shows the skematic representation of shoreline

Approximately 80% of the worldwide coasts are deteriorating with erosion rates ranging from 1 cm/year to 10 m/year (Kermani et al., 2016). It is essential to investigate and recognize the change in shoreline for various field studies such as the advancement of beachfront barrier, seaside zone administration design. The knowledge of erosion and accretion is necessary for the assessment of sediment budgets and the prediction of dynamic coastal morphology using conceptual modeling (Adlea et al., 2015).
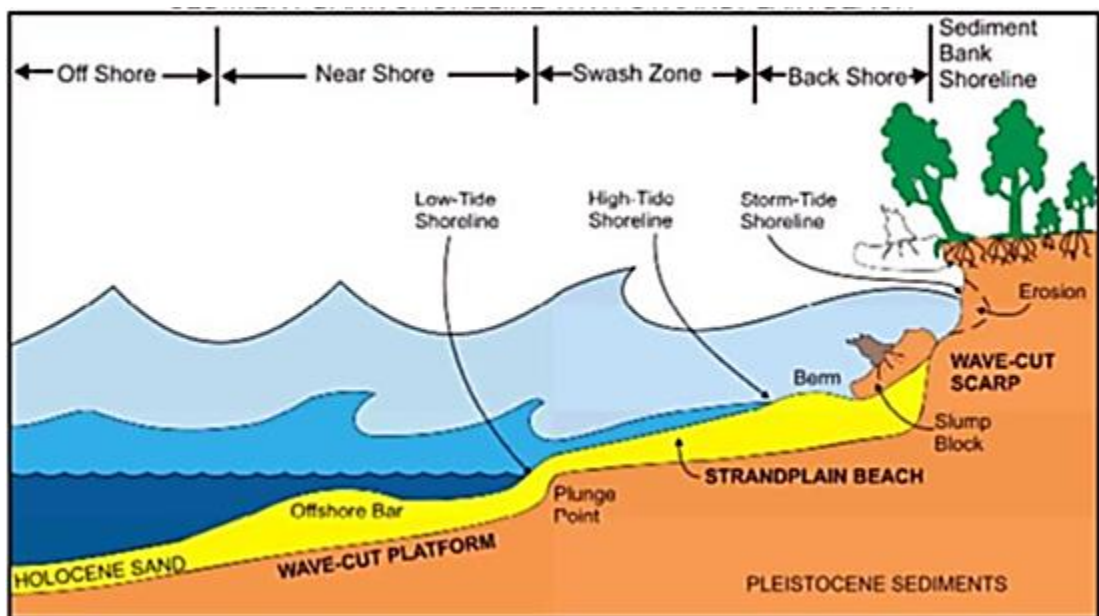
Figure 1.1 Schematic Representation of Shoreline (Source: http://www.learnnc.org)

For coastal zone monitoring, the extraction of shoreline is imperative for national development and environmental protection (Rasuly et al., 2010). Historically, the calculation of long-term and medium variation in shoreline change rates holds good for shoreline change analysis (Ford 2013). Shoreline change detection analysis and its approaches have matured and firmly recognized in the domains of investigation as well as forecasting/decision making. Initially, a topographic survey of two-dimensional field-based techniques was included, for casting perpendicular profiles alongshore (Ford 2013). However, in recent times, shoreline changes are evaluated by adopting the Remote Sensing (RS) technique to available satellite images from Landsat (It is the

longest-running enterprise for acquisition of satellite imagery of Earth), which is appreciated and became economic tool (Gens 2010). RS techniques, coupled with the Geographical Information System (GIS) tool, is used to analyze the temporal variation of shoreline, such as short-term and long-term. In various cases (Kermani et al., 2016), to obtain better and enhanced analyses of short-term change of shoreline, it is better to couple fieldwork data with RS and GIS tools. Besides, mainly from satellite images, which are less time consuming and the same used for historical analysis (Dolan et al., 1991; Thom and Hall 1991).

1.3   Effect of river sediment on the coastal zone

India's total land area is 328 million hectares, and out of that, about 17.5 crore hectares is susceptible to soil erosion. Since 1951, soil conservation measures were adopted on only 2.5 crore hectares. The country's rivers carry an approximate quantity of 6.2 tonnes of sediment per hectare area, and out of these, nearly 10% is deposited in the reservoirs (Narayana and Babu, 1983). As a result, the natural water and sediment flow towards the coastal area were affected.

The Indian coastline is about 7517 km; about 5423 km along with the mainland and 2094 km around the Andaman, Nicobar and Lakshadweep Islands. According to the naval Hydrographic charts, the main Indian land consists of nearly 43% sandy beaches, 11% rocky coast with cliffs, and 46% mudflats and marshy coasts. Numerous hypothetical and field studies have carried out to measure the volume of littoral sediment transport along the Indian coast. However, the minimal attempt has been carrying out to recognize the sources for littoral transportation, which nourish the nearshore transport system.

Rivers are the significant sources of sediments for the beach deposits into the Indian coast (Chandramohan et al., 2001). The single largest source of sediment for the Arabian Sea is the river Indus, which delivers about 0.45 billion tonnes of sediments per annum mentioned by Guptha and Hashimi (1985). There are 14 major rivers, 44 medium rivers, and more than 200 minor rivers that discharge into the Indian coast, serving as the principal sources for the littoral drift. The annual sediment load of Indian rivers is a little more than 1.2 billion tonnes, which is roughly 10% of the global

sediment flux to the world oceans (Subramanian 1993). Indian rivers show pronounced seasonal and spatial variability in their sediment discharge. Erosion and reservoir sedimentation in Indian catchments are not only severe but also accelerating (Jauhari 1999). Thus, the construction of dams and irrigation barrages has dramatically reduced the value of rivers as sediment sources for beach nourishment. Owing to the fall in the influx of sediment and concentration of wave energy, many coastal segments experience erosion. Encroachment of sea into the land has been commonly noticed near river mouths, particularly along the coasts of Karnataka, Kerala and Cauvery river mouth, due to the reduction in sediment supply and discharge, which also results in silting of the river mouth (Chandramohan et al., 2001). India is third in dam building, after China and the US. Large dam construction is the predominant form of public investment in irrigation in India.

As per the latest information compiled through the National Register of Large Dams (NRLD) maintained by the Central Water Commission (CWC), there are 5195 dams, out of which, 4847 large dams have completed, and 348 large dams are under construction. Out of completed large dams, about 76% of dams constructed before 1990 (Ministry of Water Resources – Annual Report 2014-2015). In India, government statistics on 11 of the country's reservoirs, with capacities higher than $1000mm^3$ shows that these reservoirs are filling with sediment deposition 130% to 165% over assumed rates. Based on the sediment data of reservoirs, the weight of total annual sediment deposits in all the reservoirs in India is predictable at 1080 million tonnes (World Commission on Dams, 2000), which may seriously affect the Indian coast.

1.4 Estuary

An estuary is a partially enclosed coastal body of brackish water with one or more rivers or streams flowing into it and with a free connection to the open sea (Pritchard 1967). Estuaries form a transition zone between river environments and maritime environments. They are subject both to marine influences such as tides, waves, and the influx of saline water to riverine influences such as flows of freshwater and sediment. The inflows of both seawater and freshwater provide high levels of nutrients both in

the water column and in sediment, making estuaries among the most productive natural habitats in the world mentioned by McLusky and Elliott (2004).

Most existing estuaries formed during the Holocene epoch with the flooding of river-eroded or glacially scoured valleys when the sea level began to rise about 10,000–12,000 years ago (Wolanski 2007). Estuaries are typically classified according to their geomorphological features or water-circulation patterns. They can have many different names, such as bays, harbors, lagoons, inlets, or sounds, although some of these water bodies do not strictly meet the above definition of an estuary and maybe fully saline.

The banks of many estuaries are amongst the most densely populated areas of the world, with about 60% of the world's population living along estuaries and the coast (Wolanski 2007). As a result, many estuaries suffer degradation by many factors, including sedimentation from soil erosion from deforestation, overgrazing, and other poor farming practices; overfishing; drainage and filling of wetlands; eutrophication due to excessive nutrients from sewage and animal wastes; Pollutants including polychlorinated biphenyls, radionuclides, and hydrocarbons from sewage inputs; heavy metals and diking or damming for flood control or water diversion.
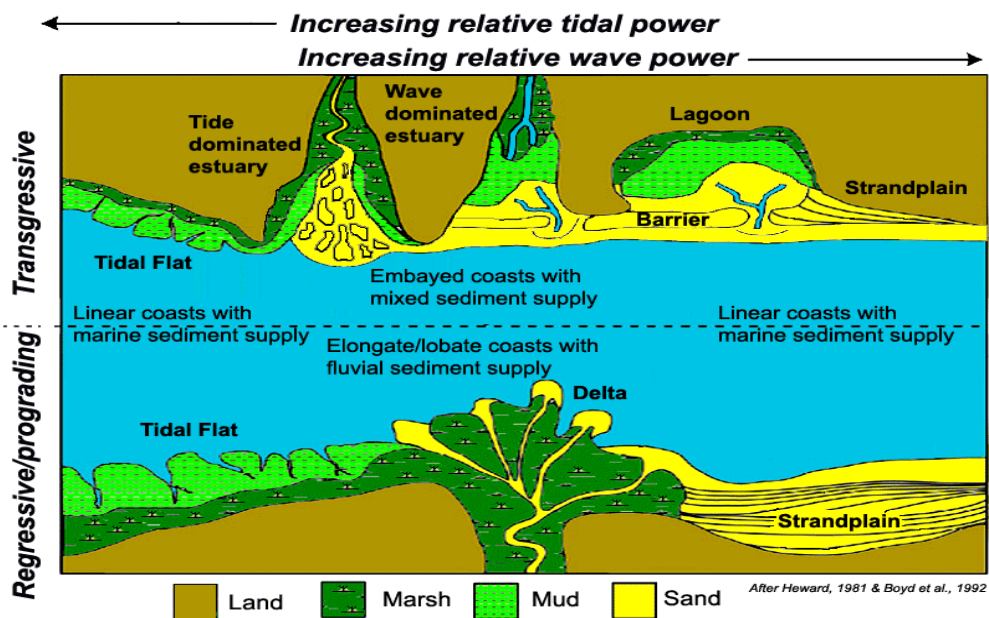
Figure 1.2 Schematic representation of estuary

1.5 Soil erosion statistics

Land degradation is not being adequately addressed but it is of vital importance to raise awareness so that future land management decisions can lead to more sustainable and resilient agricultural systems.

Table 1.1 Extent of land degradation in India, as assessed by different organizations

Organization	Assessment year	Degraded Area(Mha)
National Commission on Agriculture	1976	148.1
Ministry of Agriculture-Soil and Water Conservation Division	1978	175.0
Department of Environment	1980	95.0
National Wasteland Development Board	1985	123.0
Society for Promotion of Wastelands Development	1984	129.6
National Remote Sensing Agency	1985	53.3
Ministry of Agriculture	1985	173.6
Ministry of Agriculture	1994	107.4
NBSS & LUP	1994	187.7
NBSS & LUP (revised)	2004	146.8

The severity and extent of soil degradation in the country have been previously assessed by many agencies (Table 1.1). Water erosion is the most severe degradation problem in India, resulting in a loss of topsoil and terrain deformation. Based on the first analysis of existing soil loss data, the average soil erosion rate was 16.4 t/ha/y, resulting in an annual total soil loss of 5.3 billion tons throughout the country. Nearly 29% of total eroded soil is permanently lost to the sea, while 61% is simply transferred from one place to another, and the remaining 10% is deposited in reservoirs. In both rain-fed and irrigated areas of India, soil erosion has become a serious problem. India is losing substantial money from degraded lands. This expense is recorded by decreasing crop production, the intensity of land use, increasing crop trends, and decreasing income.

Apart from faulty agricultural activities that led to soil degradation, other human-induced land degradation activities include land clearing and careless management of forests, deforestation, over-grazing, improper management of industrial effluents and wastes, surface mining, and industrial development, etc (Bhattacharyya et al., 2015).

1.6   Factors affecting soil erosion and sedimentation

Soil erosion is a natural process that can be exacerbated by human activities and is the wearing away of the land surface by physical forces such as rainfall, flowing water, wind, ice, temperature change, gravity, or other natural or anthropogenic processes. Soil erosion is one of the most severe environmental problems in the world, as it significantly threatens agriculture, natural resources, and the environment (Rahman et al., 2009). Soil erosion risk varies from case to case, depending on the topography of the watershed, soil characteristics, local climatic conditions, land use, and land management practices. Land use, elevation, and climatic factors have a direct impact on soil erosion and sedimentation. Sedimentation reduced the storage capacity and may lead to flood generation. Therefore, proper planning is needed to implement various watershed management policies (Zare et al., 2017).

Land use and land cover changes have a significant impact on soil degradation, including soil erosion. Conversion of forest land into agricultural areas, rangelands, residential areas, development of road networks, recreational suburban areas, and residential areas, which increased the events of runoff. This runoff carries a large amount of eroded soil downstream of the river and leads to sedimentation. Various human-induced activities accelerate the LULC change as well as erosion process (Sharma et al., 2011). Over the last century, soil erosion accelerated by human activities has become a severe environmental problem (Alkharabsheh et al., 2013).

Another factor that is significantly affecting soil erosion is rainfall characteristics. Rainfall intensity, duration, as well as the number of days, increase the rate of erosion and sedimentation. The changes in LULC, along with a high amount of rainfall, are more sensitive to erosion. Soil characteristics play a significant role in land degradation and management practices. Soil with high infiltration capacity reduces the runoff and the extent of erosion but increases the groundwater yield (Zhang et al., 2016).

Physical characteristics of the basin, such as slope, the shape of basin and size etc. have significant impacts on land degradation processes. The uniform slope produced more runoff compared to concave and convex slopes. However, the total amount of soil erosion from the uniform slope was considerably higher than that of a concave or a convex slope. Steep linear slope produced more sediment compared to the gentle slope (Sensoy et al., 2014). Large drainage basins catch more precipitation. So to have a higher peak discharge compared to smaller basins, smaller basins generally have shorter lag times because precipitation does not have as far to travel. The shape of the drainage basin also affects runoff and discharge. Drainage basins that are more circular lead to shorter lag times and a higher peak discharge than that of long and thin because water has a shorter distance to travel to reach a river (https://www.internetgeography.net/).

Lag time has some role in the determination of streamflow to an extent. The larger the lag time, the higher the attenuation of the runoff rate. Vegetative cover not only increases the amount of infiltration but also reduces the flow velocity, lengthens the lag time, and increases the storage effect on the runoff rate (Yu et al., 2000). The monthly simulation gives better results compared to daily simulations (Jain et al., 2010). and a longer period of simulation gives more reliable results (Ndomba et al., 2011).

The construction of a dam alters a sedimentation process. The dam constructed across the river blocks the passage of sediment and gets trapped inside the reservoir. This leads to reservoir sedimentation, and thus, the storage capacity of the reservoir is reduced, which increases the chances of flooding (Liu et al., .2014). Sediment yield is estimated based on considering the rainfall as well as runoff characteristics. Proper estimation of runoff has significant impacts on the assessment of sediment yield of a basin. Runoff of the basin depends upon various hydrological components such as precipitation, infiltration, evapotranspiration, etc. The infiltration depends mainly on the soil properties and the intensity of the rainfall.

Further, evapotranspiration depends on vegetation, temperature, rainfall, etc. The increased rate of evapotranspiration reduces the streamflow and thus erosion rate. A proper understanding between all the hydrologic components is necessary for the accurate prediction of streamflow and sediment load.

There are several methods available for the estimation of runoff. It includes Empirical formulae and charts, by estimating losses (evaporation, transpiration, etc.), by infiltration, Unit Hydrograph method, etc. In empirical methods for estimation, the SCS curve number method is popular and widely used. It accounts for the effects of LULC, soil, slope, rainfall, temperature, and evapotranspiration (Chatterjee et al., 2001). The Hydrologic Engineering Center (HEC) software can also be used for calculating runoff. The sediment load of the basin mainly depends on runoff, slope, rainfall, soil properties, etc. Empirical and field measurement methods used to estimate sediment load from a basin. The universal soil loss equation is a commonly used method for the estimation of sediment load. Revised, as well as modified versions are available by incorporating various changes.

1.7 Dams and their impacts on sediment flow

The long-term sustainability of coasts depends on periodic deliveries of sediments from rivers and streams. However, these valuable coasts may become increasingly diminished due to sediment impoundment behind dams (Slagel and Griggs, 2008). Presently, the rivers alone contribute to about 95% of sediments entering the oceans on a global scale (Syvitski, 2003) and they naturally deliver 70 – 85% of sand to the coastline (Sherman et al., 2002). More than one-third of the world's fluvial sediment load is carried by about a dozen major rivers, wherein the Ganges and Yellow rivers alone contribute 20% of the total sediment load (Lisitzin, 1972). It is reported that the Himalayan Rivers are the major contributors, transporting about 50% of the global sediment flux (Singh et al., 2008). The construction of dams and the execution of soil erosion control programs have greatly diminished the value of a river as a source of beach sediment. Extensive alteration of fluvial systems by the construction of dams has substantially reduced the volume of sand reaching the shore. If the sediment supplies from the rivers and streams are reduced, the beach may become undernourished, shrunk, and cliff erosion may be accelerated (Wang et al., 2010), which leads to the encroachment of sea into the land. During storms, high wave energy, coupled with sea-level rise, caused extensive beach and cliff erosion and coastal structures experienced damage from wave impacts and flooding. Nation's economy will suffer when the beaches continue to narrow from lack of sediment supply. Also, narrower beaches

increase the risk to coastal property from direct wave exposure and coastal flooding. Fluvial suspended sediment is also the primary source of micronutrients to coastal waters, which can be fundamentally important in supporting the primary productivity of coastal phytoplankton.

Dams also influence the flow within a river network. There is a lack of understanding of how the influence of any particular dam propagates through the fluvial system and how many dams operated for multiple uses complicate impacts on hydrology in downstream portions of a large basin. Such information is required to assess the usefulness of dams on flood control at any location in the fluvial system, to protect the repercussions of global climate change on basin hydrology or to anticipate the network impacts of dam re-operation to rehabilitate riverine habitats (Singer, 2007).
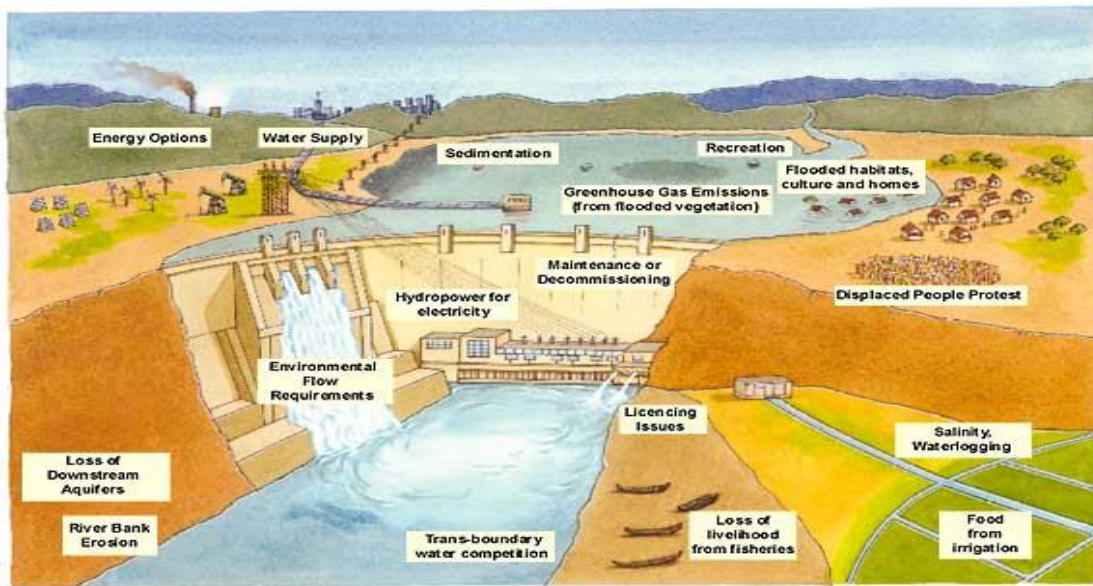
Figure 1.3 Impact of the dam (Source: www.tes.com)

The noticeable impacts of large-scale hydrological change include habitat disintegration within dammed rivers; downstream habitat changes, such as loss of floodplains, riparian zones, adjacent wetlands, deterioration, loss of river deltas and ocean estuaries. Dams disrupt the longitudinal continuity of the river system and interrupt the action of the conveyor belt of sediment transport. Figure 1.3 describes the impact of the dam. It is estimated that 77% of the total discharge of 139 largest river systems in North America north of Mexico, in Europe, and in the republics of the former Soviet Union is strongly or moderately affected by fragmentation of the river

channels by dams and by water regulation resulting from reservoir operation, interbasin diversion (Dynesius and Nilsson, 1994).

The dams also appear to cause a nearly 10% reduction in mean annual flow due to increased evaporation (Meyer et al., 2003). So, the investigation is required on the impacts of dams on hydrology, though the river network in basins, as well as how these reduced river sediment supplies play a role change in delta, estuary, and shoreline.

There are now more than 45,000 large dams throughout the world with an aggregate reservoir capacity of about 60×10^5 Mm^3 (McCully, 1996; Le Cornu, 1998) and around 70% of the world's rivers are intercepted by large reservoirs (Kummu and Varis, 2007). It is estimated that about two-thirds of the freshwater flowing to the oceans controls by dams (Naiman et al., 1993), and around 50,000Mm^3 of sediments trapped behind the world's dams every year. The volume of sediment trap is equivalent to 1% of global reservoir storage, and in total, about 11,00000 Mm^3 of sediment has accumulated in the world's reservoirs, taking up almost 1/5 of the worldwide storage capacity (Mahmood, 1987). Global annual river discharge of suspended sediments into the ocean is nearly 18000 million tonnes (Holeman, 1968), and Asia and Africa have experienced the largest reductions in sediment flux to the coast (Syvitski et al., .2005). Dams have produced 19% of the world's electricity and irrigated more than 30% of the total agricultural land till 2000. However, these dams displaced by over 40 million people, altered cropping patterns, and considerably increased salination and waterlogging of agricultural land (Adams, 2000). Worldwide, people may have concurrently augmented fluvial sediment transport through activities such as deforestation and poor farming practices and reduced the flux of this sediment to the coast through dam building.

1.8 Hydrologic modeling

Hydrologic models provide an abstract and often simplified representation of natural hydrologic processes. Hydrological models are the tools that explain the physical processes involved in the transformation of precipitation to runoff and also the interactions among various hydrological variables within the hydrologic cycle. The ultimate aim of these models is to establish a relationship between several hydrological

components such as precipitation, surface runoff, groundwater flow, evapotranspiration, and infiltration. These models range from simple unit hydrograph based models to more complex models that are based on the dynamic flow equations. There are three different categories of hydrological models: physically process-based, statistically, and empirical-based. The best model is the one that results in less configuration and parameter complexity similar to reality. The essential inputs required for all models are rainfall data, various watershed characteristics like soil properties, watershed topography, and vegetation cover, and drainage area. Lately, computerized hydrologic models have become an essential tool not only for a better understanding of the hydrologic cycle but also for a faster problem-solving in hydrology, such as ungauged catchments.

Hydrological models are increasingly being utilized to analyse the quality and quantity of streamflow, flood forecasting, reservoir system operations, groundwater development and protection, surface water and groundwater conjunctive use management, water distribution system, water use, and a range of water management activities. The sediment yield is also estimated by hydrological models, specially SWAT, which is used in present work.

1.9 Beach profile

Beach-profile surveying forms one component of the overall suite of techniques that is available to coastal managers to monitor the coastal environment. Generally, the beach will be steeper if the beach consists of larger sand particles. If the slope of the beach is gentle to foreshores and underwater slopes, then the beach consists of finer or smaller sizes of sand. Beach-profile surveys are perpendicular cross-section to the shoreline, which are undertaken at suitable geographical locations and are repeated at appropriate time intervals, will provide excellent evidence of the magnitude and frequency of the cross-shore changes which are being experienced by a particular shoreline of any sediment type. Beach level, morphology, and volume changes can be assessed by comparing surveys taken along the same profile line on different occasions. Often when undertaking such assessments, the magnitude of seasonal or short-term storm-related variations in the beach profile can be identified, together with the identification of

longer-term erosional or accretional trends. Spatial variations in beach profiles can also be assessed by comparing data that have been collected on the same date from a series of adjacent profile lines along the shoreline (Cooper et al., 2000).

1.10 Remote sensing and geographical information system (RS & GIS)

1.10.1 Remote sensing

Remote sensing is the science and art of obtaining information about an object or phenomenon through the analysis of data acquired by a device without any physical contact to the object (Lillesand et al., 2015). The electromagnetic energy sensors that are operated from airborne and spaceborne platforms to assist in inventorying, mapping, and monitoring earth resources. These sensors acquire data on the way various earth surface features emit and reflect electromagnetic energy, and this data is analysed to provide information about the resources under investigation. Figure 1.4 schematically illustrates the generalized processes and elements involved in electromagnetic remote sensing of earth resources. The two basic processes involved are data acquisition and data analysis. The elements of the data acquisition process are energy sources (a) propagation of energy through the atmosphere (b) energy interactions with earth surface features (c) retransmission of energy through the atmosphere (d) airborne and spaceborne sensors (e) resulting in the generation of sensor data in pictorial and digital form (f). In short, we use sensors to record variations in the way earth surface features reflect and emit electromagnetic energy. The data analysis process (g) involves examining the data using various viewing and interpretation devices to analyze pictorial data and a computer to analyze digital sensor data. Reference data about the resources studied (such as soil maps, crop statistics, or field-check data) used when and where available to assist in the data analysis.

Satellite remote sensing has emerged as an essential tool in earth resources management due to its essential application such as 1) Synoptic and repetitive global coverage, 2) Easy accessibility 3) Better, enhanced resolution data acquisition 4) Easily

processed and analysed 5) Multi-disciplinary utility 6) cost-effective and less time consumption (Lillisand et al., 2015).
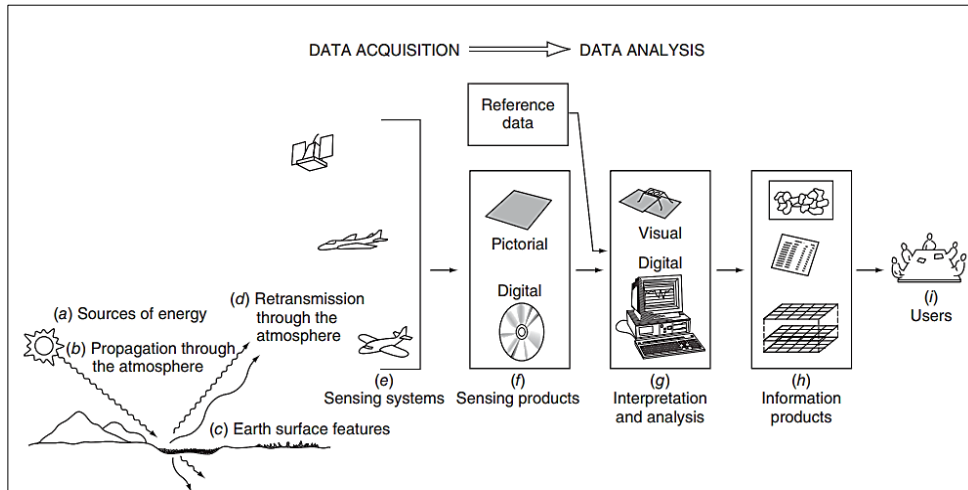
Figure 1.4 Electromagnetic Remote Sensing of Earth Resources.

1.10.2 LANDSAT mission

The Landsat mission satellite products are freely available (https://earthexplorer.usgs.gov/). The first Landsat satellite launched in 1972, the mission had collected data on the forests, farms, urban areas, and freshwater of our home planet, generating the longest continuous record of its kind. Decision-makers from across the globe use freely available Landsat data to understand environmental change better, manage agricultural practices, allocate scarce water resources, respond to natural disasters, and more. Currently, both Landsat 7 and Landsat 8 are in a near-polar orbit of our planet. Each satellite repeats its orbital pattern every 16 days, with the two-spacecraft offset so that each spot-on Earth measured by one or the other every eight days. As the Landsat satellites orbit, the instruments capture scenes across a swath of the planet that is 185 kilometers (115 miles) wide. Each pixel in these images is 30-meters across. The other Landsat missions are Landsat 1, Landsat 2, Landsat 3, Landsat 4, and Landsat 5.

The launch of Landsat 9 scheduled for late 2020, the mission will continue its legacy of monitoring key natural and economic resources from orbit. Landsat 9, managed by

NASA's Goddard Space Flight Center in Greenbelt, Maryland, will carry two instruments: The Operational Land Imager 2 (OLI-2), which collects images of Earth's landscapes in visible, near-infrared and shortwave infrared light, and the Thermal Infrared Sensor 2 (TIRS-2), which measures the temperature of land surfaces.

1.10.3 Geographical information system

A geographic information system (GIS) is a system designed to capture, store, manipulate, analyze, manage, and present spatial or geographic data. GIS applications are tools that allow users to create interactive queries (user-created searches), analyze spatial information, edit data in maps, and present the results of all these operations (Clarke 1986). GIS can refer to several different technologies, processes, techniques, and methods. It is attached to many operations and has many applications related to engineering, planning, management, transport/logistics, insurance, telecommunications, and business (Maliene et al., 2011) For that reason, GIS and location intelligence applications can be the foundation for many location-enabled services that rely on analysis and visualization. GIS can relate unrelated information by using location as the key index variable. Locations or extents in the Earth space-time may be recorded as dates/times of occurrence, and x, y, and z coordinates representing, longitude, latitude, and elevation, respectively.

1.11 SWAT model

The SWAT model has become widely accepted as a useful tool to predict the effects of watershed management on runoff, sediment, nutrients, and pesticide yields (Arnold, J G., et al., 1998). The SWAT model is a watershed scale, a physically based distributed parameter model developed to predict the impacts of land management practices on hydrologic and water quality response of complex watersheds with heterogeneous soils and land use conditions (Arnold et al., 1998). The minimum climate inputs required by the model are maximum and minimum air temperature and precipitation (Saleh et al., 2006). Surface runoff estimated by using the Soil conservation Service runoff curve number (SCS CN)(USDS-SCS,1986) method or Green and Ampt (1911) infiltration method. Potential evapotranspiration (PET) in the model estimated by the Priestly-

Taylor (Priestly and Taylor, 1972), Penman-Monteith (Monteith,1965), or Hargreaves methods(Hargreaves., 1985).

Arc-GIS SWAT extracts hydrologic information from spatial data (delineates streams and watersheds, defines HRUs and assign parameter values based on their soil type and land use, and matches sub-basins and weather stations based on locations), stores it in the data model, uses it for preparing SWAT input files, run SWAT, and writes the SWAT output on the data model (Olivera et al., 2006). The Arc SWAT 2012 version used in the present study to test the performance of the model with the global dataset. SWAT –Arc GIS interface has been selected as the modeling tool in this research.

Widely used methods to quantify the rate of soil erosion and sediment yield are USLE (Universal soil loss equation) (Wischmeier et al., 1965), RUSLE (Revised universal soil loss equation) MUSLE (Modified universal soil loss equation) (Williams et al., 1975). A modified version of the USLE model used to find out the sediment yield as a function of runoff whereas USLE estimates the soil erosion from cropland as a function of rainfall energy (Emam et al., 2016)

Drainage patterns and the physical characteristics of the basin were generated using DEM (Digital elevation model). ASTER and SRTM are commonly used DEMs. SRTM DEMs will not give the entire first order stream while delineation (Sardar et al., 2012). The resolution of DEM was not affecting the runoff, but it has a small effect on sediment yield (Al-Ansari et al., 2013). If land use, soil, and all metrological data are available, then the SWAT model can be used to predict runoff and sediment yield of basins. The estimation of sediment-yield is caused by land-use change increased with rain intensity, while the rate of sediment yield change remained unchanged (Zhang et al., 2017).

In some cases, river courses bring sediments to the reservoir, and that will lead to reservoir sedimentation. As a result of sedimentation, the water storage capacity and the efficiency of the reservoir get reduced, which leads to degradation of the reservoir. SWAT is incorporated with a module of a small dam, which used to evaluate its long-term effects on streamflow and sediment yield (Liu et al., 2014).

1.12 Global positioning system

The Global Positioning System (GPS) was originally developed for military purposes but has subsequently become ubiquitous in many civil applications worldwide, from vehicle navigation to surveying, and location-based services on cellular phones and other personal electronic devices.

Global Positioning System includes at least 24 satellites rotating around the earth in precisely known orbits, with subgroups of four or more satellites operating in each of six different orbit planes. Typically, these satellites revolve around the globe approximately once every 12 hours, at an altitude of roughly 20,200 km. With their positions in space precisely known at all times, the satellites transmit time-encoded radio signals that are recorded by ground-based receivers and can be used to aid in positioning and navigation. The nearly circular orbital planes of the satellites are inclined about 60° from the equator and are spaced every 60° in longitude. In the absence of obstructions from the terrain or nearby buildings, an observer at any point on the earth's surface can receive the signal from at least four GPS satellites at any given time (day or night) (Lillesand et al., 2015).

1.13 Outline of the thesis

The present thesis report is organized into five chapters and is as follows.

Chapter 1: Provides brief introduction of shoreline, the importance of river sediment, estuary, the impact of the dam, beach profile, RS & GIS and GPS

Chapter 2: Explains various research done by experts, research gaps, objectives of present work.

Chapter 3: Explains and gives the details of the study area considered for research work, data products used, sand sample location, field visit photographs, and dam discharge data. It also describes the methods used for shoreline analysis using DSAS and ArcGIS ® tool, sediment yield estimation using SWAT tool, grain size analysis using GRADISTAT MS Excel tool, beach profile analysis, estuary change analyzes and sediments trend analysis.

Chapter 4: Demonstrates the results obtained from different analysis and corresponding discussion as per the objectives of the present study.

Chapter 5: Explains the summary, conclusions, and limitations of the work.

CHAPTER 2

2   LITERATURE SURVEY

2.1   General

The shoreline is the boundary where land and sea meet, and it is always dynamic (Rajkumar et al., 2015). Many studies carried out regarding shoreline change. This section explains a review of recent studies, and the latest technologies used in shoreline analysis, estuarine, and dams, respectively. To analyze the shoreline change, there are two methods in general. Beginning with field-based methods usually, establish two-dimensional data carried out by topographic survey techniques, transects perpendicular to the shore profiles which surveyed regularly (Ruggiero et al., 2005; Thom & Hall, 1991). Shoreline boundary is dynamic, which changes in no time. Therefore previous dry/wet boundary or high-water lines (HWL) considered as shoreline, which can actually see to identify factors (Liu et al., 2013). Most of the time, in the coarse resolution of satellite images, tidal variations are neglected. But to proceed with improved accuracy, starting with medium and later high accuracy satellite products should be used to demarcate the positions of shoreline for historical change detection, short-term change detection, and also cost benefits should be considered (Gens 2010). Furthermore, time series of shoreline positions interpreted and analyzed using Remote Sensing (RS) and Geographical Information System (GIS), usually from aerial data coverage and satellite data with different resolutions (Ford and Murray 2013). Naturally, finding shoreline change and extraction of shoreline task is tough, overwhelming, and sometimes impossible for a whole coastal system when extraction by using standard field survey methods (Cracknell 1999). The rate of change of shoreline exhibits the overall series of actions that were influenced the shore through time, and this can present in the form of a historical shoreline position against a set of time data (Fenster et al., 1993). Several techniques like End Point Rate (EPR), Average of Rates (AOR), Minimum Description Length (MDL), Jack-Knifing (JK), Ordinary Least Squares (OLS), Reweighted Least Squares (RLS), Weighted Least Squares (WLS), Reweighted Weighted Least Squares (RWLS), Least Absolute Deviation

(LAD), Linear Regression Rate (LRR) and Weighted Least Absolute Deviation (WLAD) calculated and compared (Genz et al., 2007). To review historical shoreline movements and to forecast the future shoreline positions, several modeling techniques, computation of precise rate of change of shoreline are helpful (Addo et al., 2008).

2.2 Shoreline analysis

The shoreline is dynamic and is affected by natural events like a wave, wind, tides, sea-level rise, and many more. Shoreline change indicator can be measured with respect to vegetation line, dunes, berms, berms crest, beach scrap, wet and dry boundary, high water line, mean water line, and many more, as the reference line.

HWL defined as the wetted bound and by markings left on the beach by the last high tide. Aerial photographs were used for beach erosion rates by delineating historical shoreline position (Ly 1980) analysis. It was purely based on the use of aerial photographs before and after the construction of the dam to find out the change in shoreline position by extracting the high-water line from aerial photographs. Found that shoreline recessions on the order of 2 m to 6 m per year are experienced. Mean high water (datum-based) positions changes only with sediment transport gradients and associated morphological changes and HWL (proxy-based), which varies with high tides and large waves. These both are used as one of the indicators of shoreline. The comparison was carried out by Moore et al., (2006) using aerial photographs, and linear regression analysis, which used the least-squares method to calculate the best fit line through a series of shoreline positions, and they found out that there is a rare shift between indicator as mentioned above. If an unusual change found, both indicators could use. However, recommended for HWL as a shoreline indicator. Pajak and Leatherman's (2002) study were investigated the short-term variability in the HWL location over tidal cycles, days, and months through field observations and interpretation of videotape data. They concluded that HWL could use as a shoreline indicator. The GPS acquired shoreline positions are more accurate than photo-interpreted shoreline positions, and the same can use for coastal erosion mapping and management. In recent times Jonah et al., (2016) applied HWL proxy to define shoreline position.

The technology of modern remote sensing began with the invention of the camera more than 150 years ago (https://earthobservatory.nasa.gov/Features/RemoteSensing). Remote sensing is the use of various techniques to make observations and measurements at a target that is usually at a distance or on a scale beyond that observable to the naked eye. Remote sensing technologies include Lidar, radar, infrared radiation (IR), thermal, seismic, sonar, electric field sensing, and Global Positioning System (GPS). Depending on what is detected, these various sensors might be mounted to a satellite, airplane, boat, submarine, or an unmanned aerial vehicle (UAV) drone or from another convenient observation point such as a building top (internetofthingsagenda.techtarget.com). Remote sensing techniques benefits with rapid and more frequent data acquisition, faster and more automated processing, and a higher sampling intensity over conventional field-based techniques. Satellite products like Landsat (The Landsat program is the longest-running enterprise for acquisition of satellite imagery of Earth) image, panchromatic images, single band, multi-band, temporal and spatial images, LISS II (Linear Imaging Self Scanner), LISS III were used. It was found that the high accuracy of the analysis is achieved by using high image resolution. Malthus and Mumby (2003) made a review on remote sensing techniques was of the coastal zone for future aspects and concluded that remote sensing might be the only technique that would deliver data at a multi-scale level. Use of satellite imagery to automatically detect coastline with integrating Canny edge detection (The Canny edge detector is an edge detection operator that uses a multi-stage algorithm to detect a wide range of edges in images) and locally adaptive thresholding methods by Liu and Jezek (2004) which considered only size and continuity of the image object.

To improve the results, the parameters such as image objects, shape, texture, and relative position are essential. Shoreline modeling and erosion prediction were carried out by Srivastava et al., (2005), which gave an error on the curvature of shoreline. Implement the higher-order polynomial will lead to a better result as it considers the nature of the curve of the shoreline. Satellite data with the coarser resolution was used for shoreline change analysis by Maiti and Bhattacharya (2009), but they took longer intervals and applied the linear regression method. Calculated shoreline positions were cross-validated using Root Mean Square Error (RMSE). Accurate prediction of

shoreline changes can be made cost-effectively using satellite data of higher resolution at smaller intervals and selecting short spaced transects. Semi-automated shoreline extraction by single Radarsat-1, Synthetic-aperture radar (SAR) image data has advantages over optical data as its night sensing and cloud penetrating capabilities by Billa et al., (2011).

The ''baseline and transect'' method is the primary technique used to quantify distances and rates of shoreline movement, and to detect classification changes across time, (Jackson et al., 2012) developed AMBUR R package contains tools for new baseline and transect methods, which is, ''near'' and ''filtered,'' assisted with quantifying changes along curved shorelines that were problematic for perpendicular transect methods. It was an open-source GIS software and ESRI format file. This package provides a collection of functions for assisting with analyzing and visualizing historical shoreline change. They were also allowed the user to estimate the future location of the shoreline and store the results in a shapefile. Other utilities and tools provided in the package assist with preparing and manipulating geospatial data, error checking, and generating supporting graphics and shapefiles. Multispectral satellite data was more useful than SAR and LIDAR technology for the analysis of medium and long-term (Pardo et al., 2012). They used successive Landsat images to extract shoreline for the same location and determined level of precision. The wet/dry boundary demonstrated that it was a reliable shoreline proxy with a broad set of multi-temporal remote sensing images by Virdis et al., (2012). A new approach band ratio technique, along with a histogram threshold, was employed for TM and ETM+ satellite data to extract shoreline extraction conducted by Niya et al., (2013). Caballer et al., (2016) concluded that Landsat images were one of the satellite images used for shoreline change analysis. However, no accurate surveying measurements made when the Landsat images were registered.

Further, they carried work on whether Landsat images could use for evaluation of annual mean shoreline position. Hence their result suggests the possibility of using Landsat imagery as a new source for describing midterm changes in beaches and being much more useful if the analysis performed using annual mean shorelines obtained by tens of Landsat shorelines acquired. Liu et al., (2013) considered beach slope for

analysis of shoreline movement and used Landsat images for shoreline change detection. Supply of river sediment also a significant factor for shoreline change; this study was carried out by Li et al., (2014) on Chongming Dongtan. They used Landsat TM/ETM+ (The Landsat Enhanced Thematic Mapper Plus) images with a 30m spatial resolution data, and a total of 34 orthogonal transects generated. At a spacing of only 1000m along the baseline. Vegetation line as the shoreline indicator based on the presence of S. Marquette, which is a pioneer species in a tidal flat.

Ghoneim et al., (2015). Their study compared Landsat data with Very High Resolution (VHR) Satellite Imagery offers sub-meter resolution was one of the highest image qualities currently available from commercial remote sensing satellites. Found that Landsat images have advantages over VHR images.

Human impact also one of the reasons for shoreline change. Urban encroachment is one of the effects by man, increasing near the shoreline were studied by Appeaning Addo (2013) conducted a case study on Accra Ghana. He used aerial photographs and an orthophoto map to prepare land use maps generated by GIS. The shorelines were digitized, and the rate of change computed using the Digital Shoreline Analysis System (DSAS). The DSAS software was initially developed in the early 1990s and has undergone continuous, though episodic refinement. Which computes the rate of change statistics from multiple historical shoreline positions residing in GIS software (woodshole.er.usgs.gov/project-pages/DSAS). Appeaning Addo (2013) found that dry beach size reduced by about 35% during his study. He recommended setback lines should be put in place in the study area to prevent human development.

DSAS parameters such as End Point Rate (EPR) usually calculated by dividing the distance of shoreline movement by the time elapsed between the earliest and latest measurements. The Linear Regression Rate of change (LRR) determined by fitting a least-squares regression line to all shoreline points for a particular transect obtained. Historical changes of shoreline were one of the change analyses, where Kermani et al., (2016) carried similar kinds of research on the Jijelian sandy coast, eastern Algeria, for 1960 and 2014. They used multi dated aerial photographs and a Quick bird satellite image. Erosion and accretion calculated from statistical methods such as EPR, LRR, and WLR analyzed with DSAS. DSAS carried out in four steps: (1) shoreline

preparation, (2) baseline creation, (3) transect generation, and (4) computation of rate of shoreline change. They found that the values of shoreline change rates obtained by EPR, LRR and WLR methods are very close in all the study area and finally concluded that the methods developed in this study were found to be an effective tool for detection and assessment the changes in the shoreline position along micro-tidal coasts. Liu et al., (2013) adopted DSAS sections and the estimated beach slope, and the beach volumes calculated and compared with the area and the difference in mean shoreline position in the same intertidal zone. The analysis showed that beach volume was a reasonable indicator for assessing the patterns of erosion/accretion of tidal flat. Arc GIS and DSAS extension have become an emerging tool in recent days. Jonah et al., (2016) used this tool. Their analysis was consisting of net shoreline movement and EPR statistics, and they concluded that GIS techniques were useful and inexpensive for monitoring coastal environments.

Hegde and Akshaya (2015) carried out a shoreline transformation study of the Karnataka coast using Landsat image from 1991 to 2014 and analyzed using DSAS with LRR and EPR. It concluded that the Highest EPR (1991-2014) was noticed in the Ankola taluk, whereas the highest LRR was about in Karwar, both indicating accretion. The highest erosion seen in Honnavar. The long-term (more than ten years) shoreline changes assessed at the Tamil Nadu coast by Natesan et al., (2015) using multi-temporal satellite images from 1978 to 2014. They identified that maximum accretion and erosion observed at the South of Pulicat lagoon and Kamarajar Port (formerly Ennore Port) based on EPR, respectively. In a view to identify and quantify the erosion and accretion areas, Aedla et al., (2015) carried out for Netravati Gurpur Rivermouth using Indian Remote Sensing Satellite (IRS P6) LISS-III (2005, 2007 and 2010) and IRS R2 LISS-III (2013). Their study finds with EPR, and LRR statistical methods are shown more substantial shoreline changes at the Netravati Gurpur river mouth. A long-term analysis of the shoreline gives a minimum of ten years of temporal variations, and the short-term study of the shoreline is for min 2 years of temporal changes. The long-term analysis provides better information for shoreline analysis by Shetty et al., (2015). They considered natural events like wind, wave, tides, and sea-level rise. The remote sensing techniques (Landsat 5, 8, and LISS III) applied to understand the long-term shoreline

changes. They found about erosion and deposition along Netravathi-Gurupur and Mulky-Pavanje Spits (from 1967 to 2013). The erosion sites have shifted to south direction construction of seawalls near Netravathi-Gurupur and Mulky-Pavanje Spits. A case study on shoreline change detection from Karwar to Gokarna using IRS P6 (ResourceSat-1) satellite (LISS III) carried by Choudhary et al., (2013), which provides multispectral data in 4 bands. The spatial resolution for visible (two bands) and near-infrared (one band) is 23.5 meters, with a ground swath of 141 km. It found that the north spit of the Kali River has shifted 426.3m to the north in 30 years of span and span and out of which 109.41 m was during the seven years.

Shoreline change detection analysis carried using the Digital Shoreline Analysis System (DSAS) technique, which included semi-automated shoreline extraction techniques. Also, the Histogram threshold of band 5, Histogram threshold of band ratio, and tasselled cap transformation (TCT) (Nasar et al., 2018). The object-based image analysis technique used to extract the water on the criterion of (Normalized Difference Water Index) NDWI (Modified Normalized Difference Water Index) MNDWI and threshold level slicing (Hashmi and Ahmed, 2018).

RS and GIS applications have shown effective in the delineation of shoreline geography and coastal landforms, detection, and calculation of coastline and landform changes, extraction of shallow water bathymetry (Kumar and Jayappa 2009, Maiti and Bhattacharya, 2009). Also, these applications have validated the achievement of high-accuracy shoreline information and shoreline analysis on finer spatial and temporal scales (Li et al., 2014). Coarser pixel size data fail to the accurate position of shoreline during extraction (Gens, 2010). To extract shoreline positions from Landsat (5, 7, and 8), imagery 30m/pixel available from (Pardo-Pascual et al., 2012) suggested a methodology with RMSE values of about 5m. This accuracy has verified by comparing with 116 Landsat extracted shorelines with two shoreline segments on seawalls for a particular study area. Several locations of shoreline available annually, which are helpful to negotiate the excessively affecting by the factor cause to annual variation (Almonacid-Caballer et al., 2016). Landsat images used to analyze and digitization shorelines (Liu et al., 2013). In recent times google earth pro images with 10m resolution used for shoreline extraction (Saleem et al., 2018).

Histogram Equalization (HE) is a well-known indirect contrast enhancement method, where the histogram of the image is modified. To overcome the contrast level in the HE method, additionally, included Histogram Equalization and Adaptive Thresholding Techniques, which enhances the contrast level in the image, which was adopted by Aedla et al., (2015). They are provided the automated shoreline extraction method from satellite images using contrast enhancement and thresholding-based techniques. They found that the contrast enhancement method based on Modified Self-Adaptive Plateau-Histogram Equalization with Mean Threshold (Modified SAPHE-M) improved significant contrast enrichment of coastal edges and coastal objects for clear recognition and delineation.

For long-term and spatially extensive observations of shoreline changes, video-based technology has become a popular method because frequently, it can use to build a database. Shin and Kim (2015) utilized the fixed locations of the topographic map and the results from Ground Control Points (GCP) measurements to obtain a higher accuracy of results. Introduced the technique of utilizing the stereo image to get higher resolution images, improve the analysis results, and the resolution of coordinates.

A few automatic shoreline detection methods have proposed to overcome manual detection, which is time-consuming and needs great effort. RS and GIS techniques are overcoming the difficulties in detecting shoreline position and shoreline change analysis. There are several techniques to extract the shoreline and shoreline change detection from satellite imagery. The techniques such as image enhancement, supervised and unsupervised like ISODATA (The Iterative Self-Organizing Data Analysis Technique), Principle Component Analysis (PCA), Tasseled Cap, Normalized Difference Water Index (NDWI) were considered for multi-temporal data classification and assessment of two independent land cover classifications, density slice using single or multiple bands, and multi-spectral classification, (Mas 1999, Ryu et al., 2002 and Kuleli et al., 2011). Histogram equalization and adaptive thresholding techniques were used for automatic shoreline detection (Aedla et al., 2015).

2.2.1 Model studies on the shoreline

Several studies done shoreline using different models. These models were used to calculate shoreline change, prediction, simulation. In this section, a review has carried out on model studies on the shoreline.

A discussion of the Generalized Model for Simulating Shoreline Change (GENESIS) was carried out by Young et al., (1995). Which was designed by Hanson and Kraus during 1989, to simulate the long-term shoreline changes at coastal engineering sites resulting from spatial and temporal differences in longshore sediment transport. They reviewed that it is a one-line concept (derived from Pelnard-Considere, 1956), which means that beach/shoreface, cross-shore profile shape assumed to have remained constant as it moves landward or seaward. It requires the quality of input data. This model did not apply to simulate and randomly to fluctuate beach systems in which no trend in shoreline position is evident. Notably, it was not applicable to calculate beach changes inside inlets or in areas dominated by tidal flow, wind-generated currents, storm-induced beach erosion, cross-sediment transport, and scour at structures. Kakisina et al., (2016) used NEMOS (Nearshore Modelling of Shoreline Change) Model for abrasion mitigation. The study carried out to measurement of NEMOS modeling use of GENESIS with three scenarios that are existing conditions without protection, groin series, and groin, and seawall combination protection. Conclude that coastal protection using a combination of groins series and seawall will be capable of reducing the abrasion.

The updated ONELINE model provides practical and reliable full, time-dependent simulations of shoreline change for coasts controlled by structures and complex boundary conditions. It calculates shoreline change due to longshore sediment differentials as well as on-offshore sediment movements (Dabees and Kamphuis 1998). Further, they considered two cases; the first one features a groin field study for a 15-year simulation of a 2.6-km shoreline reach, and the second one was along the Nile Delta Coast in Egypt and included detached breakwaters, groins, seawall, and a river

mouth boundary. They compared the result and found that, consistently small prediction error on calibration and verification.

Modeling shoreline response and inlet shoal volume development on long ISLAND COAST, UNITED STATES studied by Hanson et al., (2011). They developed a new numerical model of regional sediment transport and shoreline change, combined with the inlet reservoir model, was introduced. The shoreline change model based on one-line theory following basic formulations and algorithms developed by Hanson (1987). A 20-year time series of hindcast wave data at three stations along the coast used as input data to the model. The simulated shoreline agreed well with the measured shoreline, including the accumulation updrift the inlets, the overall erosion downdrift the inlets, and the formation of salient-type features downdrift the inlets. Thomas and Frey (2013) made a review on Shoreline Change Modeling Using One- Line Models, which was GENESIS, LITPACK, UNIBEST, and GenCade. According to their results, it was found that all models represent the same major processes driving shoreline change with many small variations in approaches or capabilities. The significant differences in capabilities noted are listed below

- GenCade is the only model that allows the inclusion of inlets within the model domain and includes the impact of inlet processes and dredging on adjacent shorelines.
- UNIBEST and LITPACK include a more rigorous calculation method for longshore transport. Calculations conducted on a 2D grid (cross-shore and vertical).
- UNIBEST applies a curvilinear grid instead of linear. GenCade and GENESIS address the same issue through the addition of a regional contour. The LITPACK does not include either option.
- UNIBEST does not calculate diffraction internally.

Vitousek et al., (2007) studied Model scenarios of shoreline change at Kaanapali beach, Maui, Hawaii: seasonal and extreme events. They used the Delft3D modeling system which predicts directly observed tidal currents and wave heights, was applied for shoreline change simulation. They found that the model gave consistent results, but due

to sea-level rise may cause an accelerated seasonal response in alongshore systems and which failed in Delft3D.

Kökpinar et al., (2007) carried a study on Physical and Numerical Modeling of Shoreline Evaluation of the Kizilirmak River Mouth, Turkey. To investigate and prevent the coastal erosion at the Kızılırmak River Mouth, they made a comparative study on the physical and numerical model. Applied one-line numerical model and found that, very effective tool in the design of shore protection structures such as groins, seawall.

The PXT (Polynomials in X and time) models may provide additional information about recent change at a beach and can show how rates may have varied with time. Analyze trends of historical shoreline change. Romine et al., (2009) applied the PXT model to calculate the shoreline change rate for the beaches of southeast Oahu. They found that the PX model was held suitable for longterm analysis, and the PXT model gives results for accretion in the shoreline change rates.

Mole et al., (2012) used ShoreFor (Shoreline Forecast) model for Modelling multi-decadal shoreline variability and evolution. It was investigated using a multi-decadal dataset to assess model performance daily to decadal timescales. The model was first tested with the available offshore wave data and calibrated to each profile to examine the model performance. The model performance was minimal.

The adaptive neuro-fuzzy inference system (ANFIS) compared with harmonic analysis and autoregressive exogenous (ARX) model. Chang and Lai (2014) predicted shoreline change for monthly variation and concluded that ANFIS gives a better result than ARX models.

Laboratory study is also one of the approaches used so far; such kind of study was carried out by McCoy et al., (2015). Their study was a laboratory study of a shoreline protection structure which included wave reduction, sediment collection as well as mathematical modeling. This mathematical modeling used to determine the most sensitive variables governing sediment collection. In the end, they found out to be water depth also plays an essential role in that it reduced the sediment collection as the water became more profound.

2.3 Sediment dynamics at the estuary

An estuary is a region where the river meets the sea with sediment. This region is very important to know how sediment interacts with the sea. This section review on the sediment process at the estuary region has been done. To analyze the nature of estuary, Kitheka et al., (2005) carried work on river discharge, sediment transport, and exchange in the Tana Estuary, Kenya. Despite the decrease in sediment load, the sediment load was still high, as evidenced by the high turbidity of the river water as well as that in the Tana Estuary and Ungwana Bay. Concluded that, during spring tide, the net export of sediments is greater than the river sediment supply. During neap tide, the magnitude of net sediment export was low, and the channel deepening is limited. During the Northeast monsoon, the plume moves southward, and during the Southeast monsoon, the plume moves northward.

Studies on critical erosion and surface sediments for estuary were carried out by Bale et al., (2006). Their work was on measurements of the critical erosion threshold of surface sediments along the Tamar Estuary using a mini-annular flume. The erodibility of intertidal sediments in the region between mid-tide and low water most accurately predicted by wet sediment bulk density (in general, it is a mass of soil plus liquids/ volume as a whole) followed by water content and silt content. There was a repetitive process of erosion and deposition under tidal influences. Thus a low erosion threshold was found, and in the lower reaches, there was much less disturbance of the sediment. Shi et al., (2006) studied the bottom fine sediment boundary layer and transport processes at the mouth of the Changjiang Estuary, China. They concentrated on basic physical processes controlling the transport of fine suspended sediments at the seaward end. They carried out both point sampling, and acoustic profiling revealed that there were spring/moderate/neap tidal and intertidal (flood/ebb) variabilities of fine suspended sediment concentration. The exchange of sediment between the bed and water column affects the sediment transport in the Changjiang Estuary. They stated that further fine sediment dynamics could be integrated with numerical modeling. Shi (2010) reviewed the fine sediment processes-oriented field and simple numerical studies on Changjiang River estuary. Carried out field measurements included the point-sampling and the acoustic profiling of fine sediment suspension. It found that fine

sediment processes in the partially-mixed Changjiang River estuary are mainly forced by both estuarine circulation and tidal asymmetry. Concluded that, mean suspension concentration and bottom shear stress are two dominant physical parameters on flocculation and settling velocities.

Sediment regime also plays an essential factor, which may alter in the region of the estuary. The sediment regime controlled by a range of factors such as grain size, sediment supply, and prevailing flow conditions and can change in response to any variations in these factors. Kerner (2007) studied on Effects of deepening the Elbe Estuary on sediment regime and water quality. Long-term series of the grain size composition of sediments and sedimentation rates in the mainstream and its branches (Nebenelben) compared with changes in flow velocities and tidal water levels. Sedimentation of suspended particulate matter (SPM) used to show the effects of deepening transport regime. Nitsche et al., (2007) worked on Regional patterns and local variations of sediment distribution in the Hudson River Estuary. The distribution of sediment texture and process-related sedimentary environments; for the whole 240 km long estuary together with along river variations of depth, cross-sectional area, and grain size distribution using data set consisting of high-resolution multibeam bathymetry, side-scan sonar, and sub-bottom data, as well as over 400 sediment cores and 600 grab samples. The regional sediment distribution consists of marine sand dominated sediments near the ocean end of the estuary, a large, mud-dominated central section, and fluvial sand dominated sediments in the freshwater section of the Hudson River Estuary. They found that local morphology, bedrock type, tributary input, and human activity modified the regional sediment distribution significantly.

Hu et al., (2011), the water and sediment budgets in the Pearl River Delta (PRD) investigated with a 1D and 3D coupled model, which integrates the river network. Suggested that tide plays an essential role in seasonal deposition patterns in the wet season and erosion in the dry season and combined actions of various forcing mechanisms, including river discharge, monsoon winds, tides, coastal currents, and the gravitational circulation driven by density gradients. Their model showed the result as water and sediment fluxes in the river network unevenly distributed in space and time. Gao et al., (2013) carried research on rapid changes in dynamic sediment processes in

the Yalu River Estuary under anthropogenic impacts. Further, they investigated the changes in sediment dynamics over the past ten years through hydrodynamic calculation, as well as heavy mineral and grain size analysis. They concluded that, the long-term sediment dynamic process, geomorphological evolvement primarily affected by the decrease of water discharge and sediment supply due to human activities.

In some cases, the river no longer Reaches Sea, Zamora, et al., (2013), explained the same conditions, where they researched the case study, post dam sediment dynamics, and processes in the Colorado River estuary. This river no longer reaches the sea except during particularly high tides and anomalously wet years. They mentioned that, for Active River management, dredging needed to reconnect the river. MARV10 tide predictor program used for tidal height prediction and Malvern Master Size 2000 used for grain size distribution analysis. They quantified sedimentation rates in the river's lowermost channel section. It also found that a healthy river ocean interface can help restore nutrient cycling processes.

The physical mechanisms that cause migration of sediment deposition region and also investigation has done on large-scale structure impacts on hydro-dynamics. The model FVCOM was used for the same by Ma et al., (2013) studied numerically using the finite volume coastal ocean model (FVCOM) to calculate physical mechanisms inducing the migration of the sediment deposition region. Model results reveal that the tidal currents, as well as the sediment processes in the northern passage, are significantly changed by the structures. However, it is challenging to simulate sediment transport processes and morphological changes in a long/median term in the construction region due to daily dredging operation.

Gong et al., (2014) carried out sediment transport in response to changes in river discharge and tidal mixing by using funnel-shaped micro-tidal estuary. They considered dry and wet seasons for sediment dynamics analysis. intratidal, fortnightly, and seasonal variations of water current, salinity, and sediment concentrations were analyzed, with the changes of sediment transport patterns in the estuary. They collected hourly water temperature, salinity, and turbidity profiles made using RBR CTDs (Model XR-420) and OBS (Model OBS 3A). Their significant finding was intratidal variation of sediment concentration is mostly controlled by the tidal asymmetry in

velocity and duration at flood and ebb tides (barotropic asymmetry), and Along with the sediment transport pattern, seabed erosion expected to occur.

Franz et al., (2014) Applied MOHID model to cohesive sediment dynamics in tidal estuarine systems: a Case study of Tagus estuary, Portugal. Model results compared with velocity data from the Acoustic Doppler Current Profiler (ADCP) installed in the buoy. They considered only fortnightly and daily erosion of sedimentation cycles. The salinity effect on flocculation and the consolidation process neglected.

Yang et al., (2015) analyzed the influence of human activity on the seawater content, the sediment content, and the regional transport situation. In both flood seasons and dry seasons, as well as in the whole year, the sediment discharge rate and the suspended sediment concentration measured by (SSC) Acoustic Doppler current profiler (ADCP) method in the estuary area of the Yangtze River showed decrease trends.

Webster and Ford (2010) studied on delivery, deposition, and redistribution of fine sediments within macrotidal Fitzroy Estuary, Australia. They described the hydrodynamics and fine-sediment dynamics in the coupled Fitzroy Estuary and Keppel Bay. Cui and Li (2011) Quantified coastline change as well as accretion and erosion of the Yellow River estuary during the period from1976 to 2005, based on a systematic analysis of Landsat MSS, TM, and ETM+ data. Found relationships between the accretion–erosion of land with the sediment and runoff of the Yellow River basin. They found that change in the pattern of accretion and erosion of the Yellow River estuary using GIS and RS tools.

Kuang et al., (2014) made a comprehensive analysis of the sediment siltation in the upper reach of the deep water navigation channel in the Yangtze Estuary. A numerical hydrodynamic model of Delft3D-FLOW was used, in which hydrodynamic processes in this model included tidal flow, sediment transport, jetties and groins for the deep water navigation channel, tidal flow, and sediment transport. The model was verified using the field measured tidal level, flow velocity magnitude, direction, and SSC.

Mayerle et al., (2015) analyzed a case study of sediment transport in the Paranagua Estuary Complex in Brazil. They presented a three-dimensional model for cohesive sediment transport based on the Delft3D modeling system. The model was used to

compute current velocities, water levels, and salinities at various locations. The flow, the wave, and the sediment transport models of Delft3D coupled together, and they were calibrated and validated using relevant field measurements at different locations. They found that the effect of waves on sediment concentration and transport found to be insignificant during normal weather conditions when wind speeds are below 6 m/s, and human interactions like dredging the navigation channel will affect the flow regime and sediment transport.

Chen et al., (2015) investigated of suspended sediment transport in a tidal estuary using a 3D hydrodynamic model (SELFE). The model was calibrated and validated using the data of water surface elevation, tidal current, salinity, and SSC observed in 2010. Dai et al., (2015) carried the Morphological evolution of the South Passage in the Changjiang (Yangtze River) estuary, China. A multivariate analysis technique of the Empirical Orthogonal/Eigen Function (EOF) method used to examine the major modes of change in the long-term (over 26 years) water-depth data. They assessed the potential response of the upstream reduction of sediment supply and the impact of the natural and human-made factors near and far. Lopez and Baptista (2017) validated the sediment model coupled to the hydrodynamic model SELFE against a benchmark combined a set of idealized tests and an application to a field data-rich, energetic estuary. They were partially able to give improvement results to their scalability problems.

Human et al., (2015) investigated the two flushing events (natural and artificial), determine their effects on conditions of the estuary to those before the construction of the dam. They found that the natural flow of water is important, and it is essential over artificial flush to the estuary.

Yang et al., (2014) studied the impact of water and sediment discharges on subaqueous delta evolution in Yangtze Estuary from 1950 to 2010. They investigated the variation trends of the annual water and sediment discharges, the amounts of water and sediment in dry and flood seasons, and the distribution processes of water and sediment discharges. They revealed that the evolution of the estuary delta controlled by the water and sediment factors in the basin.

There are number works on estuary analysis carried out by Remote sensing techniques. Sreenivasulu et al., (2016) analyzed river mouth dynamics of Swarnamukhi estuary, Nellore coast, and the southeast coast of India. They carried out using multi-temporal satellite images of IRS P6 LISS-III and Landsat 8 OLI/TIRS data from 2011 to 2015 using remote sensing and GIS techniques, and there was a high erosion estimation than accretion which reflected on coastal dynamics. Also, loss or gain of sediments causes the formation of young beaches, berms, sand dunes, and sea cliffs depending on wave energy and littoral currents, changes of size and shape of the river mouth. Brocchini et al., (2016) carried a comparative study between the wintertime and summertime dynamics of the Misa River estuary. They mentioned that the continuous remotely sensed data gives to better quantify the eroded/deposited sediment volumes, especially during high flow conditions. Tian et al., (2017) used Landsat images to quantify different human threats to the Shuangtai Estuary Ramsar site, China. Especially they concentrated on wetlands where they found the expansion of cropland and built-up land. The development of the petroleum industry, aquaculture, and tourism resulted in dramatic fragmentation of the wetland landscape. They considered a moderate resolution for analysis. For better results, higher resolution is recommended, as they quoted.

2.4 Impact of dams on river sediment

Some of the prominent works have carried out relating to the impact of dams on river sediment. The study was carried out by Ly (1980). The survey of the role of the Akosombo dam on the Volta River which caused coastal erosion. After the construction of the dam, approximately 99.5% of the river drainage basin blocked. In this case, the river supplied to the shoreline only a minor quantity of sand derived from the low-lying areas of coastal plains below the dam. Kondolf (1997) studied the effect of dams and gravel mining on river channels, explicitly concerned with the response of river channels to a reduction in the supply of sediments by dams and gravel mining. Suggested that, to maintain the continuity of sediment transport through the system, in-stream mining should not be permitted in rivers downstream of dams by the lack of supply from upstream. Hill et al., (1998) compared the vegetation and hydrological regimes of regulated and unregulated systems, developed a model which predicted

based on the catchment area, however, fail to account for richness patterns at the margins of lakes enlarged by dams.

Dam operation of river discharge also plays an important role. Some dams have their capacity and operational rule. These operations have affected on sediment flow rate. Graf (2006) carried out work on the regulated dam and unregulated dam, which shows, hydrologic changes by dams have fostered dramatic geomorphic differences between regulated and unregulated reaches using aerial photographs from USGS. The used software package "Indicators of Hydrologic Adjustment" (IHA) which accepts daily flow records as input and produces summary statistics as output. Further made a comparison between regulated and unregulated reaches which shows that very large dams, on average, reduce annual peak discharges of flow 67% (in some individual cases up to 90%), decrease the ratio of annual maximum/mean flow 60%, decrease the range of daily discharges 64%, increase the number of reversals in discharge by 34%, and reduce the daily rates of ramping as much as 60%.

As the river flow regulated by the dam, the river regime and streamflow change its path. Vicente-Serrano et al., (2016) carried out the effect of reservoirs on streamflow and river regimes in a heavily regulated river basin of Northeast Spain. Identified considerable modifications of the river regimes, showed that while non- regulated basins had decreased streamflow during summer months, highly regulated basins had increasing stream-flow during summer months. The seasonal patterns and the magnitude of changes in stream-flow at gauging stations in the lower reaches of the basin differ from those observed from water releases in the primary reservoirs. Brandt (2000) reviewed that, the effects downstream from dams differ greatly depending on location, environment, and substrate, released water, sediment and concluded that, for the same change of flow, the effects might differ depending on the type of bed and bank material and the grain sizes of the transported material. Therefore, to be able to forecast changes correctly, a study should also include grain-size distributions of the released load, the erodibility of beds and banks, as well as an analysis of the existing geomorphology, including the variation of the slope.

Skalak et al., (2003) made an initial effort to document the geomorphic influence of dams on downstream channels in Pennsylvania and Maryland. They evaluated the

effects of small dams (11 of 15 sites less than 4 m high) on downstream channels at 15 locations in Maryland and Pennsylvania by using a reach upstream of the reservoir at each location to represent the downstream reach before dam construction. They evaluated differences in geomorphic and bed material characteristics between upstream reaches and downstream reaches to quantify the effects of the dams on downstream channels. Found out that the median grain diameter (D_{50}) was increased slightly by dam construction. The percentage of sand and silt and clay on the bed averages about 35% before dam construction but typically decreases to around 20% after dam construction. They stated that dam removal in streams similar to their study area should not result in significant long-term geomorphic changes. And also found that the dam removal projects in streams similar to those of their study area should not cause significant long-term geomorphic changes to the stream channels downstream.

Riverine sediment supply was a governing factor in the intertidal zone was shown by Yang et al., (2005). Stated that a significant relationship exists between intertidal wetland growth rate and riverine sediment supply that suggests the riverine sediment supply was a governing factor in the interannual to interdecadal evolution of delta wetlands. Using MapInfo software intertidal wetland calculated, then Regression analysis performed using Microsoft Excel and SPSS 12.0 software. They calculated the amount of sediment trapped in reservoirs, examined the influence of dam trapping on riverine sediment load, established a statistical relationship between riverine sediment discharge and growth rate of intertidal wetlands at the delta front. Found out that, due to lack of sediment supply, the wetlands have reduced. Their prediction shows that sensitive changes in riverine sediment supply, which will degrade wetlands. Concluded that, it will have a significant impact on the environments of the delta and nearby coastal ocean.

On Three Gorges Dam (TGD), several studies have carried out. Yang et al., (2007) conducted research on Three Gorges Dam, found out that, it has trapped around 2/3 of sediment from upstream that was the sediment flux into the estuary decreased by ≈85 mt/yr (31%) compared to a case of non-TGD in 2003–2005. It was the most important cause for the decrease in riverine sediment load and induced transformation from deposition to erosion in the delta front, which will impact the delta environment in the

future. Wang et al., (2008) confirmed that the movement monitoring of his study area Three Gorges Dam after impoundment landslide was critical during a period of low reservoir level. An et al., (2009) concluded that the change of salinity was influenced by the discharge variation of the Three Gorges Project (TGP). They applied a three-dimensional hydrodynamic module used, named ECOMSED, to deal with the effects on a salt-water intrusion in the Yangtze River estuary in dry seasons. It can be recognized that the model results were in good agreement with the measured data and able to predict the distribution of saltwater intrusion after TGP. Yang et al., (2011), their objective was collective impact both on the middle and lower courses of the river as well as the impact on the Yangtze's subaqueous delta. It found that river channel erosion, which also is reflected by the coarsening of bottom sediments, has only compensated for about 20% of the river's decreased sediment discharge due to the construction of the dam. As a result, the estuary had experienced sediment starvation and a corresponding decrease in coastal salt marsh accretion and net erosion in the subaqueous delta front, which have occurred when the river's sediment load fell below 270 Mt/yr. It will continue for the future. The impact of TGD on the Changjiang was not only limited to the river hydrology and sedimentology in the middle and lower reaches, but also the estuarine and deltaic regions near the river mouth. Changjiang Submerged Delta (CSD) went through the following phases on multi-decadal time scales: high accumulation (1958–1978); slight accumulation (1978–1997), slight erosion (1997–2002); and high accumulation (2002–2009), despite the 70% reduction of the sediment load due to the operation of the TGD since 2003. Chen et al., (2016) carried out on Changes in monthly flows in the Yangtze River, China – With particular reference to the Three Gorges Dam. They analyzed the hydrology of the Yangtze River at the monthly time scale using data that cover the period 1955– 2014, concerning temperature, precipitation, and the ongoing construction of dams. Their findings were not much change in temperature, precipitation, and significant discharge for hydroelectric generation.

Provansal et al., (2014) carried out a study on geomorphic evolution and sediment balance of the lower Rhône River (southern France) over the last 130 years: hydropower dams versus other control factors. A consequence of the changes has occurred on the

lower Rhône was a significant reduction in sediment delivery to the river mouth, with a consequence on the stability of the Rhône delta and adjacent shorelines. East et al., (2015) investigated Large-scale dam removal on the Elwha River, Washington, USA: River channel and floodplain geomorphic change where they found that the changes in topography, grain size, and channel planform resulted from a unique, artificially generated imbalance between sediment supply and transport capacity. Even though dam removed river will not carry all the sediment trapped, some part will remain and river channel and floodplain, together with renewed natural sediment and wood supply from the upper watershed, may affect the fluvial system for decades. Lu et al., (2015) worked on the sediment budget as affected by the construction of a sequence of dams in the lower Red River. The water and sediment regime of the Red River system has been significantly altered by the second dam. River channel changed from deposition to erosion and back to deposition, as affected by the constructed dams.

Syvitski et al., (2009) used Shuttle Radar Topography Mission (SRTM) data to find the sinking of the delta. They concluded that 85% of the deltas in the world received heavy flooding, which resulted in temporary submergence. They also estimated that the delta surface is vulnerable due to sea-level rise; if the sediment supply did not reach the delta.

Rao et al., (2010), studied on dam construction in the river catchments and impact on the shoreline behavior in the respective deltas. They had taken up the Krishna and Godavari deltas as a case study to examine the changes along the delta-front shoreline during the pre-dam and post-dam periods in correlation with the trends in water discharges and suspended sediment loads through these two rivers and revealed that the Krishna–Godavari delta-front shoreline had shifted significantly during the past seven decades. Mentioned that due to sediment supply is diminished, the continued land subsidence, which is common to delta-front regions, probably led to a relative sea-level rise and coastal submergence. One of the significant facts that the decreasing sediment delivery and increasing erosion along the Krishna–Godavari delta-front coast during the past four decades, which witnessed large scale sediment retention at the burgeoning dams across these two rivers in peninsular India.

Smith et al., (2016) carried out on Dam-induced and natural channel changes in the Saskatchewan River below the E.B. Campbell Dam, Canada. Compared pre- and post-

dam sediment sizes using grain-size data for channel-bed samples collected from their study area. Carried out bedload transport, and channel cross-section surveys found out that, all channel cross-sections up to 81 km below the dam have coarsened and enlarged since the closure, resulting in excavation, enlargement.

2.5   Sediment trend analysis (STA)

It is a technique by which the process of net sediment transport from the relative spatial changes in the grain size distributions of all naturally occurring sediments, can determine. The changes in grain size distributions can be measured with the help of three-grain size parameters, Mean Size, Sorting, and Skewness. Sediment movement patterns and the dynamic behaviour of sediments in a study environment can be inferred by performing the grain size analysis of collected sediment samples and comparing the changes in grain size parameters at different sampling locations. It provides an understanding of sediment pathways, sources, and sinks.

STA was first published by McLaren and Bowles (1985) the key points from their study are in a case of complete deposition; the deposit will be finer, better sorted and more negatively skewed (Case I). The lag remaining after erosion must be coarser, better sorted, and more positively skewed (Case II). Two cases of selected deposition were recognized, in which either the deposit can be finer (Case IIIa) or coarser (Case IIIb) than the source, but the sorting will be better, and skewness will be more positive. Grain size parameters can be obtained easily by using a mathematical or graphical approach. There are Various formulae proposed by several researchers (Krumbein and Pattijohn1938, Trask 1930, Otto 1939, Inman 1952, Folk and Ward 1957, Mc Cammon 1962). Of all these, the Folk and Ward method preferred for performing STA (McLaren 1985). Folk and Ward method have shown relatively good efficiency when compared to the rest of the formulae. (McCammon 1962).

In the present study, Sediment Trend Matrix (STM) has prepared by the help of grain size parameters obtained from Folk and Ward formulae. This STM was used to draw Sediment Transport Paths (STP) for the samples collected. The dynamic characteristics of the beach are varying temporarily by changing wave conditions during post-monsoon and pre-monsoon seasons, having different environmental conditions. Therefore, to assess the dynamic behaviour of the coastal region for pre-monsoon and

post-monsoon season, it is essential to carry out Seasonal Beach Profiling. The changes in sedimentary beach volumes are commonly evaluated using measurements of the beach or seabed height over a small number of selected profiles during a long-time interval. The direction of sediment motion is added based on various morphological and geological features such as erosion & deposition, which identified using the change in shoreline from pre-monsoon to post-monsoon season.

2.6 Land use land cover (LULC)

Land use and land cover (LULC) change is a complex process that can affect erosion and sediment load rates in a watershed. Climate and several human activities are capable of exacerbating LULC change and the dynamics of erosive processes. The studies found that the hydrological cycle and erosion processes are closely connected to land cover changes. Other studies focused on the impact of urbanization on hydrology, reporting that an increase of human settlements causes a decrease in infiltration and an increase in runoff. Few studies have addressed the combined effect of land use and climate changes on hydrology and surface water. Remote sensing data, processed using geographic information system (GIS) software, have proven to be a very useful tool in land use studies, especially to detect, map, and model land cover patterns occurring in a given area over a determined period (Romano et al., 2017).

Remote sensing techniques can be used to investigate the impact of land use/cover change on land surface temperatures (LST). Land-based conventional meteorological stations are not distributed along with wide areas, and therefore, they could not provide sufficient land surface temperature data. Advance and progress in remote sensing technology allowed for highlighting land use/cover change and extracting LST data in high temporal and spatial resolutions from multiple sensors and at different scales. MODIS is one of the recent satellites which was launched in the third millennium and proved to be robust for providing information about the dynamics of the terrestrial system on the earth (Hereher 2017).

Erosion, flood, and overflow events are frequently experienced due to changes in land use in watersheds where human impacts are intensive. It is essential to understand the effects of land-use types on erosion at a watershed scale. This knowledge can then be

used to manage soil and water resources in watersheds better (Guzha et al.,2018). Korkanc (2017) conducted a study to determine the surface runoff and soil loss under simulated rainfall conditions on the plots under different land uses/covers. According to the results of the study, areas where agricultural activities are performed, are the areas with the potential for surface runoff and erosion formation. There are many studies that evaluate the impact of LULC change on various temporal and spatial scales (Fan and Shibata, 2015; Zhou et al., 2013). As a result of anthropogenic activities, there has been a subsequent increase in impervious areas. The LULC leads to the alteration of the water balance of the catchment, with an increase in runoff, decrease in evapotranspiration, and groundwater recharge (Leopold and Dunne 1978). Factors like altitude, slope, distance from the river, type of agricultural practices, type of soil and magnitude of erosion, frequency of drought and flood, population density, and distance from a built-up area affect the rate of LULC change (Lin et al., 2009). The magnitude of impacts depends on several factors like soil depth (FAO 2008), precipitation events (FAO 2008), the spatial layout of deforestation areas (National Research Council 2008), area of the watershed (Biswas et al., 2014), etc.

2.7 Soil erosion

Erosion, which is of global significance, is shown to be one of the most important areal resources of deterioration and pollution in water resources. The average surface runoff, erosion rate, and runoff coefficient are affected by land use/cover changes. Agricultural use, grazing, and the recent abandonment of cultivated land are important causes of erosion and healthy pastureland vegetation, and afforestation works that will provide a good soil cover will reduce the surface runoff and soil loss (Korkanc 2017). The findings obtained from this study will contribute to the studies on the development of watershed management strategies in watersheds, the soil protection, the management of soil and water resources, and the development of adaptation strategies to the climate change since they reveal the hydrological effects of different land uses/cover types and their effects on the surface runoff and soil loss. Not only topography, but climate also has an impact on soil erosion. Investigations conducted using the soil and water assessment tool (SWAT) model and maps of land-use and soil types, together with meteorological data from six gauging stations. Estimation of runoff and sediment yield

under typical rainfall conditions and different land-use scenarios. In all the land-use change scenarios, the value of sediment yield change caused by land-use change increased with rain intensity, while the rate of sediment yield change remained unchanged (Zhang, S. et al., 2017). While evaluating the benefits of soil conservation in different regions, the soil type and rainfall levels need to be taken into consideration. Land Change Modeller (LCM) module to identify transitions from the one land cover type to the other. The model produced a predicted land use map by using Markov Chain analysis. Annual Agricultural Non-Point Source Pollution Model (Ann AGNPS) was used to estimate the effect of the predicted land-use changes on sediment load. Land-use change analysis and erosion modeling, which gives a soil erosion trend in the future (Romano, G. et al., 2017). A rapidly growing population and climate change expected to influence land use and soil sustainability. Considering the effect of these changes in the future, it is necessary to forecast land use patterns and investigate soil erosion scenarios. Revised Universal Loss Equation and Markov Cellular Automata can also be used for the future sediment yield estimation. The land use change from forest area to settlements will be the most significant factor in erosion induced by land use change. Meanwhile, land use change is the only soil erosion risk factor that can be modified by policymakers at reasonable costs and decrease future soil loss by water erosion (Zare et al., 2017).

Gully erosion is one of the major threats for soil as well as for watercourse. Soil conservation strategies have focused more on terracing than on gully control techniques since the contribution of gully sediment yield in the overall soil loss from watersheds is unknown. The different investigations done to quantify the sediment yield provided by head-cut as well as sidewall–floor erosion of first-order gullies. For any period, the two main processes of gully erosion (that is sidewalls-floor and head-cut erosions) increased significantly with the slope gradient. The head-cut sediment yield on steep slope catchments (Slope gradient>15%) was almost three times that of gentle slope (slope gradient<5%) for the 48 years of study. The gully sidewalls–floor sediment yield on a steep slope was almost four times that of a gentle slope. Sidewalls–floor erosion contributed more than head-cut to total gully sediment yield. This contribution was, on average, 81.5% for the gentle slopes and 77.8% for the steep slopes. While total gully

erosion was on average 1.66 m3 ha−1 year−1 for the gentle slopes and 5.603m3 ha−1 year−1 for the steep slopes, these values were derived from the study of micro-catchments, where first-order gully density is relatively higher than in larger watersheds. Therefore, these sediment yield figures should be reduced to smaller values as the watershed area increases (Bouchnak et al., 2009).

2.8 Sedimentation

Sedimentation is the process by which material is transported by suspended in or deposited by streams. Reservoir sedimentation affects the sustainability of hydraulic schemes because of sediment accumulation, which successively reduces the water storage capacity. Thus, in the long-term, reservoir efficiency reduces. Reservoirs are only sustainable if sedimentation is controlled. Hydropower is renewable energy, but reservoir silting up can threaten, especially the use of storage power plants (Jenzer Althaus et al., 2015). Dams and associated reservoirs have notable effects on soil and water dynamics in prairie streams. The simulation module of small dams in the soil and water assessment tool (SWAT) is used to evaluate their long-term effects on streamflow and water quality at a watershed scale. It is important to overcome the challenges in characterizing small storage and short retention time in small reservoir routing. The concepts of equivalent reservoir storage and equivalent reservoir discharge are applied by which the average daily storage and daily discharge of the small reservoirs were calculated. The sediment deposition and nutrient abatement within the reservoir can be computed using available SWAT routines. The Universal Soil Loss Equation (USLE) has been used for the estimation of on-site erosion rates (Rao et al., 2015). The effects of small dams in the reduction of daily peak flow, sediment, and nutrient loads at the watershed outlet are obtained by summing the effects of all small dams within the watershed considering both reservoir and channel processes. The simulation results show that the combined effect of these small dams can reduce daily peak flow by 0–14% at the watershed outlet depending on climate and initial reservoir storage conditions. The on-site effects of individual small dams much higher depending on its size, location, shape, drainage area, and land use compositions in the contribution area(Liu et al., 2014). Small dams are also effective in reducing nutrient loading from agricultural runoff. However, reservoir maintenance, such as dredging, spill

management, and debris cleaning during flood events, is required to ensure proper operation of the small dams and prevent pollution caused by the failure of the small reservoirs (Greg Schellenberg et al., 2017). The impacts due to soil erosion have severe effects on the reservoir as well as river sedimentation and a certain extent on floods. The deposition of detached material takes place when the transport capacity of flow is smaller than the quantity of material being transported. Hence it is concluded that suitable erosion control measures are to be implemented for preventing further negative impacts so that reservoirs can be maintained with their storage capacity and damages due to floods can be minimized (Rao et al., 2015).

SWAT can also be used to identify critical erosion-prone areas based on the average annual sediment yield of each sub-watershed. It is also helpful to select and adopt suitable soil conservation measures to reduce soil erosion. A management plan can be developed to treat the sub-watersheds with conservation practices. These plans will decrease the sedimentation rate and thereby increase the life of the reservoir (Sardar et al., 2014). A modified version of the USLE model used to find out the sediment yield as a function of runoff, whereas USLE estimates the soil erosion from cropland as a function of rainfall energy (Emam et al., 2016).

2.9 SWAT application

Models are important tools to understand hydrologic processes. There are many models that have been developed to simulate the sediment transport and runoff discharge from the watershed as well as to predict the impact of watershed management practices or land-use changes on sediment transport (Zhang et al., 2019). The SWAT (Soil and Water Assessment Tool) (Arnold et al., 1998) model was developed in the early 1990s by the U.S. Department of Agriculture, Agricultural Research Service (USDA-ARS). The detail of the model features, capabilities, scientific details, framework, strengths, limitations, and application history will be described in a later chapter.

The applicability of the Soil and Water Assessment Tool (SWAT) model in estimating daily discharge and sediment delivery from mountainous, forested watersheds and the assessment of the impact of forest cover types on stream discharge patterns and sediment load was carried out in two small watersheds located in lower Himalaya,

India. Results showed the higher ET, lower mean annual surface runoff, lower water yield, and lower sediment yield from the dense forest than that from the degraded forest indicated the effect of forest cover types on these hydrological variables (Tyagi et al., 2014).

The performance of the SWAT model, to some extent, can be affected by the resolution of the time series dataset used in the calibration and validation of the model. In general, the model is known to perform well with monthly data compared to daily data (Jain et al., 2010). The development of the SWAT model was primarily for long periods (2 years and more) simulations. But, this didn't prevent the researchers from applying the model to short simulation periods less than one year. Having a much longer period of daily flow record for both calibration and validation likely would have resulted in better comparisons between recorded and simulated daily flows, because a longer record would not be affected by a few anomalous high values of the discharge as a short record (Saleh et al., 2009).

The SWAT model was applied to simulate the runoff and sediment yield in the Miyun river catchment, China. The physiography of the watershed is characterized by mountain ranges, steep slopes, and deep valleys. The model accurately predicted the daily and monthly runoff and sediment yield with the value of Nash-Sutcliffe efficiency of greater than 0.6 (Xu et al., 2009). The application of the SWAT model to a data-scarce tropical complex catchment showed that the model could be used in ungauged catchments for identifying hydrological controlling factors/parameters. The study also showed that the length of the period of simulation affects the result i.e., the longer the period, the more reliable is the result (Ndomba et al., 2011).

The impact of DEMs generated from different data sources, DLG5m (local Digital line graph, 5m interval), ASTER30, and SRTM90 respectively, on predicting runoff, sediment, total phosphor (TP) and total nitrogen (TN) were studied. The study compared the quality and performance of remote sensing-derived data (ASTER30m, SRTM 90m). The results indicate that SWAT predicted outputs, which were based on ASTER 30m and SRTM90m, were close to each other. Predicted TN based on SRTM90 m provided a little more accurate estimate of the area but a little less accurate estimate of a mean slope than the ASTER 30m (Lin et al., 2010).

The SWAT model was applied to the Lake Tana basin for modeling of the hydrological water balance. The objective of the study was to test the applicability of the SWAT model for the prediction of streamflow in the basin. The model was successfully applied to the basin in simulating the daily and monthly stream flows and found out that the flow was more sensitive to the HRU definition thresholds than the sub-basin discretization effect (Setegn et al., 2008). The impact of the watershed subdivision on the water balance components was studied for Nagwan watershed in eastern India. The result of the study revealed that the number and size of sub-watersheds do not significantly affect surface runoff but had a noticeable effect on other components of the water balance: evapotranspiration, percolation, and soil water content. Therefore, it is possible to conclude that the watershed subdivision affects the water balance in general. The number and size of sub-watersheds for a given catchment depends on the resolution of spatial data used in the model. High-resolution data results in a higher number of sub-watersheds and thereby enhance the water balance prediction of the model (Tripathi et al., 2006).

The SWAT model was applied to the Blue Nile basin, Ethiopia, and found out that the SWAT model incapable of realistically model gully erosion. The study showed that the SWAT model underpredicted the sediment from a basin where gully erosion is high. To compensate for this, the USLE soil erodibility factor (USLE_K) in MUSLE (Modified Universal Soil Loss Equation) was increased (Easton et al., 2010).

Singh et al., (2013) used SWAT CUP software to describe and demonstrate the use of different approaches such as the Sequential Uncertainty domain parameter Fitting (SUFI-2), Generalized Likelihood Uncertainty Equation (GLUE) for stream-flow measurement and best parameter estimation for stabilizing the correlation between the simulated parameters and observed parameters. Laouacheria and Mansouri (2015) used the Watershed Bounded Network Model (WBNM) and Hydrologic Engineering Center-Hydrologic Modeling System (HEC-HMS) hydrological models to predict the runoff hydrographs of urban catchments and also evaluated the effect of parameters on the shape of the runoff hydrograph. It was inferred that catchment size did not affect the routing calculations, but it had a direct influence on the unit hydrograph.

2.10 Studies carried out on Kali river

Manjunathaa et al., (1996) carried research on transport of elements from soils around Kaiga to the Kali River, southwest coast of India. They investigated the behaviour of alkali, alkaline earth and transition elements during weathering, their consequent delivery into the adjoining river system and their surficial and sub surficial distributions in the soils around Kaiga, In 1997 investigation carried out by Department of Marine Biology Karnataka University P.G. & Research centre, Karwar Karnataka state and published a report on Hydrobiological studies of Kali river before the construction of Kadra reservoir and commissioning of Kaiga atomic power plant Funded by Nuclear power corporation Mumbai. They established the spatial and temporal variation of the following factors in the Kali River during the pre-construction period of Kadra dam and pre-operational period of the Kaiga Atomic Power Plant. a. Hydrological parameters b. Sedimentological parameter.

During the pre-construction period of Kadra dam and pre-operational period of the Kaiga Atomic Power Plant. Recorded the composition and distribution of the following biotic elements Such as Microorganisms of water and sediment, Phyto and Zooplankton, Benthic meio and macrofauna, Fish fauna in the Kali River;

Yadav et al., (2008) studied the ecological Status of Kali River Flood Plain, mainly concentrated on Western Ghat biodiversity. Vipin and Jayappa (2011) worked on Hypsometric analysis of Kali River Basin, Karnataka, India, and using geographic information systems. The hypsometric analysis provides valuable information on landform evolution and tectonics. Their study was limited to the evaluation of hypsometric parameters which provided valuable information on the type of erosive processes operating in the Western Ghats regions. Vipin and Jayappa (2016) estimated Soil loss and prioritization of sub-watersheds of the Kali River basin using the Revised Universal Soil Loss Equation (RUSLE) model and GIS. But they have not validated model results due to lack of direct field measurements of soil erosion. Further monitoring sediment load in the river basin and measurement of sediment deposition in reservoirs that exist in the watershed is necessary to estimate they suggested.

The present study is to know the impacts of these dams on the river hydrology, sediment flow, and how it is affecting coastal regions such as estuary and shoreline. The findings

of this study will be useful in the water resource department and coastal engineering and management since such studies are not conducted so far for this study area.

2.11 Summary and research gaps

There is extensive literature available for the impacts of dams, sediment analysis at the estuary, and shoreline change detection. Many studies had been carried out throughout the world for the following mentioned aspects. But in the context of sediment characteristics, there is less research work present which links from the trapping of sediments behind the dams to estuary and shoreline change.

Based on the literature review, the following research gaps in the area of river sediment on estuary and shoreline change are drawn.

1) Limited studies were carried out on the impact of dams, which are restricted to the downstream channel, trap of sediments behind the dams, and hydrological regime. Major studies are required in shoreline change concerning the impact of dams.

2) In estuary region, studies were carried out on sediments that occur in that region only such as metal contamination, suspended sediments, bed loads, and change detection of estuary due to wind, wave, and tidal inlets, respectively. Minimal studies carried out which links between changes of the estuary to the shoreline change analysis.

3) Shoreline change detection was carried out by considering wind, wave, tides, HWL, MWL, LWL, sediment transport, which present on shoreline respectively, and different type resolution data with RS and GIS techniques used. But rarely river sediment parameters had been considered.

4) Statistical, mathematical, computational modeling, and simulation studies were carried out. All these studies were limited to the impact of the dam, estuary, and shoreline changes separately. The combined study of the impact from the above factors is not yet considered for the research in India.

2.12 Scope of the work

Karnataka is a state in the southwestern region of India, which is bordered by the Arabian Sea on the west coast. Karnataka is the eighth largest state by population.

Karnataka's coastline extends over a length of 320km. It is one of the most intended shorelines with numerous river mouths, lagoons, bays, creeks, promontories, cliffs, spits, dunes, and long beaches. Unlike the east coast of India, the coastal stretch of Karnataka has no major delta formation. The shelf of Karnataka has an average width of 80 kilometers, and the depth of the shelf break is between 90 and 120 meters. There are a few islands off the coast, the major group being St. Mary's island, 4 kilometers off the coast near Malpe. Fourteen rivers drain their water, the shore water of Karnataka. The important estuaries include the Netravati-Gurpur, Gangolli, Hangarkatta, Sharavati, Aganashini, Gangavali, and Kali. Sand bars have developed most of the estuaries. There are a number of barrier spits at Tannirbhavi, Sasithitlu, Udyavara, Hoode, Hangarkatta, and Kirimanjeswara formed due to migration of coastal rivers. There are also 90 beaches with varying aesthetic potential. Among these beaches at Someshwar-Ullal, Malpe, St. Marys Island, Belekeri, and Karwar excellent with a potential for international tourism. Twenty-two beaches are classified as unfit for use due to coastal erosion, human settlements, and activities linked to ports and harbours, industries and fisheries.

The coastal zone is relatively poor with respect to mineral wealth. The fresh deposits lime shell in the backwater of Kali, Gangavalli, Aghanashini, Sharavathi, Gurpur, Pavanje, and Mulki declining as 90 percent of claims are harvested every year. About 50 percent of the area under coastal zone (4,90,000 hectares) is subjected to moderate soil erosion and 6 percent of the area (56,000 hectares) to severe soil erosion. These erosions may be the insufficient sediment flow from the river through dams.

Kali River and its estuary become much more complicated when its river system and estuarine topography are taken into consideration. It is found that the north split of the Kali River has shifted 109.41m to the north. The northern part near river mouth shows an accretion of 0.1758km^2 and erosion of 0.08km^2, whereas the southern part is accreted by 0.1086km2, no erosion found about 1.2km (Choudhary et al., 2013). Kali River consists of 5 reservoirs before it joins the Arabian Sea. Therefore, it is clear that as the amount of sediment discharge into the sea continues to decline due to the construction of the dam, an assessment of shoreline behaviour on a finer spatial and temporal scale is essential to gain a comprehensive understanding of the evolution of the entire Kali River estuary region.

The present study was carried out to analyse erosion and accretion, using layer stack processed for Landsat MM, Landsat 4-5, Landsat-7 ETM+, and Landsat-8 images data for the years 1975-2017. For Landsat-8 image for May and October, which is for Pre-monsoon and Post-monsoon. An extension of ArcGIS®, Digital Shoreline Analysis System (DSAS) tool, version 4.3 (April 2012), has been used for the analysis of shoreline changes of Ravindranath Tagore beach and Devabagh beach area. The erosion and accretion depend on sediment supply. Dams trap these sediments; the present study area has a series of dams, starting from Supa dam, Bommanahalli dam, Tattihalla dam, Kodasalli dam, and Kadra dam. Therefore, it is essential to find the shoreline configuration keeping in view of pre-construction dam and post-construction of the dam. How seasonal variation acts on shoreline configuration. The change detection at Kali estuary due to disturbed sediment supply, effect of construction of dam on sediment yield at the downstream, impact of sediment supply on dynamics of beach face sand beach nourishment and also to find sediment transport around the shoreline.

2.13 Objectives

The present study is planned to address the following issues:

1) To study the long-term shoreline configuration with respect to the pre-construction dam and post-construction of the dam.

2) To study the seasonal variation on shoreline configuration.

3) To study the Kali estuary, change with the response to sediment.

4) To assess the impact of the dam on sediment yield.

5) To understand the sediment dynamics of beach face sand using the granulometric method.

6) To quantify the seasonal coastal process in terms of beach sand volume.

CHAPTER 3

3 MATERIALS AND METHODOLOGY

3.1 Kali river basin

The study area, Kali river basin (Fig.3.1) lies between 74° 05' 7.63" to 74° 57' 39.05" East longitude, and 14° 43' 11.8" to 15° 33' 44.9" North latitude and the river basin spreads over an area of 4943.43 sq. Km. And covers the entire taluks of Supa, Haliyal, Karwar, and partially covers the districts of Ankola and Yellapur from the Uttara Kannada district. Annual average rainfall measured was found to be 3200 mm. The river runs 184 kilometres before reaching the Karwar beaches and joins the Arabian Sea west coast of India. Figure 3.1 shows the details of shoreline and area of interest.
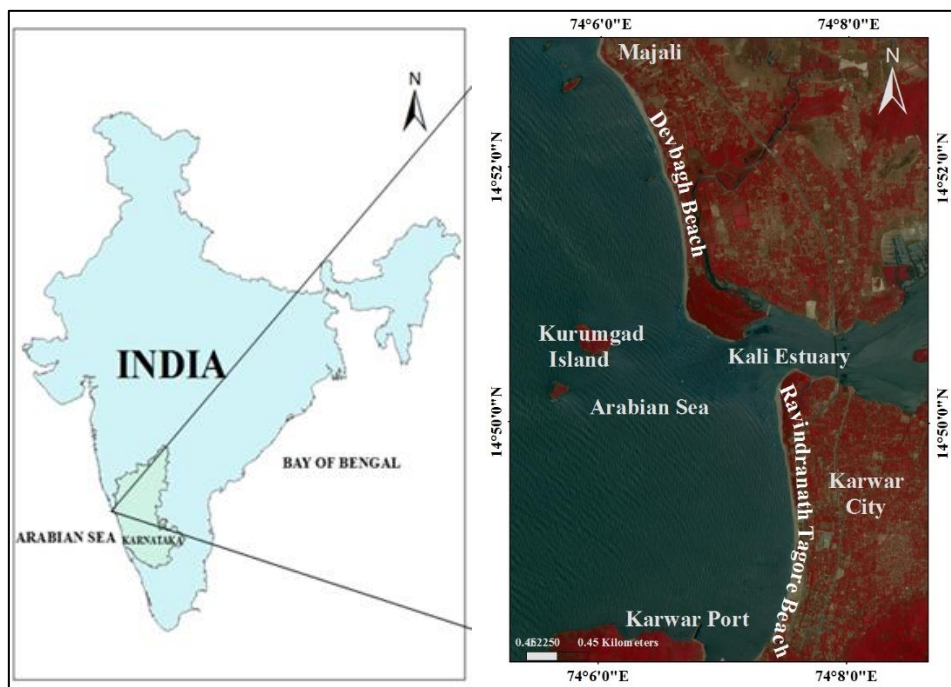
Figure 3.1 Location of the Study Area, Shoreline of Karwar Coast

Red soil, Lateritic soil, and black soil are the types of soils present in the study area (National Bureau of Soil Survey and Land Use Planning – NBSSLUP). The elevation of the study area varies between 1-1037 m above the mean sea level.

In this Kali river basin, there are five major hydroelectric dams have constructed over the 32,000 acres of the rich forest area of Western Ghats of India. The Supa dam built-in 1985 is one of the biggest dams across Kali river. The other dams across Kali River

are Kodasalli dam, Kadra dam, Tattihalla dam, Bommanahalli dam. The five dams, when to work together, generate electricity of 1200 MW. Moreover, the Kaiga power plant generates an additional 400 MW. The location of all the dam is shown in   Figure 3.2. The river is a lifeline for nearly 4 lakh people in the district, and it supports the livelihoods of thousands of people on the coast of Karwar. Untreated effluents from the industries are released directly into the river, and improper sand mining in the Supa Dam region resulted in hazardous disturbances to the river's ecology.
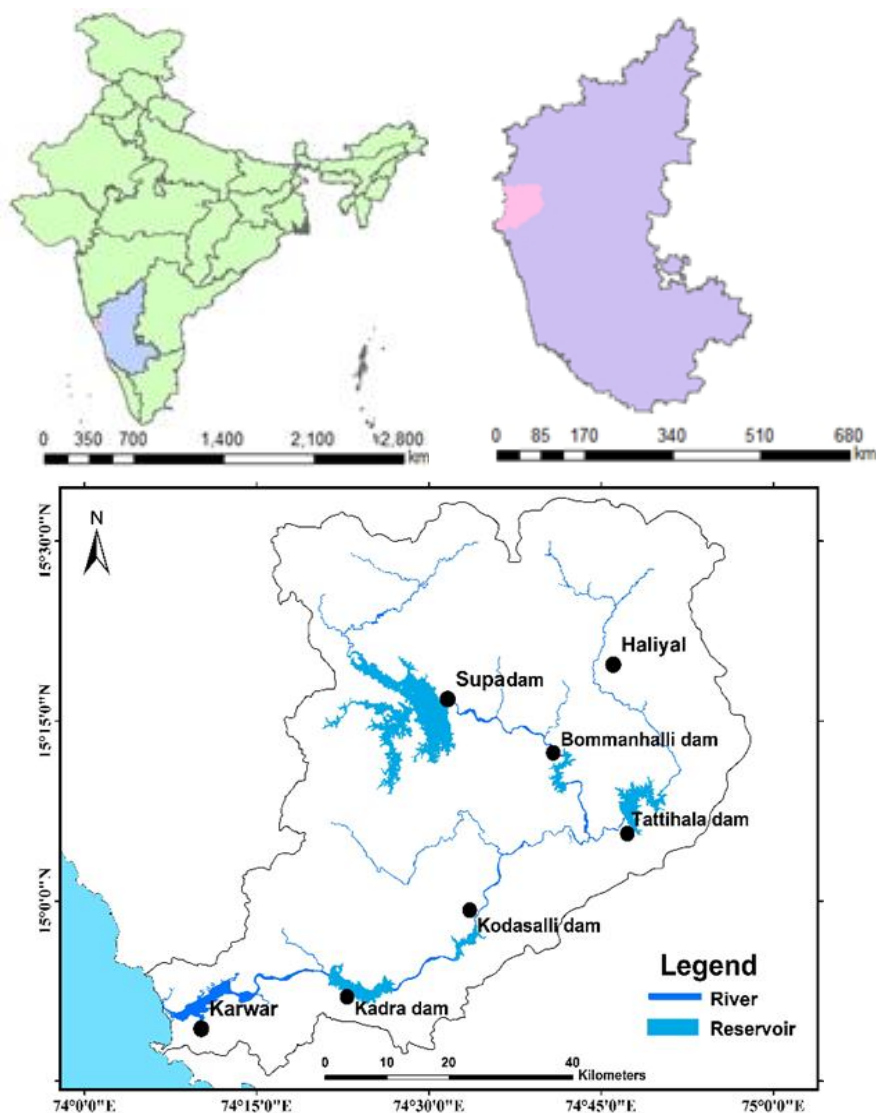
Figure 3.2 Location of the study area, Kali river basin

Kali river basin does not contain any CWC observation station for streamflow and sediment, but it includes a series of the reservoir with inflow and outflow data (KPCL Ganeshgudi).

3.2 Aghanashini river basin
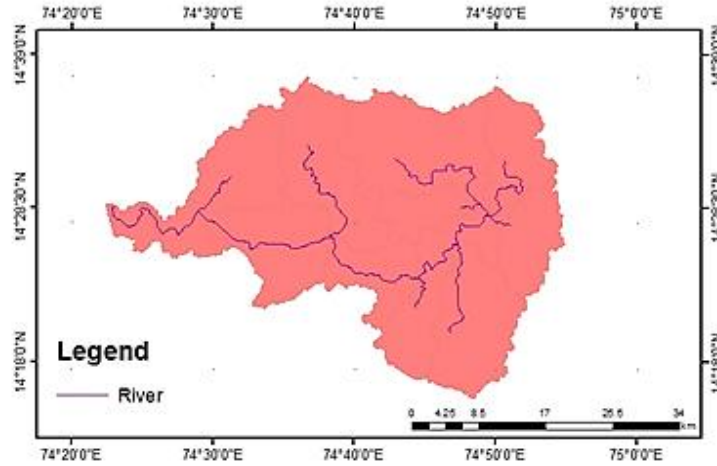
Figure 3.3 Location of Aghanashini river basin

River Aghanashini (Figure 3.3) located at 14.52116°N and 74.36432°E, which originates at Manjguni of Sirsi taluk. It flows about 127 km before it joins with the Arabian Sea at Belekan, Kumta. Catchment spreads about 1149 sq. Km is distributed across taluks of Kumta, Sirsi, Siddapur, Honavar, Ankola.
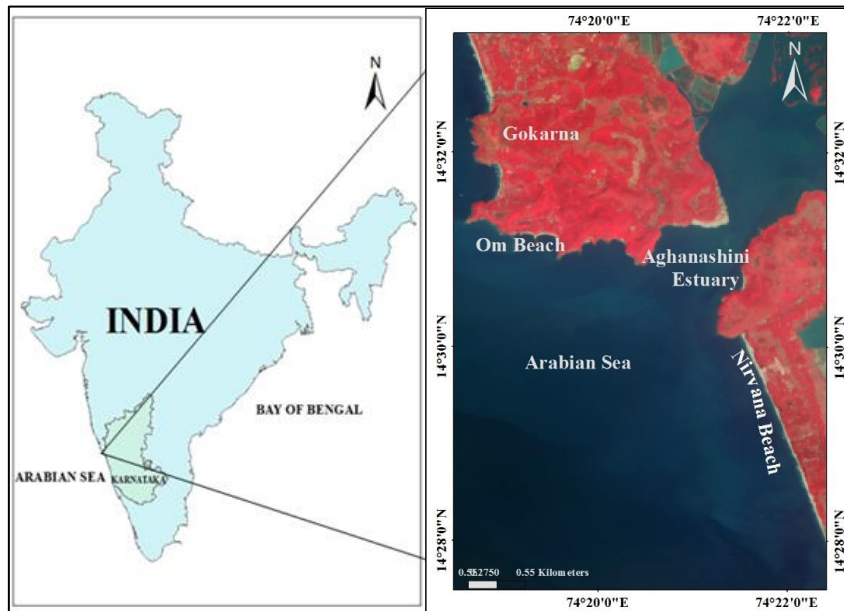
Figure 3.4 Location of Aghanashini Coast

The average annual rainfall measured was found to be 3500mm. Figure 3.4 gives the details of the shoreline related to the Aghanashini river.

Aghanashini river has a natural, unobstructed flow of water that carries the natural sediments and supplies to the Arabian sea coast through its estuary (Ramachandra et al., 2018).

3.3   Data products and data source

Geometrically corrected and orthorectified Landsat MSS (Multispectral Scanner System), Landsat 5, Landsat-7 ETM+ (The Enhanced Thematic Mapper Plus), The Operational Land Imager (OLI) and Thermal Infrared Sensor (TIRS) Landsat-8 satellite data set have used for shoreline analysis studies of Devbagh beach and Ravindranath Tagore beach. The information about satellite data and other data sets used are provided in Table 3.1 and Table 3.2, respectively.

Table 3.1 Details of Satellite data

Sl No.	Satellite & Sensor	Acquired date	Acquisition time (+/- 15 minutes)	Path / Row	Resolution (m)
01	Landsat MSS	06/05/1975 to 21/10/1980	10.11 am	146/50	30
02	Landsat-5	21/12/1989 to 30/12/1998	10.11 am	146/50	30
03	Landasat-7 ETM+	07/11/1999 to 20/12/2009	10.11 am	146/50	30
04	Landsat-8 OLI/TIRS	13/05/2013 to 08/05/2017	10:11 am	146/50	30

Table 3.2 Data type and its sources

Data	Description	Source
DEM	SRTM DEM 30 m resolution	https://earthexplorer.usgs.gov/
Land use	Landsat (30 m × 30 m)	https://earthexplorer.usgs.gov/
Soil	Description of soil types (1 km×1 km)	Food and Agriculture Organization (FAO)
Meteorological Data	Daily data	Indian Meteorological Department, India
Streamflow Data (For Aghnashini River)	Daily data	Santeguli, Kumta Taluk , Uttara Kannada West flowing rivers from Tapi to Tadri Karnataka Lat, Long -14.4344, 74.5889 Central Water Commission, India http://indiawris.gov.in/wris/#/DataDownload
Reservoir operational data	Daily Data	Karnataka Power corporation Limited, Ganeshgudi

3.3.1 Reservoir operation data

There are five dams built across the Kali river, starting from Supa dam (Table 3.3), Bommanahalli dam(Table 3.4), Tattihalla dam(Table 3.6), Kodasalli dam(Table 3.5) and Kadra dam (Table 3.3). The inflow and outflow details of the dam operations are needed as an input for SWAT to carry out the analysis.

Table 3.3 Supra and Kadra Dam Discharge data

Supa Dam Discharge data			Kadra Dam Discharge data		
Years	Cum inflow (M Cum)	Cum Discharge (M Cum)	Years	Cum inflow (M Cum)	Cum Discharge (M Cum)
1995-96	2031.37	2893.68	1997	3309.35	3960.45
1996-97	2091.75	2083.49	1998	1452.89	1413.52
1997-98	3197.97	2935.71	1999	5601.15	4778.95
1998-99	2033.19	2223.4	2000	5246.81	5185.47
1999-00	3311.71	3244.19	2001	4523.62	4613.96
2000-01	2702.1	2690.92	2002	3663.37	3539.05
2001-02	2008.02	2495.95	2003	3501.87	3225.7
2002-03	1915.98	1967.08	2004	3488.65	3970.29
2003-04	1909.42	1768.46	2005	5526.07	4426.56
2004-05	2314.26	2285.84	2006	7385.98	7360.21
2005-06	3379.86	2346.76	2007	8878.63	6848.34
2006-07	3853	4370.93	2008	6154.3	6110.9
2007-08	3252.38	3585.07	2009	5036.83	4982
2008-09	2908.24	2943.18	2010	4431.46	4318.22
2009-10	2661.83	2636.2	2011	6588.34	6499.15
2010-11	2412.48	2323.49	2012	4421.91	4423.48
2011-12	3624.26	3717.33	2013	5156.93	5253.12
2012-13	2481.98	2142.62	2014	6104.06	6081.1
2013-14	3538.26	3106.61	2015	3794.23	4290.92
2014-15	2994.94	2769.17	2016	2502.29	2466.38
2015-16	1508.86	2065.61	2017	3828.44	2633.57
2016-17	1830.22	1504.31			

Table 3.4 Bommanahalli Dam Discharge data

Years	Cum inflow (M Cum)	Cum Discharge (M Cum)
2008	2096.15	2170.82
2009	3108.48	3091.86
2010	2975.25	3276.23
2011	4219.59	4316.01
2012	3193.14	5297.79
2013	3184.01	3201.73
2014	4725.76	4879.42
2015	2895.48	2881.69
2016	1719.72	1750.45
2017	1214.49	1059.41

Table 3.5 Kodasalli Dam Discharge data

Years	Cum inflow (M Cum)	Cum Discharge (M Cum)
1999	3232.88	3112.94
2000	3817.74	3661.33
2001	4094.84	3989.18
2002	2915.62	2930.77
2003	2578.35	2565.52
2004	2805.03	4461.51
2005	3547.44	3510.14
2006	6095.75	6129.4
2007	5569.6	5575.11
2008	4942.17	4905.18
2009	3996.82	4003.76
2010	3377.52	3373.11
2011	5071.95	5021.73
2012	3436.88	3567.67
2013	3936.4	4018.22
2014	5098.51	5062.75
2015	3000.53	2974.96
2016	1870.3	1871.55
2017	2024.83	2841.57

Table 3.6 Tattihallai Dam Discharge Data

Years	Cum inflow (M Cum)	Cum Discharge (M Cum)
2008	196.71	78.5
2009	259.42	331.82
2010	208.35	47.81
2011	298.76	267.73
2012	72.06	164.28
2013	168.02	163.62
2014	226.57	217.7
2015	39.28	111.89
2016	29.26	33.02

3.4   Collection and location of beach face sediment data

The granulometric analysis is carried for beach face sediment. The samples were collected from the Devbag beach and the Ravindranath Tagore beach. The location of the beach face sediment is listed below in Table 3.7

Table 3.7 Beach Face Sediment Sample Locations And Period Of Data Collection

Sl. No	Sample Station	Latitude	Longitude	Period of data collection
1	RT 1st point	$14^0 48'42''$N	$74^0 07'32''$E	26/10/2017, 31/3/2018, 29/01/2018 and 26/5/2018
2	RT Middle Point	$14^0 49'35''$N	$74^0 07'31''$E	
3	RT Estuary	$14^0 50'24''$N	$74^0 07'35''$E	
4	Devbagh Estuary	$14^0 50'40''$N	$74^0 07'12''$E	
5	Devbagh Middle Point	$14^0 51'50''$N	$74^0 06'33''$E	
6	Devbagh Endpoint	$14^0 52'50''$N	$74^0 05'59''$E	

3.4.1 Field visit

Figure 3.5 (a) Plate 1, (b) Plate 2, (c) Plate 3, (d) Plate 4, (e) Plate 5 and (f) Plate 6

Figure 3.6 (a) Plate 1:Kali River Estuary, (b) Plate 2: Sand Sample, (c) Plate 3: Acquiring GPS point and (d) Plate 4: Sand sample

The above Plate from plate 1 to plate 4 were photos of Ravindranath Tagore beach during the field visit. It clears that it contains Mangrove forest, cliffs, and vegetation line. Sand samples collected with GPS points for the analysis of grain size distribution analysis. Plate 1 is the collection point at Kali river estuary; Plate 2 is a collection of the sand samples; Plate 3 is the collecting GPS of the sample point.

3.5 Methodology

The coastal zone one of the important sources of the economy of the country. It plays a major part in the development of the nation and coastal protection. Sediments from the river which are available from estuary are responsible for beach nourishment. Estimation of sediment yield, shoreline change detection, seasonal wise variation, coastal process, beach profile, effects of pre-construction of the dam, post-construction of dam, and mapping and analysis rate of change of shoreline are foremost activities. There are many conventional, remote sensing, and GIS technique options that are available to study the shoreline configuration in the coastal zone. In the present study, the shoreline change rate analyzed by considering the pre-construction of the dam, post-construction of the dam. Remote sensing provides historical, decadal data and database so that that analysis can be carried out. Conventional methods of collection of data provide ground truth data, which are accurate, less error, but requires laborious work and time-consuming. But remote sensing provides repetitive, inaccessible, and larger data.

Further analysis can be carried out within less time. At present remote sensing techniques are largely used to study shoreline configuration. This chapter explains the data and methodologies developed to address the established objectives for the present study.

3.6 Shoreline analysis

Shoreline analysis was carried for 42 years (1975-2017), which is regarded as long-term analysis and also carried out for short-term of 5 years analysis (2013-2017). Landsat MMS, Landsat-4 & 5, Landsat-7 ETM+, and ortho-rectified satellite images of the study area from the sensors Landsat-8 were collected from USGS Earth Explorer web tool. The tidal range along the study region is about 1.5 m, and the submergence of the land associated with the high tide period is less than 5-6 m (Hegde and Akshaya, 2015). Hence no additional corrections are undertaken for the delineation of shoreline other than approximately common acquisition time and period of the year. Flow chart of shoreline analysis is shown in Figure 3.7and Figure 3.8
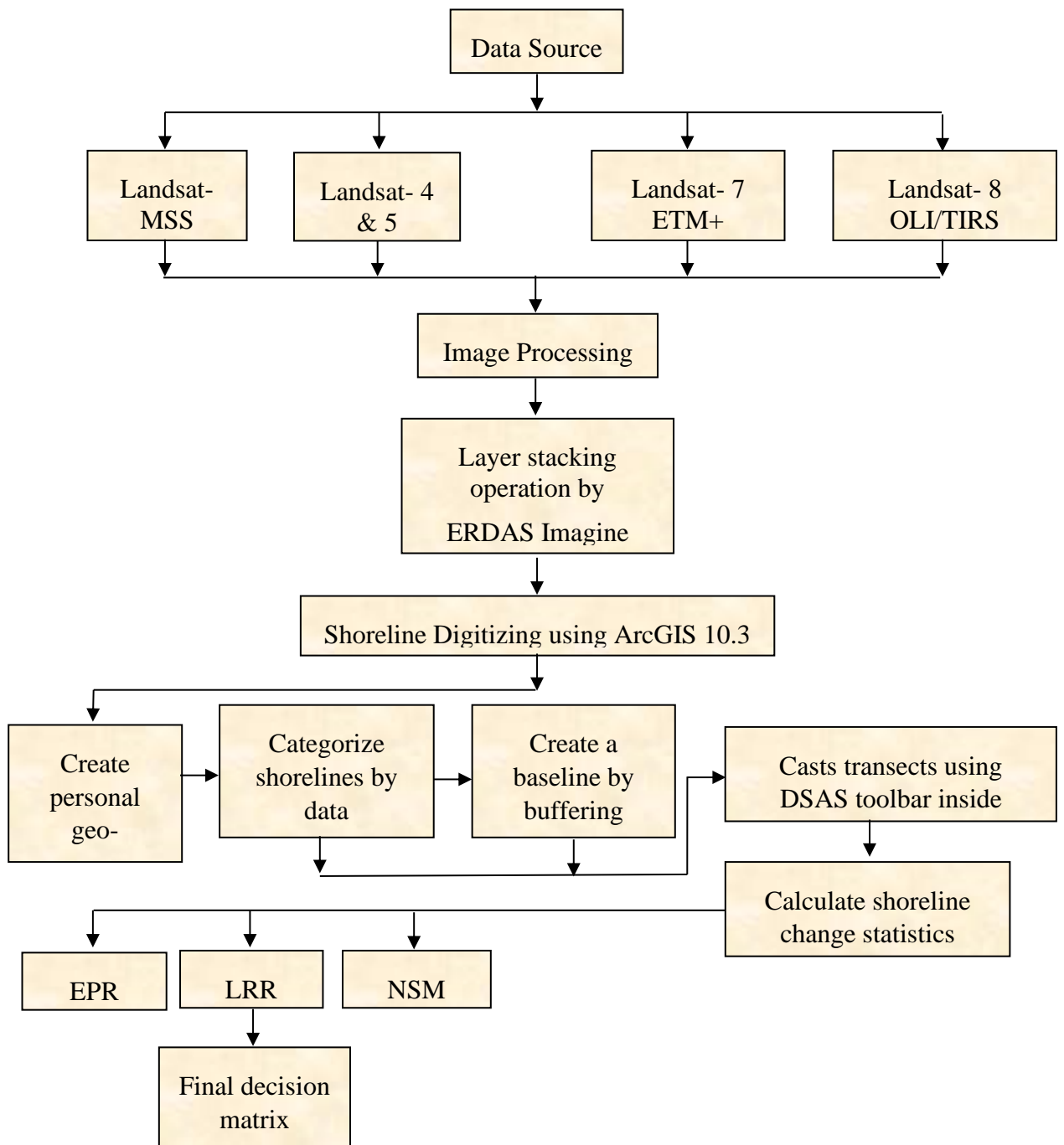
Figure 3.7 Flowchart of the Entire Methodology of Shoreline Change Analysis
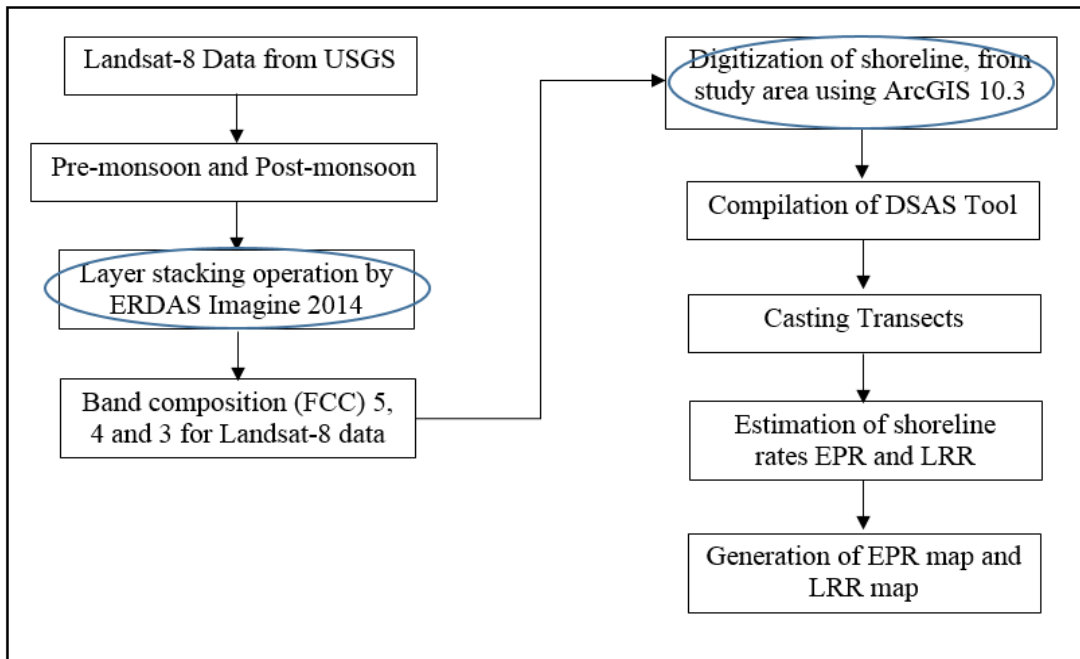
Figure 3.8 Flow chart of shoreline analysis for Pre and Post-monsoon season

3.7 Image processing

The geocoded Landsat-8 satellite images acquired, undergone for spectral pre-processing. Layer stacking method (Layer stacking is a process for combining multiple images into a single image. In order to do that, the images should have the same extent (number of rows and number of columns), which means you will need to resample other bands that have different spatial resolutions to the target resolution. In other words, all images/bands should have the same spatial resolution to be able to perform layer stacking. The layer stacking was applied for all the bands of the Landsat satellite data. It was further adapted into a False Colour Composite (FCC) for bands 5, 4 and 3 of Landsat 8 satellite image using the ERDAS Imagine 2014 tool and projected to Universal Transverse Mercator (UTM) with reference to WGS 1984 UTM zone 43N datum. Further, the nearest neighbour interpolation method applied for resampling of the input satellite images using the ERDAS imagine 2014 tool. The resampled size was 30m, which is a pixel size of Landsat-8.

3.7.1 Shoreline extraction

The shorelines datasets from the Landsat-8 satellite images from 2013-2017 were extracted using ArcGIS® 10.3 tool. Using the manual digitization extraction method in the ArcGIS® 10.3 tool, a high water line boundary was demarcated as shoreline proxy.

3.7.2 Shoreline change analysis

The digitized shorelines were superimposed, and erosion/accretion rates were calculated at 50m intervals by casting transects along Devbagh beach and Ravindranath Tagore beach using Digital Shoreline Analysis System, an ArcGIS® extension introduced by USGS. Before casting of transects by DSAS, it asks to load digitized shoreline and baseline with proper attribute data. In this present study, shoreline and baseline were kept approximately about 100m distance apart. These transects were connecting baseline and shorelines in the perpendicular direction. DSAS includes several statistical methods that were automatically generated, such as Shoreline Change Envelope (SCE), Net Shoreline Movement (NSM), EPR, LRR, WLR, and Least Median of Squares (LMS). Frequently EPR or LRR being used for erosion and accretion calculation (Natesan et al., 2015). To estimate the change of rates and to compute the movement of shoreline, LRR statistical approach has been applied normally. EPR considers earliest and latest shoreline measurements, it is calculated by taking the ratio of the distance of shoreline movement to the time elapsed between those two measurements and LRR considers all the shoreline, it can be estimated by fitting a least-squares regression line to all shoreline points for a particular transect obtained from the analysis. In this analysis, shoreline changes were determined by two statistical computation, such as EPR and LRR.

3.7.3 Calculation of rates of erosion and accretion

There are a few information investigation methods that can be utilized to figure shoreline erosion and accretion rates (Theiler et al., 2009). Present examination, shoreline change positions are figured using four information investigation methods. The End Point Rate (EPR) is basically completed through partitioning the separation

isolating the two shorelines in the quantity of time duration (Eq. 1). This is the most common basic strategy to figure shoreline development rates, and it is generally utilized by various seaside specialists (Ford 2013).

$$EPR= (D_1-D_2)/(T_1-T_0) \qquad\qquad (3.1)$$

Where:

D_1 and D_2: the distance between the shoreline and baseline.

T_0 and T_1: the period (days or years) of the position of two shorelines.

Linear Rate Regression (LRR) is the second technique utilized for computing erosion rates. This technique comprises fitting a minimum squares relapse line to different positions of shoreline, focusing on a specific transect (Theiler et al., 2009). The shorelines are crossed by transects and establishing the linear regression equation given by (Kermani et al., 2016) (Eq. 2)

$$Y= mX + c \qquad\qquad (3.2)$$

Where (Y) denotes the length of the space from baseline, in meters, (X) duration (years), (m) represents the rate of change in shoreline, and (c) represents Y-intercept (Kermani et al., 2016).

3.8 Types of uncertainty

There are two types of uncertainty: positional uncertainty and measurement uncertainty (Fletcher et al., 2011). Five primary sources of error were evaluated in detecting shoreline positions used for this study, namely seasonal error, tidal fluctuation error, digitizing error, pixel error, and rectification error (Fletcher et al., 2011; Romine and Fletcher 2012).

3.8.1 Positional uncertainties

It is including errors related to seasons, tides, and T-sheet HWL-to-LWM shoreline conversions, which are related to all phenomena that reduce the precision and accuracy of defining a shoreline position in a given year. These uncertainties mostly on the nature

of the shoreline position at the time an aerial photo/satellite image were captured. (Fletcher et al., 2011).

3.8.2 Seasonal error (E_s)

It is the error from movements in shoreline position (seasonal shoreline fluctuations) under the action of the waves and storms. Because seasonal change is cyclical, the probability of a photograph depicting a summer shoreline is equal to the probability of a photograph depicting a winter shoreline. Therefore, a uniform distribution is an adequate approximation of seasonal uncertainty. Generally, the mean and standard deviation of seasonal changes were calculated from the absolute values of differences between summer and winter shoreline positions. The standard deviation of the distribution is the seasonal error (Fletcher et al., 2011).

3.9 Tidal fluctuation error (E_t)

It is the error associated with horizontal variability in shoreline position due to tides. Like seasonal error, a uniform distribution is an adequate approximation of tidal uncertainty. A uniform distribution is generated that incorporates the mean and two times the standard deviation as the minimum and maximum values. The tidal error is the standard deviation of the distribution. (Fletcher et al., 2011).

3.9.1 Measurement uncertainties

They are related to shoreline digitization, image resolution, and image rectification. For photos, measurement uncertainty is associated with the orthorectification process and onscreen delineation of the shoreline.

3.9.2 Digitizing error (E_d)

It is the error related to shoreline digitization; one analyst digitizes the shorelines for all satellite images to eliminate the possibility of different interpretations by multiple analysts. The error is the standard deviation of the differences (distances) between

repeated digitization by several analysts. (Fletcher et al., 2011). The digitizing error was estimated about ± 4.5 m (Romine and Fletcher 2012).

3.9.3 Pixel error (E_p)

It relates to image precision (resolution). It is the pixel size of the image. The pixel size in orthorectified images is 0.5 m, which means that any feature smaller than 0.5 m cannot be resolved (Fletcher et al., 2011). The Landsat image pixel size is 30m. The graphic restitution of the coastline reveals a maximum deviation of ± 2 pixels (Courtaud 2000).

3.9.4 Rectification error (E_r)

It is calculated from the orthorectification process. Aerial photographs are corrected, or rectified, to reduce displacements caused by lens distortions, refraction, camera tilt, and terrain relief using the PCI ortho engine (http://www.pcigeomatics.com/pdf/TrainingGuide-Geomatica-OrthoEngine.pdf). The RMS values calculated by the tool are measures of the offset between points on a photo and established GCPs. The rectification error is the RMS value. It is the square root of the mean error of the image rectification process (Fletcher et al., 2011; Romine and Fletcher 2012).

3.9.5 Total positional uncertainty

The total positional uncertainty (U_t). It is defined as the square root of the sum of the squares of the sources of previous errors (Fletcher et al., 2011; Romine and Fletcher 2012). It was calculated using (1):

$$U_t = \pm\sqrt{E_s^2 + E_t^2 + E_d^2 + E_p^2 + E_r^2} \qquad (3.3)$$

Where E_s is the seasonal error, E_t is the tidal error, E_d is the digitizing error, E_p is the pixel error, and E_r is the rectification error.

The annualized uncertainty (U_a) is the uncertainty in the rate-determining model (error for the shoreline change rate) (Addo et al., 2011; Fletcher et al., 2011). The shoreline

change rate is expressed in m/yr. It was calculated as the square root of the sum of the squares of total positional uncertainty for each shoreline divided by the analysis period, as in (2) (Fletcher et al., 2011)

$$U_a = \frac{\pm\sqrt{\sum_1^n U_{ti}^2}}{T} \qquad (3.4)$$

Where i is an index of the shoreline, U_{ti} is the total positional uncertainty for each shoreline i, and T is the period of analysis. From error calculation, the error was found to be ± 3.98 m/yr.

3.10 Tools used

In order to extract the shoreline from the satellite image, the present study adopted Earth Resources Data Analysis System (ERDAS) Imagine 9.2, a digital image processing software, ArcGIS® 10.3, GIS software and Digital Shoreline Analysis System (DSAS) 4.3, a GIS tool for shoreline change rate analysis. ERDAS IMAGINE is the image processing software, which is designed for the purpose of accessing, interpreting, and analyzing multispectral satellite imagery. It has a wide range of features for enhancing and manipulating a large number of image files. It also enables to develop new models for satellite image processing based on earth applications.

ERDAS Imagine includes an innovative set of tools for extraction of earth surface features and allows geospatial data layers to be created and maintained through the use of remotely sensed imagery. In ERDAS Imagine, satellite remotely sensed imagery and geospatial data of all categories' Earth application could be analyzed to produce GIS-ready mapping.

GIS is an information system used to store, retrieve, manipulate, and analyze geographically referenced or geospatial data. DSAS is a GIS software tool, used to calculate the rate-of-change statistics from multiple significant shoreline positions (Thieler et al., 2005). DSAS computes the shoreline movement and its changes through statistical methods such as End Point Rate (EPR), Linear Regression Rate (LRR), Net Shoreline Movement (NSM), Weighted Linear Regression Rate (WLR), Shoreline

Change Envelope (SCE), Least Median of Squares (LMS) and Jackknife (J). The SCE and NSM report a distance, not a rate. The SCE represents the total change in shoreline movement for all available shoreline positions and is not related to their dates. The NSM is associated with the dates of only two shorelines. The NSM represents the total distance between the oldest and youngest shorelines.

3.11 Estuary change analysis

The study area includes the Kali river estuary. Both RT beach and Devbagh beach is separated by the Kali river estuary. From the historical satellite image, it is shown that estuary belongs to Devbgh beach, i.e., northern side of Kali river estuary experienced erosion and some area has vanished. Further to quantify the change in the estuary area, the area change analysis has been carried out using Landsat satellite image (1976-2018). Landsat 5, 7, and 8 level 2 data are used. This is available as corrected errors of radiometric and geometric correction, and ERDAS imagine tool has been used for image processing. The steps of change detection analysis are as shown in Figure 3.9.
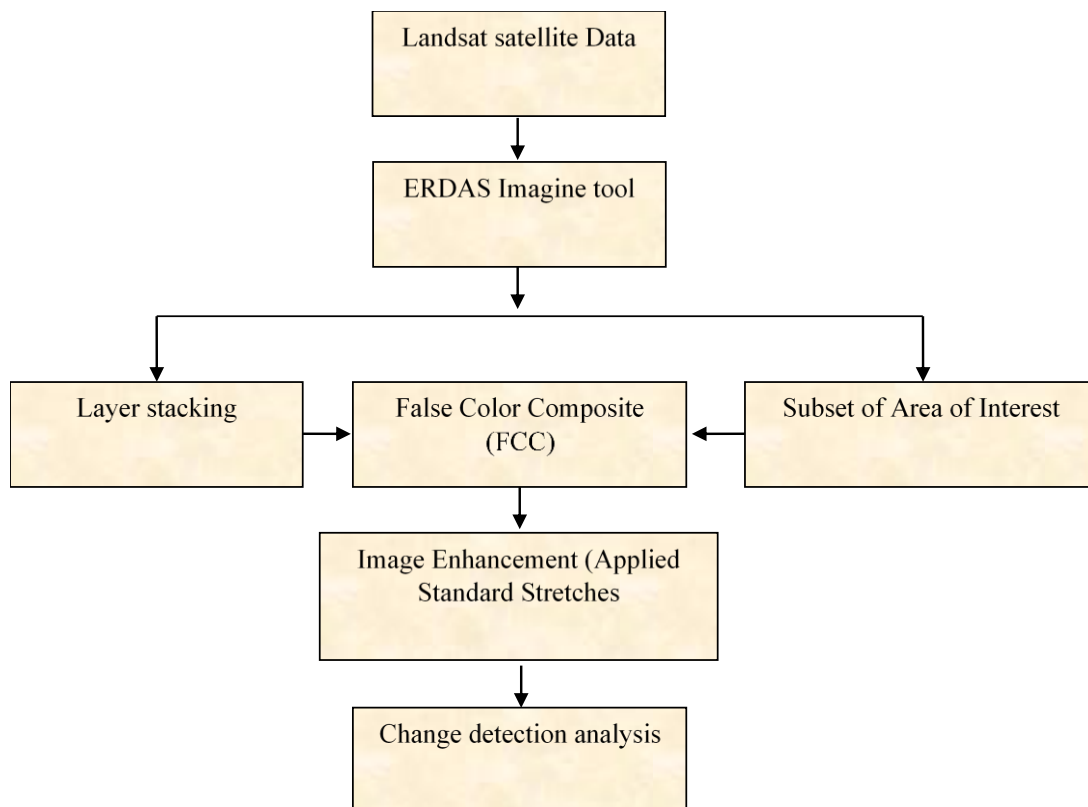
Figure 3.9 Flow Chart of Estuary Change Detection Analysis

3.12 Hydrological model

Hydrological models are tools that describe the physical processes controlling the transformation of precipitation to stream flows. The focus of these models is to establish a relationship between various hydrological components such as precipitation, evapotranspiration, surface runoff, groundwater flow, and soil water movement (infiltration). These models range from simple unit hydrograph-based models to more complex models that are based on the dynamic flow equations. Three different categories of hydrological models can be distinguished: physically process-based, empirical and statistically based. The best model is the one that gives results close to reality with fewer parameters and model complexity. The important inputs required for all models are rainfall data and drainage area and also watershed characteristics like soil properties, vegetation cover, and watershed topography and soil moisture content.

3.12.1 Software used

Various software used for this research work is Arc-GIS, Arc-SWAT, SWAT-CUP. Arc-GIS is a geographic information system (GIS) for working with maps and geographic information. It is useful for creating and using maps, compiling geographic data, analyzing mapped information, sharing and discovering geographic information, using maps and geographic information in a range of applications, and managing geographic information in a database. Arc-SWAT is an Arc-GIS and Arc-View extension and interfaces for SWAT. It is a small watershed to river basin-scale model used to simulate the quality and quantity of surface and groundwater and predict the environmental impact of land use, land management practices, and climate change. SWAT is widely used in assessing soil erosion prevention and control, non-point source pollution control, and regional management in watersheds. SWAT-CUP is a calibration/uncertainty or sensitivity program interface for SWAT. The program links SUFI2, PSO, GLUE, Parasol, and MCMC procedures to SWAT. It enables sensitivity analysis, calibration, validation, and uncertainty analysis of SWAT models.

3.12.2 Soil water assessment tool (SWAT)

To estimate the sediment yield with and without a dam, SWAT has been used in the present study. The inputs are used from the website (https://swat.tamu.edu/software/india-dataset/), which suits the Indian conditions. Additionally, the dam discharge data collected from KPCL Ganeshgudi was used as reservoir input for the SWAT. Finally, the model was run using ArcSWAT version 2012.10.21, which is an extension and interface for SWAT.

The SWAT is a basin-scale model built by the USDA Agricultural Research Service. It is used to quantify the influence of different land management practices on water quantity and quality in complex watersheds with heterogeneous soils, land use, and management. The model was spatially semi-distributed, process-based, computationally efficient, and capable of continuous simulation over long periods at a daily time scale. It is capable of simulating a single basin or a system of multiple basins that were hydrologically connected. It could model hundreds to thousands of square kilometers of area. Weather, soil temperature and properties, hydrology, plant growth, pesticides, nutrients, bacteria and pathogens, and land management are the key model components.

In the SWAT model initially, the basin was divided into sub-basin and further into HRU, which is the fundamental unit of SWAT modeling. In the present study, the multiple combinations of land use, soil, and slope, this creates HRU with a threshold set as 10. This means that if anyone of the particular such as land use or soil type percentage is less than 10, then these land-use or soil type would be disregarded and replaced by the adjacent soil or land use type. This approach gives 15 sub-basins in the Aghanashini river basin with 45 HRU's, 32 sub-basins in the Kali river basin with 86 HRU's.

There are different methods to estimate soil erosion. They are USLE, RUSLE, and MUSLE. Modified Universal Soil Loss Equation (MUSLE), which is a modified version of USLE (Universal Soil Loss Equation), was considered to estimate the erosion and yield from rainfall and overland flow. A modified version of the USLE model used

to find out the sediment yield as a function of runoff, whereas USLE estimates the soil erosion from cropland as a function of rainfall energy.

The USLE for estimating average annual soil erosion is:

A = RKLSCP.. (3.5)

> A = average annual soil loss in t/a (tons per acre)
>
> R = rainfall erosivity index
>
> K = soil erodibility factor
>
> LS = topographic factor - L is for slope length & S is for slope
>
> C = cropping factor

P = conservation practice factor

SWAT is based on the laws of physics, but it also permits the use of measurements in simulations. Each watershed is first divided into sub-basins and then into hydrologic response units (HRUs) based on the land use, slope, and soil distributions. It is capable of simulating large watersheds in a relatively short time. The hydrological cycle simulated by SWAT model is based on the water balance equation,

$$SWt = SW0 + \sum_{t=1}^{n}\left(R_{day} - Q_{surf} - E_a - W_{perc} - Q_{gw}\right) \qquad (3.6)$$

where, SWt and SW0 are final and initial soil water content (mm/d) respectively; t is the time (day); R_{day} is the precipitation(mm/d); Q_{surf} is the runoff (mm/d); Ea is the evapotranspiration(mm/d); W_{perc} is the percolation (mm/d); Q_{gw} is the return flow (mm/d).

Modified Universal Soil Loss Equation (MUSLE), which is a modified version of the Universal Soil Loss Equation (USLE) developed by Wischmeier and Smith (1965, 1978), is used for computing soil erosion caused by rainfall and runoff (Williams, 1975). The MUSSLE equation is given by,

$$sed = [11.8(Q_{surf}.q_{peak}.area_{hru})^{0.56}(K_{USLE}.C_{USLE}.P_{USLE}.LS_{USLE}).CFRG \quad (3.7)$$
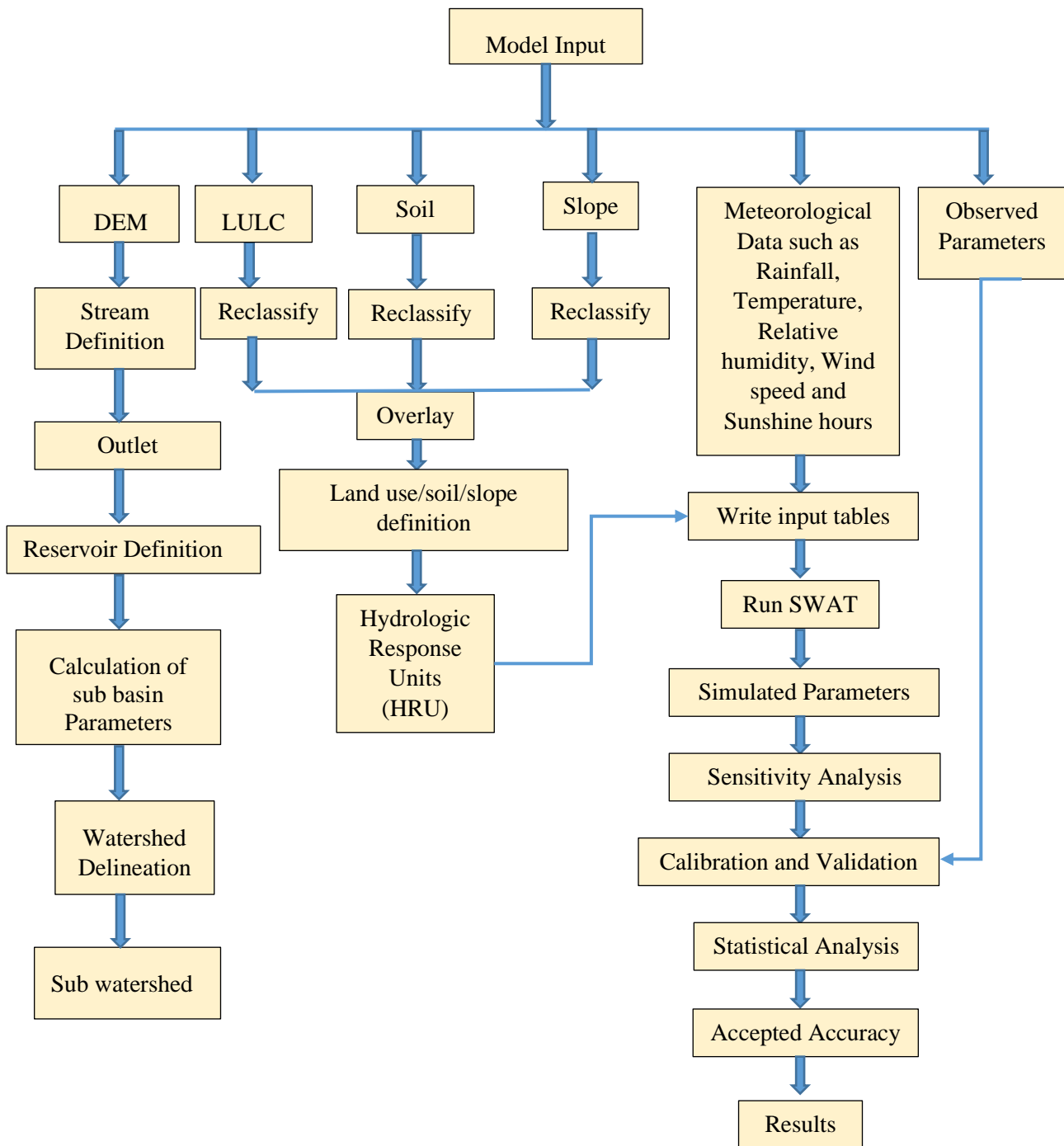
Figure 3.10 Flow Chart of Estimation of Sediment Yield Using SWAT

Where sed is the sediment yield on a given day, Q_{surf} is the surface runoff volume, q_{peak} is the area of HRU (ha), K_{USLE} is the USLE soil factor, C_{USLE} is the cover and management factor, P_{USLE} is the USLE support practice factor, LS_{USLE} is the USLE topographic factor CFRG is the coarse fragment factor (Neitsch et al., 2011, Bieger et al., 2015).

3.12.3 Data preparation

In the case of hydrological modeling, the difficult task is to collect the data sets. This is due to the constraint of quality and adequacy of data sets. The collection of all hydrological variables at different time scales appropriate to catchment scale processes is a laborious task. Although, if these difficulties overcome and provide information is necessary to analyse the behaviour of catchment and response to hydrological events. Several datasets are required for this study, which includes topographic data (DEM), land use/land cover data, soil data, daily climatic data being, daily data of precipitation, maximum and minimum temperature, relative humidity, wind speed and solar radiation. Data used in this research was collected from various organizations and agencies. Further DEM collected from the USGS website, land cover, and other important inputs were provided on the website such as https://swat.tamu.edu/data/india-dataset/ and all the dam discharge were collected from Karnataka Power Corporation Limited (KPCL).

3.12.4 SWAT model inputs

The necessary input spatial data sets were projected to WGS/UTM Zone 43N, which is the Transverse Mercator projection parameters for India, using ArcGIS®10.3. For the analysis of the drainage pattern of land surface terrain, the watershed is delineated by using DEM. The land use/land cover spatial data were reclassified into SWAT land cover. Further, to identify the SWAT code for different categories of land use/land cover on the map as per the required format, a user lookup table was created. The watershed delineation process includes five major steps, DEM setup, stream definition, outlet and inlet definition, watershed outlets selection and definition, and calculation of sub-basin parameters. After setting up of the model using the default parameter values, the default simulations of streamflow were carried out for the calibration period.

The spatially distributed model used in the GIS platform needed for the ArcSWAT interface includes the Digital Elevation Model (DEM), soil data, land use/land cover, weather data, and stream network layers. Data on River discharge and sediment were also used for calibration of streamflow and prediction purposes.

3.12.5 Digital elevation model

The digital elevation model (DEM) is the digital representation of the land surface elevation with respect to any reference datum.
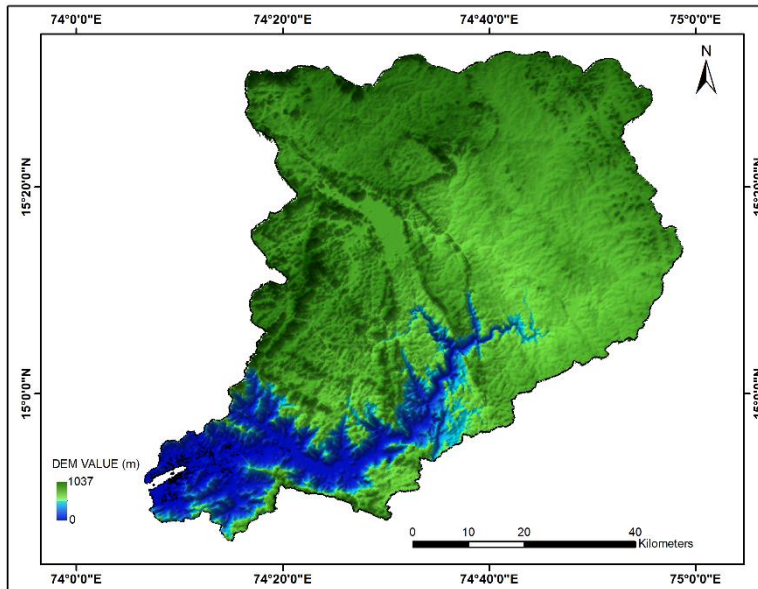
Figure 3.11 DEM of Kali River Basin
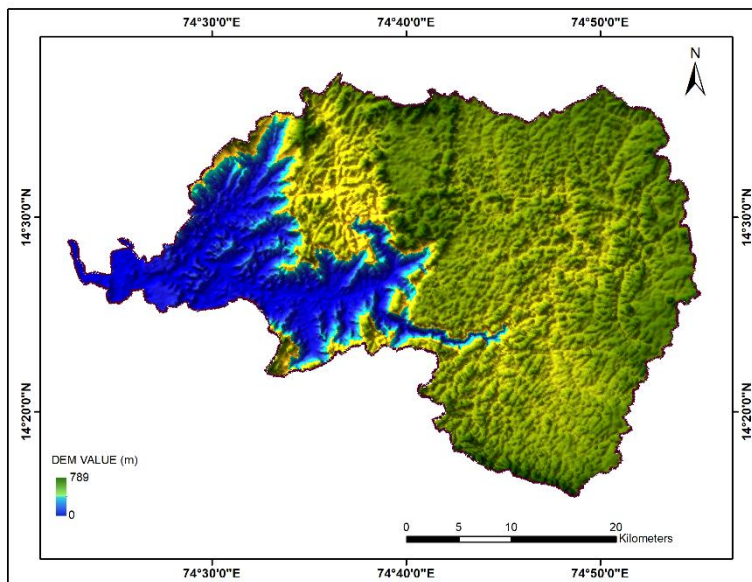
Figure 3.12 DEM of Aghanashini River Basin

DEM's are used to determine terrain attributes such as elevation, slope, and aspect. The Shuttle Radar Topography Mission (SRTM) 30 m resolution digital elevation models were used for the study to delineate the watershed and to extract the stream network in the catchment.

The maximum elevation of the Kali basin found to be 1037 m, and the minimum is 1 m. For the Aghanshini river, the elevation lies in an interval of 3 - 789 m.

3.12.6 Precipitation

SWAT requires daily precipitation as well as daily maximum and minimum air temperature data. There are 36 rain gauge stations with daily data located inside and around the Kali basin, five stations for the Aghanashini catchment (IMD). Average annual rainfall of the Kali basin found to be 3200 mm and Aghanashini basin, with similar characteristics as the Kali, receives about 3500 mm.
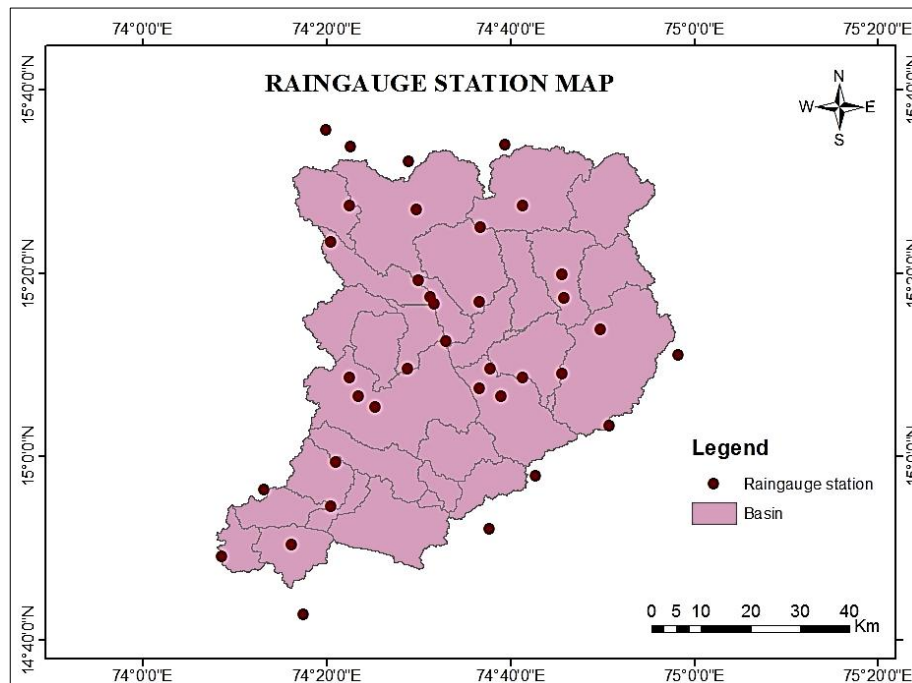
Figure 3.13 Rainfall Map of Kali River Basin

3.12.7 Temperature

SWAT requires daily maximum and minimum air temperature. The average annual temperature of the Kali river is 26.5 °C, and for Aghanashini river is 27.12 °C.

3.12.8 Land use/Landcover

Land use found in the Kali basin is Built-up, forest, Agricultural, barren land, shrub, and grassland, etc.

For Aghanasini basin land use land cover found are forest, Agricultural, barren land, shrub, and grassland etc. The details of LULC of the Kali river basin is shown in Table 3.8, and Table 3.9 gives the details regarding the LULC of the Aghanashini river basin.
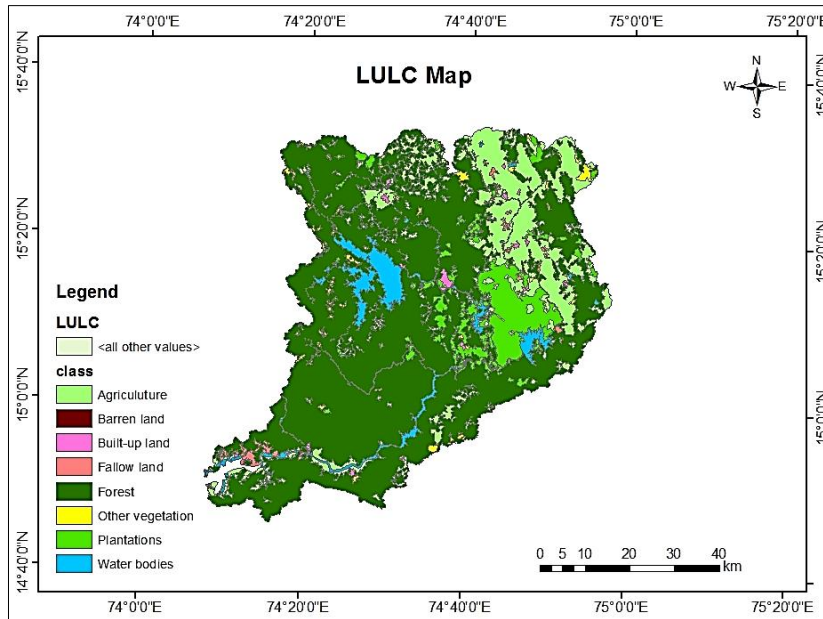
Figure 3.14 LULC of Kali River Basin for the year 2005
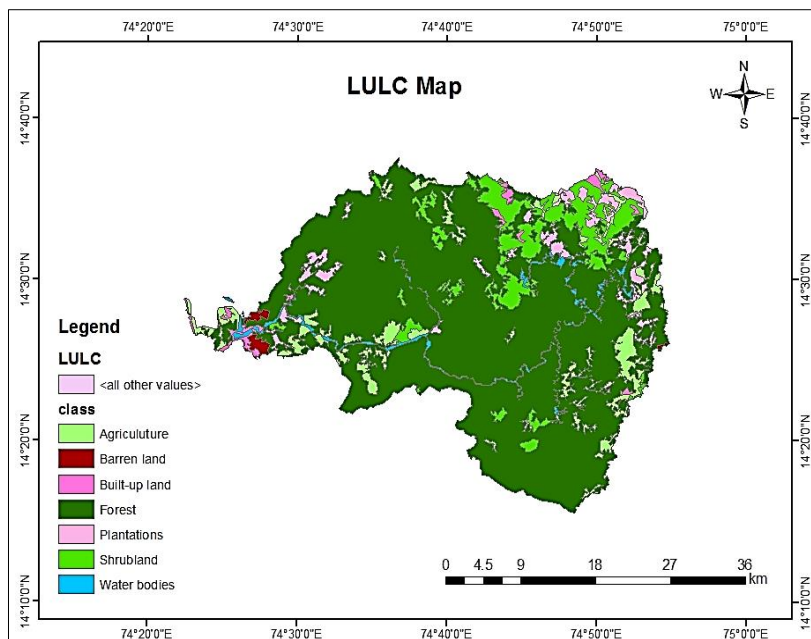
Figure 3.15 LULC of Aghanshini river for the year 2005

Table 3.8. Kali River Basin

LULC	1985(%)	1995(%)	2005(%)
Agriculture	15.56	17.09	18.90
Barren land	4.34	4.01	3.65
Built up	1.26	2.10	3.77
Fallow land	3.12	2.72	2.56
Forest	69.47	65.11	62.57
Other vegetation	2.58	3.21	3.12
Plantations	1.98	2.07	2.34
Water bodies	1.69	3.69	4.09

Table 3.9 Aghanashini River Basin

LULC	1985(%)	1995(%)	2005(%)
Agriculture	6.97	8.65	10.78
Barren land	2.67	3.78	4.87
Built up	0.74	1.19	2.75
Shrub land	2.23	2.87	3.04
Forest	80.35	75.6	69.34
Plantations	5.34	5.78	6.33
Water bodies	1.70	2.13	2.89

3.12.9 Soil map

The soli map gives important information about soils such as its types, characteristics, types zones, and so on. Soils of Kali basin and Aghanashini are Red soil, Lateritic soil, and black soil
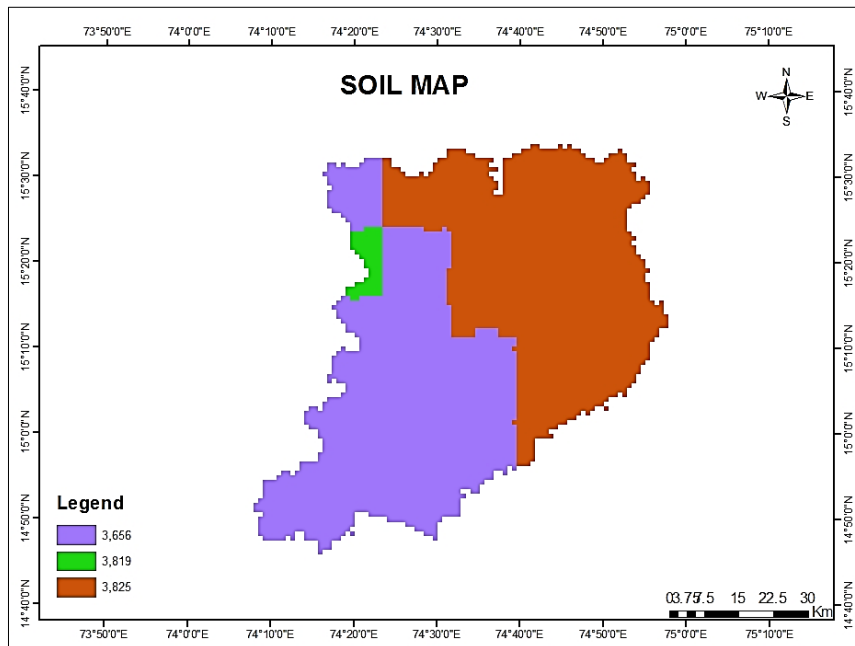
Figure 3.16 Soil map of Kali River Basin
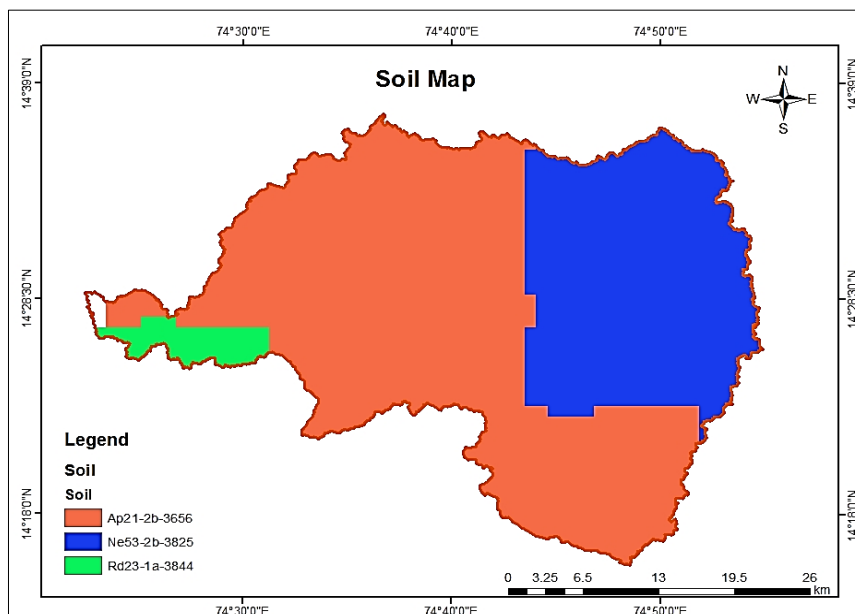
Figure 3.17 Soil Map of Aghanashini River Basin

3.13 Model performance evaluation

The performance of the model was evaluated by using the coefficient of determination (R2), Nash-Sutcliffe efficiency (NSE) index, and Percent bias (PBIAS).

3.13.1 Coefficient of determination (R^2)

In statistics, the coefficient of determination denoted R^2 or r^2 and pronounced "R squared" is the proportion of the variance in the dependent variable that is predictable from the independent variable(s). It is a good method to signify the consistency among observed and simulated data by following the best fit line. R squared values range from 0 to 1 and are commonly stated as percentages from 0 to 100%. An R-squared of 100% means movements in the independent variable completely explain all movements of a dependent variable. Higher values indicating less error variance and values greater than 0.50 are considered acceptable.

$$R^2 = \left[\frac{\sum_{i=1}^{n}(Q_{obs}-\bar{Q}_{obs})(Q_{sim}-\bar{Q}_{sim})}{\sqrt{\sum_{i=1}^{n}(Q_{obs}-\bar{Q}_{obs})^2}\sqrt{\sum_{i=1}^{n}(Q_{sim}-\bar{Q}_{sim})^2}} \right]^2 \qquad (3.10)$$

3.13.2 Nash - Sutcliffe efficiency (NSE)

The Nash–Sutcliffe model efficiency coefficient (NSE) is used to assess the predictive power of hydrological models. It is defined as,

$$NSE = 1 - \frac{\sum_{i=1}^{n}(Q_{obs}-Q_{sim})^2}{\sum_{i=1}^{n}(Q_{obs}-\bar{Q}_{obs})^2} \qquad (3.11)$$

Nash–Sutcliffe efficiency can range from $-\infty$ to 1. An efficiency of 1 (NSE = 1) corresponds to a perfect match of modeled discharge to the observed data. An efficiency of 0 (NSE = 0) indicates that the model predictions are as accurate as of the mean of the observed data, whereas an efficiency less than zero (NSE < 0) occurs when the observed mean a better predictor than the model. Essentially, the closer the value of model efficiency is to 1, the more accurate value from the model analysis obtained. Nash–Sutcliffe efficiency can be used to describe the accuracy of model outputs other than discharge quantitatively.

3.13.3 Percent bias (P-bias)

PBIAS indicates whether the model results are consistently under or overestimated compared to the observations. It is defined by the range -10 to10. The equation of the coefficient is,

$$PBIAS = \frac{\sum_{I=1}^{N}(Q_{obs}-Q_{sim})}{\sum_{i=1}^{n} Q_{obs}} \times 100 \qquad (3.12)$$

The optimal value of PBIAS is 0.0, with low magnitude values indicating accurate model simulation. Negative values indicate overestimation bias, whereas positive values indicate model underestimation bias (Gupta et al., 1999).

3.13.4 Model calibration

Model calibration involves the modification of parameter values and comparison of the predicted output of interest to measured data until a defined objective function is achieved. Model calibration is an important process in a hydrological model. Calibration is an iterative process that compares simulated and observed data of interest through parameter evaluation. This approach consists of manual calibration involving the following steps: (1) perform the simulation; (2) compare measured, and simulated values; (3) assess if reasonable results have been obtained; (4) if not, adjust input parameters based on expert judgment and other guidance within reasonable parameter value ranges; and (5) repeat the process until it is determined that the best results have been obtained.

3.13.5 Model validation

The purpose of model validation is to establish whether the calibrated model can predict streamflow comparing to observed streamflow for later periods without making a further adjustment of parameters that may adjust during the calibration process. This validation process is also conducted using the Arc SWAT program.

3.13.6 SWAT –CUP Description

SWAT Calibration and uncertainty programs (SWAT-CUP) are an interface that was developed from SWAT.SWAT –CUP software is used for auto-calibration and

uncertainty analysis of SWAT models. The SWAT CUP supports programs like SUFI2, PSO, GLUE, Parasol, and MCMC procedures to SWAT. Sensitivity analysis is usually used to measure the effect of parameters on output. Effective calibration of a distributed model like Arc-SWAT begins by developing a proper mechanism for reducing the number of parameters to be calibrated. Therefore sensitivity analysis is to be conducted. Arc SWAT provides an interface for parameter sensitivity analysis. In this study, the SUFI2 program is used for calibration and validation.

3.13.7 Sequential uncertainty fitting version 2 (SUFI2)

The Sequential Uncertainty Fitting version 2 (SUFI2) program parameter uncertainty accounted for all sources of uncertainties such as uncertainty in driving variables. The degree to which all uncertainties are accounted for is quantified by a measure referred to as the P –factor, which is the percentage of measured data bracketed by the 95% prediction uncertainty (95PPU). Another measure quantifying the strength of a calibration uncertainty analysis is the R factor, which is the average thickness of the 95PPU band divided by the standard deviation of the measured data. SUFI-2 seeks to bracket most of the measured data with the smallest possible uncertainty band.

The goodness of fit and the degree to which the calibrated model accounts for the uncertainties are assessed by the above two measures. Theoretically, the value for P factor ranges between 0 and 100%, while that of R factor ranges between 0 and infinity. A P factor of 1 and the R factor of zero is a simulation that corresponds to measured data.

3.14 Grain size distribution of collected sample

Sand samples have been collected for both Devbagh and Tagore beach of Karwar coast for the year of 2018. Particularly for the pre-monsoon and post-monsoon season. The first sample collection made at Kali river estuary point, second sample collection approximately 2 km away from Kali river estuary and final sample point collected about 4 km distance from Kali river estuary. Further, the analysis is carried out using GRADISTAST V8. The GRADISTAST V8 is a Microsoft Excel tool to find the calculation of Mean, Sorting, Skewness, and Kurtosis by applying Moment method and

Folk and Ward method. The moment method includes an Arithmetic method, Geometric method, and Logarithmic method. The Folk and Ward method consists of geometric and logarithmic (Blot and Pye 2001).

3.15 Sediment trend analysis

Beach face sediment samples were collected by using hand grasp method in 3 locations along the study area for both pre-monsoon & post-monsoon season. The collected samples were initially washed to remove salts and then allowed to oven dried for 24 hours at 105°C - 110°C to remove moisture. After drying, 500 grams of each sample was taken for performing dry sieve analysis by using Ro– Top machine for about 15 minutes as recommended in IS: 2720-1965 (Part–IV). With these results, log probability distribution curves were plotted with grain size (φ) on X-axis and cumulative percentage on Y-axis. Statistical parameters such as mean, sorting and skewness were computed using Folk and Ward method (1957). A grain size distribution and statistics package called GRADISTAT developed by Blott and Pye (2001) was used for calculating statistical parameters and plotting log probability distribution curves.

3.16 Estimation of sand volume from beach profiling

The dynamic characteristics of the beach were varying temporarily with changing wave conditions during post-monsoon and pre-monsoon seasons by different environmental conditions. Therefore, to assess the dynamic behavior of the coastal region for pre-monsoon and post-monsoon season, it is essential to carry out seasonal beach profiling. In the present study, an extensive field survey was carried out using total station instrument to obtain the beach profiles of post-monsoon and pre-monsoon seasons along 3kms long coastal stretch with variable geomorphology of Karwar (Ravindranath Tagore) beach for computation of volume of sand/sand accretion/erosion along the beaches. A total of 20 profiles have been surveyed at different locations i.e. two profiles at each location for post and pre-monsoon season of 2017. From a depth of 1.5 m below the mean sea level, the volume of sand between consecutive beach profiles, i.e., at an interval of 150m was estimated using trapezoidal rule for both pre-monsoon & post-monsoon season. The D_{50} grain size of sediment at each cross-section was determined.

CHAPTER 4

4   RESULTS AND DISCUSSIONS

4.1   General

The construction of a dam plays a major role in the coastal zone. This makes an impact on the natural river flow and the beach nourishment. This impact makes huge causes to the nature of the coastal zone. Hence, the present research work intends to carry out the analysis of shoreline for pre-construction of the dam, post-construction of the dam, pre-monsoon season and post-monsoon season using the DSAS tool. Shoreline analysis can be performed for long-term and short-term analyses depending upon the availability of the data set. Further, the sediment estimation was also carried out for the Kali river basin and the Aghanashini river to check the effect and difference between these both river basins by considering with and without the dam. The SWAT tool has been used for the sediment estimation. The granulometric analysis carried out for collected beach face sand samples of both Ravindranath Tagore (RT) beach and Devbagh beach and also the sand movement has been analyzed. In addition to this, the beach profile has been carried out for only RT beach of 3 km stretch using a total station.

4.1.1   Shoreline analysis for pre-construction of dam and post-construction of dam

In the present section results of the analysis of satellite data and DSAS are discussed in detail. DSAS generated 114 transects for Devbagh beach and 110 transects for RT beach These transects oriented perpendiculars to the baseline at 50 m spacing along 9.5 km length of Devbagh beach to RT beach. Kali estuary region was not selected which, separates both these beaches. The baseline is user-defined which projected approximately 100 m distance is from the digitized shorelines. Shoreline change rates have been calculated using the DSAS tool with two different statistical techniques such as EPR and LRR.
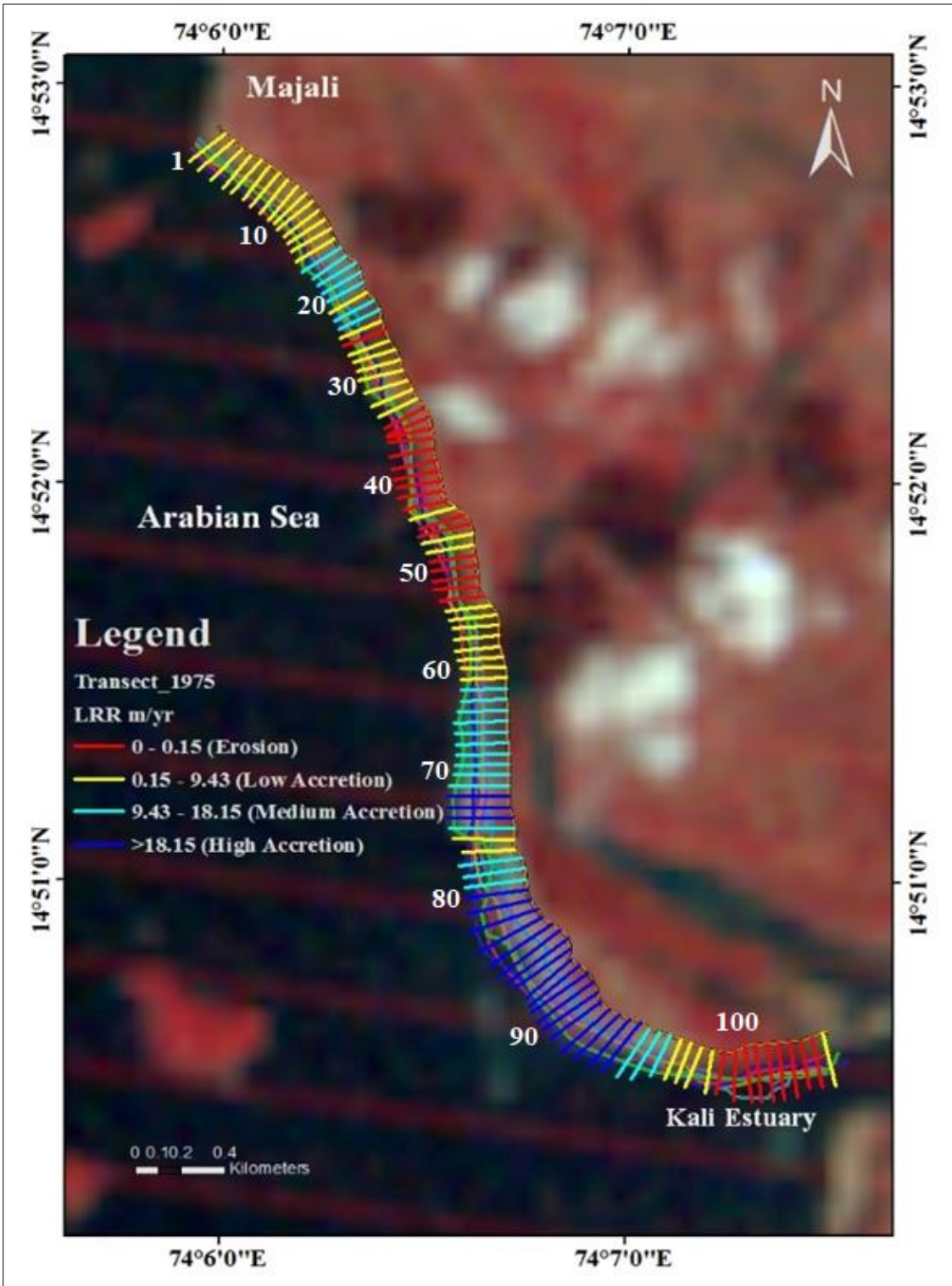
Figure 4.1: Devbagh Beach Pre-Construction of the Dam (1975-1980)
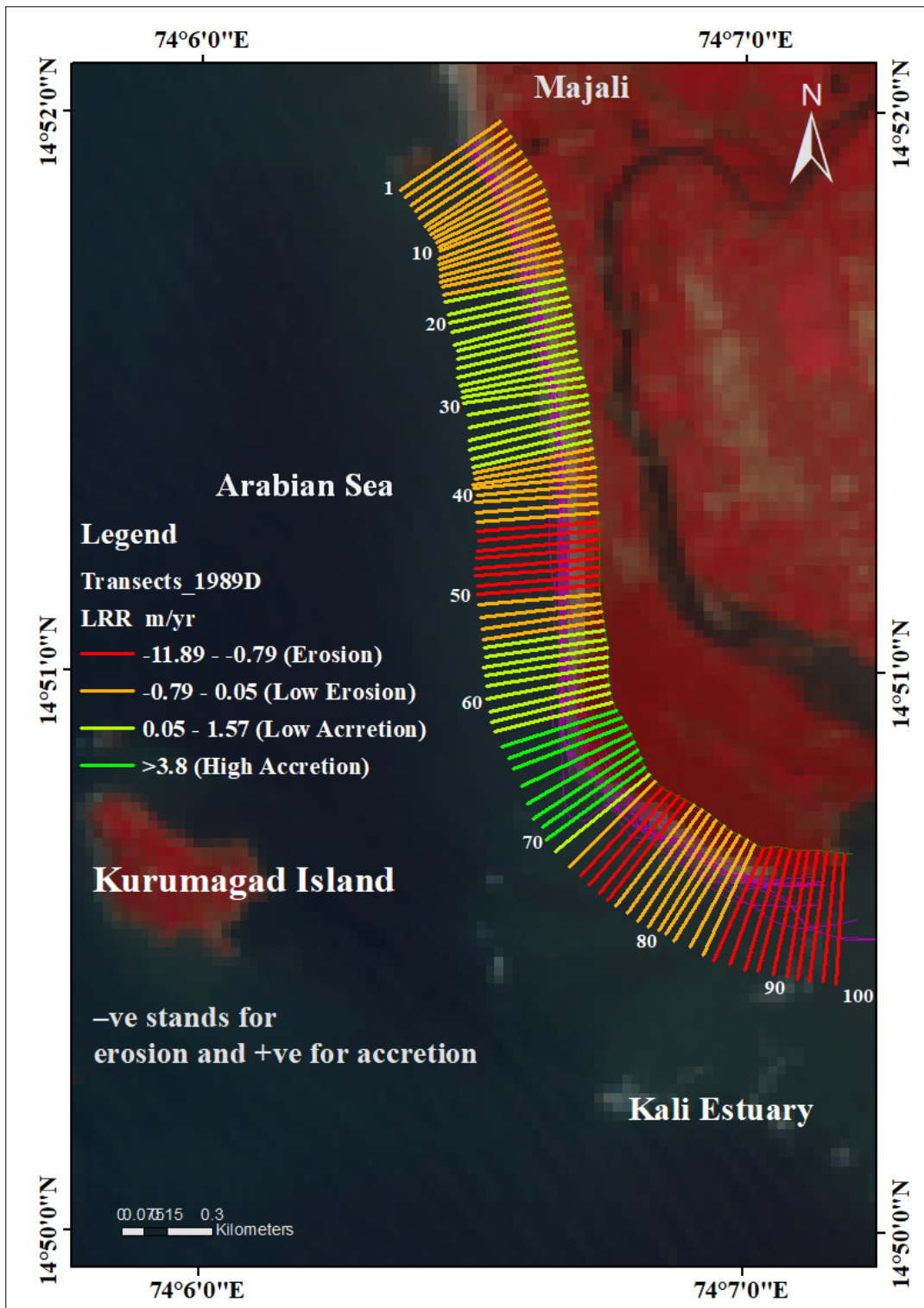
Figure 4.2: Devbagh beach post-construction of the dam (1990-2017)

Figure 4.1 shows the map of Devbagh beach pre-construction of the dam. From the analysis, it is clear that from 1975 to 1980, the beach had accretion at the rate of 6.96 m/yr (EPR) and 8.39 m/yr (LRR). Transects number from 1 to 32 were accretion 6.15 m/yr (EPR), 7.34m/yr (LRR) and 53 to 104 were having accretion of 13.29m/yr (EPR), 16.41m/yr (LRR). Figure 4.2 shows the map of Devbagh beach post-construction of the dam. The shoreline analysis carried out from 1990 to 2017. It seems to be after the construction of the dam beach is under erosion at the rate of -0.93 m/yr (EPR) and -0.47 m/yr (LRR). The maximum erosion found to be at the Kali estuary region.

The graph of Devbagh beach for pre and post-construction of the dam is as shown in Figure 4.2(a & b). It is noticed that during the pre-construction of the dam, Devbagh beach found to be dynamic in case of the supply of sediment through the river. In the case of the post-construction of the dam, Devbagh beach observes reduced sediment supply, and the maximum part of the beach is under erosion. In the case of Ravindranath Tagore beach during 1975-1980, the beach has accretion at the rate of 7.25 m/yr (EPR) and 2.7 m/yr (LRR). The maximum accretion found between transects from 82 to 107, which is 16.03 m/yr (EPR) and 8.83 m/yr (LRR). The accretion found in the Kali estuary region. The result is expressed in Figure 4.3. further, the shoreline analysis was carried out from 1990-2017 to find the shoreline change of Ravindranath Tagore beach for the period, which is post-construction of the dam. From Figure 4.4, it is evident that the accretion rate has dramatically decreased and at the Kali estuary region has turned from accretion state to erosion state, which is -0.75 m/yr (EPR) and -0.97 m/yr (LRR). But from transects 6 to 19 shows accretion of 7.26 m/yr (EPR) and 5.59 m/yr (LRR). This part of the beach is near to the breakwater, and it was constructed in 2005, which is 250m. The graph shows the shoreline rates, such as EPR and LRR, are drawn, and it is shown in Figure 4.5.

Pre-construction of it is found to be dynamic sediment supply through the river. In the case of pre-construction of the dam, most of the Ravindranath Tagore Beach is observed deposition of sediment, and the beach was in accretion state. In the case of the post-construction of the dam, Ravindranath Tagore Beach received less sediment supply, and the maximum part of the beach is in erosion state.

Figure 4.2 (a) Rate of change of Devbagh beach of Pre-construction of the dam for the period of 1972- 1980 and (b) Rate of change of Devbagh beach of Post-construction of the dam for the period of 1990- 2017.

Figure 4.3 Ravindranath Tagore Beach Pre-Construction of the Dam (1975-1980)

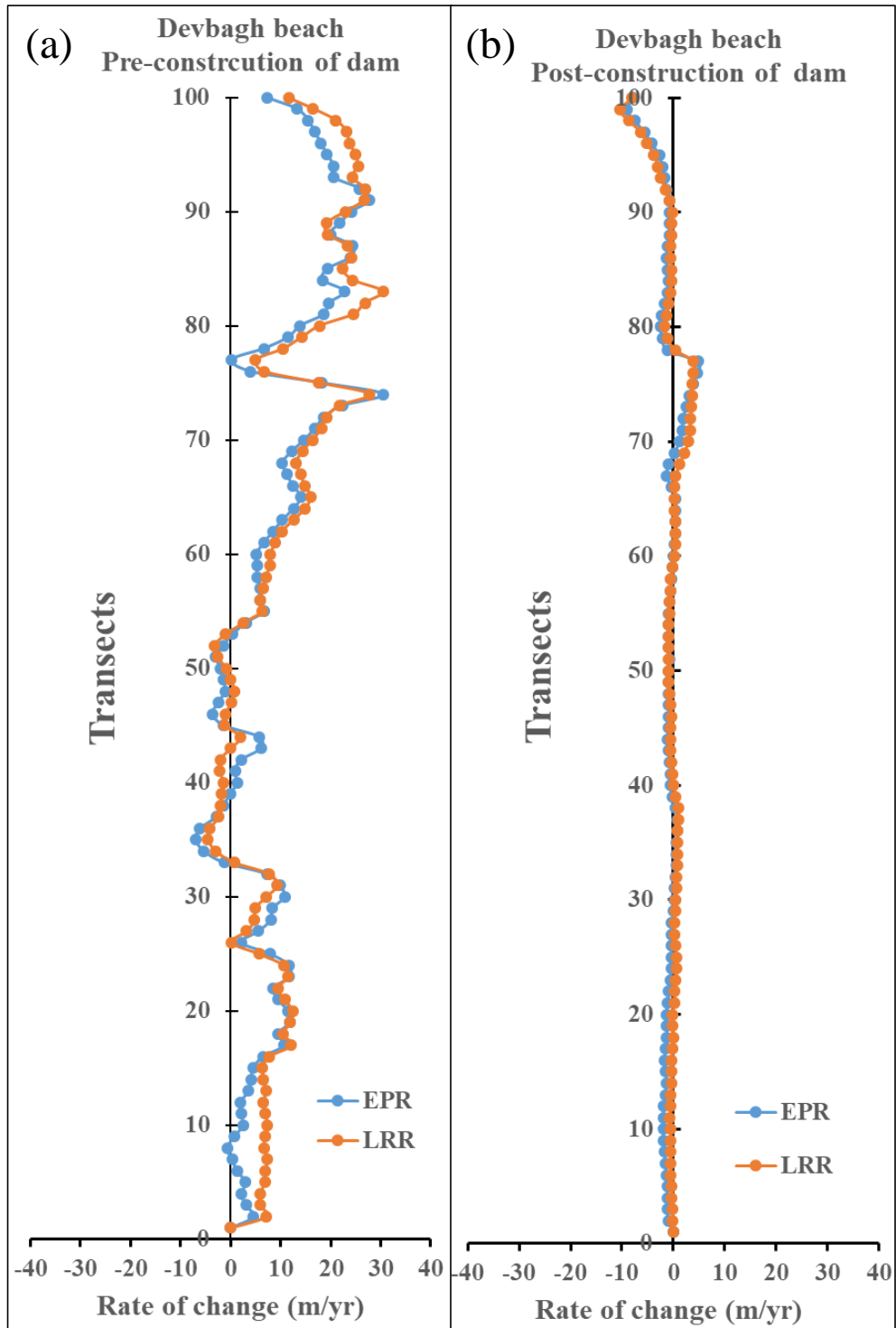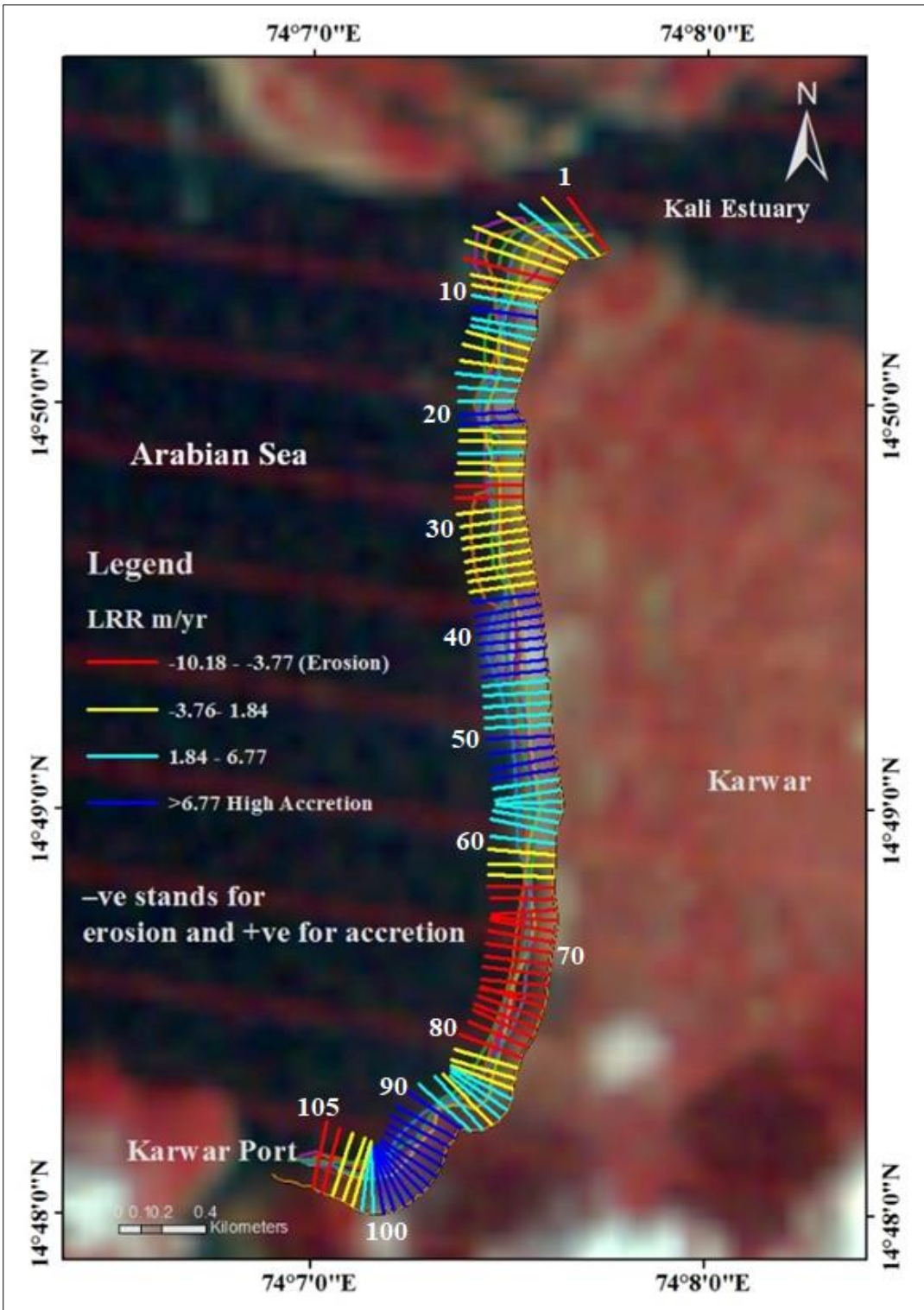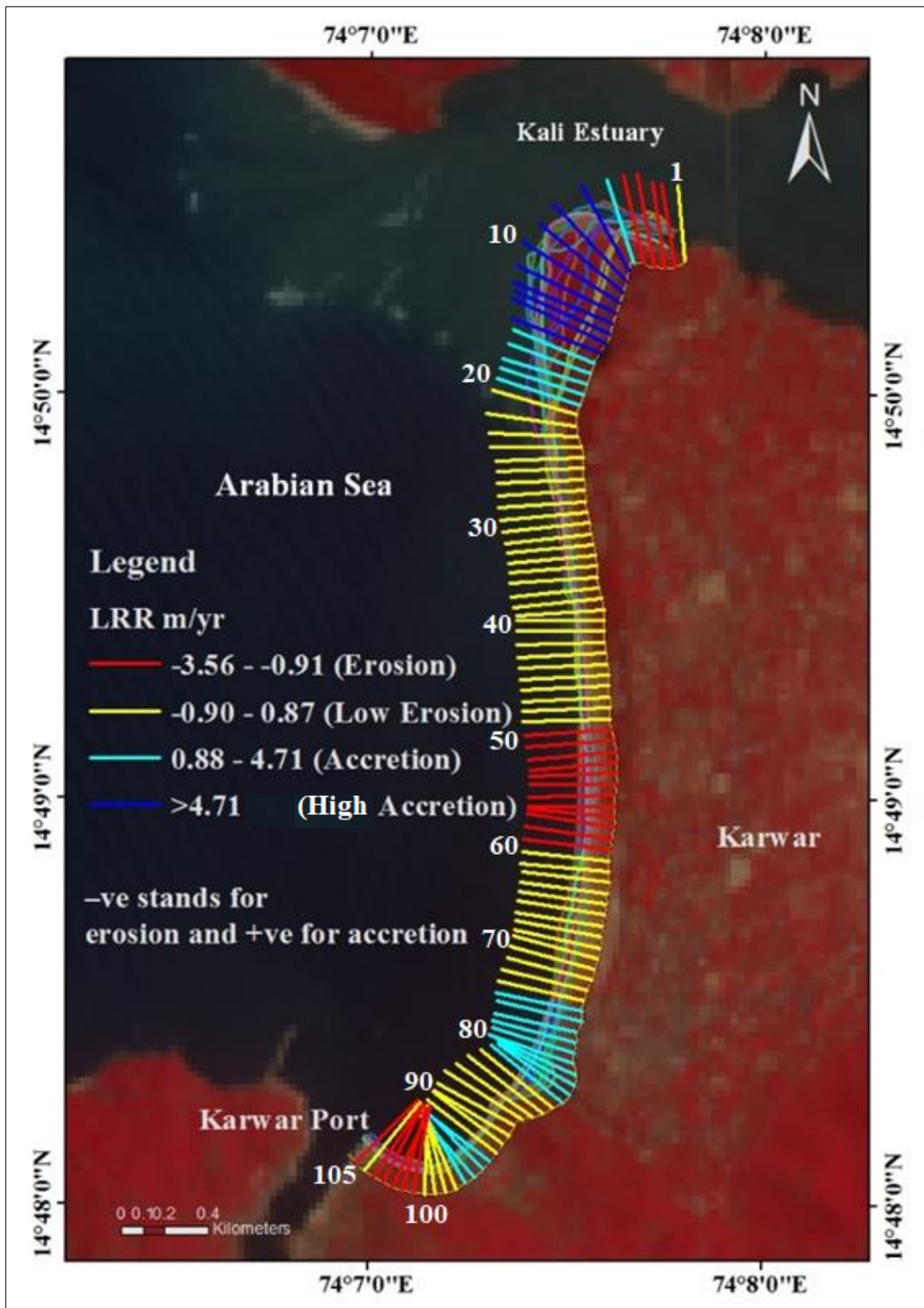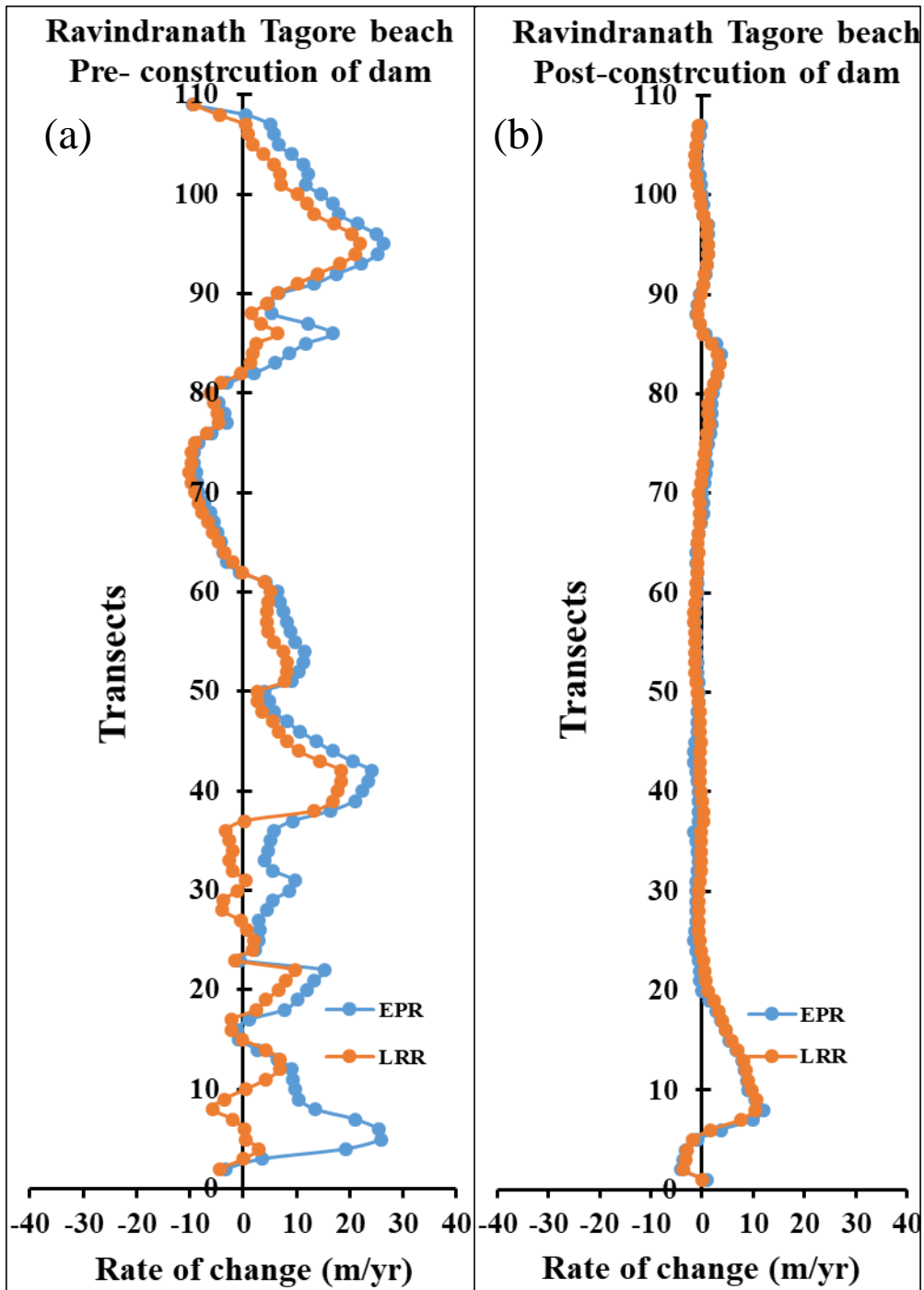Figure 4.4 Ravindranath Tagore Beach Post-Construction of the Dam (1990-2017)

Figure 4.5 (a) Rate of change of Ravindranath Tagore beach Pre-construction of the dam for the period of 1972- 1980 and (b) Rate of change of Ravindranath Tagore beach Post- construction of the dam for the period of 1990- 2017.

4.1.2 Shoreline analysis of Aghnashini river coast

Similarly, the shoreline analysis was carried out for the Aghnashini river joining coast. The main objective is to find about the coast experiences a change in the state due to river sediment. Aghanashini river has similar hydrological characteristics compared with the Kali river basin as it flows down to the Arabian sea.

The analysis carried out for shoreline change for two cases, that is Pre and Post construction of the dam. From the analysis, it is found to be changed in shoreline and beaches belonging to them. The analysis shows that the Pre-construction of the dams across the Kali river, the beaches such as Devbagh and Ravindranath Tagore beach were experienced the natural phenomenon in case of sediment supply from the Kali river. Since the post-construction of the dam, both beaches have undergone erosion state, which means the beach is nourishment is decreased; the natural phenomenon is not observed, and also river flows are regulated discharge from dams. To compare this study, the Aghanashini river basin and the coast is considered. Because the Aghanashini river exists approximately 60 km away from Karwar coast, and there is no dam build across to this river. The river flows naturally and meets the Arabian ocean at the Aghanashini estuary. After the analysis, the graph plot showing the X-axis as the rate of change (m/yr), and the Y-axis shows as transects.

At the upper part of the Aghanashini river estuary is under the Western ghats region, and it is of the rocky crop area. There is no formation of beach found, hence the shoreline analysis carried out for the lower part of the estuary. From Figure 4.6, it was found to be, the transects number 0 to 127 the beach undergone the only accretion of EPR 17.98 m/yr and 13.61 m/yr. The average accretion of EPR 8.92 m/yr and LRR of 6.92m/yr. Which shows that the coast is still under the accretion zone. This Aghanashini coast shoreline analysis gives evidence that the natural flow of the river, the natural phenomenon at the estuary region, and the sediment supply from the river. Since there is no dam built across this river, the sediment seems to be supplied sediment from the Aghanashini river naturally. It plays one of the important roles in the case of beach nourishment of a particular coast. This result shows that if there is no dam is constructed across the river; then the coast is going to remain natural as it is. If the dam built across

the river, then certainly the beach is diminished in nourishment due to decreased sediment supply from the river.
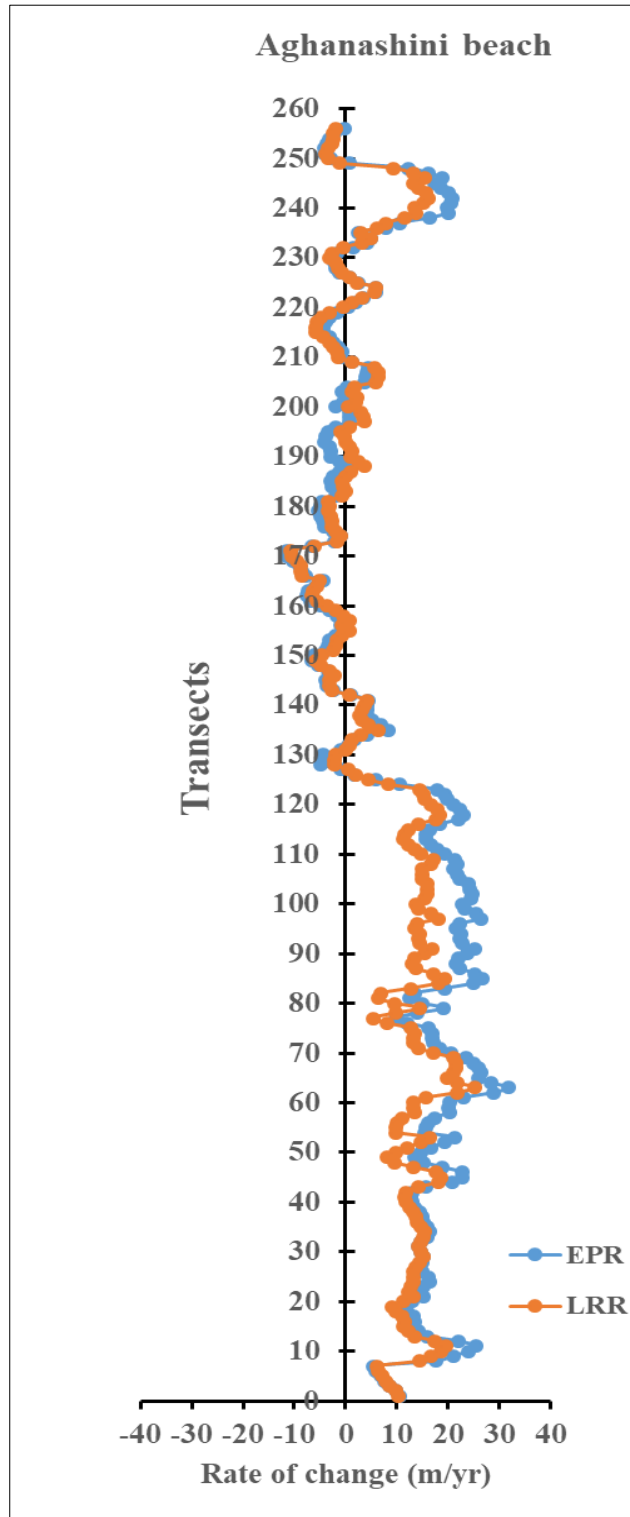

Figure 4.6 Rate of change of Aghnashini beach

4.1.3 Shoreline analysis for pre-monsoon and post-monsoon after the construction of the dam

DSAS generated 99 transects for Devbagh beach and 102 transects for Ravindranath Tagore beach. The above analysis was the same for both Pre-monsoon and Post-monsoon shoreline analysis. Shoreline change rates have been calculated using the DSAS tool with two different statistical techniques, such as EPR and LRR. The baseline is user-defined, which is projected approximately 100m distance from the latest 2017 shoreline. Total 201 transects were generated with 50 m spacing along a 9.5 km stretch of the study area.

The transect map generated from the DSAS tool gives the results of LRR and EPR for Pre-monsoon and Post-monsoon of Devbagh beach shown in Figure 4.7 and Figure 4.8, respectively. Similarly, the transect map of LRR and EPR for Pre-monsoon and Post-monsoon for Ravindranath Tagore beach shown in Figure 4.10 and Figure 4.11, respectively. This map explains the pattern of erosion and accretion.

From Figure 4.7, Pre-monsoon of Devbagh beach, from transects 1 to 79 shows only erosion of shoreline change rate is -8.23 m/yr (EPR) and -6.33 m/yr (LRR). From the erosion place visit, it was found that it is mainly due to lack of sediment supply, lack of deposition. Very near to this part of the shoreline, fishers are located, and it's exposed to the sea. The seawall is constructed at this erosion place. Transect 83 and 84 show the maximum shoreline accretion of 21.31 m/yr (EPR) and 21.02 m/yr (LRR). This place shows accretion due to accumulation of sediment from kali river, which is a healthy deposition and it was witnessed. Simultaneously, at transect 92 and 93 maximum shoreline erosion of -20.58 m/yr (EPR) and -20.05 m/yr (LRR) this region is very close to Kali estuary and again seawall are constructed to keep away from erosion, this seawall very close to the study area which is found attached after the transect number 99. And the average erosion rate is -7.54 m/yr (EPR) and 5.57 m/yr (LRR).

From Figure 4.8, Post monsoon of Devbagh beach, considered shoreline change rate (EPR) and (LRR) from 2013-2016. At transect 92 maximum shoreline accretion of 29.65 m/yr (EPR) and 27.10 m/yr (LRR) as mentioned this region very close to Kali estuary during monsoon, it supplies sediments which nourished beach after post-monsoon. At transect 80 maximum shoreline erosion of -37.43 m/yr (EPR) and -28.33

m/yr (LRR). And average erosion rate is 0.34 m/yr (EPR) and 0.46 m/yr (LRR). Devbagh beach at the Kali estuary during pre-monsoon high erosion and high accretion during post-monsoon was found and compared by a field visit.

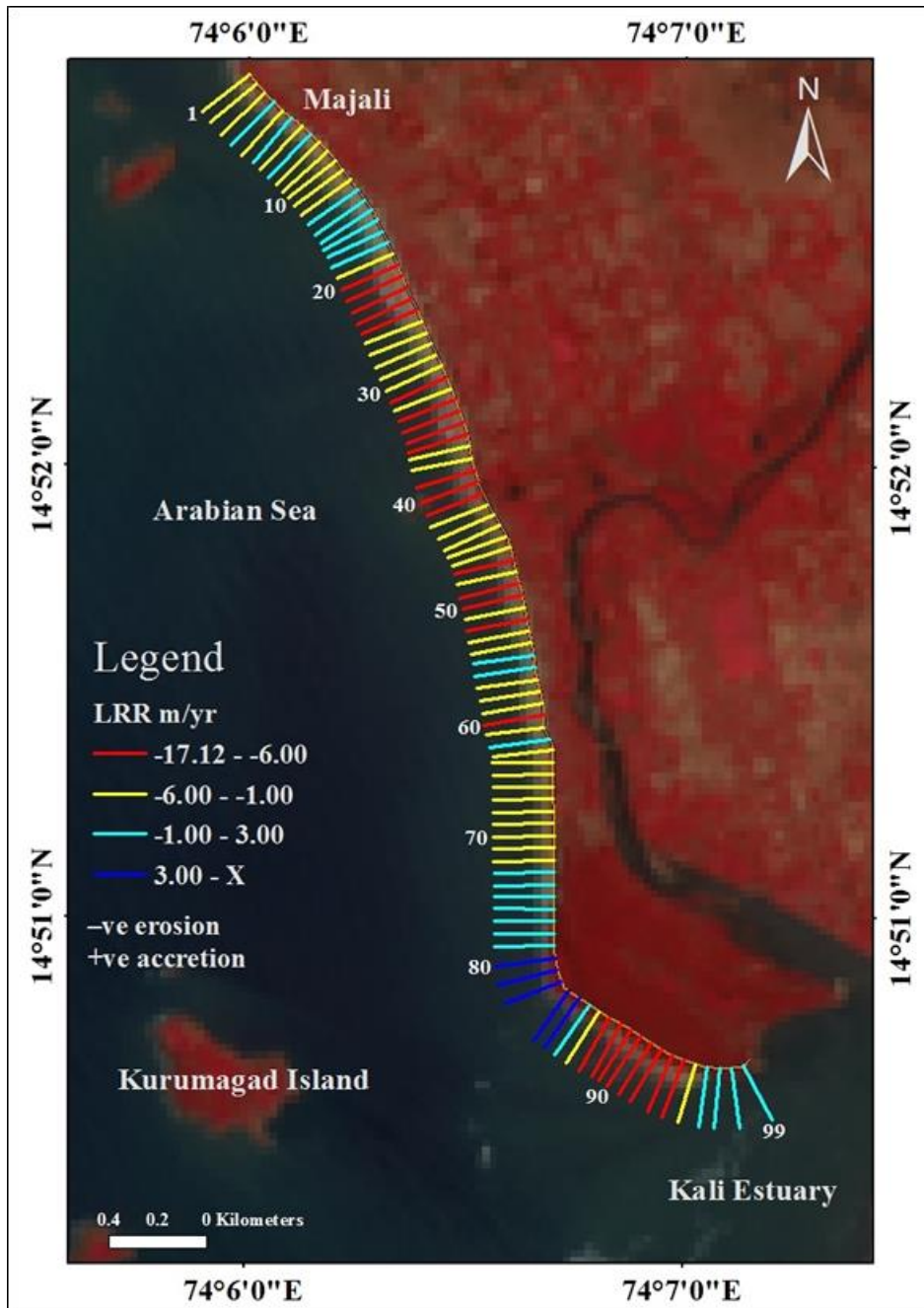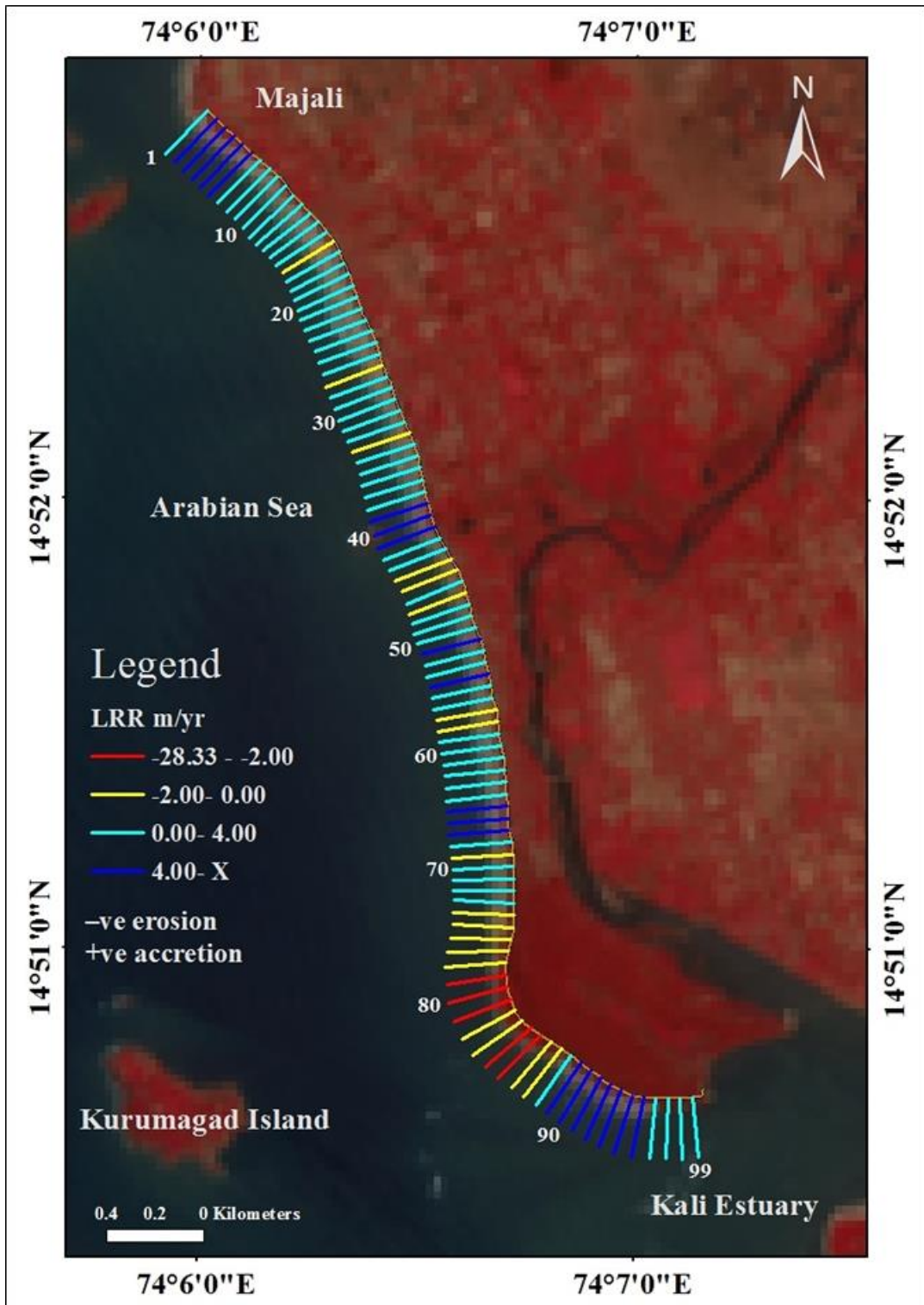Figure 4.7 Pre-monsoon of Devbagh beach

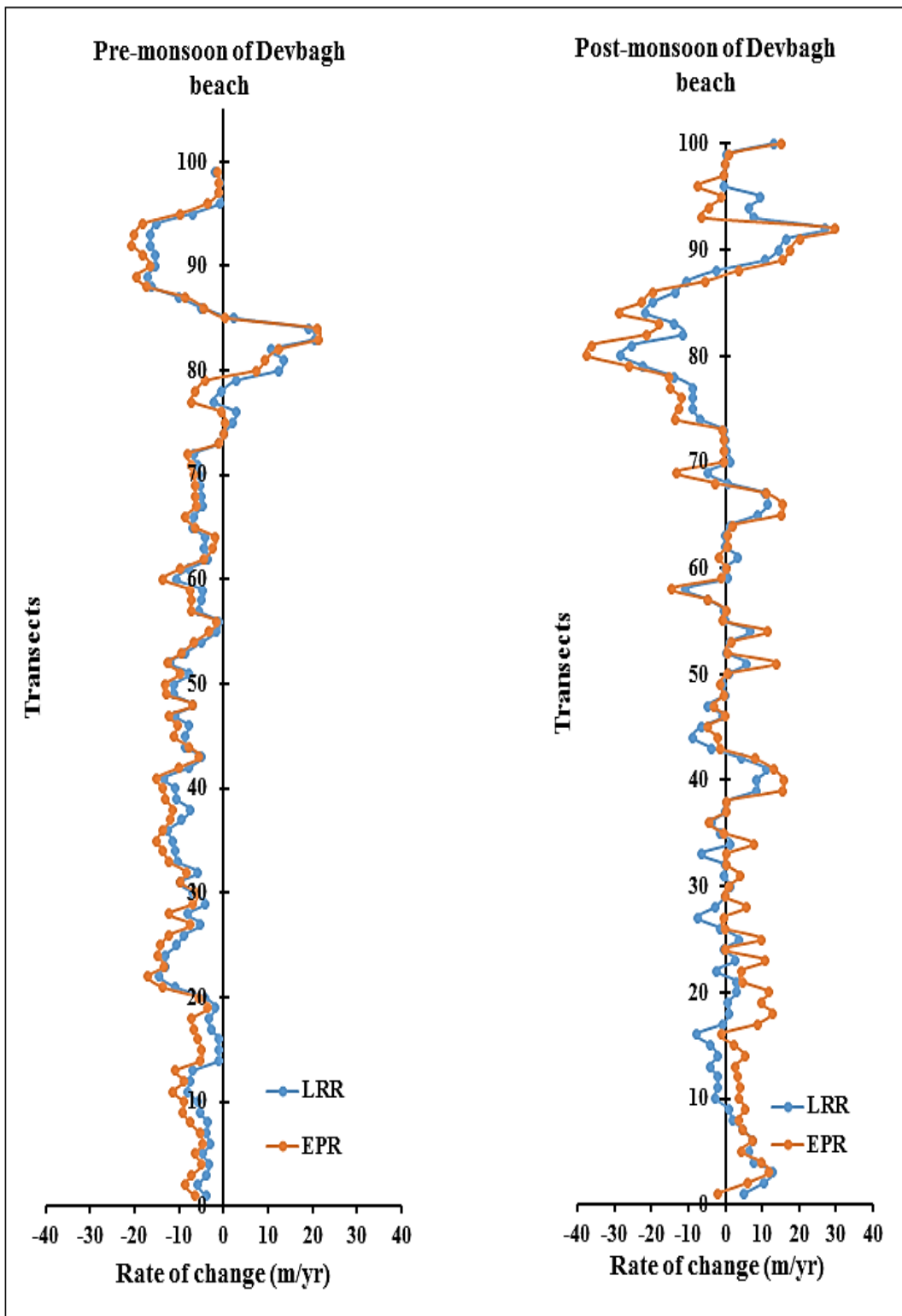Figure 4.8 Post-monsoon of Devbagh beach

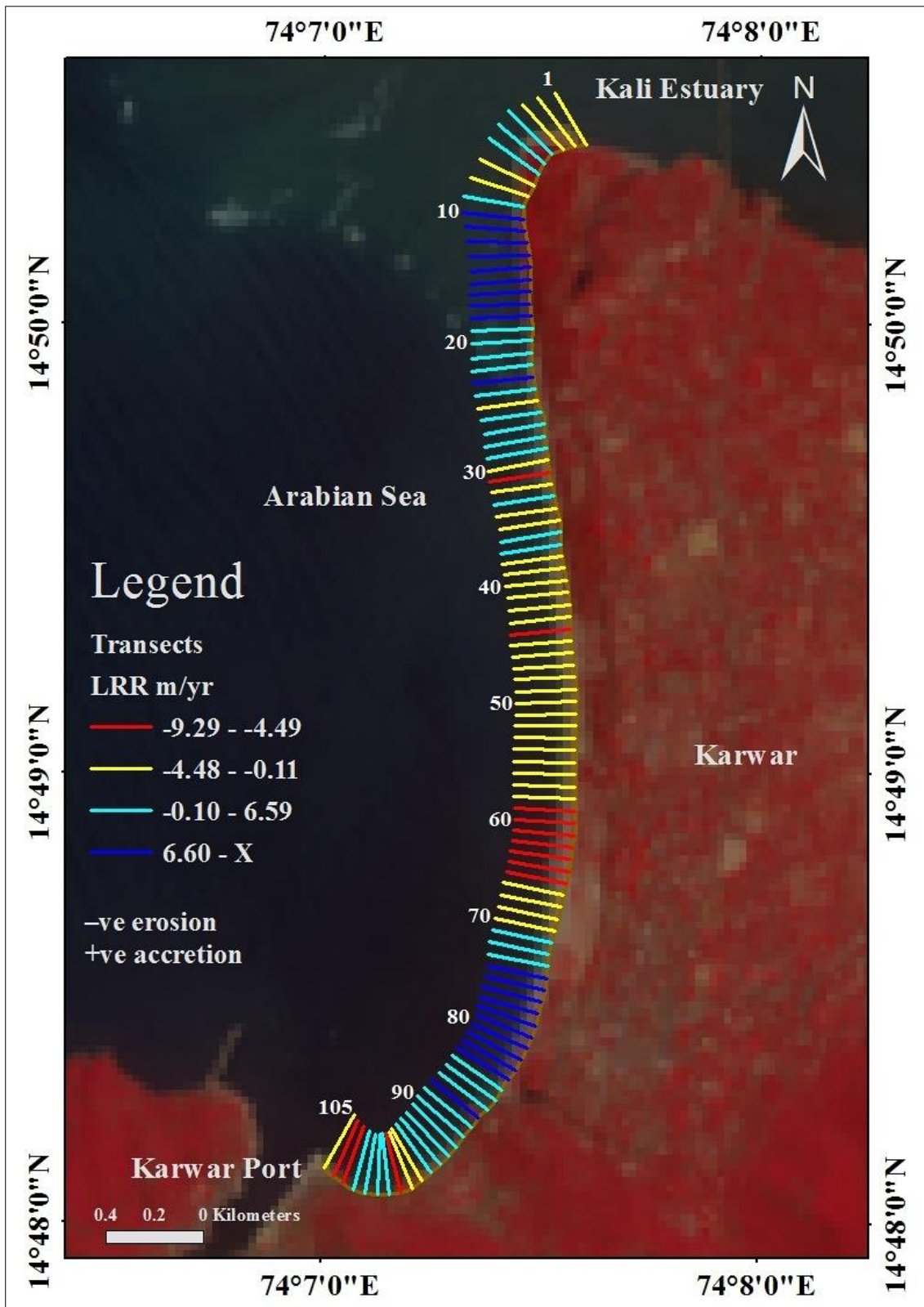Figure 4.9 Graphs of Devbagh beach of Pre and post-monsoon season

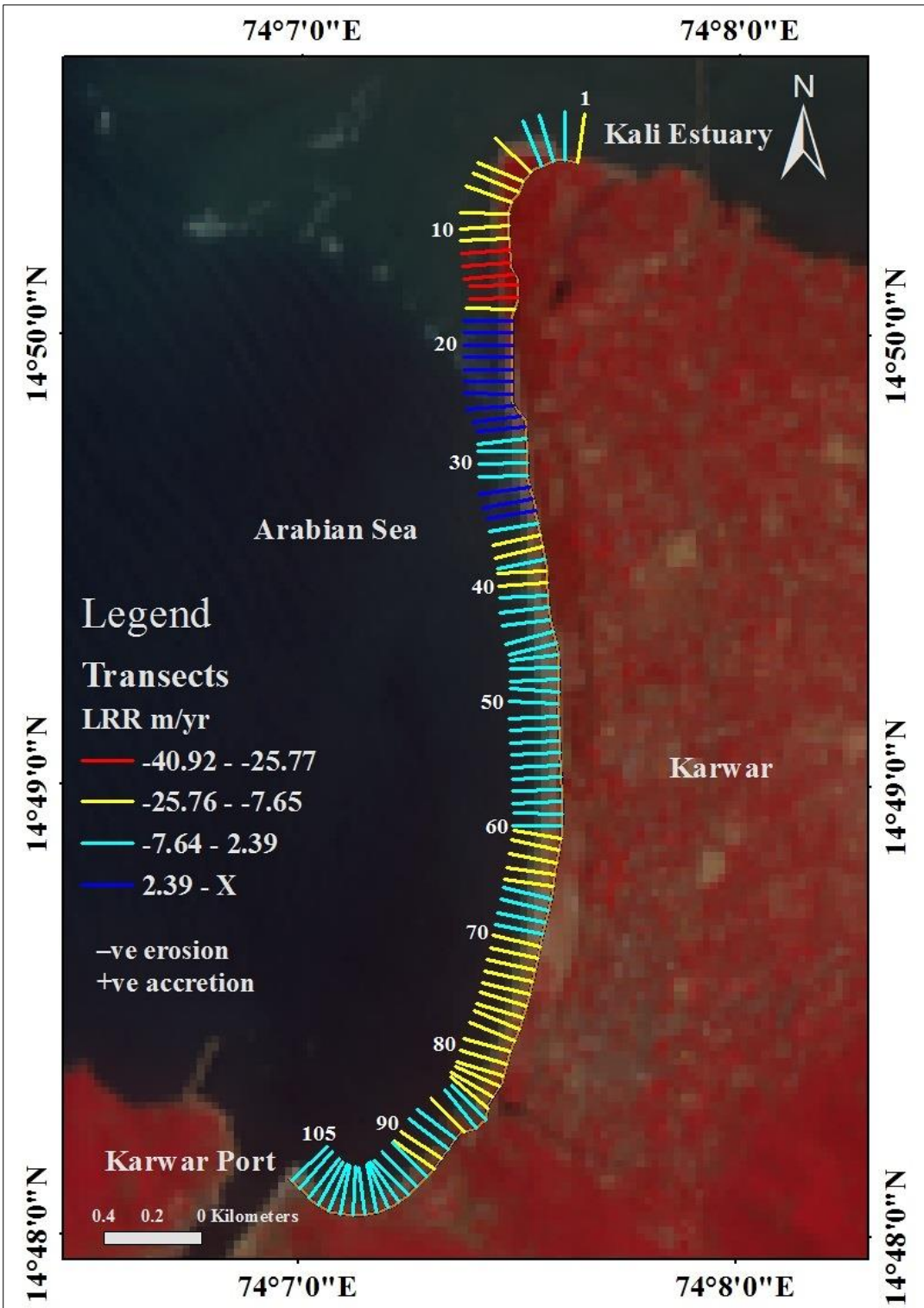Figure 4.10 Pre-monsoon of Ravindranath Tagore Beach

Figure 4.11 Post-monsoon of Ravindranath Tagore beach

From Figure 4.10, Pre-monsoon of Ravindranath Tagore beach, from transects shoreline analysis, was carried out from 2013 to 2017. At transect, 77 maximum

shoreline accretion of 15.13 m/yr (EPR) sediment from Kali estuary is responsible for the accretion on the beach. At transect 13 maximum shoreline accretion 20.16 m/yr (LRR) in this region breakwater was constructed (was commissioned on 2005, 250m west breakwater), due to this accretion may be possible. At transect 63 maximum shoreline erosion of -11.71 m/yr (EPR) and -9.29 m/yr (LRR). And the average shoreline rate is 0.004 m/yr (EPR) and 1.67 m/yr (LRR).

From Figure 4.11, Post-monsoon of Ravindranath Tagore beach considered shoreline change rate (EPR) and (LRR) from 2013 to 2016. At transect 25 maximum shoreline accretion of 16.82 m/yr (EPR) and 14.45 m/yr (LRR) due to sediment transport from estuary and breakwater constructed in this region. At transect 16 maximum shoreline erosion of -36.52 m/yr (EPR) and -40.92 m/yr (LRR). And average erosion rate is -5.77 m/yr (EPR) and -6.55 m/yr (LRR). From the above results, it is evident that the shoreline change rate differs according to the season.

Figure 4.12 shows that during pre-monsoon Ravindranath Tagore beach experiences both accretion and erosion. Sediment transport found to be north to south direction and south to north direction in the case of post-monsoon. From transects 0 to 20 has abrupt changes for Rabindranath Tagore beach; this is due to these transects comes under Kali estuary were sediment supplied and also change in the orientation of the shoreline. These transects receive high energy, and, in the region, it is observed that during pre-monsoon high erosion and high accretion during post-monsoon. Erosion place visit it was evident that Ravindranath Tagore beach most of the region stable in nature and attracted by a lot of tourist and tourism activities. This may also be due to the enhanced human interference along the coast owing to urbanization, harbor development, naval base establishment, and series construction dam to Kali river. On the other hand, Devbagh beach is also stable, except in the estuary and seawall region. This beach has natural breakwater, and, in that region, we witnessed a stable beach.
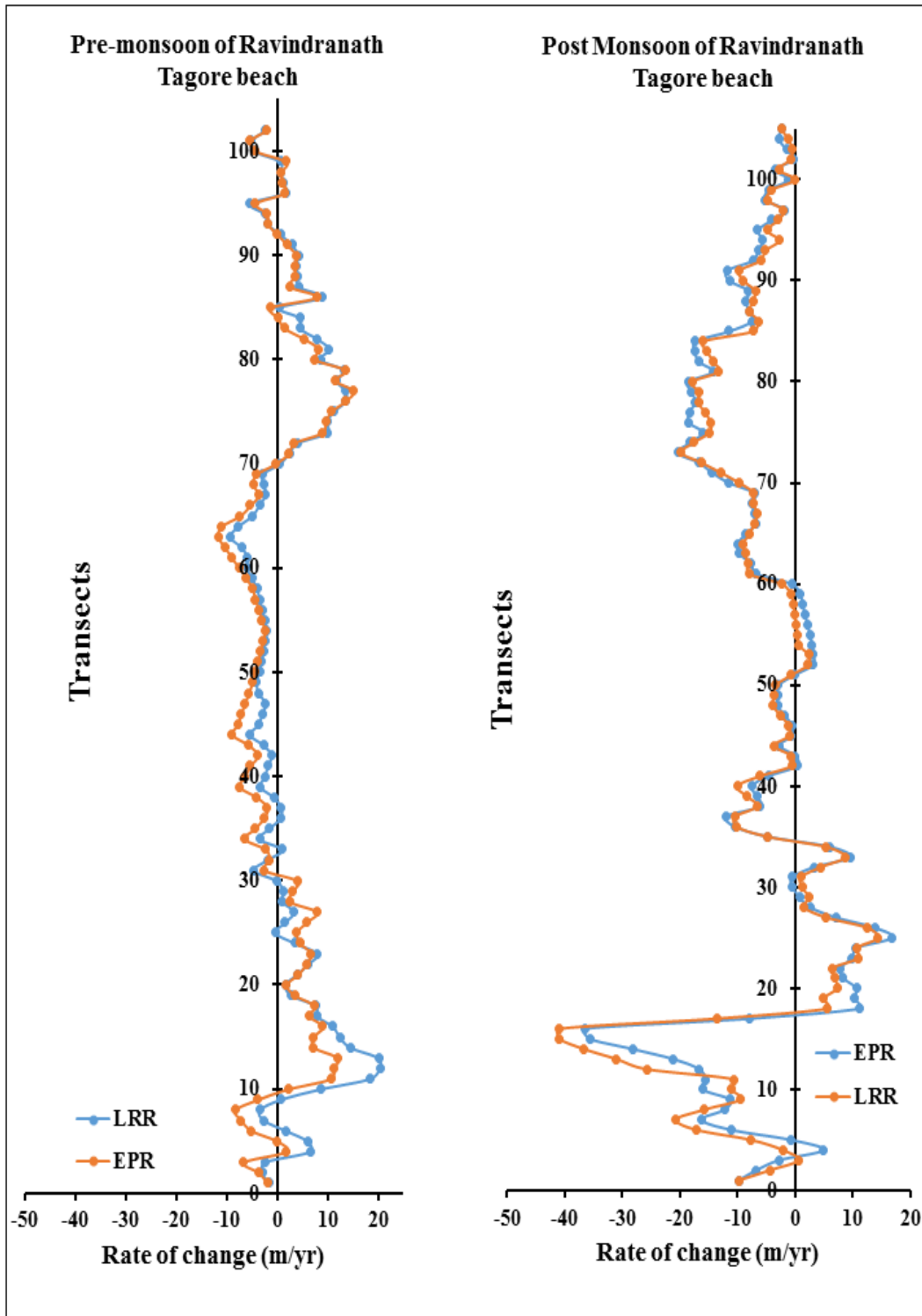
Figure 4.12 Graphs of EPR and LRR for Ravindranath Tagore beach

4.2 Estuary change analysis

The estuary change analysis has been carried for the period from 1976 to 2018. The Landsat satellite for mentioned year collected particularly for December (26/12/1976, 21/12/1989, 20/12/2009 and 21/12/2018). The change in the area of estuary detected, as shown in the map of 1976, 1989, and 2018. It is noticed that the upper part that is estuary region related Devbagh beach is experienced more erosion, and also, the lower part that is estuary region is related to RT beach is experienced less erosion. The lower part beach width is reduced. Earlier the estuary region was with the small passage at the river and sea meeting region. As the year progresses, post-construction of the dam, the passage has been increased. The regulated discharged of water and the sediment trap behind the dam leads to a heavy impact on Kali estuary, especially on the upper part of it. In the case of the lower part of the estuary, the beach width was naturally stable, and the land after that was not exposed to wind, tides, and currents, which can be noticed through the images shown. The river channel near to estuary also eroded, which leads widened of the river channel. The supply of sediment to the estuary is diminished, which leads to a decrease in the beach width.
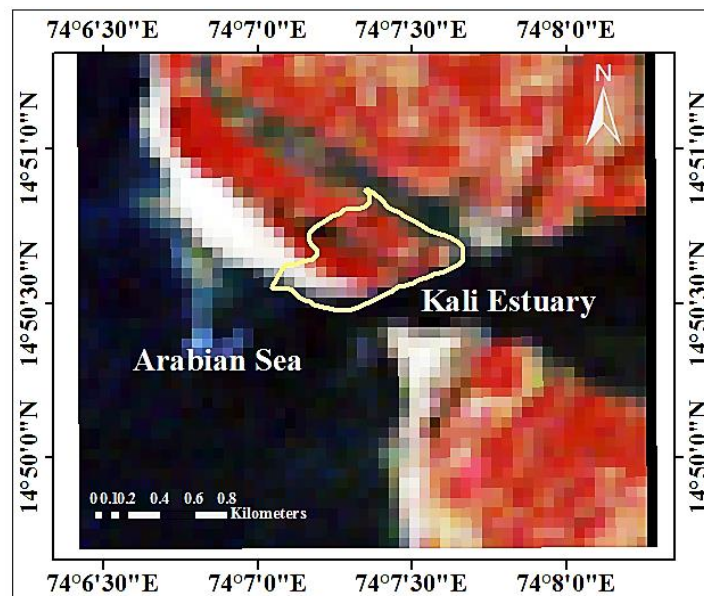
Figure 4.13 The Map of Kali Estuary During 1976

In the lower part, the meandering of the river channel has noticed due to regulated water discharge. Once the regulated water is discharged, the river water becomes raw water,

and hence it starts to erode the river channel bank. This may be the reason for drastic changes in the estuary region as well as the river network channel. The results with figures discussed below.
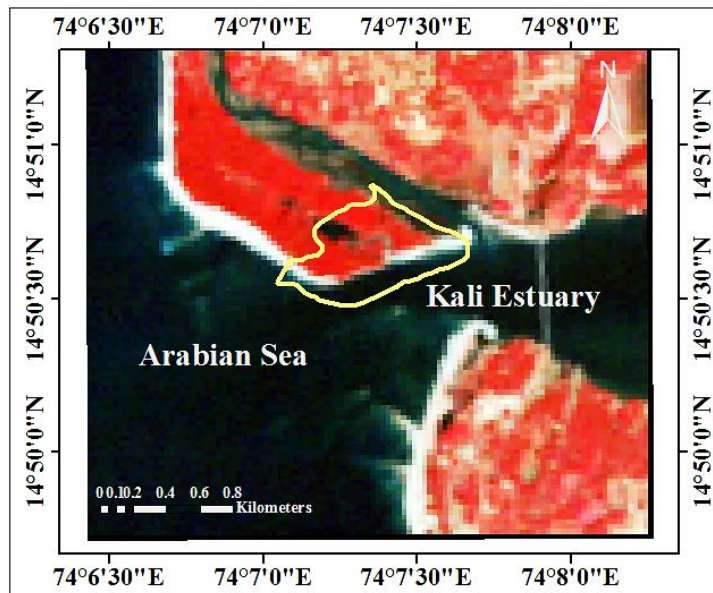
Figure 4.14 The Map Of Kali Estuary During 1989
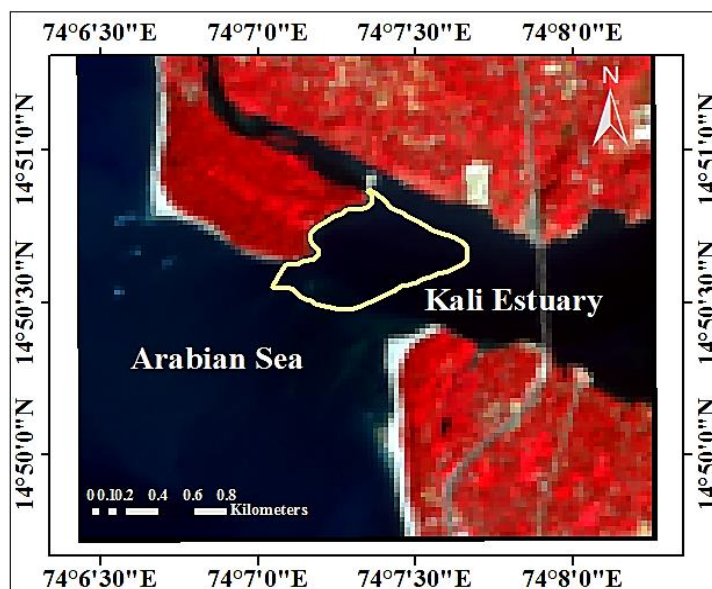
Figure 4.15 The Map of Kali Estuary During 2018

Map during 1976, which is shown in Figure 4.13 considered as a base map for change detection. The area is marked in the yellow color region is experiencing the erosion.

During the pre-construction of the Supa dam, the estuary was in cyclic, the natural flow of water and sediments deposited naturally.

But from the change detection analysis using these maps, the estuary region, which is related to Devabagh beach, is experiencing erosion. Figure 4.14 and Figure 4.15 show the change in the area of the estuary with respect to the year. The area calculation is tabulated in Table 4.1.

Table 4.1 The Details of Kali Estuary of Upper Part Area Vanished (All Calculation with respect to 1976)

Sl. No	Years	Area of Erosion (m^2)
Base	1976	0
	1989	39696.22
	2009	340258.59
	2018	420068.59

Figure 4.16 shows the graph of the area changed and also explains the trend of change in the area. From the graph, it is clear that the area keeps on vanishing from 1976 to 2018, nowhere the indication shown regarding the recovery of the area. This is being linear trendline. From the analysis, it is found to be 420068.59 m^2 been vanished.
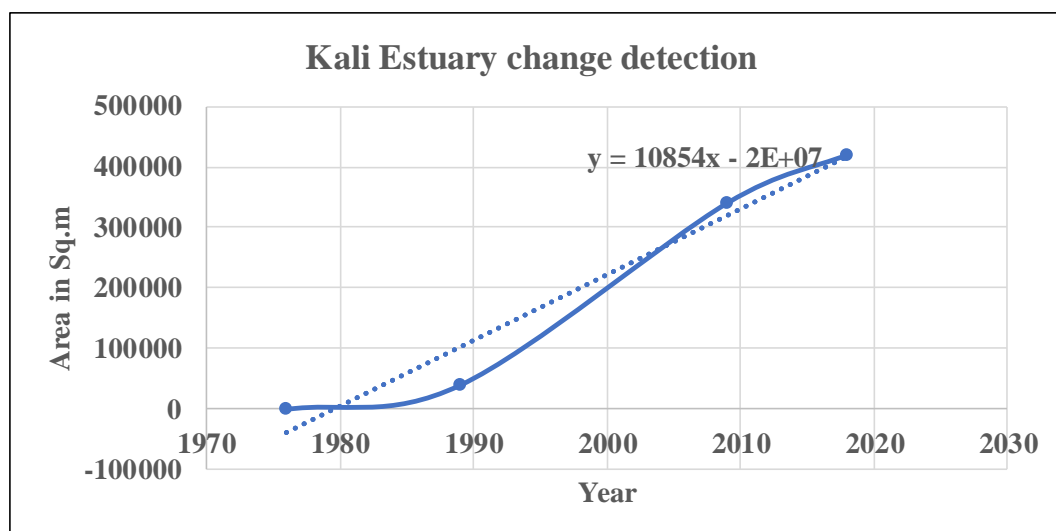
Figure 4.16 The Trend of Area Change In Kali Estuary

During the year 1989, the lower part of the Kali Estuary has experienced more erosion of 159837.23 m^2, and later the years 2009 and 2018, it is noticed that both accretion and erosion are experienced. The details are given in Table 4.2. In the year 2018, the accretion rate is increased when compared to erosion, which may be meandering of river direction towards the lower part of the estuary, which can be noticed from the image.
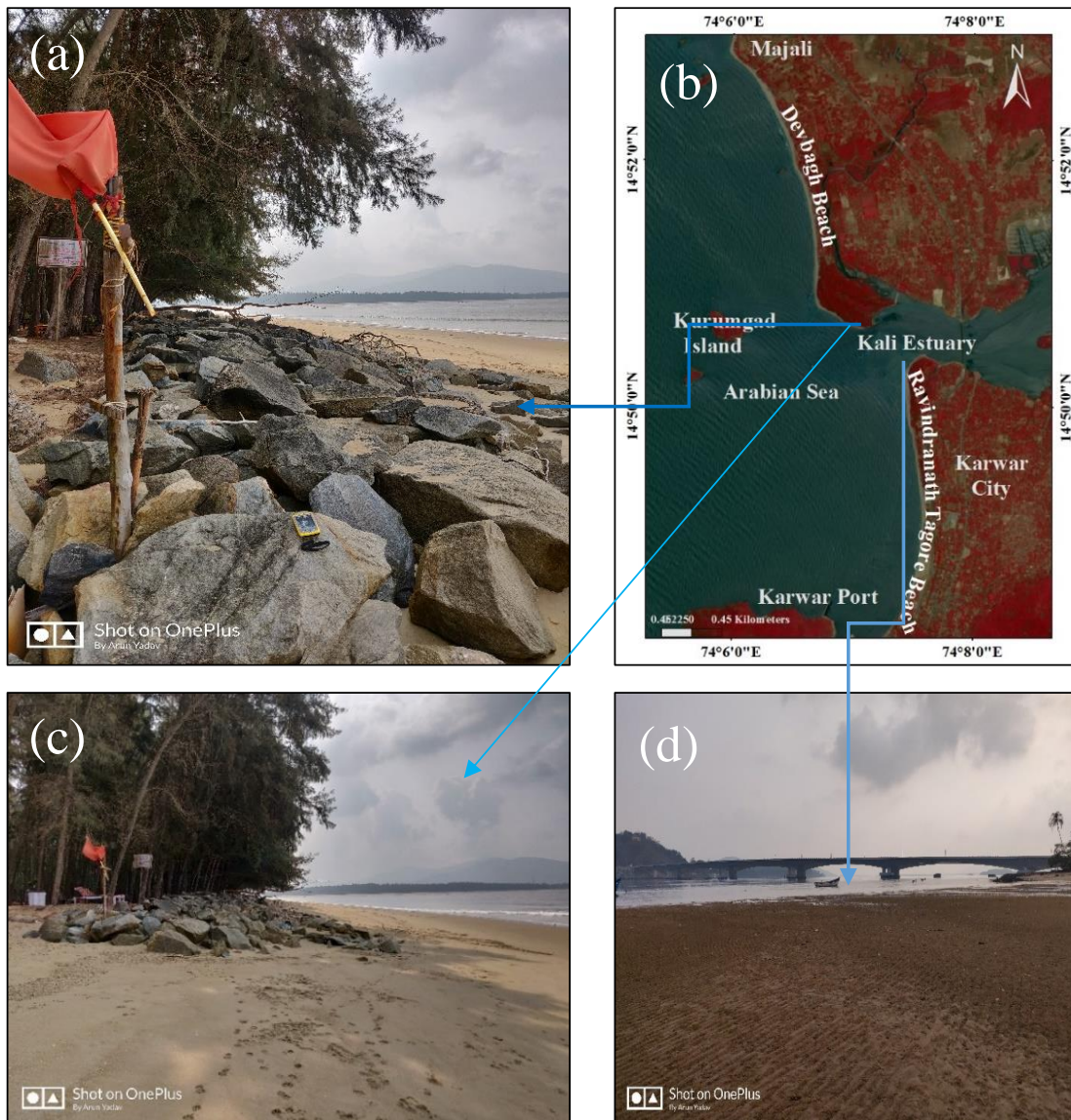
Figure 4.17 (a) Plate 1. Sea wall at Devbagh beach,   (upper part) Kali estuary (b) Location of area (c) Plate 2. Devbagh beach, (upper part) Kali estuary, and (d) Plate 3. The lower part of Kali estuary

During the site visit, it was witnessed that, sea wall has been constructed in the upper part of the estuary region. This sea wall is constructed to avoid erosion in a particular region.

Plate 1 and Plate 2 show the sea wall constructed at the upper part of the Kali estuary, and Plate 3 shows the lower part of the Kali estuary. From plate three it is evident that, due to the regulated discharge of water from the dam, the Kali river is not met to the Kali estuary naturally.

Table 4.2 The Details of Kali Estuary of Lower Part Area Vanished (All Calculation with respect to 1976)

		Accretion	Erosion
Base	1976	0.00	0.00
	1989	0.00	159837.23
	2009	17744.21	57320.89
	2018	21636.62	45770.71

4.3 Land use land cover change analysis

Land use land cover of the three study areas was studied in different decades.ie; 1985,1995 and 2005. In Kali and Aghanashini basin, the forest cover is more. Down the decade's forest cover has been decreasing due to various developmental activities. In the Kali river basin, construction of the dam is one of the major reasons for the changes of LULC. The result obtained is presented in Table 4.3 and Table 4.4 for the Kali river basin and the Aghanashini river, respectively.

Table 4.3 Kali River Basin

LULC	1985(%)	1995(%)	2005(%)
Agriculture	15.56	17.09	18.90
Barren land	4.34	4.01	3.65
Built up	1.26	2.10	3.77
Fallow land	3.12	2.72	2.56
Forest	69.47	65.11	62.57
Other vegetation	2.58	3.21	3.12
Plantations	1.98	2.07	2.34
Water bodies	1.69	3.69	4.09

Table 4.4 Aghanashini River Basin

LULC	1985(%)	1995(%)	2005(%)
Agriculture	6.97	8.65	10.78
Barren land	2.67	3.78	4.87
Built up	0.74	1.19	2.75
Shrub land	2.23	2.87	3.04
Forest	80.35	75.6	73.34
Plantations	5.34	5.78	6.33
Water bodies	1.70	2.13	1.89

4.4 Impact of the dam on sediment yield

4.4.1 Calibration and validation of streamflow Kali river basin

Kali river basin has five series of the dam, as mentioned in chapter 3. The data of all discharged dams are collected and given as a dam input file. The calibration and validation result is shown one by one, starting from the Supa dam to the Kadra dam, respectively.

4.4.2 Supa dam with gridded data

The uppermost portion of the Kali river basin consists of a dam, Supa was constructed in 1987. Calibration and validation up to the Supa dam were done using dam inflow data. IMD gridded rainfall data were available up to 2013, and from 2011, station data is available. Therefore, from1989 to 2010 model uses IMD data for simulation and from the 2011 model used station data.
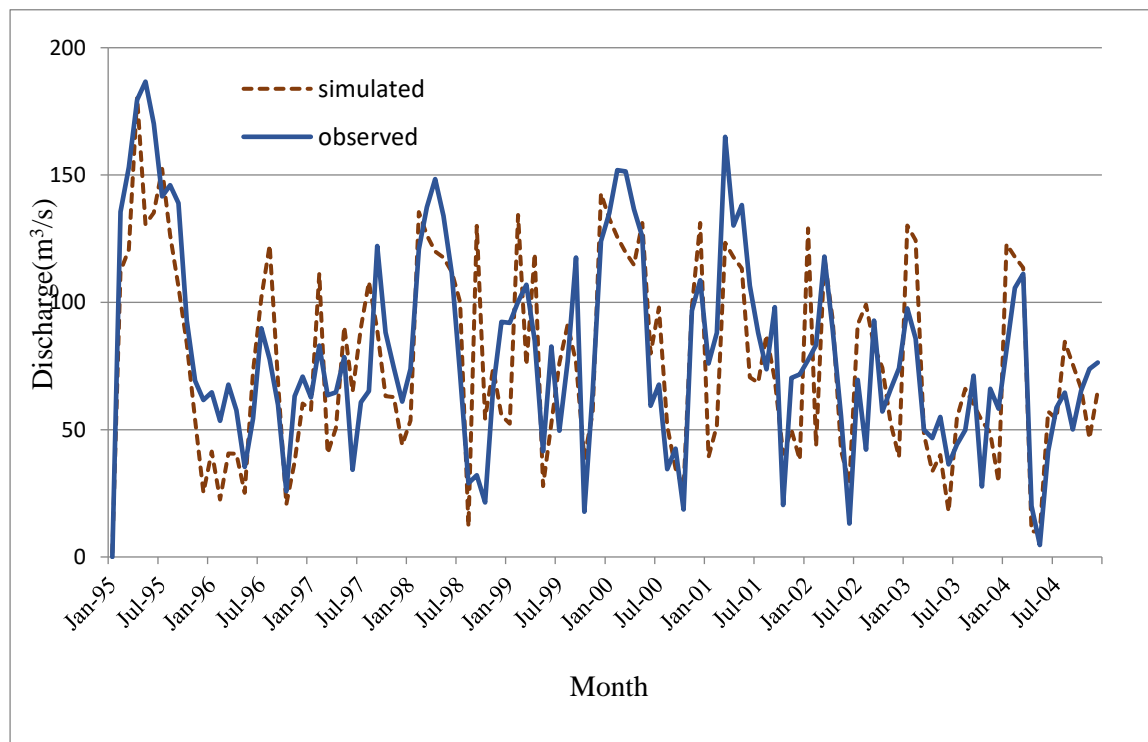
Figure 4.18 Observed v/s Simulated for Calibration using Gridded Rainfall Data

Figure 4.19 Scatter plot for Calibration using Gridded Rainfall Data
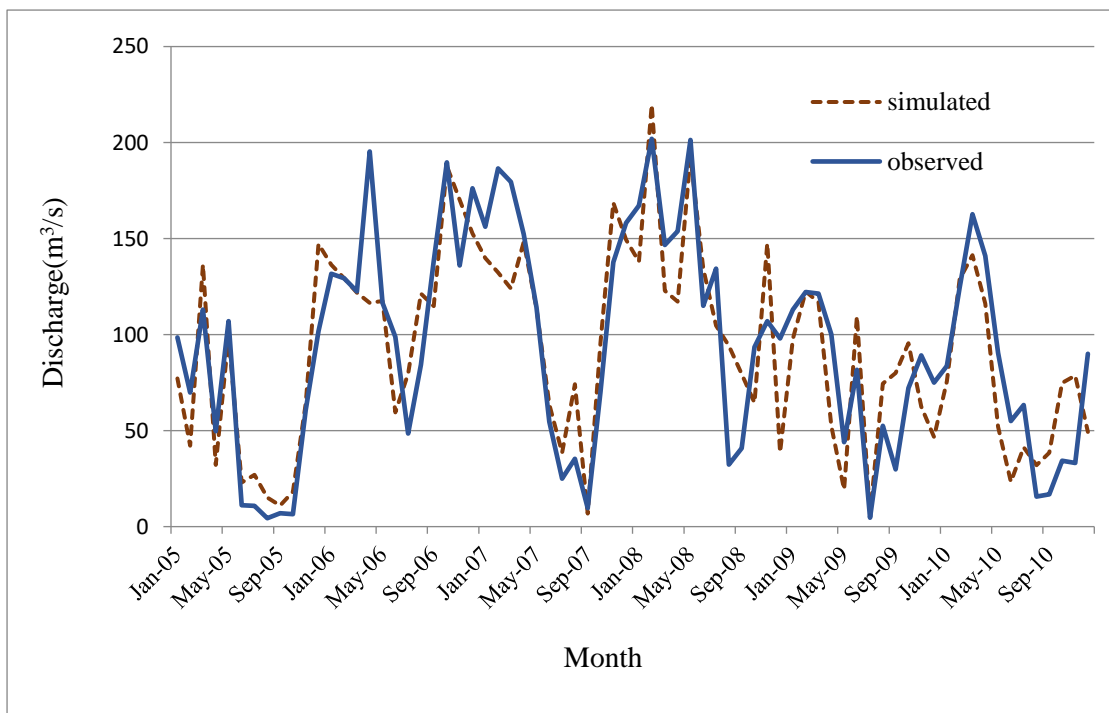
Figure 4.20 Observed V/S Simulated for Validation using Gridded Rainfall Data

Figure 4.21 Scatter plot for Validation using gridded rainfall data

By using IMD gridded data model gives an R2 of 0.60 during calibration and 0.71 during validation. Station data gives better results, and it is represented in table 4.7 and 4.8 repectively. During calibration, NSE is 0.65 PBIAS is 3.09%, and during validation, NSE is 0.66, and PBIAS is 4.78%.

4.4.3 Supa dam with rain gauge station data

The rainfall station data is available from 2011 to 2017. The model was simulated for calibration of 2011 to 2015 and simulated for validation from 2016 to 2017.

Figure 4.22 Observed V/S Simulated for Calibration using Station data

Figure 4.23 Scatter plot for Calibration using Station data

Figure 4.24 Observed V/S Simulated for Validation using Station data

From the above graphs, it is found to be, the calibration using station data gives an R^2 of 0.77, NSE of 0.73, and PBIAS of 6.22%.
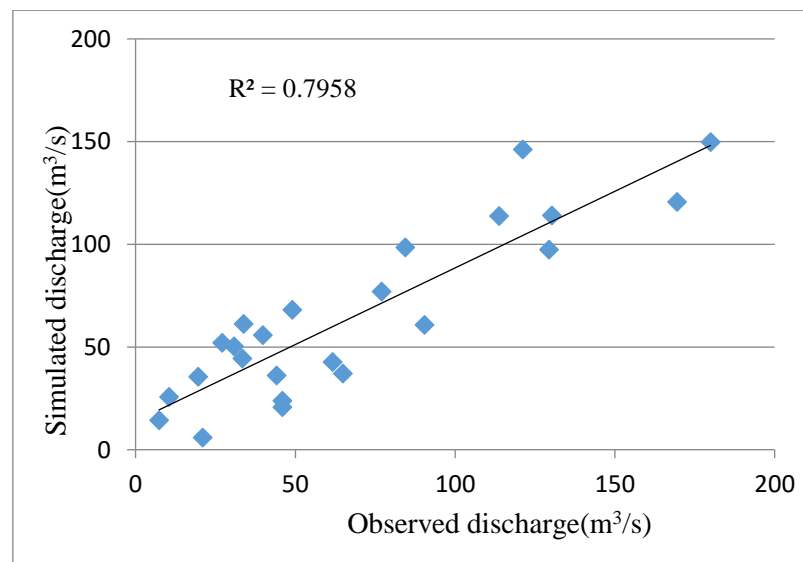
Figure 4.25 Scatter plot for Validation using Station Data

Validation gives an R^2 of 0.79, NSE of 0.78, and PBIAS of 8.76%. This result implies that the result obtained from station data are more reliable.

4.4.4 Bommanahalli dam

Bommanahalli dam constructed in 1979 and data was available from 2009. Station rainfall data used for calibration and validation.

Figure 4.26 Observed V/S Simulated for Calibration using Station data

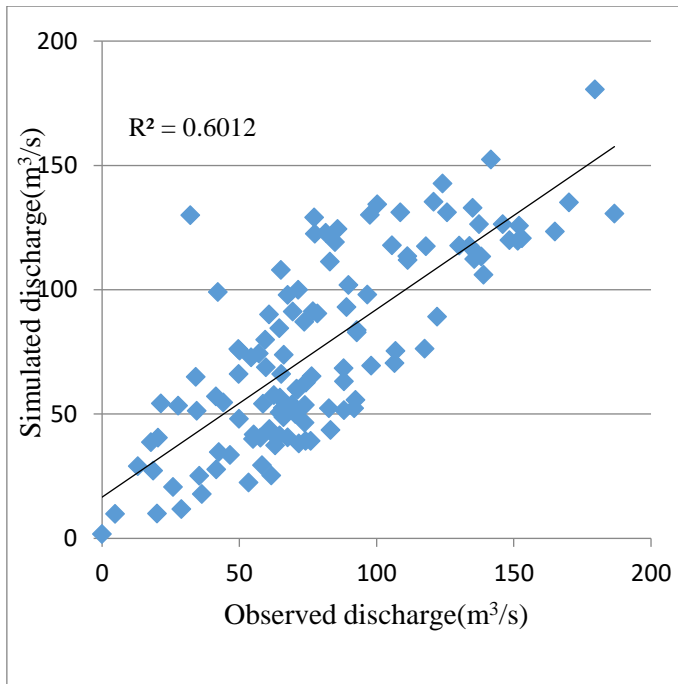

Figure 4.27 Scatter plot for Calibration using Station data

Figure 4.28 Observed V/S Simulated for Validation using Station data
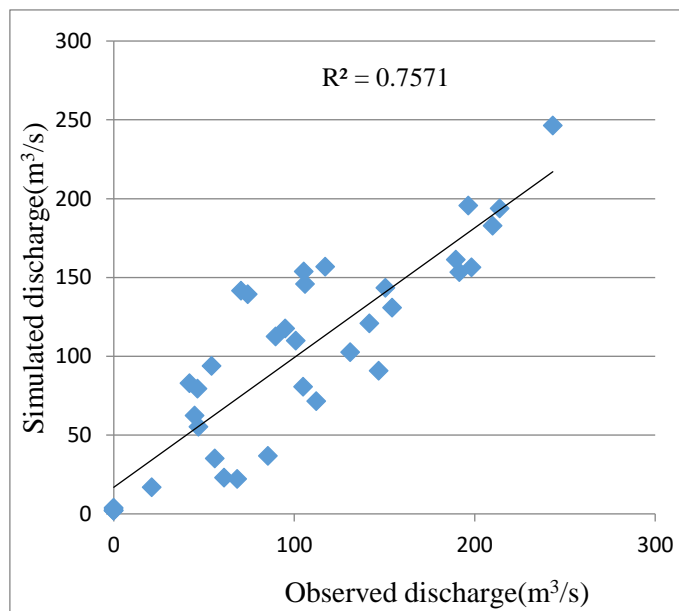
Figure 4.29 Scatter plot for Validation using Station data

Calibration gives an R^2 of 0.64, NSE of 0.62, and PBIAS of 16.78%. Validation gives an R^2 of 0.75, NSE of 0.71, and PBIAS of 13.25%.

4.4.5 Thattihalla dam

Dam data is available from 2009. Therefore, Calibration and validation conducted using rainfall station data.

Figure 4.30 Observed V/S Simulated for Calibration using Station data

Figure 4.31 Scatter plot for Calibration using Station data

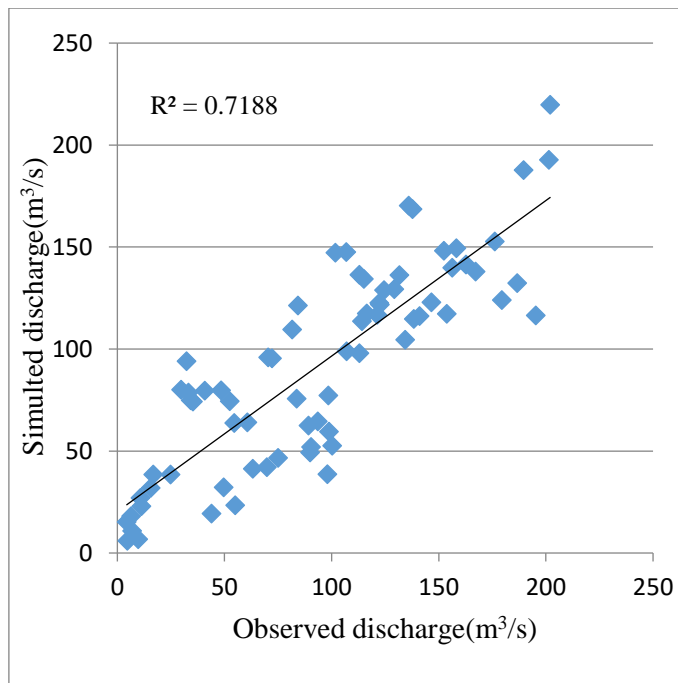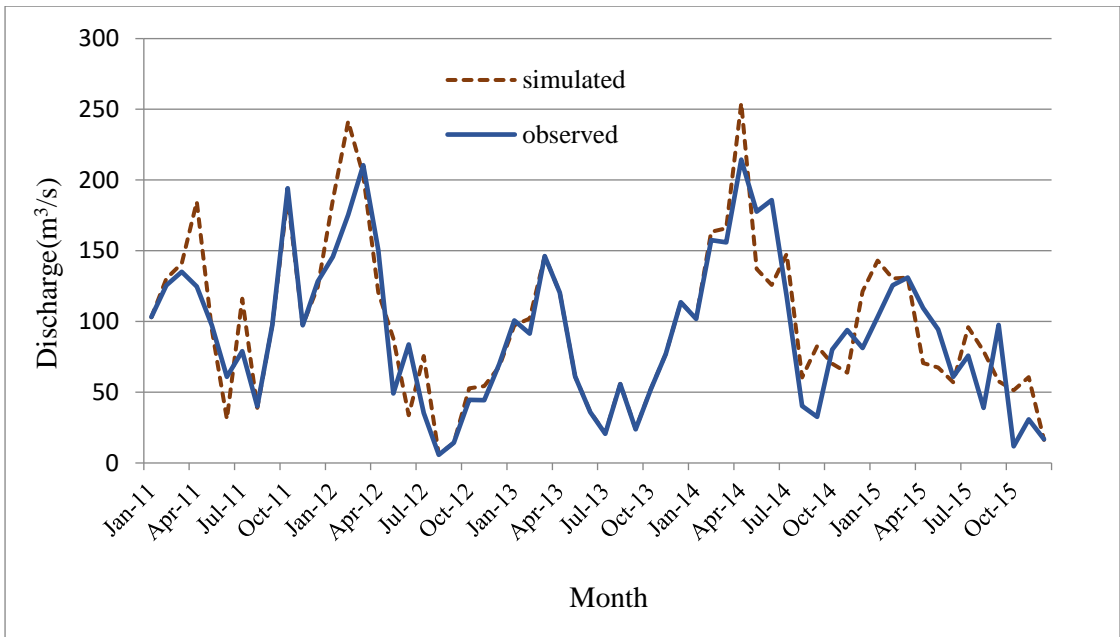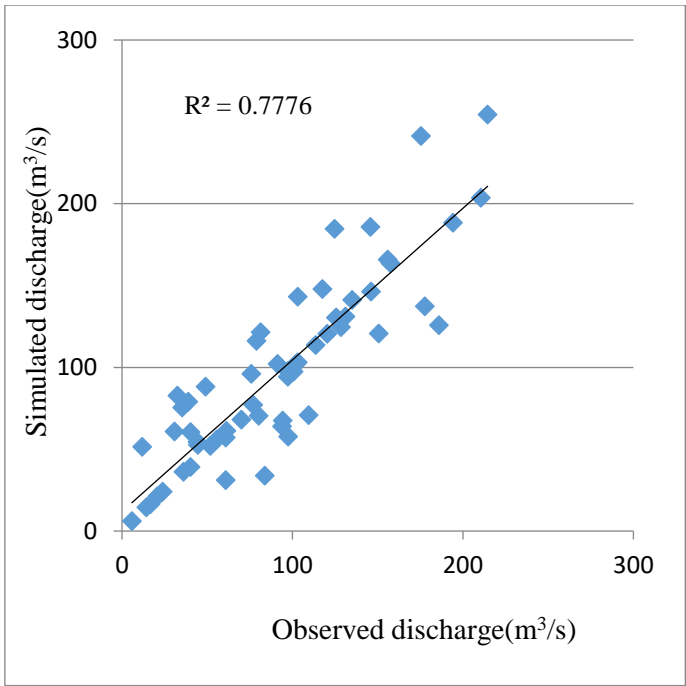Figure 4.32 Observed V/S Simulated for Validation using Station data

Figure 4.33 Scatter plot for Validation using Station data

Calibration gives an R^2 of 0.69, NSE of 0.64, and PBIAS of 13.78%. Validation gives an R^2 of 0.66, NSE of 0.64, and PBIAS of 18.25%.

4.4.6 Kodasalli dam

For the Kodasalli dam, data is available from 2000. From 2000 to 2010, rainfall gridded data used for simulation. From 2011 to 2017, station data used.

Figure 4.34 Observed V/S Simulated for Calibration using gridded data

Figure 4.35 Scatter plot for Calibration using gridded data

Figure 4.36 Observed V/S Simulated for Validation using gridded data
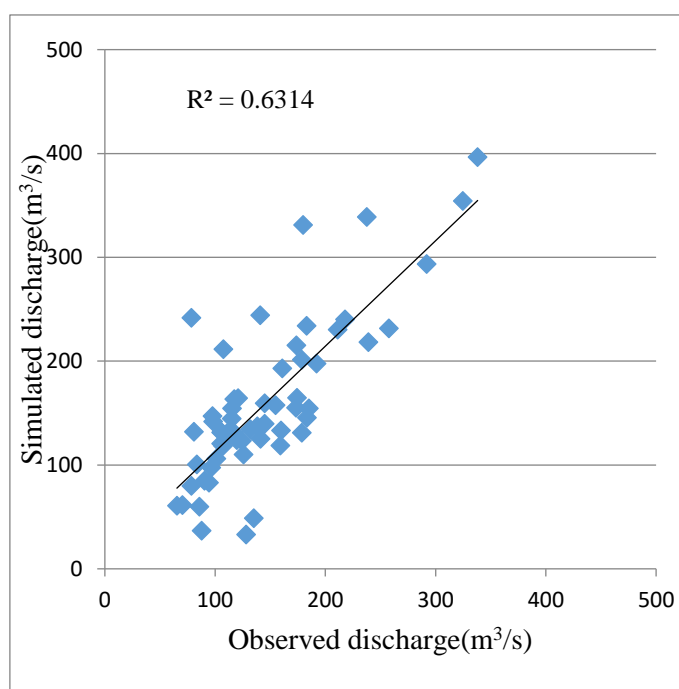
Figure 4.37 Scatter plot for Validation using gridded data

Calibration results using gridded rainfall data shows an R^2 of 0.62, NSE of 0.60, and PBIAS of 18.97%. Validation gives an R^2 of 0.63, NSE of 0.60, and PBIAS of 12.34%.

4.4.6.1 Kodasalli dam with rain gauge station data
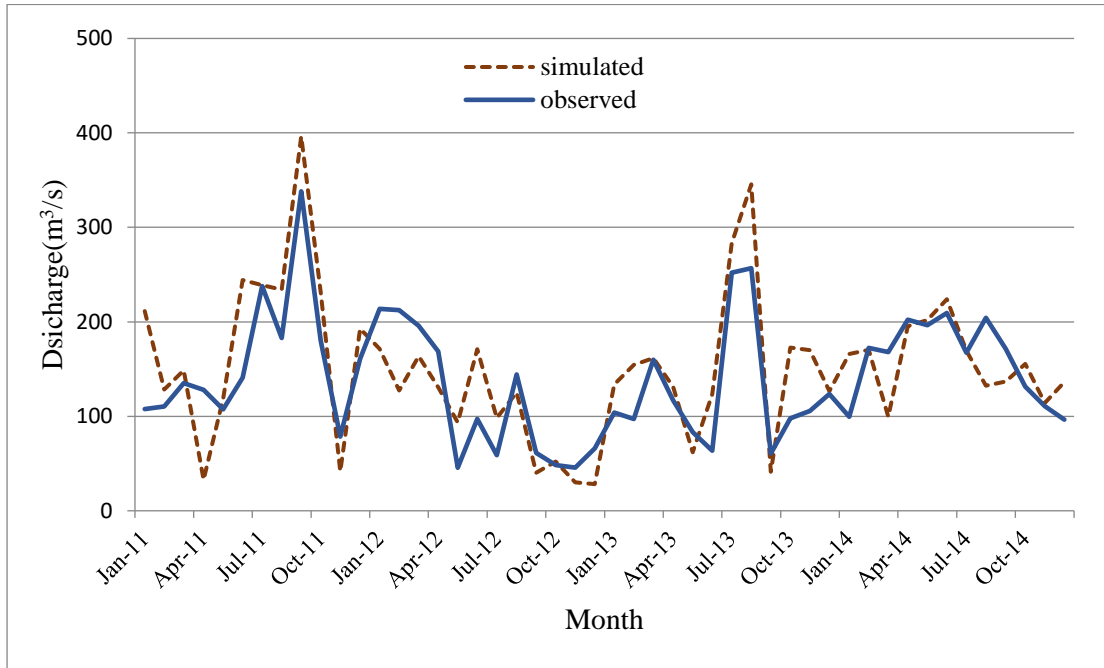
Figure 4.38 Observed V/S Simulated for Calibration using Station data
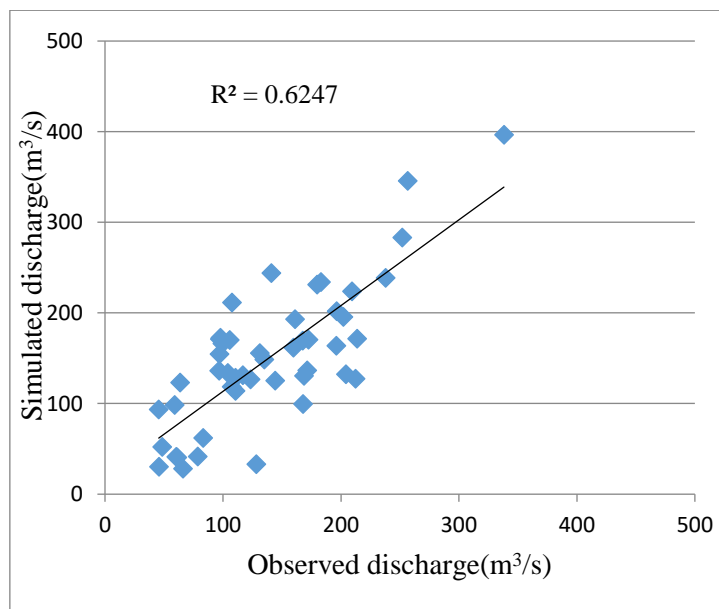
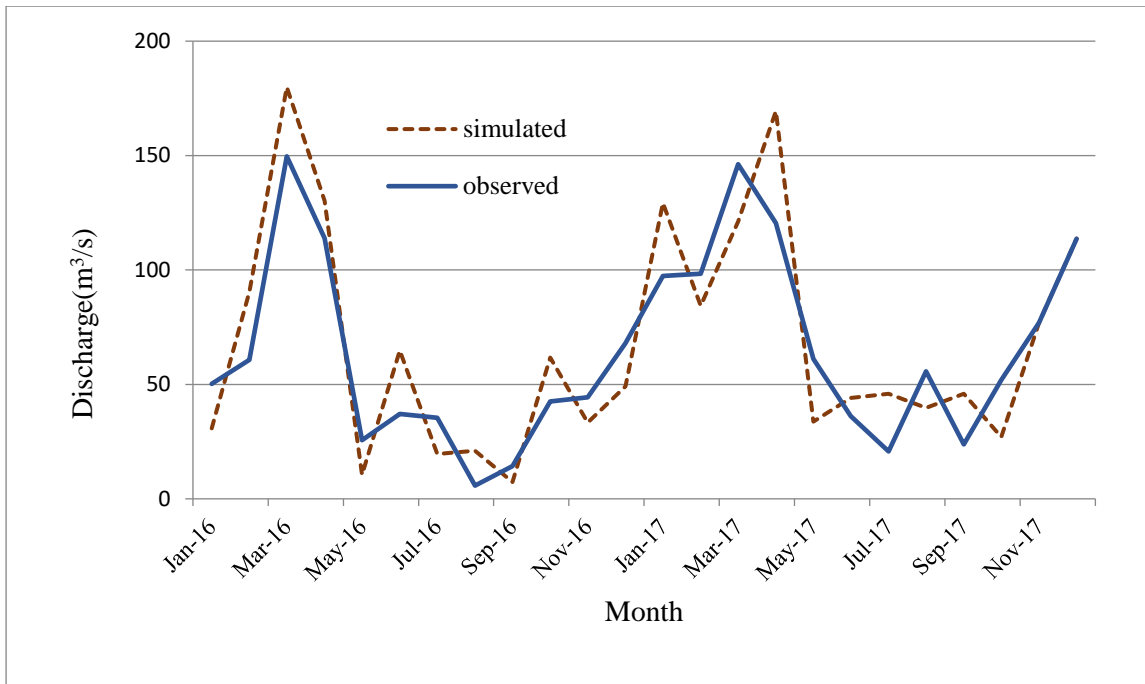Figure 4.39 Scatter plot for Calibration using Station data
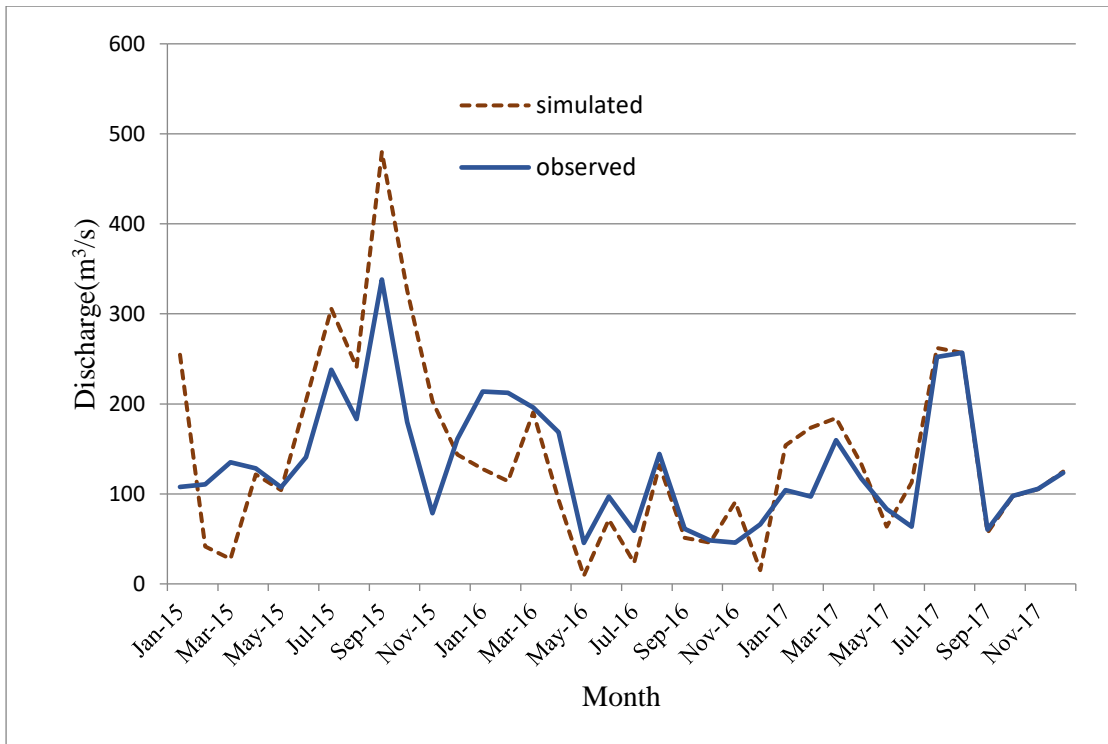
Figure 4.40 Observed V/S Simulated for Validation using Station data
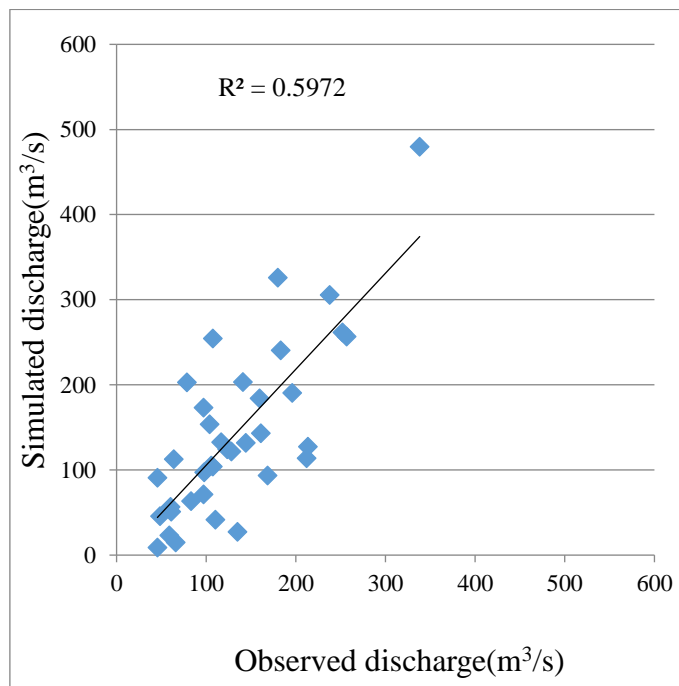
Figure 4.41 Scatter plot for Validation using Station data

Calibration results using gridded rainfall data shows an R^2 of 0.65, NSE of 0.64, and PBIAS of 12.97%. Validation gives an R^2 of 0.67, NSE of 0.61, and PBIAS of 6.34%.

4.4.7 Kadra dam

For Kadra also simulation was made with IMD gridded data and station data. The results presented in the figure below.
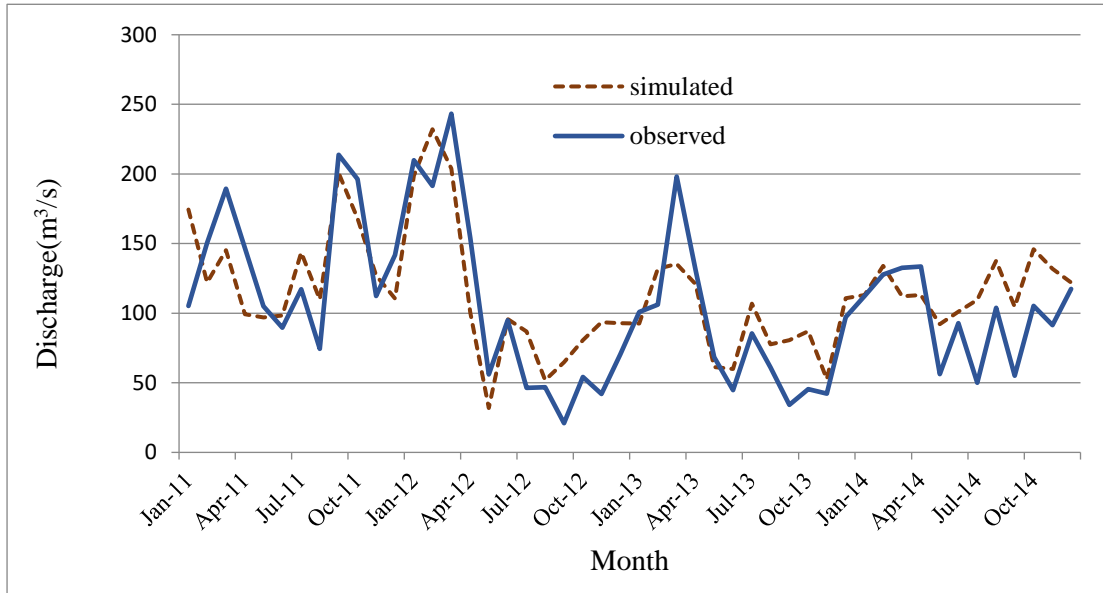

Figure 4.42 Observed V/S Simulated for Calibration using gridded data
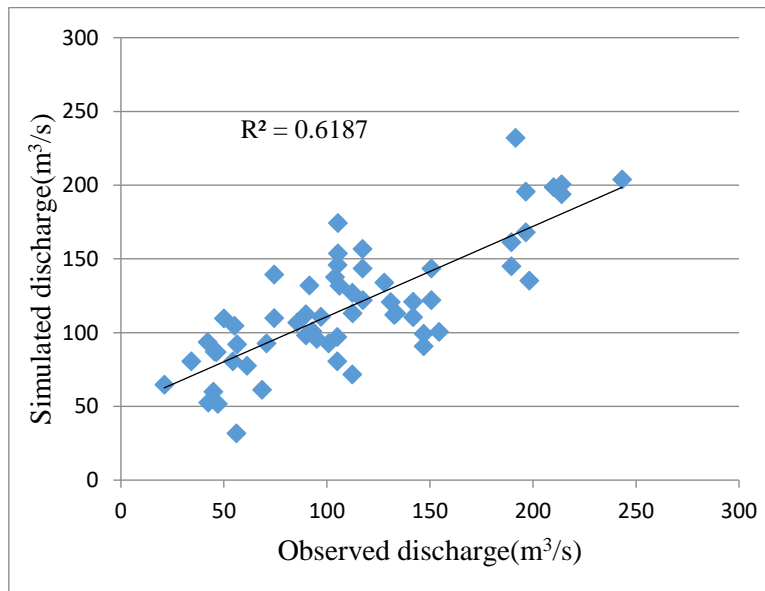

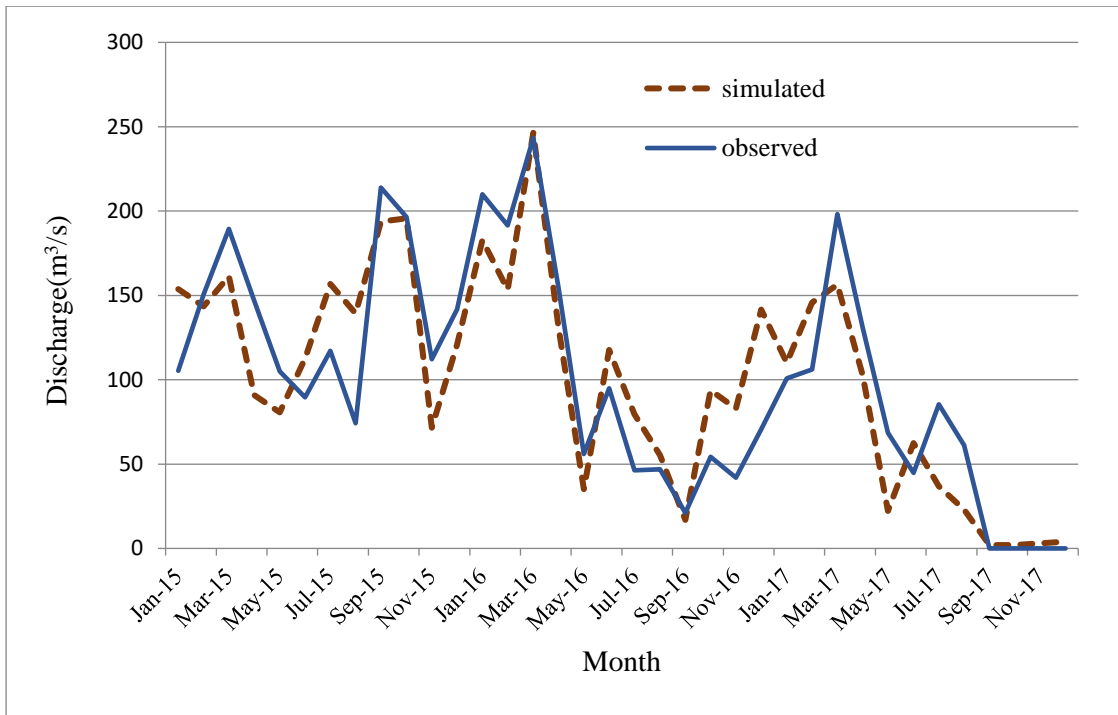Figure 4.43 Scatter plot for Calibration using gridded data
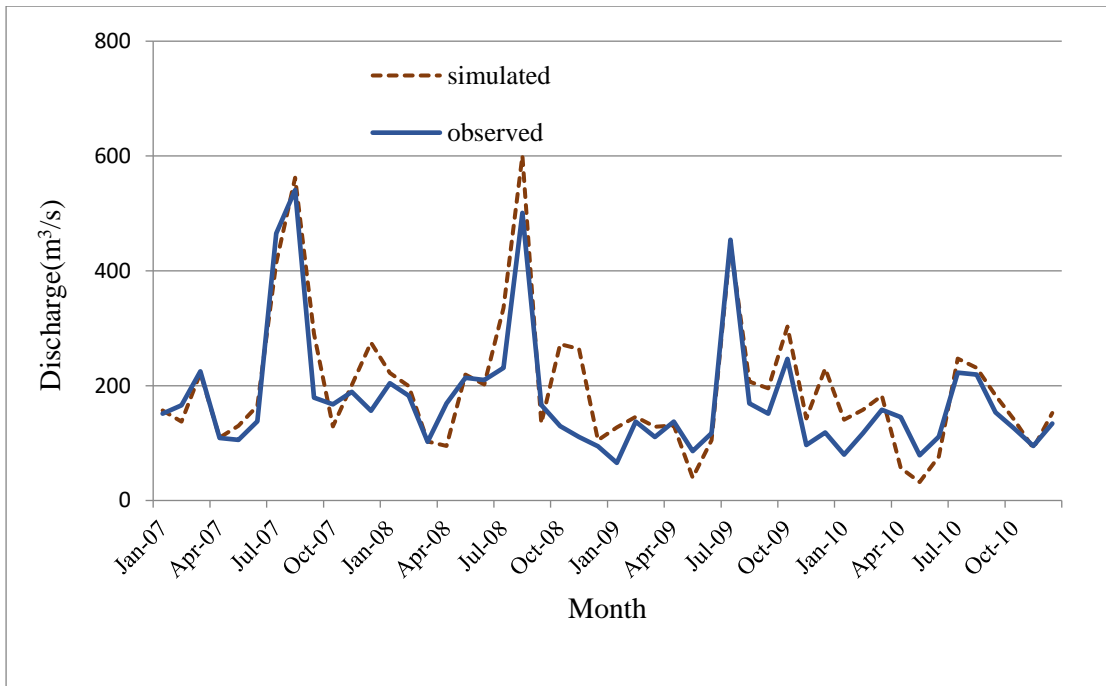
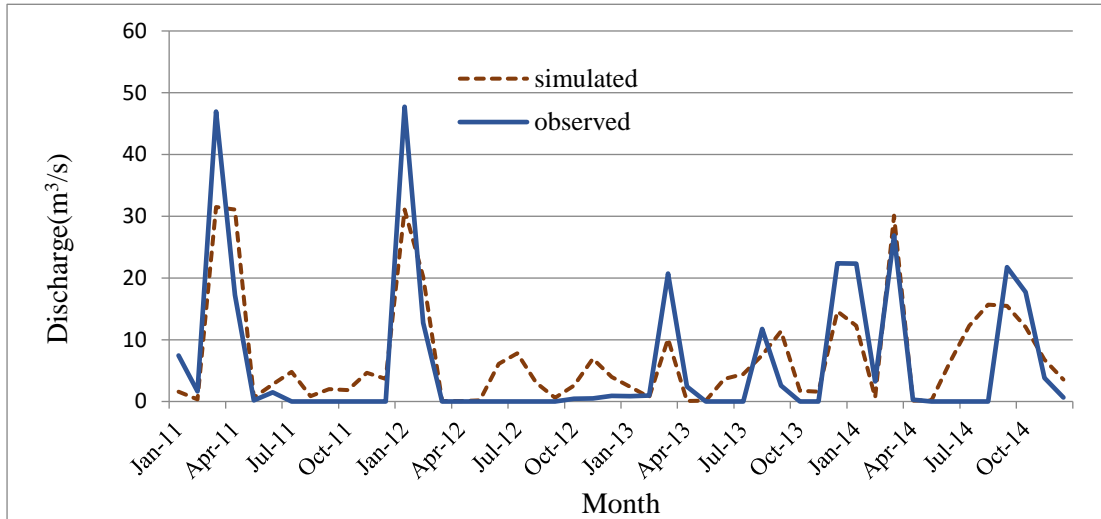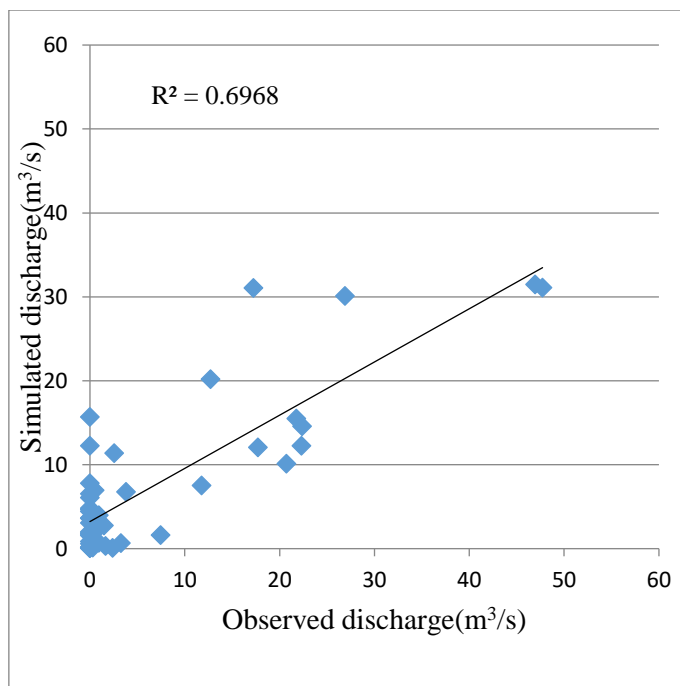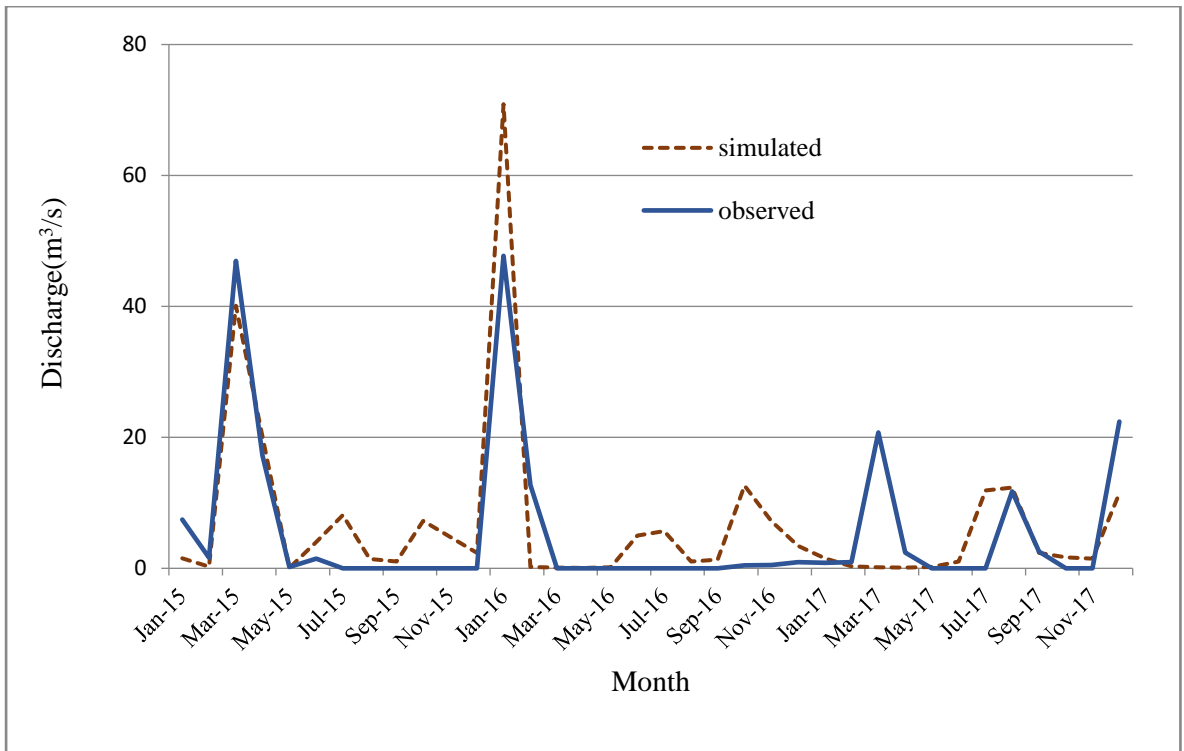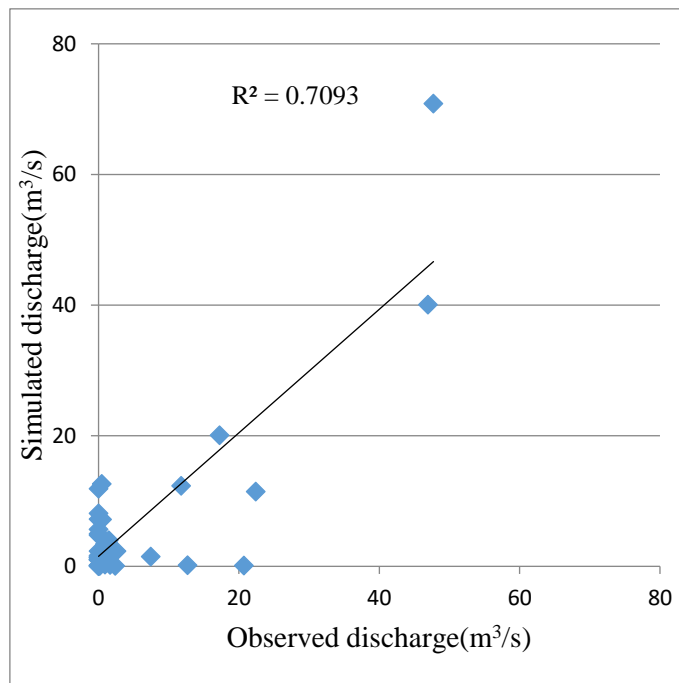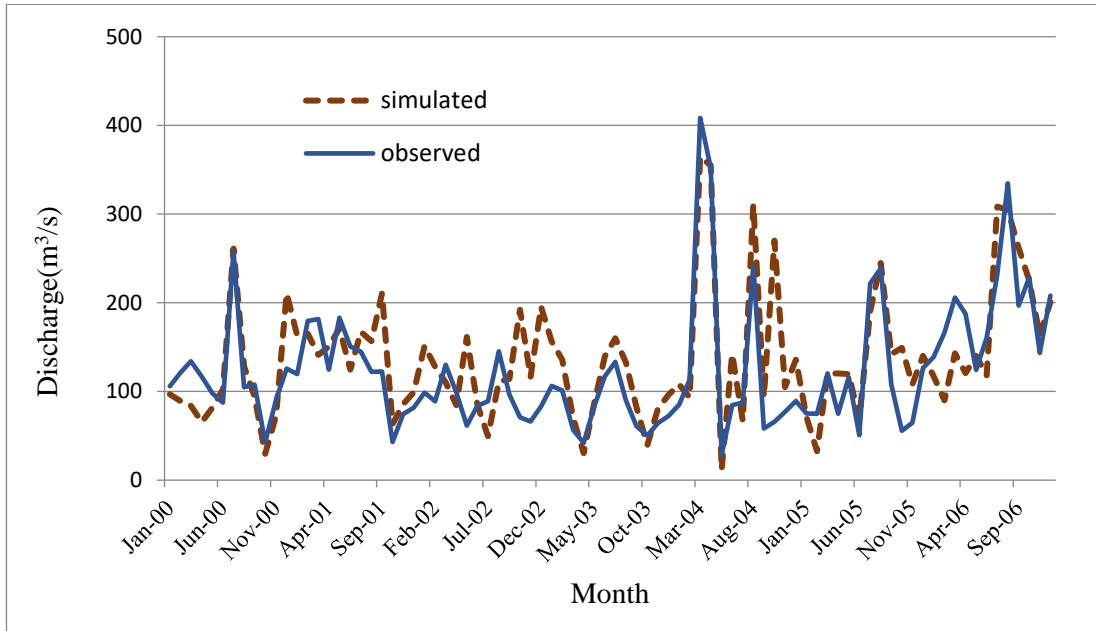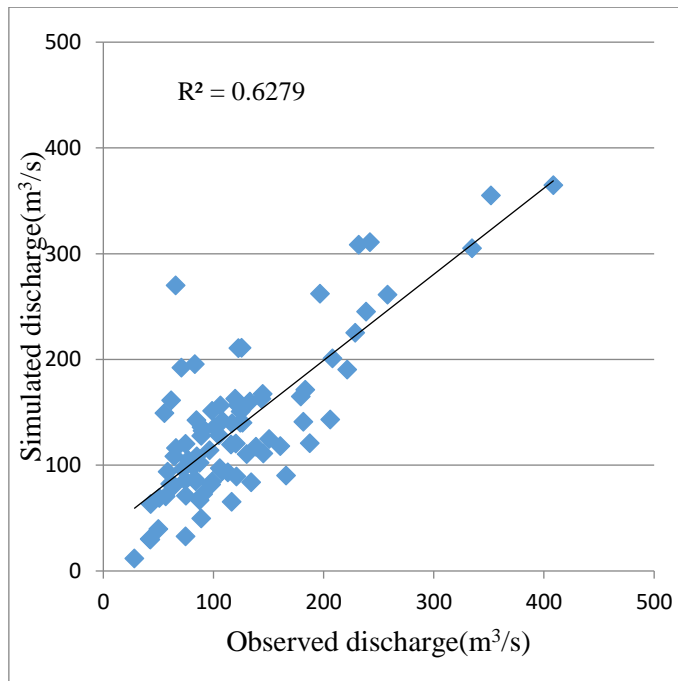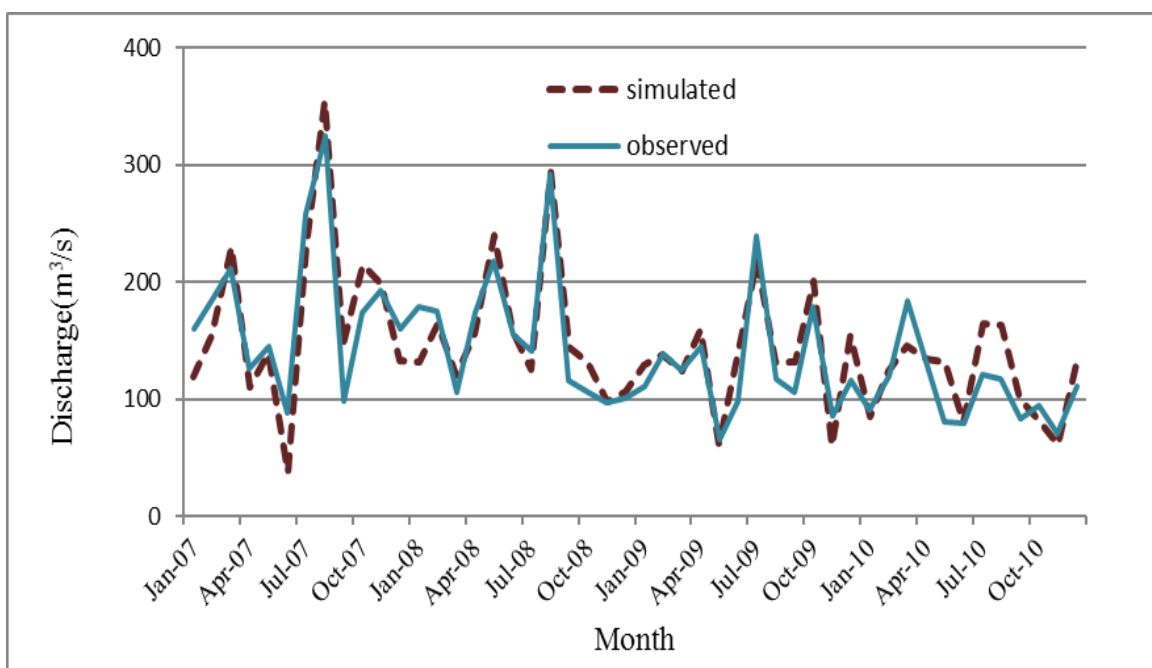Figure 4.44 Observed V/S Simulated for Validation using gridded data
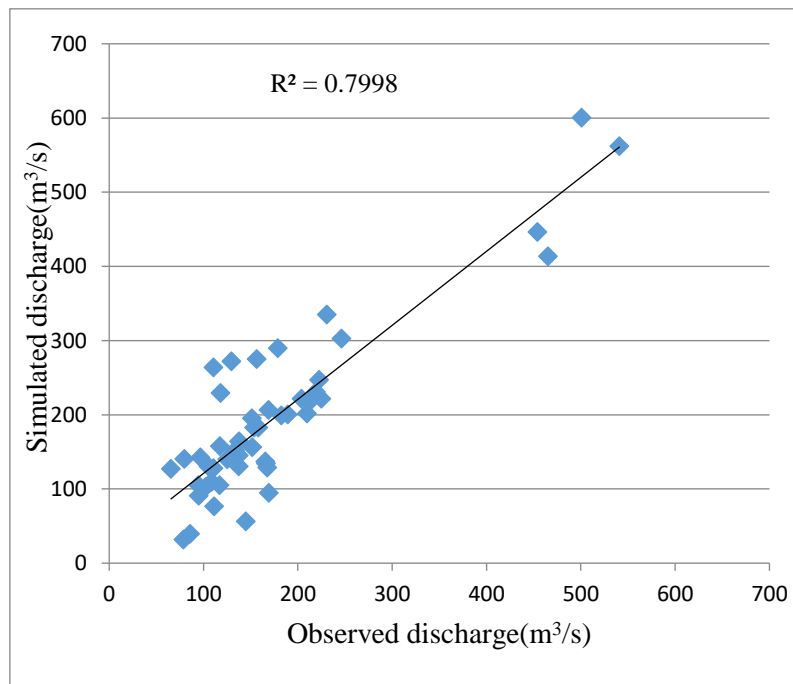
Figure 4.45 Scatter plot for Validation using gridded data

Calibration shows an R^2 of 0.77, NSE of 0.69, and PBIAS of 17.02%, and validation gives an R^2 of 0.79, NSE of 0.71, and PBIAS of 14.37%.

4.4.7.1 Kadra dam rain gauge station data

At the outlet of the Kali basin, river discharge data was predicted and compared at one of the downstream dam points, Kadra, the last dam before joining the Arabian sea from 2011-2017. The comparison was with the available observed data for the Aghanasini basin. This data was available from 2010-2016 at Santeguli station. The physical and hydro metrological characteristics of the basin imply the hydrological response with the similarity of the two basins (Table 5.2). So, we use the same parameter for streamflow simulation of both the basins.

The SWAT model calibrated at a daily time scale based on the river discharge data for the Kali river basin. Four years (2012–2015) were chosen for calibration and two years (2016–2017) for the validation processes with one year as a warm-up period (2011). Several parameters have influenced more on the output, were selected after the sensitivity analysis. These parameters were used to calibrate the model by the SWAT-CUP program. The parameter was used to run for the Kali river basin and compared the streamflow results with the Kadra reservoir inflow data. The existence of a series of the reservoir in the Kali river basin with the regulated flow, which gives the comparison plot of simulated and observed data. From the scatter plot between observed and simulated data for both calibration and validation, shows the performance of the model.

Table 4.5 Characteristics of Kali and Aghanashini basins*(Source: Oudin et al., 2010)*

River	Area (km²)	Slope (%)	Average Rainfall (mm)	Elevation (m)	Soil	Length (km)
Kali river	4188	139%	3200	1-1037m from MSL	Red soil, Lateritic and black soil	184
Aghanshini river	1449	119%	3500	0-931m from MSL	Red soil, Lateritic and black soil	127

Statistical analysis results that obtained from calibration and validation are R^2= 0.81, NSE=0.78, PBIAS = 9.4%, and R2=0.79, NSE= 0.73, PBIAS= -6.5% respectively. It leads to satisfactory results that may occur due to the highly regulated flow of reservoir

in the Kali river basin. Therefore, the model can be used for further hydrological studies in similar areas.
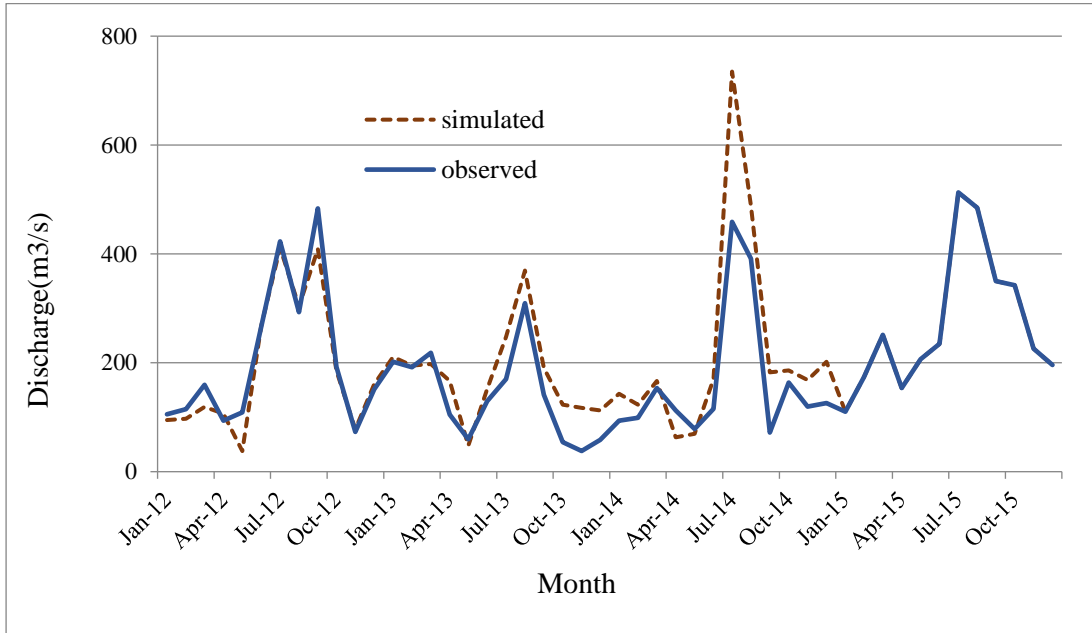
Figure 4.46 Observed V/S simulated for calibration of Kali river basin
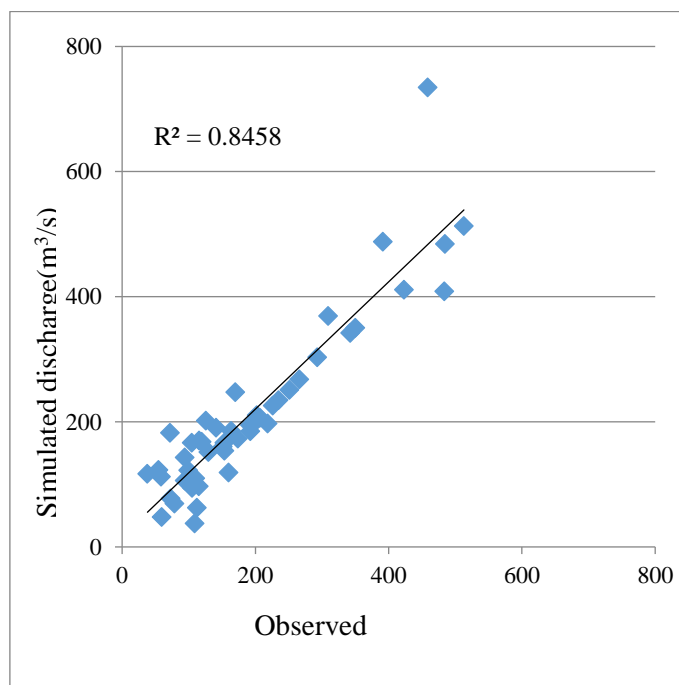
Figure 4.47 Scatter plot for calibration of Kali river basin
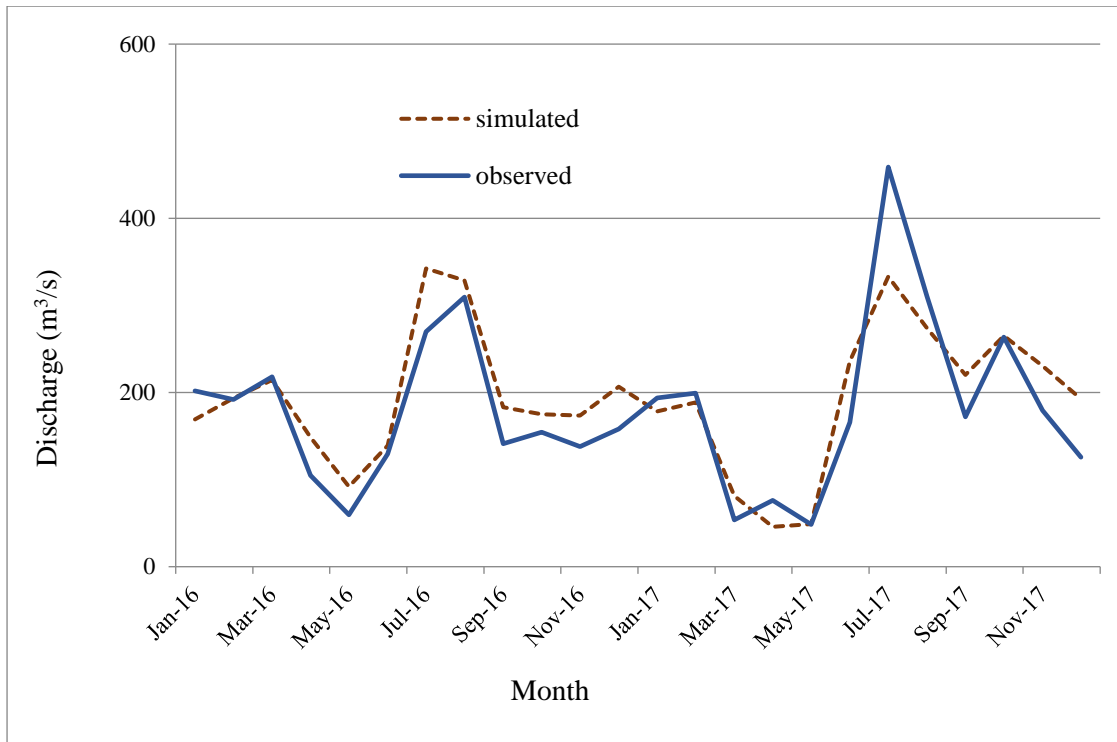
Figure 4.48 Observed V/S simulated for validation of Kali river basin
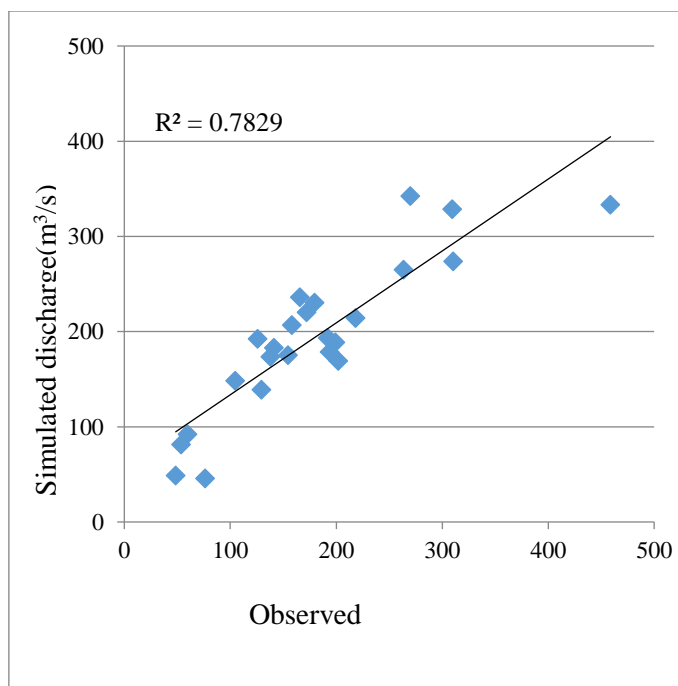
Figure 4.49 Scatter plot for validation of Kali river basin

4.4.7.2 Without dam condition

SWAT runs from 1955 to 2017 using both gridded data as well as station data.
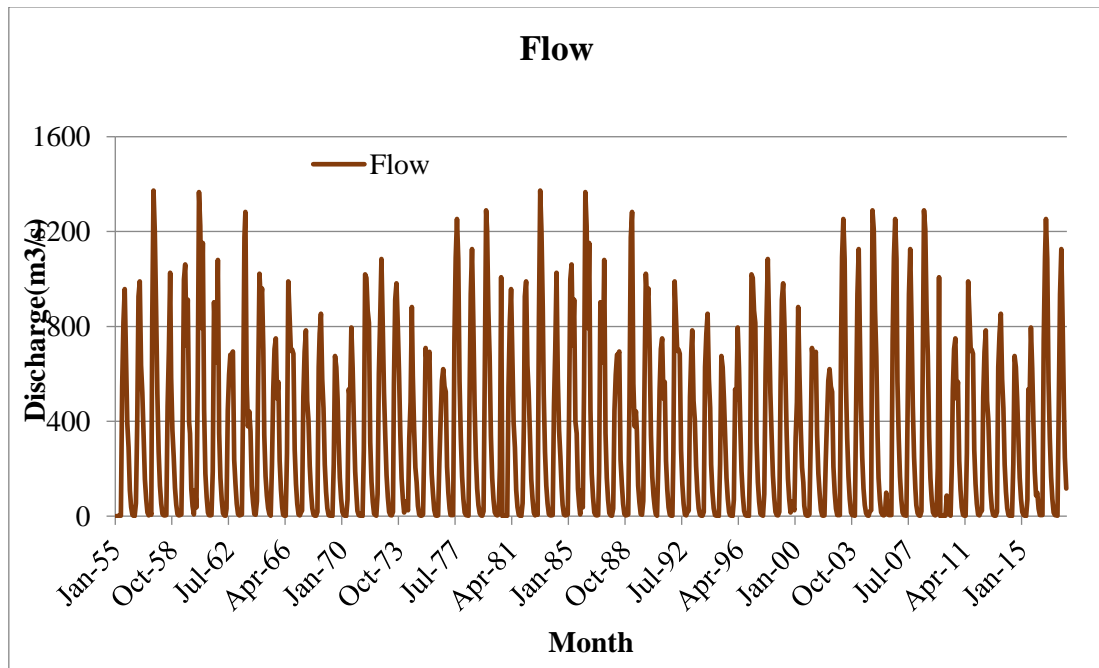
Figure 4.50 Streamflow at the outlet of the basin using without dam condition

The presence of a reservoir alters the flow irregularly. Simulation without considering the dam gives a regular flow, and sediment yield at the outlet of the basin found to be 4.19 t/ha.

4.5 Aghanashini river basin

The SWAT model was calibrated at a monthly time-based scale on the river discharge data for the Aghanashini river basin. Four years (2012–2015) was chosen for calibration and two years (2016–2017) for the validation processes with one year as a warm-up period (2011) using station data. Calibration and validation were also done with gridded rainfall data from 1991 to 2009 with a three-year warm-up period. Simulation using station data gives more accurate results. Several parameters have more influence on the output, were selected after the sensitivity analysis. These parameters were used to calibrate the model by the SWAT-CUP program.
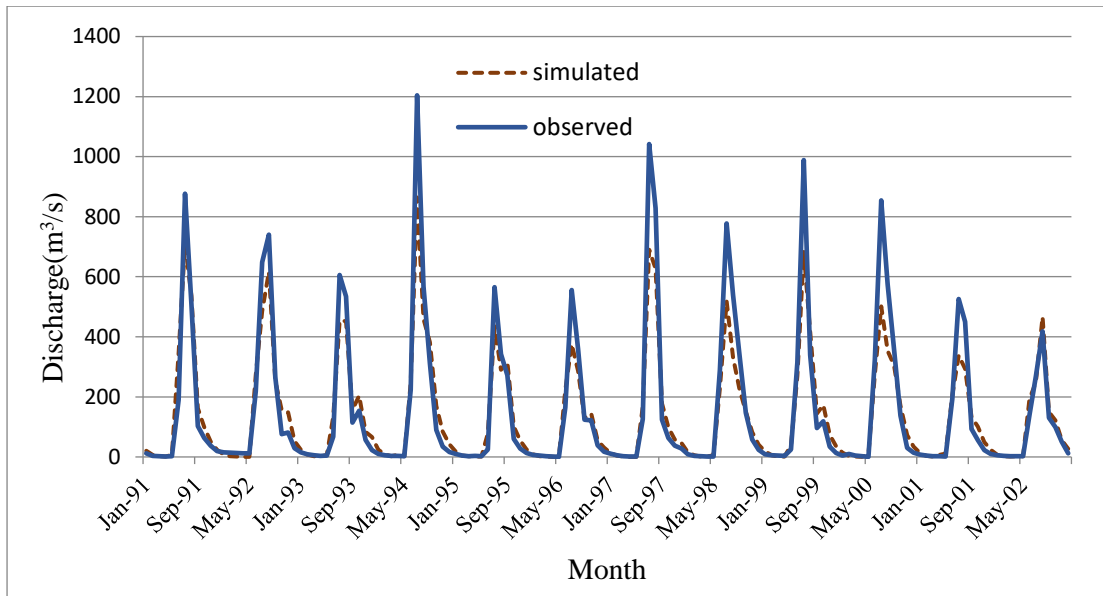
Figure 4.51 Observed V/S Simulated for Calibration using gridded rainfall data

Calibration results of the Aghanashini river show that the simulated flow smoothly matched with the observed flow with an R^2 of 0.93, NSE of 0.88, and PBIAS of 4.1% for gridded data. The validation results for the same basin gives an R^2 of 0.89, NSE of 0.85 and PBIAS 8.8%.
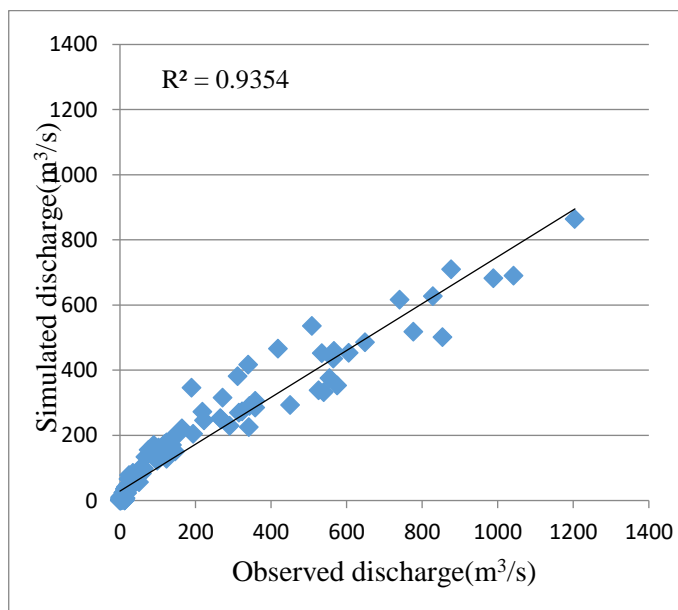
Figure 4.52 Scatter plot for Calibration using gridded rainfall data
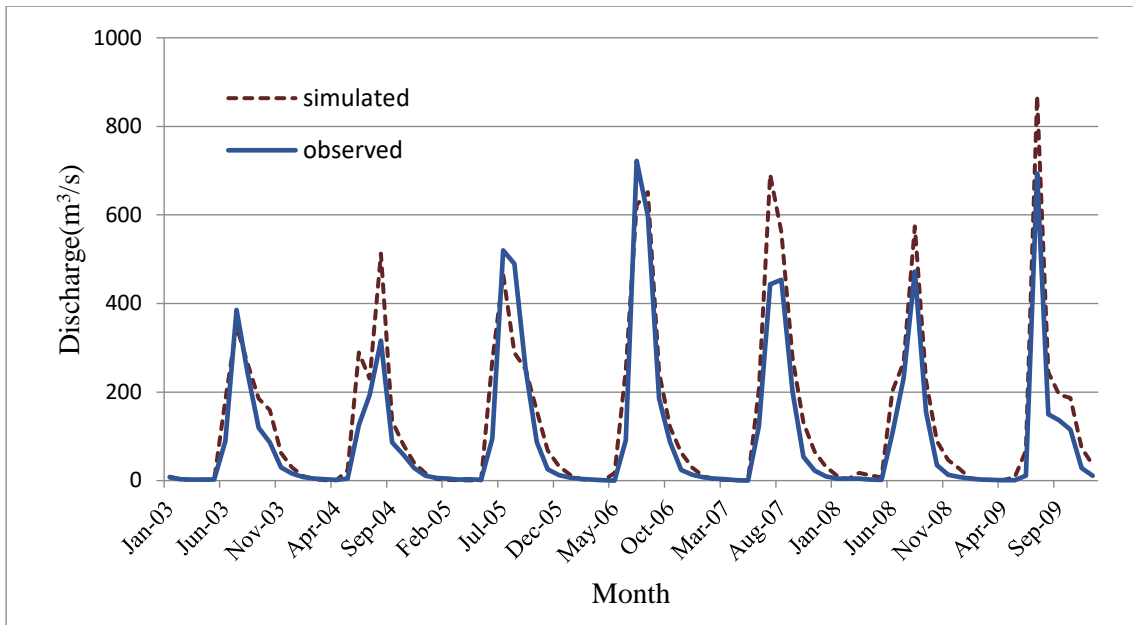
Figure 4.53 Observed V/S Simulated for Validation using gridded rainfall data
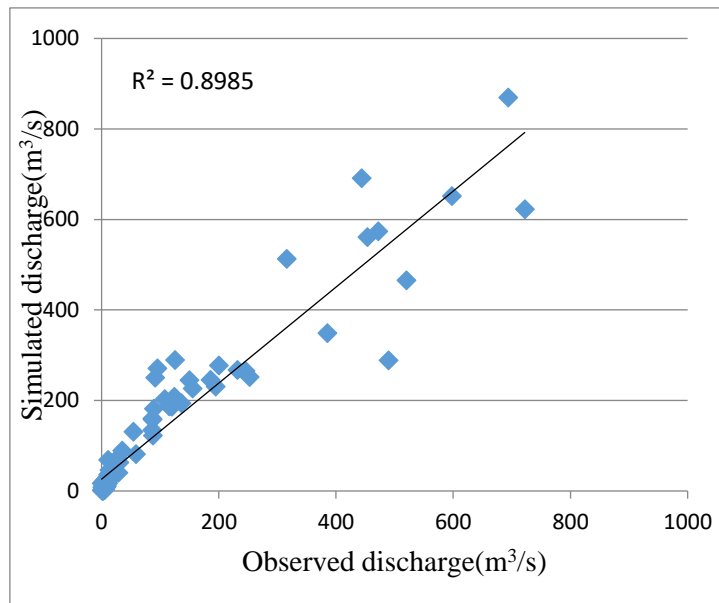
Figure 4.54 Scatter plot for Validation using gridded rainfall data

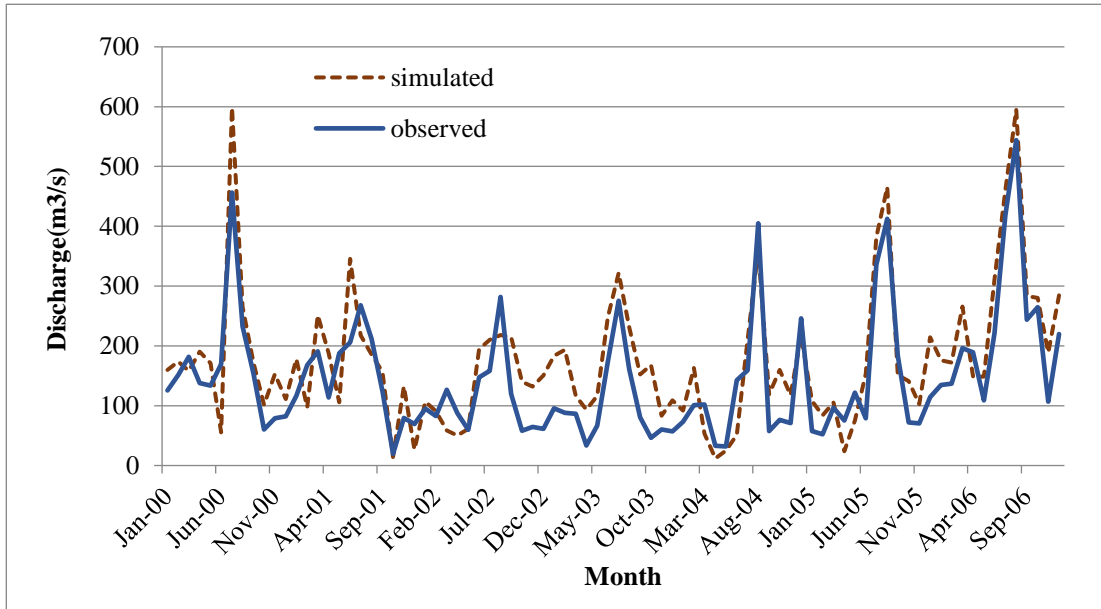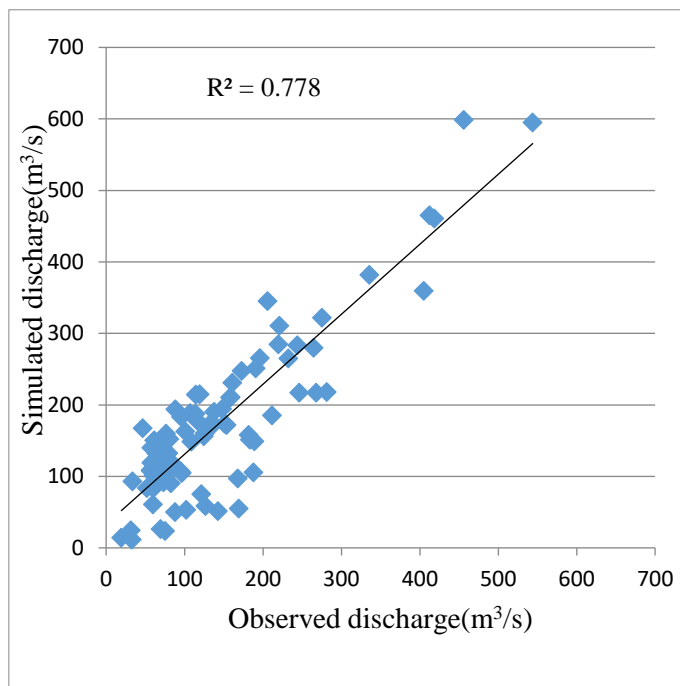## 4.6 Aghanashini river basin with rain gauge station data
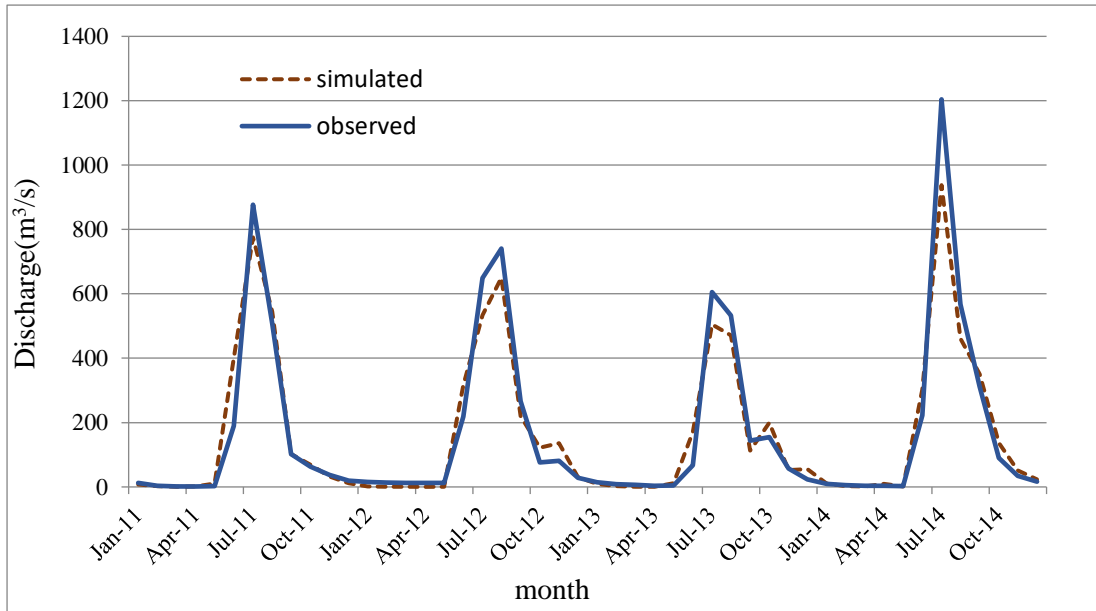
Figure 4.55 Observed V/S Simulated for Calibration using station data
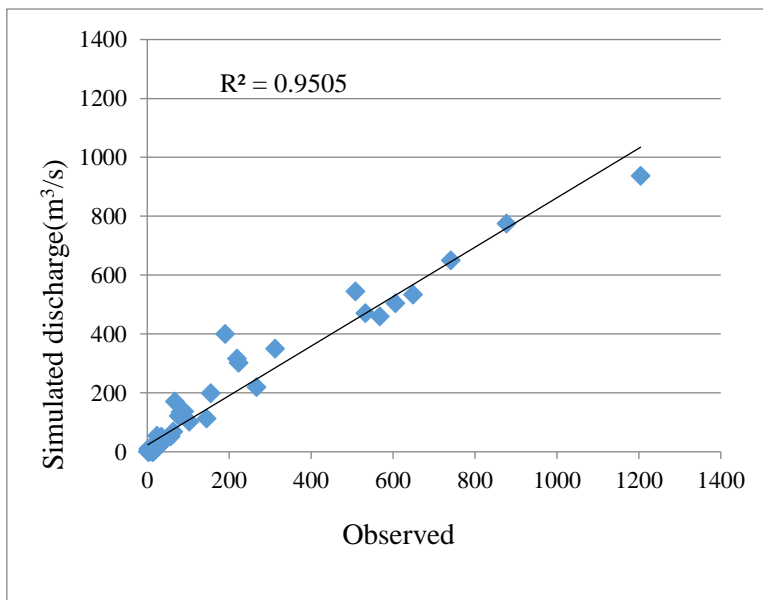
Figure 4.56 Scatter plot for Calibration using station data
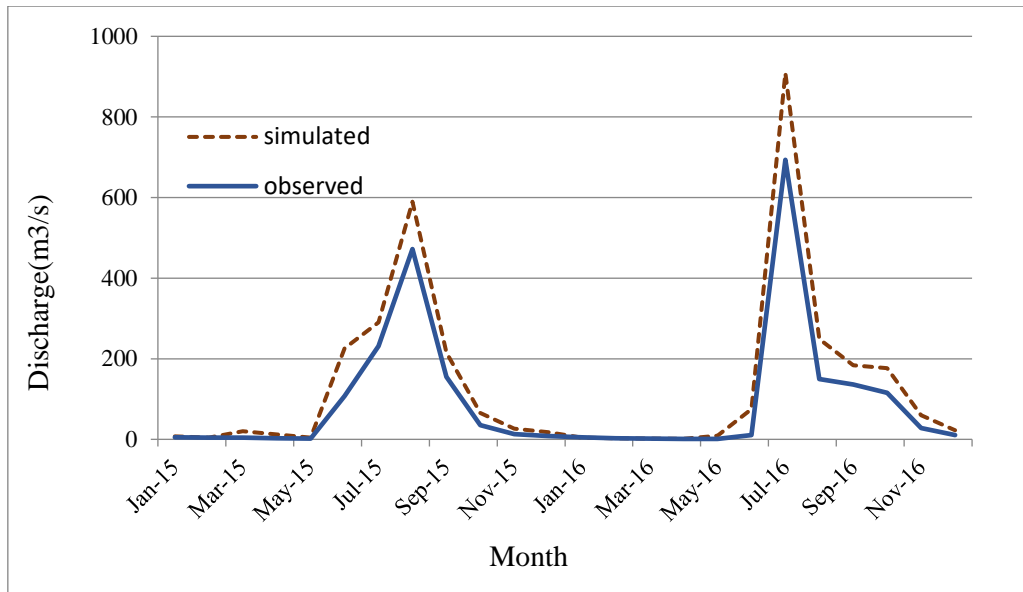
Figure 4.57 Observed V/S Simulated for Validation using station data
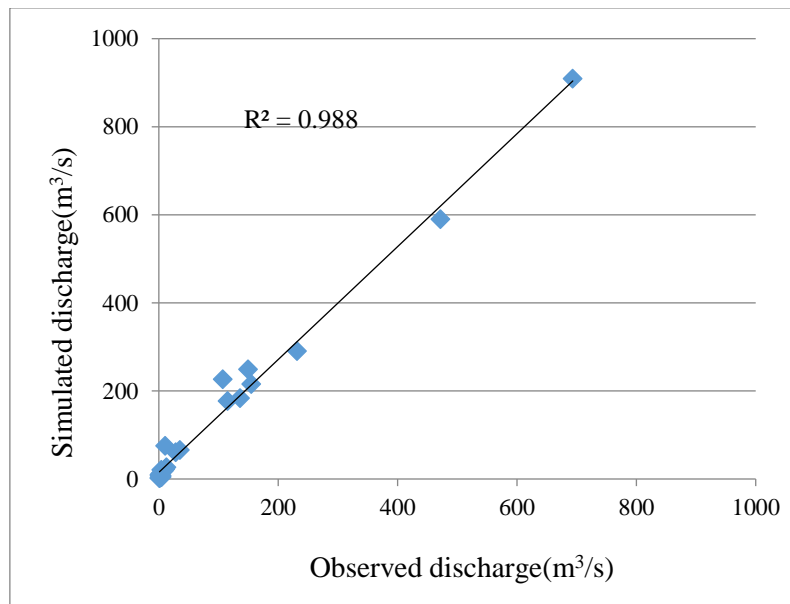
Figure 4.58 Scatter plot for Validation using station data

Simulation using station data gives an R^2 of 0.95, NSE of 0.90, and PBIAS of 4.1% for calibration, and validation gives an R^2 of 0.90, NSE of 0.80, and PBIAS of 12.3%.

The model is well-calibrated and validated with a good model performance. The unobstructed passage of water through the river makes the results more reliable. The average sediment yield at the outlet of the basin at the end of simulation was found to

be 4.38t/ha/yr. Since there is a lack of CWC observation point for sediment, no calibration, and validation conducted.

Simulation of sediment yield at the outlet of Kali and Aghanashini is important, because the construction of dam sediment load had been reduced to 1.39t/ha/year in the Kali river basin. Also, without a dam, the sediment load found to be 4.69t/ha/year. From the Aghanashini basin, sediment yield was obtained as 4.58t/ha/year for a period from 2010-2016. The high sediment yield of the Aghanashini river compared to the Kali river is due to the unhindered passage of water and sediment, since the catchment does not contain any reservoir. The details of the parameter and their ranges during streamflow calibration the sediment yield are given in Table 4.6 Parameter and their ranges during streamflow calibration   Table 4.7. Sediment yield at the outlet of each dam. The performance rating of gridded and station data is given in Table 4.8 and Table 4.9, respectively.

Table 4.6 Parameter and their ranges during streamflow calibration

Sl. No	Parameter	Range
1	CN2	80-90
2	ALPHA-BF	0.85-0.95
3	GW-DELAY	0-500
4	GWQ MN	1000-2000
5	CH-K2	2-4
6	CH-N2	0.014-0.2
7	ESCO	0.5-1
8	GW-REVAP	0-0.2
9	RCHRG-DP	0-1
11	SOL-AWC	0-1
13	SURLAG	0-4

Table 4.7 Sediment yield at the outlet of each dam

Name of the dam	Sediment yield(t/ha/yr)
Supa dam	1.23
Bommanahalli dam	0.73
Thattihalla dam	0.90
Kodasalli dam	1.07
Kadra dam	1.34

Table 4.8 Performance rating index using gridded rainfall data

Station name	Calibration			Validation		
	R^2	NSE	PBIAS	R^2	NSE	PBIAS
Aghanashini river basin	0.93	0.88	4.1%	0.89	0.85	8.8%
Supa	0.66	0.65	3.09%	0.71	0.66	4.78%
Kodasalli	0.62	0.60	18.97%	0.63	0.60	12.34%
Kadra	0.77	0.69	17.02%	0.79	0.71	14.34%

Table 4.9 Performance rating index using rain gauge station data

Station name	Calibration			Validation		
	R^2	NSE	PBIAS	R^2	NSE	PBIAS
Aghanashini river basin	0.95	0.90	4.1%	0.90	0.80	12.3%
Supa	0.77	0.73	6.22%	0.79	0.78	8.76%
Bommanahalli	0.64	0.62	16.78%	0.75	0.71	13.25%
Thattihalla	0.69	0.64	13.78%	0.66	0.64	18.25%
Kodasalli	0.65	0.64	12.97%	0.67	0.61	6.34%
Kadra	0.81	0.78	9.4%	0.79	0.73	6.5%

To find the effect of land use, land cover changes, and reservoir on sediment yield. Analysis of LULC was done in 3 decades, i.e., 1985, 1995, and 2005. The sediment yield of each of the basin with different LULC and dam condition is represented below in Table 4.10.

Table 4.10 Sediment yield from the different basin

Sediment yield	1985		1995		2005	
	t/ha/yr	t/yr	t/ha/yr	t/yr	t/ha/yr	t/yr
Kali basin(with dam)	1.08	506310.48	1.23	576631.38	1.39	651640.34
Aghanashini basin	3.64	463051.68	3.92	498671.04	4.38	557188.56
Kali basin(without dam)	3.96	1856471.7	4.02	1884600.12	4.69	2198700.14

The comparison of sediment yield with dam and without the dam of the graph is plotted against sediment yield vs year. From the graph, it shows that, with the natural flow of the Kali river and joining to the Arabian sea, during this scenario, the sediment yield was naturally normal. Further, due to the regulated discharge of the Kali river from the series of dams, the sediment yield is certainly reduced. Approximately 30% of the sediment yield has been reached to the Arabian sea. The detailed comparison of sediment yield of pre and post-construction of the dam is given in Figure 4.59.
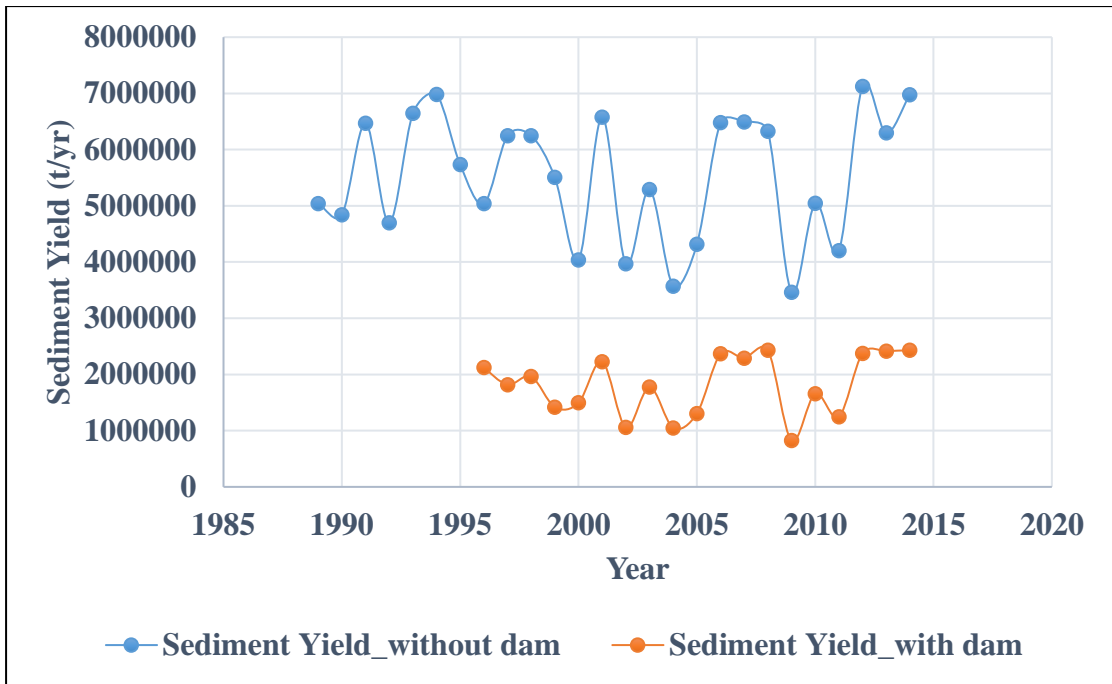
Figure 4.59 Comparison of Sediment Yield with and Without Dam

4.7 Granulometric analysis

The sand samples collected throughout the post-monsoon of 2017 and pre-monsoon of 2018. These samples were kept for dry in an oven at a temperature of 108°C for 24 hrs. For the grain size, 500gms of the sample considered. The analysis was carried out by GRADISTAST V8 for Tagore and Devbagh beaches of the Karwar coast. The result of the analysis shown in Figure 4.60 and Figure 4.61.
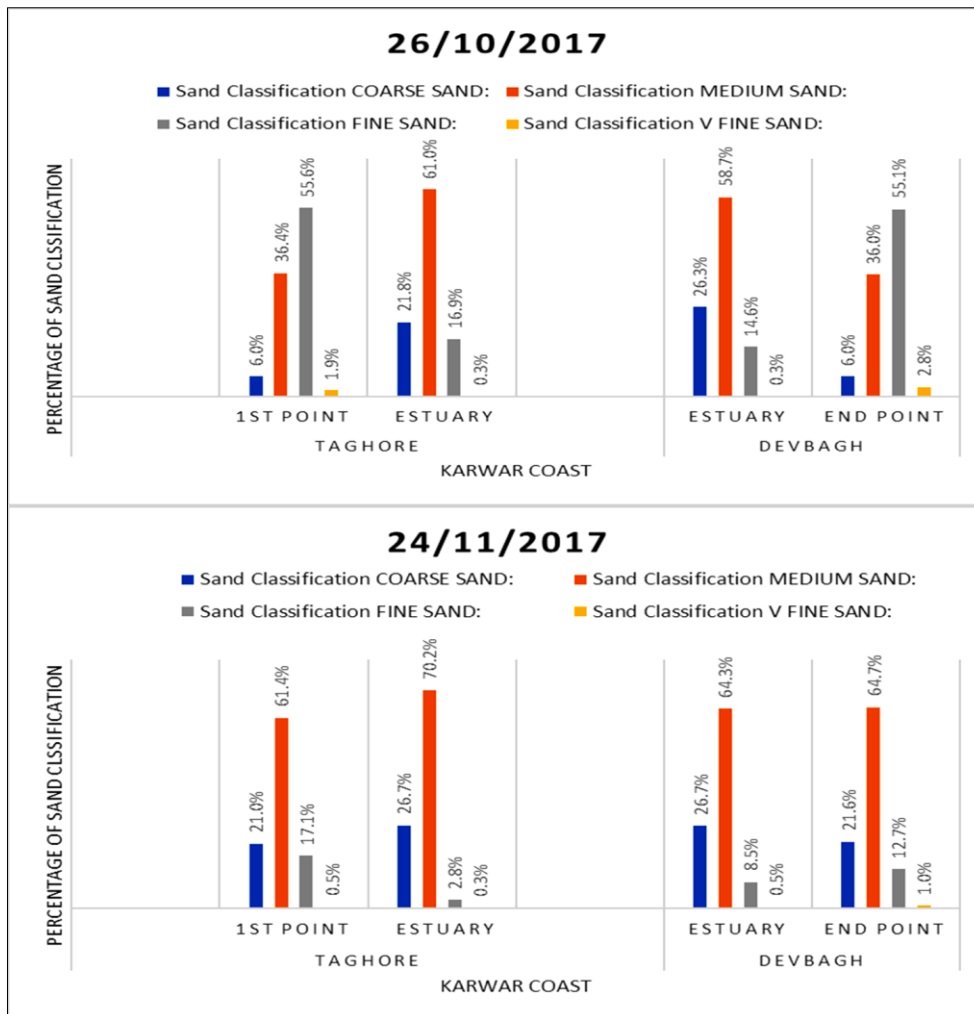
Figure 4.60 Sand classification of Post-monsoon season of 2017

From Figure 4.60, it is found for the month 26/10/2017, and 24/11/2017 medium sand and coarser sand are more at the estuary region of both the beaches have less fine sand.

Similarly, fine sand is more away from the estuary. This means coarser and medium sand particles are present in the region of the estuary for both Tagore's and Devbagh beach of Karwar coast. Fine sand is present at 4 km away from the estuary region.

From Figure 4.61, it is found for the month of 31/03/2018 it is medium sand found to be 69.9%, and coarser sand is 25.1% for Kali estuary at Tagore beach. 58.3% medium sand and 36.3% coarser sand found in the Kali river estuary at Devbagh beach.
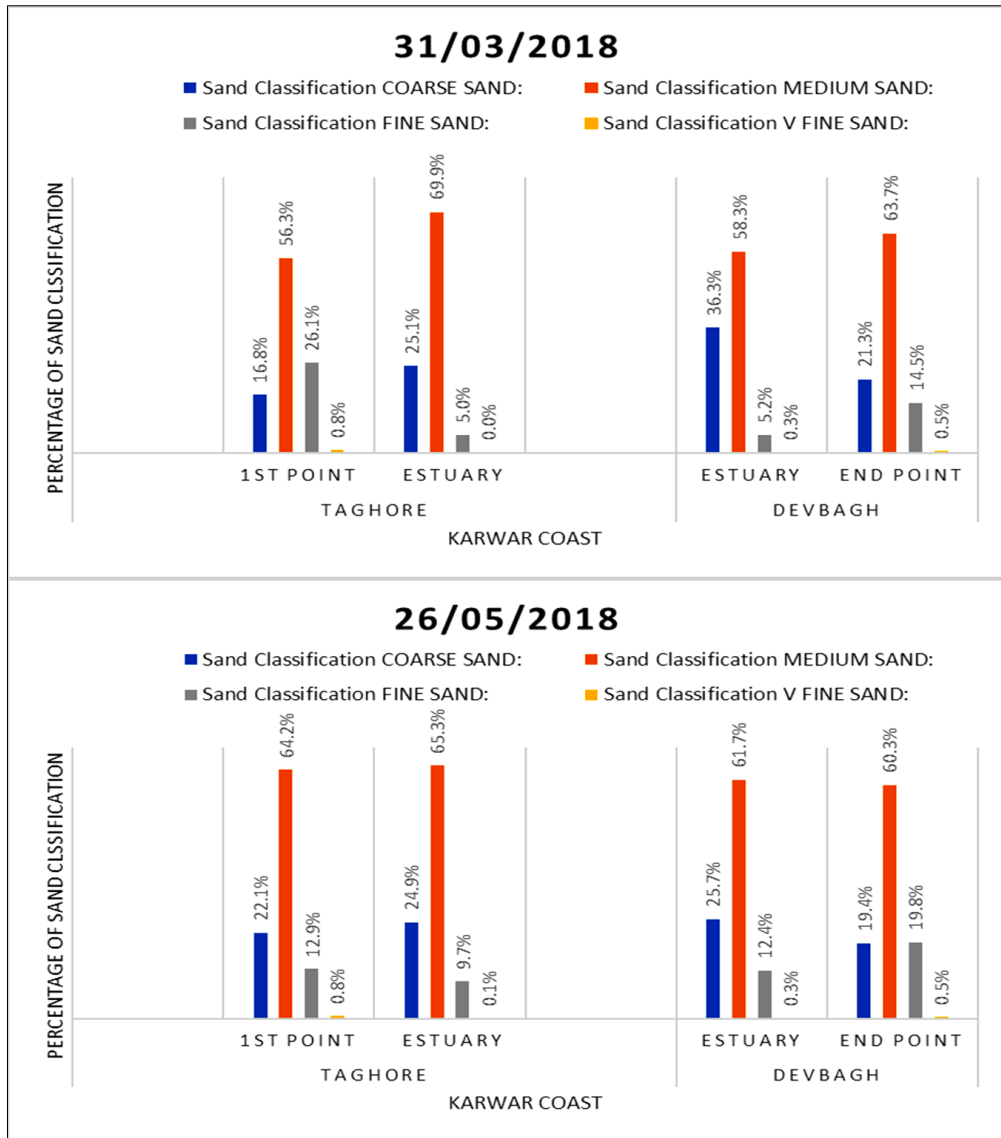
Figure 4.61 Sand classification of Pre-monsoon season of 2018

At Tagore beach 1st point (4kms away from estuary) medium and coarser sand found to be comparatively less. During 26/05/2018, medium sand (65.3% and 64.2%) and coarser sand (24.9% and 22.1%) is almost the same percentage at the Kali estuary region and Tagore 1st point sample point of the beach. For Devbagh beach during 26/05/2018, medium sand evenly found at Kali estuary and endpoint sample location. In the case of coarser sand at Kali estuary at Devbagh beach found of 25.7% and at another sample point is found to be 19.4%. Hence during the pre-monsoon season, the approximately the sand particle distribution is even.

4.8   Sediment Trend Matrix (STM) & Sediment Transport Path (STP) along RT beach

Grain size analysis results for pre-monsoon season and post-monsoon season are tabulated in Table 4.11 and Table 4.12, respectively.

Table 4.11 Grain Size Analysis results for samples collected during Pre-Monsoon Season

MEAN	STANDARD DEVIATION	SKEWNESS
0.336	0.142	-0.86
0.406	0.17	-0.87
0.37	0.15	-0.96

Table 4.12 Grain Size Analysis results for samples collected during Post-Monsoon Season.

MEAN	STANDARD DEVIATION	SKEWNESS
0.305	0.12	-0.91
0.379	0.14	-1.01
0.389	0.13	-1.13

STM developed by using the grain size parameters (Mean, Sorting, and Skewness) computed above for both pre-monsoon & post-monsoon season of RT beach, as shown in Table 4.13 & Table 4.14, respectively.

Table 4.13 STM along RT beach during Pre-Monsoon Season

Sample	S1	S2	S3	Grain Size Characteristics	Inferences
S1		C B +	C B +	Mean Sorting Skewness	S2→S1 S3→S1
S2	F P -		F P +	Mean Sorting Skewness	
S3	F P -	C B -		Mean Sorting Skewness	

Table 4.14 STM along RT beach during Post-Monsoon Season

Sample	S1	S2	S3	Grain Size Characteristics	Inferences
S1		C B +	C B +	Mean Sorting Skewness	S2 → S1 S3 → S1
S2	F P -		C P +	Mean Sorting Skewness	
S3	F P -	F B -		Mean Sorting Skewness	S2 → S3
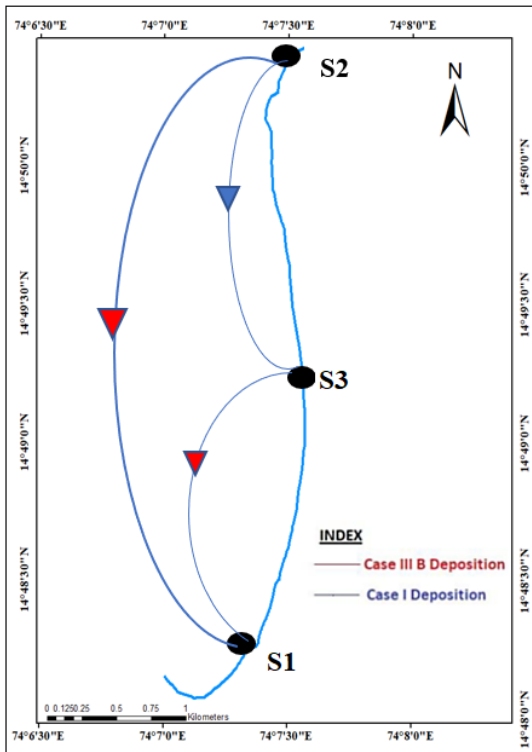
Figure 4.62 STP along RT beach during Pre-monsoon Season
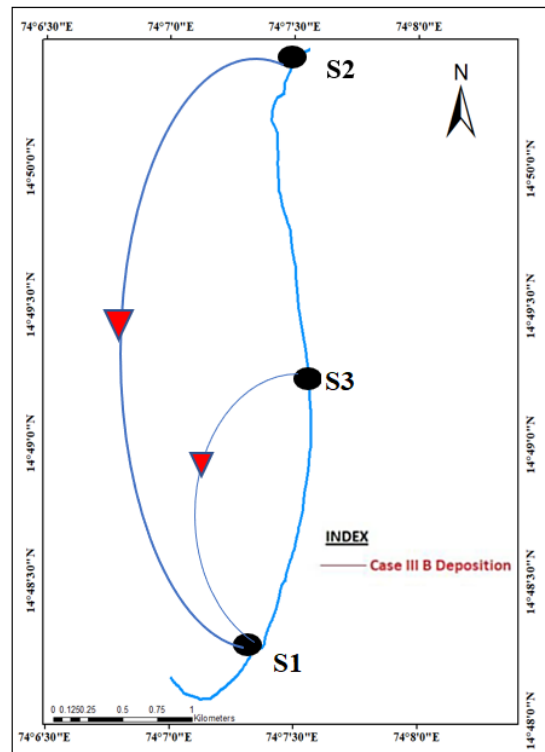
Figure 4.63 STP along RT beach during Post-monsoon Season

141

4.9   Beach profile analysis of RT beach and volume estimation

4.9.1   Beach profile analysis of RT beach

The beach profile is carried out for Ravindranath Tagore beach of 3 km stretch for the pre-monsoon and post-monsoon seasons of 2017, between May and November, respectively. Beach profile analysis carried out using a total station instrument. Figure 4.64 shows the comparison of the RT profile during the seasons.
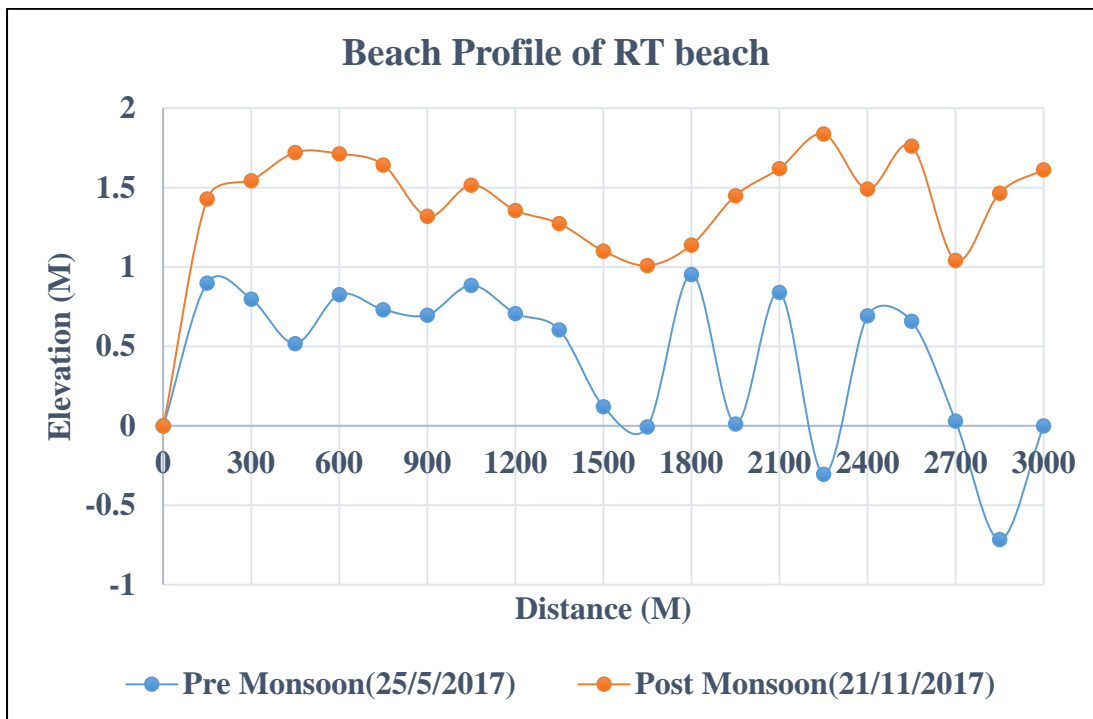
Figure 4.64 RT profile during Pre and Post monsoon seasons of 2017

From the graph, which is shown in figure 4.64, it is evident that profile changes according to the seasons. During the pre-monsoon season, the beach seems to be less accretion, and some parts experienced erosion. This is maybe due to wave and wind energy interaction, and also sediment supply from the river is decreased. On the other hand, during the post-monsoon season, the profile is experienced accretion thought considered study area. This may be due to the decreased effect of wind and wave energy. Also, sediment supply from the Kali river probably increased with river flow at the estuary. Further, for the same study, the area of cross-section of profile carried out using the total station. This survey brings how the cross-section being changed

142

according to the season. From the survey it is noticed that, during the pre-monsoon season, all the cross-section of RT beach has reduced its elevation with respect to datum. The following Figure 4.65, Figure 4.66, Figure 4.67, shows the graph of cross-sections of the RT beach one by one.
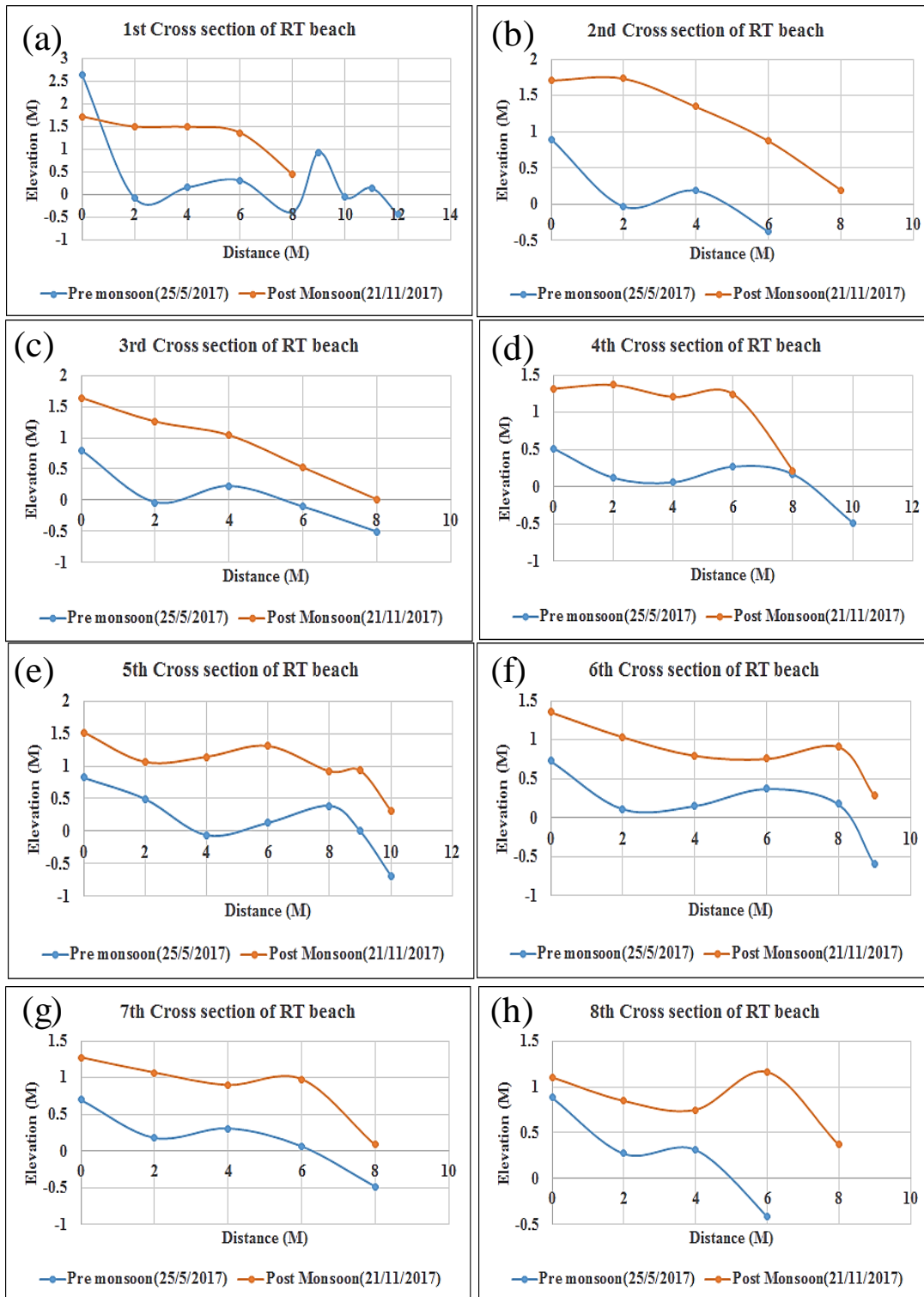
Figure 4.65 (a) 1st Cross Section (b) 2nd Cross Section (c) 3rd Cross Section (d) 4th Cross Section (e) 5th Cross Section (f) 6th Cross Section (g) 7th Cross Section and (h) 8th Cross Section of RT beach
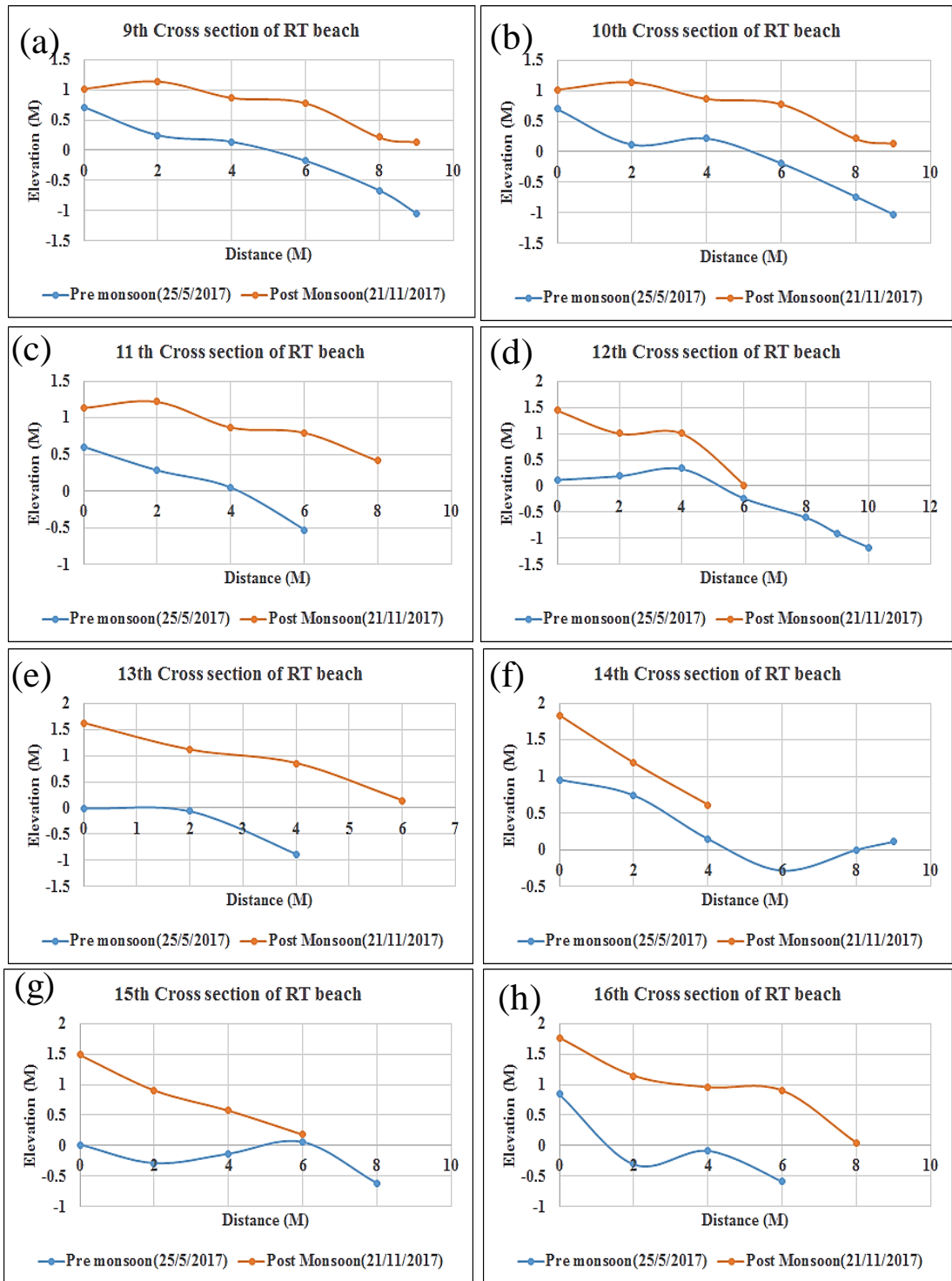
Figure 4.66 (a) 9th Cross Section (b) 10th Cross Section (c) 11th Cross Section (d) 12th Cross Section (e) 13th Cross Section (f) 14th Cross Section (g) 15th Cross Section and (h) 16th Cross Section of RT beach
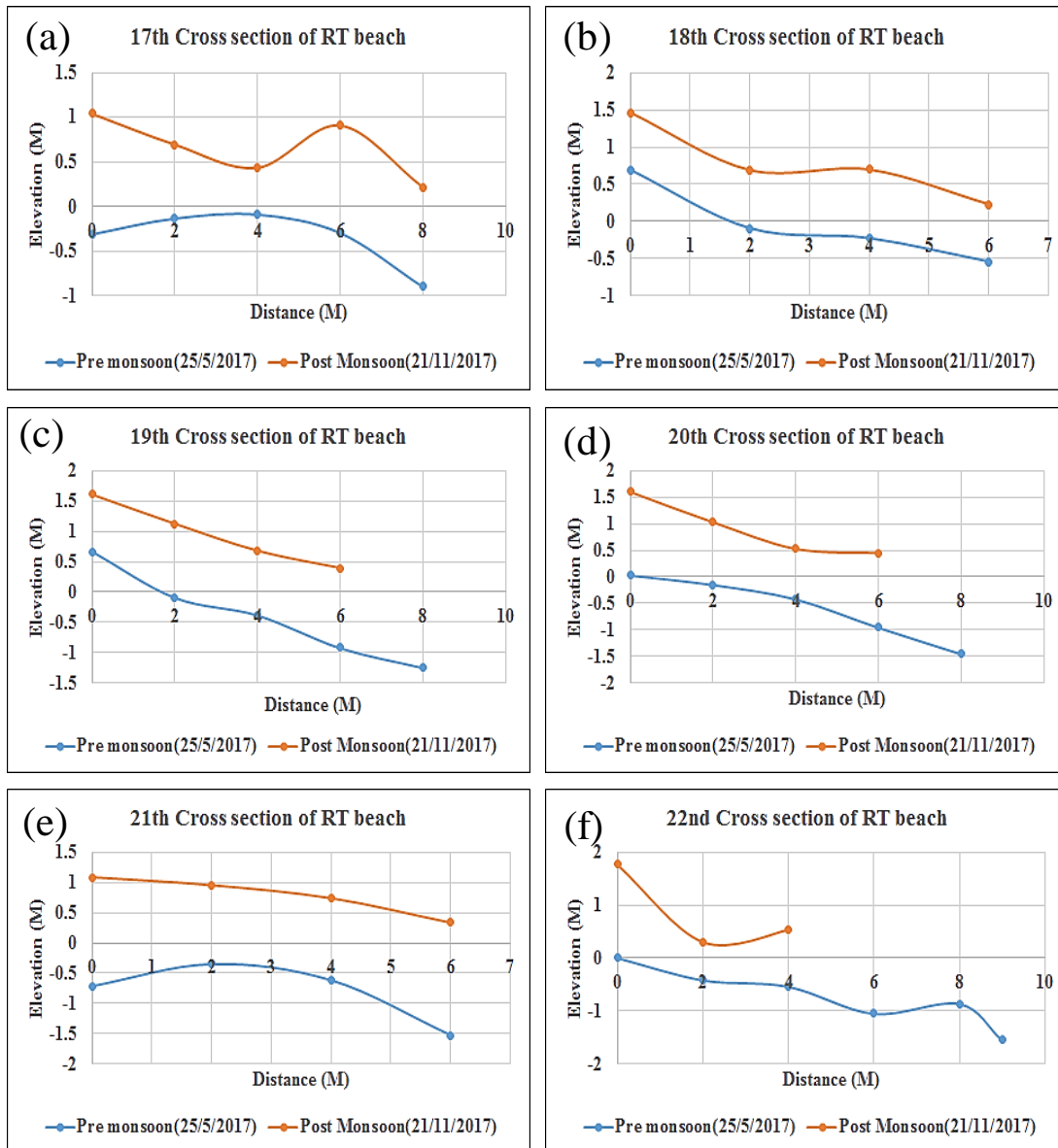
Figure 4.67 (a) 17th Cross Section (b) 18th Cross Section (c) 19th Cross Section (d) 20th Cross Section (e) 21th Cross Section and (f) 22th Cross Section

4.9.2 Estimation of sand volume of beach

In this present study, the estimation of the sand volume of RT beach is done. The total station instrument, measuring tape, and prism has been used for the profile leveling of the beach. The profile leveling includes of a) Longitudinal profile and b) Cross-section profile. The pre-monsoon season and post-monsoon season of the 2017 year are considered. This study is to know how these seasonal conditions play a role in terms of volume of beach or beach nourishment. The estimation of area and volume of pre and the post-monsoon season is given in Table 4.15 and Table 4.16, respectively.

Table 4.15 Details of pre-monsoon season

Profile	Area (Sq. Mt)	Volume (Cubic. Mt)
1	14.04	4212
2	10.23	3069
3	12.04	3612
4	**15.96**	**4788**
5	15.20	4560
6	13.95	4185
7	13.92	4176
8	9.84	2952
9	11.48	3443
10	9.41	2822
11	7.41	2223
12	11.16	3348
13	4.24	1272
14	7.98	2394
15	8.25	2475
16	9.33	2799
17	11.04	3312
18	7.47	2241
19	**4.08**	**1224**
20	6.12	1836
Total	**203.15**	**60943**

The trapezoidal formula adopted for the estimation of the area and volume of the beach. From the table it was found to be, the total area of all 20-cross-section profile was 203.15 Sq. MT, and 60943 Cubic. Mt in case of pre-monsoon of 2017.

Table 4.16 Details of post-monsoon season

Profile	Area (Sq. Mt)	Volume (Cubic. Mt)
1	19.52	5856
2	16.23	4869
3	18.92	5676
4	19.72	5916
5	**24.80**	**7440**
6	20.75	6224
7	18.44	5532
8	16.59	4977
9	19.89	5967
10	19.08	5724
11	14.43	4329
12	12.45	3735
13	10.60	3180
14	**10.46**	**3138**
15	15.03	4509
16	16.20	4860
17	19.88	5964
18	15.81	4743
19	14.55	4365
20	15.18	4554
Total	**338.525**	**101557.5**

On the other hand, the post-monsoon season had an experienced a volume of 101557.5 cubic.mt, and the total area of the cross-section is 338.525 sq.mt. The analysis gave the result as the RT beach accreted, and cross-sectional, and sand volume increased compared to pre-monsoon season. The nourishment of the beach is good in the case of post-monsoon than pre-monsoon season. To understand the differences in area and volume according to the seasons, the graph is plotted. Figure 4.68 shows the estimation of the area according to the seasons of 2017.
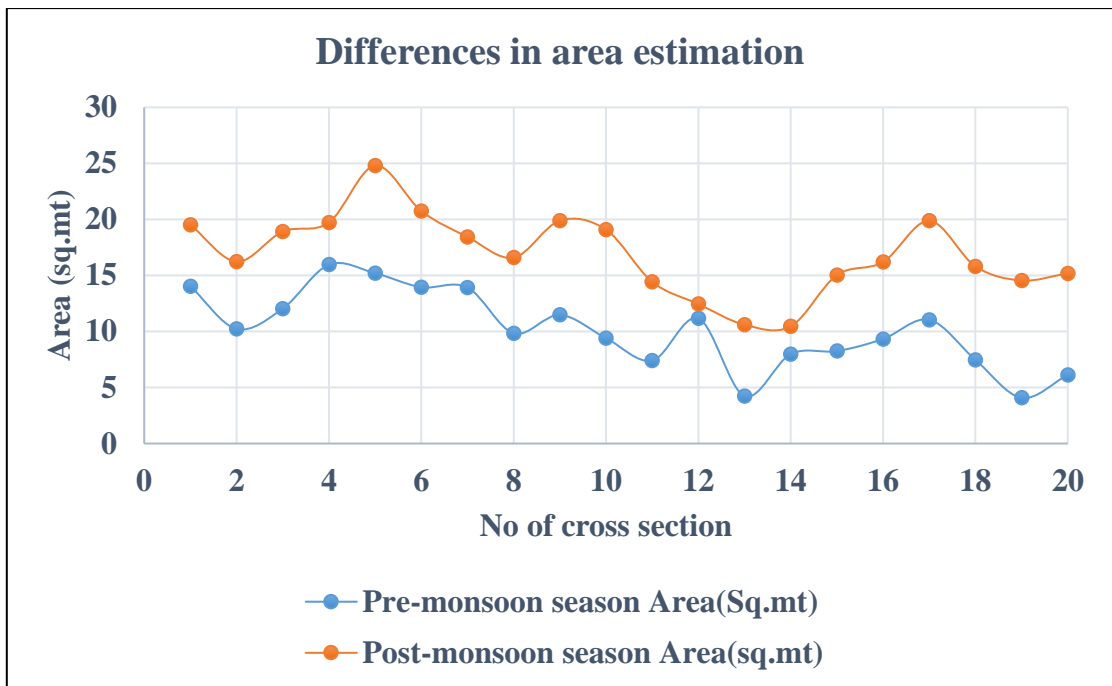
Figure 4.68 Estimation of area of pre and post monsoon season
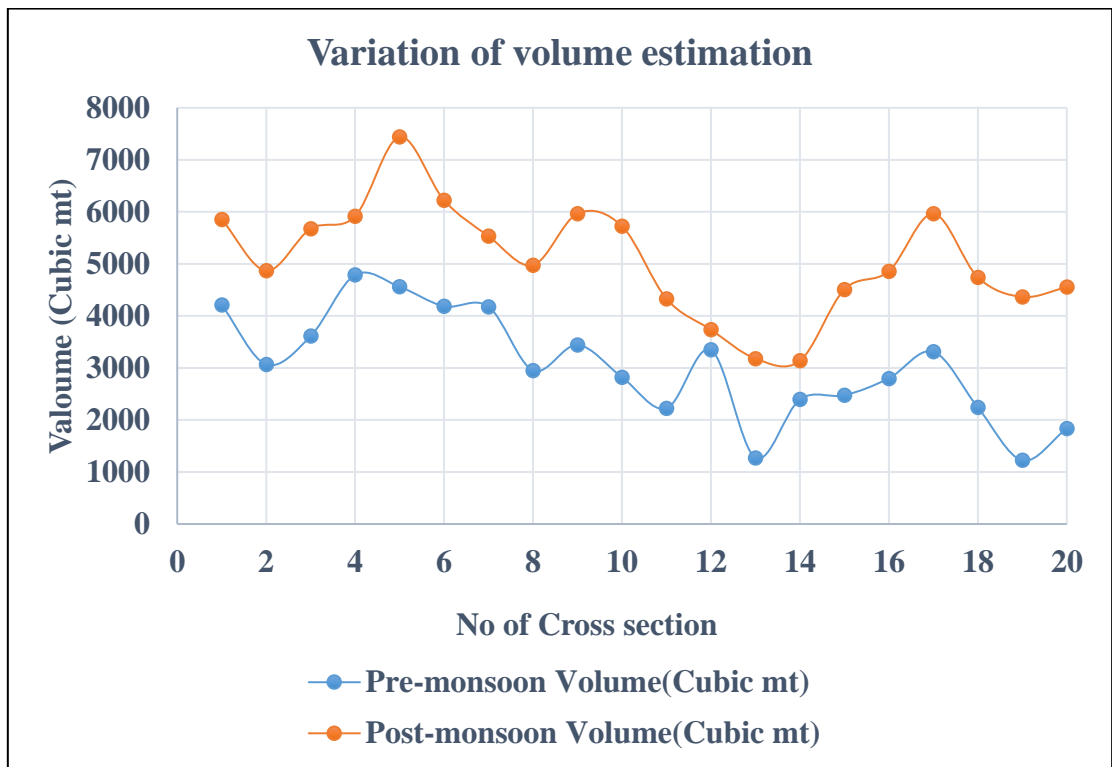
Figure 4.69 Estimation of volume of pre and post-monsoon season

The highest area is estimated as 25 sq .mt at the 5th cross-section, and the lowest area is estimated at 10.46 sq.mt at the 14th cross-section during post-monsoon. In the case of pre-monsoon season, at 4th cross-section, the max area is found to be 15.96 sq.mt, and on the 19th cross-section of the beach, the lowest area of 4.08sq.mt found. Similarly, the max volume for the post-monsoon season is 7440cubic mt. At 5th cross-section and lowest of 3138cubic.mt at the 14th cross-section. In the case of pre-monsoon, the maximum volume estimation found to be 4788cubic mt. At 4th cross-section and lowest of 1224cubic mt. At the 19th cross-section. The graphical representation of area and volume is provided in Figure 4.68 and Figure 4.69, respectively.

CHAPTER 5

5   SUMMARY AND CONCLUSIONS

5.1   General

The major focus of this dissertation was to study and compare the impact of the dam on shoreline configuration as a case study of the Kali river basin, shoreline belonging to the Karwar coast, such as Devabagh beach and RT beach. In this process of accomplishing this major objective, the present research work specifically addressed: a) Impact of pre-construction of dam and post-construction of dam on shoreline configuration b) Seasonal variation on shoreline configuration using DSAS, RS & GIS tool c) Analysis of impact of dam on sediment yield before joining to sea using SWAT tool d) Grain size analysis and Gradistat analysis for beach face sand sample e) Estimation of volume of sand using beach profile survey for the pre monsoon season and post monsoon season f) To find the sediment and the sediment transport path.

This chapter provides summary and major conclusions drawn based on the obtained results. The summary is presented under above mentioned themes. Also, the limitations of the study for further studies are added.

5.2   Summary

5.2.1 Impact of pre-construction of the dam and post-construction of the dam on shoreline configuration

The DSAS analysis carried out for shoreline configuration by considering the construction period of the dam. The impact analysis of the dam on the coastal zone is necessary to analyze as the dam is responsible for the trap of river sediment. The major findings of the study are as follows:

1. From the study, it was found to be of Devbagh beach Pre-construction of the dam; from 1975 to 1980, the beach had an accretion at the rate of 6.96 m/yr (EPR) and 8.39 m/yr (LRR).

2. Post-construction of the dam, the shoreline analysis was carried out from 1990 to 2017. The beach was under erosion at the rate of -0.93 m/yr (EPR) and -0.47 m/yr (LRR).

3. In the case of RT beach from 1975 to 1980, that was pre-construction of the dam, and it was an experienced accretion at the rate of 7.25 m/yr (EPR) and 2.7 m/yr (LRR).

4. Post-construction of the dam at RT beach, the erosion of the experience, which is -0.75 m/yr (EPR) and -0.97 m/yr (LRR).

5. Finally, both the beaches have changed from the accretion zone to the erosion zone.

6. The maximum erosion found to be at the Kali estuary region.

5.2.2 Seasonal variation on shoreline configuration using DSAS, RS & GIS tool

The present research work carried out for seasonal variation such as Pre-monsoon season and Post-monsoon season of shoreline configuration using LANDSAT-8 (OLI/TIRS) satellite data only from 2013 to 2017. The outcome of the analysis as follows:

1. Devbagh beach during Pre-monsoon season had an average shoreline change rate of -7.54 m/yr (EPR) and -5.57 m/yr (LRR), and during Post-monsoon season, it is experienced that an average rate between 0.34 m/yr (EPR) and -0.46 m/yr (LRR).

2. RT beach during Pre-monsoon season had an average shoreline change with the rate of 0.004 m/yr (EPR) and 1.67 m/yr (LRR) and on post-monsoon is -5.77 m/yr (EPR) and -6.55 m/yr (LRR).

3. The direction of longshore currents during post-monsoon found to be the majority of northern currents superimposed by onshore currents.

4. During pre-monsoon, the current direction showed both northerly and southerly majority with superimposed onshore currents.

5.2.3 Estuary Change analysis

1. The analysis of estuary change results states that the upper part of Kali estuary, which belongs to Devbagh beach, experienced erosion. 420068.59 m^2 of the area had vanished due to erosion in the Kali estuary for the period from 1976 to 2018.

2. Also, the lower part, which belongs to Ravindranath Tagore Beach, had experienced both accretion and erosion. The maximum erosion of 159837.23 m^2 found in the year 1989, which is after the construction of the Supa dam and the maximum erosion of 45770.71m^2, the maximum accretion of 21636.62 m^2 located in the year 2018.

5.2.4 Analysis of the impact of the dam on sediment yield before joining to sea using swat tool

The estimation of sediment yield is done by considering two cases. a) Estimation of sediment with a dam and without a dam. b) Gridded Rainfall data and rainfall data from rain gauge station. Further, the SWAT tool implemented in the Kali river basin, the Aghanashini river basin in order to compare the impact of the dam on streamflow and sediment yield. The following inferences are drawn:

1. The streamflow of the Kali river basin is calibrated and validated using Dam discharge data of each dam of the Kali river basin. The performance of the SWAT model gave good results.

2. For gridded rainfall data, the R^2, NSE, and PBIAS values gave very good results for the Aghanashini river basin, and for the Kali river basin, it was estimated reasonably good results.

3. For Rain gauge station data, R^2, NSE, and PBIAS values gave very good results for the Aghanashini river basin. For the Kali river basin dam, Supa dam, and Kadra dam, it was estimated very good results. Also, for the remaining dam, the model performance is reasonably good.

4. The sediment yield estimated at Kali river basin outlet, without the dam, is 4.19 t/ha/yr, and with the dam, it is estimated to be 1.42t/ha/yr. Similarly,

for the Aghanashini river basin outlet, the sediment yield found to be 4.58t/hr/yr.

5.2.5 Grain size analysis and gradistat analysis for beach face sand sample

The beach face sand samples of RT beach collected for pre-monsoon season and post-monsoon season of the 2017 year. At three different locations of the beach, the sand samples collected. The following results are listed based on the analysis:

1. It was found for the month 26/10/2017, and 24/11/2017 medium sand and coarser sand was more at the estuary region of both the beaches and had less fine sand.

2. It was found for the month of 31/03/2018 is, medium sand found to be 69.9%, and coarser sand was 25.1% for Kali estuary at RT beach. On the other hand, 58.3% medium sand and 36.3% coarser sand found in the Kali river estuary at Devbagh beach.

3. From the analysis, it was found in the case of pre-monsoon season, and approximately the sand particle distribution was even.

5.2.6 Estimation of volume of sand using beach profile survey for the pre-monsoon season and post-monsoon season

Beach profile survey of RT beach is carried out for pre-monsoon season and post-monsoon season of the year 2017. The observation and reading used for the beach volume estimation. The following results were drawn based on survey readings:

1. The total area of all 20 cross-section profiles was 203.15 sq.mt, and the volume estimated was 60943 cubic.mt in case of pre-monsoon season of 2017.

2. In the case of the post-monsoon season had an experienced a volume of 101557.5 cubic.mt, and the total area of the cross-section was 338.525 sq.mt.

3. The RT beach had accreted a cross-sectional, and sand volume was increased compared to the pre-monsoon season.

4. The nourishment of the beach was proper in the case of post-monsoon than pre-monsoon season.

5.2.7 To find the Sediment Transport Path

The sediment transport path was found for RT beach for both pre-monsoon season and post-monsoon season. The analysis of STP is listed below:

1. During the pre-monsoon season of 2017, the sand sample travelled path was from S2 location to S1 with coarser sand deposition, and it was similar for the sand sample from S3 to S1. Further, the sand sample was travelled from S2 to S3 with a finer deposition of finer sand.

2. In the case of post-monsoon, the sand sample travelled path was from sample location S2 to S1. Particularly at S2 location coarser sand deposition occurred.

3. Hence it was found that, in the case of both seasons, the sand sample was moved to south direction in the RT beach with respect to north direction.

4. Also, during the post-monsoon season, coarser sand deposition is found throughout the RT beach, and during the pre-monsoon season, coarser sand was found in location from S3 to S1. Finer sand was found between the location of S2 to S3.

5.3 Conclusions

1. The result of the study shows that shoreline configuration was changed due to the construction of the dam. Pre-construction of the dam, both the beaches of the Karwar coast, were experiencing a natural beach cyclic process. Due to the construction of the dam, it had impacted on natural beach cyclic process, and both the beaches turned into erosion zone.

2. In the case of seasonal shoreline configuration from the analysis it was found to be, the direction of longshore current during post-monsoon found to be the majority of northerly currents superimposed by onshore currents, whereas during the pre-monsoon season, the current direction shows both northerly and southerly majority with superimposed onshore currents.

3. It may be due to the meandering of the Kali river in the estuary region. Construction of the dam was responsible for the meandering of the dam, which leads to regulate the discharge of water and sediment trap behind the

dams and also sand mining catalyst to change of the Kali estuary. The critical zone is the upper part of Kali estuary, and already seawall had been constructed. Since the fisheries community was located in those areas, the rehabilitation of lost areas needs to be fixed, which was very important.

4. A Soil Water Assessment Tool (SWAT) implemented in the Kali river basin, the Aghanashini river basin in order to compare the effect of the reservoir on streamflow and sediment yield. This model was well-calibrated with the river discharge data. Prediction of sediment yield at the river mouth of both the basins gave an idea about how the presence of a reservoir affects streamflow and sediment yield of a basin. About 30 percent of sediment had trapped from the dam, which was not supplied to the Karwar coast.

5. The obtained results show that the Kali river basin had highly regulated flow and comparatively less sediment yield at the river mouth due to the presence of series of the reservoir. However, the Aghanashini River had a free flow across the catchment with the unrestricted passage of sediments to the downstream. The sediment yield was found to be 4.58t/ha/year at the river mouth due to the absence of a reservoir in the catchment.

6. The GRADISTAST V8 tool was very user-friendly, which gives results for the moment method and Folk and Ward method at a time. Sand sample results show that coarser sand particle and more medium sand particle found in the estuary region than from another sampling point at the beach.

7. Beach profile survey using total station given good observation and readings; in fact, it gave an advantage to plot in AutoCAD and also provides readings in text format, which allowed to draw a better graph. Beach profile survey also provided an idea about beach volume and how it is changing according to the seasons.

8. STP analysis gave an idea about sand travel or movement depending upon the season.

9. Remote sensing and geospatial techniques coupled with DSAS, an extension ArcGIS® tool, are useful to analyze shoreline configuration. It would be useful for long-term and short-term shoreline analysis, including seasonal

wise monitoring. It delivered a complete view of erosion and accretion rate of the shore areas, which was economically significant.

10. The present study submitted that multi-dated satellite data, seasonal wise along with statistical practices, could be effectively used for shoreline analysis.

5.4   Limitations of the study

1. Since the study of shoreline configuration on the impact of the dam, the satellite imagery resolution had to be considered depending upon the time limit. Also, during the analysis application of wave, wind, the tide was not considered.

2. The LANDSAT satellite imagery was 30m resolution, but it was freely available data.

3. The accuracy of the result could be increased using high-resolution data of satellite imagery.

4. To validate the sediment yield on the ungauged basin, the sediment gauge station should be developed.

5. The SWAT model calibration efficiency was limited due to the lack of measured data for a selected period of 1989-2017.

6. The field seasonal variation analysis should be carried out for at least more than one year.

5.5   Scope for future studies

1. The study on the nature of sediment transport budget carried in the Karwar coastal zone by considering longshore/ littoral currents.

2. The study on the reversing wind pattern and wave action contributes to the overall to the sediment budget for the Karwar coast can be carried with suitable data.

3. The accuracy of shoreline analysis and LULC can be generated with freely available higher resolution satellite data.

4. The installation of a sediment gauge station, the validation of the sediment yield can be done.

6 REFERENCES

- Adams, A. (2000). "Social impacts of an African dam: equity and distributional issues in the Senegal River Valley. Cape Town": *World Commission on Dams* (Dam Report Series).

- Aedla, R., Dwarakish, G. S., & Reddy, D. V. (2015). "Automatic shoreline detection and change detection analysis of netravati-gurpurrivermouth using histogram equalization and adaptive thresholding techniques". *Aquatic Procedia*, 4, 563-570.

- Almonacid-Caballer, J., Sánchez-García, E., Pardo-Pascual, J. E., Balaguer-Beser, A. A., & Palomar-Vázquez, J. (2016). "Evaluation of annual mean shoreline position deduced from Landsat imagery as a mid-term coastal evolution indicator". *Marine Geology*, 372, 79-88.

- An, Q., Wu, Y., Taylor, S., & Zhao, B. (2009). "Influence of the Three Gorges Project on saltwater intrusion in the Yangtze River Estuary". *Environmental Geology*, 56(8), 1679-1686.

- Aouiche, I., Daoudi, L., Anthony, E. J., Sedrati, M., Ziane, E., Harti, A., & Dussouillez, P. (2016). "Anthropogenic effects on shoreface and shoreline changes: Input from a multi-method analysis, Agadir Bay, Morocco". *Geomorphology*, 254, 16-31.

- Appeaning Addo, K. (2013). "Shoreline morphological changes and the human factor. Case study of Accra Ghana". *Journal of coastal conservation*, 1-7.

- Asaeda, T., & Rashid, M. H. (2012). "The impacts of sediment released from dams on downstream sediment bar vegetation". *Journal of hydrology*, 430, 25-38.

- Atallah, T. A. (2002). "A review on dams and breach parameters estimation".

- Bale, A. J., Widdows, J., Harris, C. B., & Stephens, J. A. (2006). "Measurements of the critical erosion threshold of surface sediments along the Tamar Estuary using a mini-annular flume". *Continental Shelf Research*, 26(10), 1206-1216.

- BaMasoud, A., & Byrne, M. L. (2013). "The predictive accuracy of shoreline change rate methods in Point Pelee, Canada". *Journal of Great Lakes Research*, 39(1), 173-181.

- Baxter, R. M. (1977). "Environmental effects of dams and impoundments". *Annual Review of Ecology and Systematics*, 8(1), 255-283.

- Belkova, I. N., & Finagenov, O. M. (2001). "Effect of Thawing Soil on the Stability of the Downstream Slope of the Dam for the Ust'-Srednekan Hydroelectric Plant". *Power Technology and Engineering (formerly Hydrotechnical Construction),* 35(4), 182-188.

- Benzagouta, M. S., & Amro, M. M. (2009). "New approach for reservoir assessment using geochemical analysis: Case study". *Journal of Petroleum Science and Engineering*, 68(3), 171-179.

- Bigda-Peyton, H., Nowicki, S., & Wodehouse, H. The Ecological and Social Impacts of Hydroelectric Dams on the Rio Chico and Chiriquí Viejo Watersheds.

- Billa, L., & Pradhan, B. (2011). "Semi-automated procedures for shoreline extraction using single RADARSAT-1 SAR image". *Estuarine, Coastal and Shelf Science*, 95(4), 395-400.

- Bin, C. H. E. N., & Kai, W. (2008). "Suspended sediment transport in the offshore near Yangtze Estuary** Project supported by the National Natural Science Foundation of China (Grant No. 40576017), the National Basic Research Program of China" (973, Program, Grant No. 2007CB411804). *Journal of Hydrodynamics*, ser. B, 20(3), 373-381.

- Birasal, N. R. (2014). "Do We Need Some More Dams? Past, Present and Future of Freshwater Bodies in Karnataka State–A Perspective". *International Journal of Scientific Research in Agricultural Sciences*, 1(3), 32-42.

- Birasal, N. R., Nadkarni, V. B., & Gouder, B. Y. M. (1987). "The first five months of the supa reservoir, river Kali, India". *River Research and Applications*, 1(3), 275-281.

- Brandt, S. A. (2000). "Classification of geomorphological effects downstream of dams". *Catena*, 40(4), 375-401.

- Brocchini, M., Calantoni, J., Postacchini, M., Sheremet, A., Staples, T., Smith, J., ... & Corvaro, S. (2017). "Comparison between the wintertime and summertime dynamics of the Misa River estuary". *Marine Geology*, 385, 27-40.

- Brune, G. M. (1953). "Trap efficiency of reservoirs. Eos", *Transactions American Geophysical Union*, 34(3), 407-418.

- Buzzelli, C., Doering, P. H., Wan, Y., Sun, D., & Fugate, D. (2014). "Modeling ecosystem processes with variable freshwater inflow to the Caloosahatchee River Estuary, southwest Florida. I. Model development". *Estuarine, Coastal and Shelf Science*, 151, 256-271.

- Cady, P. (2011). "A riverbank filtration demonstration project on the Kali River, Dandeli, Karnataka, India". *University of Rhode Island*.

- Chandramohan, P., Jena, B. K., & Kumar, V. S. (2001). "Littoral drift sources and sinks along the Indian coast". *Current Science*, 292-297.

- Chang, F. J., & Lai, H. C. (2014). "Adaptive neuro-fuzzy inference system for the prediction of monthly shoreline changes in northeastern Taiwan". *Ocean Engineering*, 84, 145-156.

- Chen, J., Finlayson, B. L., Wei, T., Sun, Q., Webber, M., Li, M., & Chen, Z. (2016). "Changes in monthly flows in the Yangtze River, China–With special reference to the Three Gorges Dam". *Journal of Hydrology*, 536, 293-301.

- Chen, W. B., Liu, W. C., Hsu, M. H., & Hwang, C. C. (2015). "Modeling investigation of suspended sediment transport in a tidal estuary using a three-dimensional model". *Applied Mathematical Modelling*, 39(9), 2570-2586.

- Choudhary, R. I. C. H. A., Gowthaman, R., & SanilKumar, V. (2013). "Shoreline change detection from Karwar to Gokarna-South West coast of India using remotely Sensed data". *International Journal of Earth Sciences and Engineering*, 6(3), 489-494.

- Chu, A., Wang, Z., & de Vriend, H. J. (2015). "Analysis on residual coarse sediment transport in estuaries. Estuarine", *Coastal and Shelf Science*, 163, 194-205.

- Chu, Z. X., Sun, X. G., Zhai, S. K., & Xu, K. H. (2006). "Changing pattern of accretion/erosion of the modern Yellow River (Huanghe) subaerial delta, China: Based on remote sensing images". *Marine Geology*, 227(1), 13-30.

- Clarke, K. C. (1986). "Advances in geographic information systems. Computers", *environment and urban systems,* 10(3-4), 175-184.

- Coulombier, T., Neumeier, U., & Bernatchez, P. (2012). "Sediment transport in a cold climate salt marsh (St. Lawrence Estuary, Canada), the importance of vegetation and waves". *Estuarine, Coastal and Shelf Science*, 101, 64-75.

- Cooper, N. J., Leggett, D. J., & Lowe, J. P. (2000). "Beach-Profile Measurement, Theory and Analysis: Practical Guidance and Applied Case Studies." *Water and Environment Journal,* 14(2), 79-88.

- Cui, B. L., & Li, X. Y. (2011). "Coastline change of the Yellow River estuary and its response to the sediment and runoff (1976–2005)". *Geomorphology*, 127(1), 32-40.

- Dabees, M., & Kamphuis, J. W. (1999). "Oneline, a numerical model for shoreline change". *In Coastal Engineering 1998*, 2668-2681.

- Dada, O. A., Li, G., Qiao, L., Ding, D., Ma, Y., & Xu, J. (2016). "Seasonal shoreline behaviours along the arcuate Niger Delta coast: Complex interaction between fluvial and marine processes". *Continental Shelf Research*, 122, 51-67.

- Dai, Z., & Liu, J. T. (2013). "Impacts of large dams on downstream fluvial sedimentation: an example of the Three Gorges Dam (TGD) on the Changjiang (Yangtze River)". *Journal of Hydrology*, 480, 10-18.

- Dai, Z., Liu, J. T., & Wen, W. (2015). "Morphological evolution of the south passage in the Changjiang (Yangtze River) estuary, China". *Quaternary International*, 380, 314-326.

- Dai, Z., Liu, J. T., Wei, W., & Chen, J. (2014). "Detection of the Three Gorges Dam influence on the Changjiang (Yangtze River) submerged delta". *Scientific reports*, 4.

- Dandekar, P., & Thakkar, H. (2014). "Shrinking and Sinking Deltas: Major role of Dams in delta subsidence and effective sea level rise". *South Asia Network on Dams Rivers and People*, 1-14.

- Dolan, R., Fenster, M. S., & Holme, S. J. (1991). "Temporal analysis of shoreline recession and accretion". *Journal of coastal research*, 723-744.

- Dora, G. U., Kumar, V. S., Vinayaraj, P., Philip, C. S., & Johnson, G. (2014). "Quantitative estimation of sediment erosion and accretion processes in a micro-tidal coast". *International Journal of Sediment Research*, 29(2), 218-231.

- Dynesius, M., & Nilsson, C. (1994). "Fragmentation and flow regulation of river systems in the northern third of the world". Science-new york then washington-, 753-753.

- East, A. E., Pess, G. R., Bountry, J. A., Magirl, C. S., Ritchie, A. C., Logan, J. B., ... & Liermann, M. C. (2015). "Large-scale dam removal on the Elwha River, Washington, USA: River channel and floodplain geomorphic change". *Geomorphology, 228,* 765-786.

- East, A. E., Pess, G. R., Bountry, J. A., Magirl, C. S., Ritchie, A. C., Logan, J. B., ... & Liermann, M. C. (2015). "Large-scale dam removal on the Elwha River, Washington, USA: River channel and floodplain geomorphic change". *Geomorphology, 228,* 765-786.

- Erskine, W. D. (1985). "Downstream geomorphic impacts of large dams: the case of Glenbawn Dam, NSW". *Applied Geography*, 5(3), 195-210.

- Fearnside, P. M. (2014). "Impacts of Brazil's Madeira River dams: Unlearned lessons for hydroelectric development in Amazonia". *Environmental Science & Policy, 38,* 164-172.

- Fencl, J. S., Mather, M. E., Costigan, K. H., & Daniels, M. D. (2015). "How big of an effect do small dams have? Using geomorphological footprints to quantify spatial impact of low-head dams and identify patterns of across-dam variation". *PLoS one*, 10(11).

- Feng, L., Hu, C., Chen, X., & Song, Q. (2014). "Influence of the Three Gorges Dam on total suspended matters in the Yangtze Estuary and its adjacent coastal waters: Observations from MODIS". *Remote Sensing of Environment, 140,* 779-788.

- Feng, Z., Liu, B., Zhao, Y., Li, X., Jiang, L., & Si, S. (2016). "Spatial and temporal variations and controlling factors of sediment accumulation in the

Yangtze River estuary and its adjacent sea area in the Holocene, especially in the Early Holocene". *Continental Shelf Research*, 125, 1-17.

- Franz, G., Pinto, L., Ascione, I., Mateus, M., Fernandes, R., Leitao, P., & Neves, R. (2014). "Modelling of cohesive sediment dynamics in tidal estuarine systems: Case study of Tagus estuary, Portugal". *Estuarine, Coastal and Shelf Science*, 151, 34-44.

- Fu, K., & He, D. (2007). "Analysis and prediction of sediment trapping efficiencies of the reservoirs in the mainstream of the Lancang River". *Chinese Science Bulletin*, 52, 134-140.

- Gao, G., Falconer, R. A., & Lin, B. (2013). "Modelling importance of sediment effects on fate and transport of enterococci in the Severn Estuary, UK". *Marine pollution bulletin*, 67(1), 45-54.

- Garel, E., & D'Alimonte, D. (2017). "Continuous river discharge monitoring with bottom-mounted current profilers at narrow tidal estuaries". *Continental Shelf Research*, 133, 1-12.

- Gens, R. (2010). "Remote sensing of coastlines: detection, extraction and monitoring". *International Journal of Remote Sensing*, 31(7), 1819-1836.

- Ghoneim, E., Mashaly, J., Gamble, D., Halls, J., & AbuBakr, M. (2015). "Nile Delta exhibited a spatial reversal in the rates of shoreline retreat on the Rosetta promontory comparing pre-and post-beach protection". *Geomorphology*, 228, 1-14.

- Gong, W., & Shen, J. (2009). "Response of sediment dynamics in the York River Estuary, USA to tropical cyclone Isabel of 2003". *Estuarine, Coastal and Shelf Science*, 84(1), 61-74.

- Gong, W., Jia, L., Shen, J., & Liu, J. T. (2014). "Sediment transport in response to changes in river discharge and tidal mixing in a funnel-shaped micro-tidal estuary". *Continental Shelf Research*, 76, 89-107.

- Gourgue, O., Baeyens, W., Chen, M. S., de Brauwere, A., de Brye, B., Deleersnijder, E., ... & Legat, V. (2013). "A depth-averaged two-dimensional sediment transport model for environmental studies in the Scheldt Estuary and tidal river network". *Journal of Marine Systems*, 128, 27-39.

- Graf, W. L. (1999). "Dam nation: A geographic census of American dams and their large-scale hydrologic impacts". *Water resources research*, 35(4), 1305-1311.

- Graf, W. L. (2006). "Downstream hydrologic and geomorphic effects of large dams on American rivers". *Geomorphology*, 79(3), 336-360.

- Guerin, T., Bertin, X., & Chaumillon, E. (2016). "Wave control on the rhythmic development of a wide estuary mouth sandbank: A process-based modelling study". *Marine Geology*, 380, 79-89.

- Gupta, H., Kao, S. J., & Dai, M. (2012). "The role of mega dams in reducing sediment fluxes: A case study of large Asian rivers". *Journal of Hydrology*, 464, 447-458.

- Guptha, M. V. S., & Hashimi, N. H. (1985). "Fluctuation in glacial and interglacial sediment discharge of the river Indus as seen in a core from the Arabian Sea".

- H., & Jezek, K. C. (2004). "Automated extraction of coastline from satellite imagery by integrating Canny edge detection and locally adaptive thresholding methods". *International Journal of Remote Sensing,* 25(5), 937-958.

- Hanson, H., Larson, M., & Pham, T. N. (2011). "Modeling shoreline response and inlet shoal volume development on long island coast, united states". *Coastal Engineering Proceedings*, 1(32), 88.

- Hegde, A. V., & Akshaya, B. J. (2015). "Shoreline transformation study of Karnataka Coast: Geospatial Approach". *Aquatic Procedia*, 4, 151-156.

- Heinemarm, H. G. (1981). "A new sediment trap efficiency curve for small reservoirs". *JAWRA Journal of the American Water Resources Association*, 17(5), 825-830.

- Hill, N. M., Keddy, P. A., & Wisheu, I. C. (1998). "A hydrological model for predicting the effects of dams on the shoreline vegetation of lakes and reservoirs". *Environmental Management*, 22(5), 723-736.

- Holeman, J. N. (1968). "The sediment yield of major rivers of the world". *Water Resources Research*, 4(4), 737-747.

- Hu, J., Li, S., & Geng, B. (2011). "Modeling the mass flux budgets of water and suspended sediments for the river network and estuary in the Pearl River Delta, China". *Journal of Marine Systems*, 88(2), 252-266.

- Human, L. R. D., Snow, G. C., & Adams, J. B. (2016). "Responses in a temporarily open/closed estuary to natural and artificial mouth breaching". *South African Journal of Botany*, 107, 39-48.

- Jackson, C. W., Alexander, C. R., & Bush, D. M. (2012). "Application of the AMBUR R package for spatio-temporal analysis of shoreline change: Jekyll Island, Georgia, USA". *Computers & Geosciences,* 41, 199-207.

- Jain, S. K., Tyagi, J., and Singh, V. (2010). "Simulation of runoff and sediment yield for a Himalayan watershed using SWAT model." Journal of Water Resource and Protection, 2(03), 267.

- Jauhari, V. P. (1999). "Operation, monitoring and decommissioning of large dams in India. Contributing paper", *World Commission on Dams*, 1-168.

- Jonah, F. E., Boateng, I., Osman, A., Shimba, M. J., Mensah, E. A., Adu-Boahen, K., ... & Effah, E. (2016). "Shoreline change analysis using end point rate and net shoreline movement statistics: An application to Elmina, Cape Coast and Moree section of Ghana's coast". *Regional Studies in Marine Science*, 7, 19-31.

- Jothiprakash, V., & Vaibhav, G. A. R. G. (2008). "Re-look to conventional techniques for trapping efficiency estimation of a reservoir". *International Journal of Sediment Research*, 23(1), 76-84.

- Kakisina, T. J., Anggoro, S., & Hartoko, A. (2016). "NEMOS (Nearshore Modelling of Shoreline Change) Model for Abrasion Mitigation at the Northern Coast of Ambon Bay". *Aquatic Procedia*, 7, 242-246.

- Karunarathna, H., Horrillo-Caraballo, J., Burningham, H., Pan, S., & Reeve, D. E. (2016). "Two-dimensional reduced-physics model to describe historic morphodynamic behaviour of an estuary inlet". *Marine Geology*, 382, 200-209.

- Kermani, S., Boutiba, M., Guendouz, M., Guettouche, M. S., & Khelfani, D. (2016). "Detection and analysis of shoreline changes using geospatial tools and

automatic computation: Case of jijelian sandy coast (East Algeria)". *Ocean & Coastal Management*, 132, 46-58.

- Kerner, M. (2007). "Effects of deepening the Elbe Estuary on sediment regime and water quality". *Estuarine, coastal and shelf science*, 75(4), 492-500.

- Kesel, R. H. (1988). "The decline in the suspended load of the lower Mississippi River and its influence on adjacent wetlands". *Environmental Geology*, 11(3), 271-281.

- Kitheka, J. U., Obiero, M., & Nthenge, P. (2005). "River discharge, sediment transport and exchange in the Tana Estuary, Kenya". *Estuarine, Coastal and Shelf Science*, 63(3), 455-468.

- Kökpinar, M. A., Darama, Y., & Güler, I. (2007). "Physical and numerical modeling of shoreline evaluation of the Kizilirmak river mouth, Turkey". *Journal of Coastal Research*, 445-456.

- Kondolf, G. M. (1997). "Profile: hungry water: effects of dams and gravel mining on river channels". *Environmental management*, 21(4), 533-551.

- KUANG, C. P., Wei, C., Jie, G., & HE, L. L. (2014). "Comprehensive analysis on the sediment siltation in the upper reach of the deepwater navigation channel in the Yangtze Estuary". *Journal of Hydrodynamics, Ser. B*, 26(2), 299-308.

- Kummu, M., & Varis, O. (2007). "Sediment-related impacts due to upstream reservoir trapping, the Lower Mekong River". *Geomorphology*, 85(3-4), 275-293.

- Lajczak, A. (1996). "Modelling the long-term course of non-flushed reservoir sedimentation and estimating the life of dams". *Earth surface processes and landforms*, 21(12), 1091-1107.

- Le Cornu, J. (1998). "Dams and Water Management". Report of ICOLD Secretary General to the International Conference on Water and Sustainable Development, Paris, March 19-21.

- Leuven, J. R. F. W., Kleinhans, M. G., Weisscher, S. A. H., & van der Vegt, M. (2016). "Tidal sand bar dimensions and shapes in estuaries". *Earth-Science Reviews*, 161, 204-223.

- Li, X., Zhou, Y., Zhang, L., & Kuang, R. (2014). "Shoreline change of Chongming Dongtan and response to river sediment load: a remote sensing assessment". *Journal of Hydrology*, 511, 432-442.

- Li, X., Zhu, J., Yuan, R., Qiu, C., & Wu, H. (2016). "Sediment trapping in the Changjiang Estuary: Observations in the North Passage over a spring-neap tidal cycle". *Estuarine, Coastal and Shelf Science*, 177, 8-19.

- Lillesand, T., Kiefer, R. W., & Chipman, J. (2015). "Remote sensing and image interpretation." *John Wiley & Sons*.

- Lisitizin, A. P. (1972). "Sedimentation in the World Ocean: Tulsa". *Society of Economic Paleontologists and Mineralogists Special Publication*, No. 17.

- Liu, H., & Jezek, K. C. (2004). "Automated extraction of coastline from satellite imagery by integrating Canny edge detection and locally adaptive thresholding methods". *International Journal of Remote Sensing*, 25(5), 937-958.

- Liu, X., Jia, Y., Zheng, J., Shan, H., & Li, H. (2013). "Field and laboratory resistivity monitoring of sediment consolidation in China's Yellow River estuary". *Engineering Geology*, 164, 77-85.

- Liu, Y., Huang, H., Qiu, Z., & Fan, J. (2013). "Detecting coastline change from satellite images based on beach slope estimation in a tidal flat". *International Journal of Applied Earth Observation and Geoinformation*, 23, 165-176.

- Lopez, J. E., & Baptista, A. M. (2017). "Benchmarking an unstructured grid sediment model in an energetic estuary". *Ocean Modelling*, 110, 32-48.

- Lu, X. X., Oeurng, C., Le, T. P. Q., & Thuy, D. T. (2015). "Sediment budget as affected by construction of a sequence of dams in the lower Red River, Viet Nam". *Geomorphology*, 248, 125-133.

- Lu, X. X., Oeurng, C., Le, T. P. Q., & Thuy, D. T. (2015). "Sediment budget as affected by construction of a sequence of dams in the lower Red River, Viet Nam". *Geomorphology*, 248, 125-133.

- Luo, X. X., Yang, S. L., & Zhang, J. (2012). "The impact of the Three Gorges Dam on the downstream distribution and texture of sediments along the middle and lower Yangtze River (Changjiang) and its estuary, and subsequent sediment dispersal in the East China Sea". *Geomorphology,* 179, 126-140.

- Ly, C. K. (1980). "The role of the Akosombo Dam on the Volta River in causing coastal erosion in central and eastern Ghana (West Africa)". *Marine Geology*, 37(3-4), 323-332.

- Ma, G., Shi, F., Liu, S., & Qi, D. (2013). "Migration of sediment deposition due to the construction of large-scale structures in Changjiang Estuary". *Applied Ocean Research*, 43, 148-156.

- Mahmood, K. (1987). "Reservoir Sedimentation: Impact, Extent and Mitigation". *World Bank Technical Paper*, 71.

- Maiti, S., & Bhattacharya, A. K. (2009). "Shoreline change analysis and its application to prediction: a remote sensing and statistics-based approach". *Marine Geology*, 257(1), 11-23.

- Manjunatha, B. R., Balakrishna, K., Shankar, R., Thiruvengadasami, A., Prabhu, R. K., Mahalingam, T. R., & Iyengar, M. A. R. (1996). "The transport of elements from soils around Kaiga to the Kali river, southwest coast of India". *Science of the total environment*, 191(1), 109-118.

- Maliene, V., Grigonis, V., Palevičius, V., & Griffiths, S. (2011). "Geographic information system: Old principles with new capabilities". *Urban Design International,* 16(1), 1-6.

- Markose, V. J., & Jayappa, K. S. (2011). "Hypsometric analysis of Kali River Basin, Karnataka, India, using geographic information system". *Geocarto International*, 26(7), 553-568.

- Markose, V. J., & Jayappa, K. S. (2016). "Soil loss estimation and prioritization of sub-watersheds of Kali River basin, Karnataka, India, using RUSLE and GIS". *Environmental monitoring and assessment*, 188(4), 1.

- Marren, P. M., Grove, J. R., Webb, J. A., & Stewardson, M. J. (2014). "The impact of dams on floodplain geomorphology: are there any, should we care, and what should we do about it?". *7th Australian Stream Management Conference/asn events*.

- Mayerle, R., Narayanan, R., Etri, T., & Wahab, A. K. A. (2015). "A case study of sediment transport in the Paranagua Estuary Complex in Brazil". *Ocean Engineering,* 106, 161-174.

- McCoy, N., Tang, B., Besse, G., Gang, D., & Hayes, D. (2015). "Laboratory study of a novel marsh shoreline protection structure: Wave reduction, silt-clay soil collection, and mathematical modelling". *Coastal Engineering*, 105, 13-20.

- McCully, P. (1996). "Silenced Rivers: The Ecology and Politics of Large Dams. Zed Books", *London*. 350.

- Ministry of Water Resources- Annual Report, 2005 - 2006. Chapter. 6, Central Water Commission, 6-10.

- McLusky, D. S., & Elliott, M. (2004). "The estuarine ecosystem: ecology, threats and management". *Oxford University Press on Demand.*

- Meyer, J., Alber, M., Duncan, W., Freeman, M., Hale, C., Jackson, R., ... & Sheldon, J. (2003). "Summary report supporting the development of ecosystem flow recommendations for the Savannah River below Thurmond Dam". *University of Georgia, Athens*.

- Ministry of Water resources – Annual Report 2014-2015.

- Mole, M. A., Davidson, M. A., Turner, I. L., Splinter, K. D., Goodwin, I. D., & Short, A. D. (2012). "Modelling multi-decadal shoreline variability and evolution".

- Moore, L. J., Ruggiero, P., & List, J. H. (2006). "Comparing mean high water and high water line shorelines: should proxy-datum offsets be incorporated into shoreline change analysis?". *Journal of Coastal Research*, 894-905.

- Müller, B., Berg, M., Yao, Z. P., Zhang, X. F., Wang, D., & Pfluger, A. (2008). "How polluted is the Yangtze river? Water quality downstream from the Three Gorges Dam". *Science of the total environment*, 402(2), 232-247.

- Mulu, A., & Dwarakish, G. S. (2015). "Different Approach for Using Trap Efficiency for Estimation of Reservoir Sedimentation. An Overview". *Aquatic Procedia*, 4, 847-852.

- Naiman, R. J., Decamps, H., & Pollock, M. (1993). "The role of riparian corridors in maintaining regional biodiversity". *Ecological applications*, 3(2), 209-212.

- Narayana, D. V., & Babu, R. (1983). "Estimation of soil erosion in India". *Journal of Irrigation and Drainage Engineering*, 109(4), 419-434.

- Natesan, U., Parthasarathy, A., Vishnunath, R., Kumar, G. E. J., & Ferrer, V. A. (2015). "Monitoring longterm shoreline changes along Tamil Nadu, India using geospatial techniques". *Aquatic Procedia*, 4, 325-332.

- Nguyen, K. D., Guillou, S., Chauchat, J., & Barbry, N. (2009). "A two-phase numerical model for suspended-sediment transport in estuaries". *Advances in Water Resources*, 32(8), 1187-1196.

- Nitsche, F. O., Ryan, W. B. F., Carbotte, S. M., Bell, R. E., Slagle, A., Bertinado, C., ... & McHugh, C. (2007). "Regional patterns and local variations of sediment distribution in the Hudson River Estuary". *Estuarine, Coastal and Shelf Science*, 71(1), 259-277.

- Niya, A. K., Alesheikh, A. A., Soltanpor, M., & Kheirkhahzarkesh, M. M. (2013). "Shoreline Change Mapping Using Remote Sensing and GIS-Case Study: Bushehr Province". *International Journal of Remote Sensing Applications*, 3(3), 102-107.

- Pajak, M. J., & Leatherman, S. (2002). "The high water line as shoreline indicator". *Journal of Coastal Research*, 329-337.

- Pardo-Pascual, J. E., Almonacid-Caballer, J., Ruiz, L. A., & Palomar-Vázquez, J. (2012)." Automatic extraction of shorelines from Landsat TM and ETM+ multi-temporal images with subpixel precision". *Remote Sensing of Environment*, 123, 1-11.

- Pickup, G. (1980). "Hydrologic and sediment modelling studies in the environmental impact assessment of a major tropical dam project". *Earth Surface Processes and Landforms*, 5(1), 61-75.

- Pizzuto, J. (2002). "Effects of Dam Removal on River Form and Process: Although many well-established concepts of fluvial geomorphology are relevant for evaluating the effects of dam removal, geomorphologists remain unable to forecast stream channel changes caused by the removal of specific dams". *BioScience*, 52(8), 683-691.

- Pohl, M. M. (2002). "Bringing down our dams: trends in American dam removal rationales". *JAWRA Journal of the American Water Resources Association*, 38(6), 1511-1519.

- Pritchard, D. W. (1967). "What is an estuary: physical viewpoint". *American Association for the Advancement of Science.*

- Priya, K. L., Jegathambal, P., & James, E. J. (2016). "Salinity and suspended sediment transport in a shallow estuary on the east coast of India". *Regional Studies in Marine Science*, 7, 88-99.

- Provansal, M., Dufour, S., Sabatier, F., Anthony, E. J., Raccasi, G., & Robresco, S. (2014). "The geomorphic evolution and sediment balance of the lower Rhône River (southern France) over the last 130years: Hydropower dams versus other control factors". *Geomorphology*, 219, 27-41.

- Rahman, A. F., Dragoni, D., & El-Masri, B. (2011). "Response of the Sundarbans coastline to sea level rise and decreased sediment flow: A remote sensing assessment". *Remote Sensing of Environment*, 115(12), 3121-3128.

- Rajkumar, P., Kumar, R. S., Kumarvel, S., Bagyaraj, M., Rajaprian, K., & Venkatesan, S. (2015). "A Study on Shoreline Changes in Parts of Pondicherry and Tamil Nadu Using Remote Sensing and GIS Techniques". *International Journal*, 3(12), 917-932.

- Rao, K. N., Subraelu, P., Kumar, K. C. V., Demudu, G., Malini, B. H., & Rajawat, A. S. (2010). "Impacts of sediment retention by dams on delta shoreline recession: evidences from the Krishna and Godavari deltas, India". *Earth Surface Processes and Landforms,* 35(7), 817-827.

- Ren, J., & Wu, J. (2014). "Sediment trapping by haloclines of a river plume in the Pearl River Estuary". *Continental Shelf Research*, 82, 1-8.

- Romine, B. M., Fletcher, C. H., Frazer, L. N., Genz, A. S., Barbee, M. M., & Lim, S. C. (2009). "Historical shoreline change, southeast Oahu, Hawaii; applying polynomial models to calculate shoreline change rates". *Journal of Coastal Research*, 1236-1253.

- Sherman, D. J., Barron, K. M., & Ellis, J. T. (2002). "Retention of beach sands by dams and debris basins in southern California". *Journal of Coastal Research*, 36(sp1), 662-674.

- Shetty, A., Jayappa, K. S., & Mitra, D. (2015). "Shoreline change analysis of Mangalore coast and morphometric analysis of Netravathi-Gurupur and Mulky-Pavanje spits". *Aquatic Procedia*, 4, 182-189.

- Shi, J. Z. (2010). "Tidal resuspension and transport processes of fine sediment within the river plume in the partially-mixed Changjiang River estuary, China: a personal perspective". *Geomorphology*, 121(3), 133-151.

- Shi, J. Z., Zhang, S. Y., & Hamilton, L. J. (2006). "Bottom fine sediment boundary layer and transport processes at the mouth of the Changjiang Estuary, China". *Journal of Hydrology*, 327(1), 276-288.

- Shin, B., & Kim, K. (2015). "Estimation of Shoreline Change Using High Resolution Images". *Procedia Engineering*, 116, 994-1001.

- Singer, M. B. (2007). "The influence of major dams on hydrology through the drainage network of the Sacramento River basin, California". *River Research and Applications*, 23(1), 55-72.

- Singh, O., Sharma, M. C., Sarangi, A., & Singh, P. (2008). "Spatial and temporal variability of sediment and dissolved loads from two alpine watersheds of the Lesser Himalayas". *Catena*, 76(1), 27-35.

- Skalak, K. J., Pizzuto, J. E., & Jenkins, P. (2003). "The Effects of Dams on Downstream Channel Characteristics in Pennsylvania and Maryland: Assessing the Potential Consequences of Dam Removal". *In AGU Fall Meeting Abstracts.*

- Slagel, M. J., & Griggs, G. B. (2008). "Cumulative losses of sand to the California coast by dam impoundment". *Journal of Coastal Research*, 571-584.

- Slinger, J. H. (2017). "Hydro-morphological modelling of small, wave-dominated estuaries. Estuarine", *Coastal and Shelf Science*, 198, 583-596.

- Smith, N. D., Morozova, G. S., Pérez-Arlucea, M., & Gibling, M. R. (2016). "Dam-induced and natural channel changes in the Saskatchewan River below the EB Campbell Dam, Canada". *Geomorphology*, 269, 186-202.

- Sreenivasulu, G., Jayaraju, N., Reddy, B. S. R., Prasad, T. L., Lakshmanna, B., Nagalakshmi, K., & Prashanth, M. (2016). "River mouth dynamics of Swarnamukhi estuary, Nellore coast, southeast coast of India". *Geodesy and Geodynamics*, 7(6), 387-395.

- Srivastava, A., Niu, X., Di, K., & Li, R. (2005). "Shoreline modeling and erosion prediction". *In Proceedings of the ASPRS Annual Conference*,7-11.

- Stanley, E. H., & Doyle, M. W. (2002). "A geomorphic perspective on nutrient retention following dam removal: Geomorphic models provide a means of predicting ecosystem responses to dam removal". *AIBS Bulletin*, 52(8), 693-701.

- Subramanian, V. (1993). "Sediment load of Indian rivers". *Current Science*, 928-930.

- Syvitski, J. P., Kettner, A. J., Overeem, I., Hutton, E. W., Hannon, M. T., Brakenridge, G. R., ... & Nicholls, R. J. (2009). "Sinking deltas due to human activities". *Nature Geoscience*, 2(10), 681.

- Syvitski, J. P., Vörösmarty, C. J., Kettner, A. J., & Green, P. (2005). "Impact of humans on the flux of terrestrial sediment to the global coastal ocean". *Science*, 308(5720), 376-380.

- Tahmiscioğlu, M. S., Anul, N., Ekmekçi, F., & Durmuş, N. (2007). "Positive and negative impacts of dams on the environment". *In International Congress on River Basin Management*, 22-24.

- Thomas, R. C., & Frey, A. E. (2013). "Shoreline change modeling using one-line models: General model comparison and literature review"

- Tian, Y., Luo, L., Mao, D., Wang, Z., Li, L., & Liang, J. (2017). "Using Landsat images to quantify different human threats to the Shuangtai Estuary Ramsar site, China". *Ocean & Coastal Management*, 135, 56-64.

- Van Maren, D. S., Oost, A. P., Wang, Z. B., & Vos, P. C. (2016). "The effect of land reclamations and sediment extraction on the suspended sediment concentration in the Ems Estuary". *Marine Geology*, 376, 147-157.

- Verstraeten, G., & Poesen, J. (2000). "Estimating trap efficiency of small reservoirs and ponds: methods and implications for the assessment of sediment yield". *Progress in Physical Geography*, 24(2), 219-251.

- Vicente-Serrano, S. M., Zabalza-Martínez, J., Borràs, G., López-Moreno, J. I., Pla, E., Pascual, D., ... & Peña-Gallardo, M. (2017). "Effect of reservoirs on

streamflow and river regimes in a heavily regulated river basin of Northeast Spain". *Catena*, 149, 727-741.

- Vijith, V., Shetye, S. R., Baetens, K., Luyten, P., & Michael, G. S. (2016). "Residual estuarine circulation in the Mandovi, a monsoonal estuary: A three-dimensional model study". *Estuarine, Coastal and Shelf Science*, 173, 79-92.

- Virdis, S. G., Oggiano, G., & Disperati, L. (2012). "A geomatics approach to multitemporal shoreline analysis in Western Mediterranean: the case of Platamona-Maritza beach (northwest Sardinia, Italy)". *Journal of Coastal Research*, 28(3), 624-640.

- Wang, F., Zhang, Y., Huo, Z., Peng, X., Araiba, K., & Wang, G. (2008). "Movement of the Shuping landslide in the first four years after the initial impoundment of the Three Gorges Dam Reservoir, China". *Landslides*, 5(3), 321-329.

- Wang, H., Bi, N., Saito, Y., Wang, Y., Sun, X., Zhang, J., & Yang, Z. (2010). "Recent changes in sediment delivery by the Huanghe (Yellow River) to the sea: causes and environmental implications in its estuary". *Journal of Hydrology*, 391(3), 302-313.

- Webster, I. T., & Ford, P. W. (2010). "Delivery, deposition and redistribution of fine sediments within macrotidal Fitzroy Estuary/Keppel Bay: southern Great Barrier Reef, Australia". *Continental Shelf Research*, 30(7), 793-805.

- Wolanski, E. (2007). Estuarine Ecohydrology. Amsterdam: Elsevier.

- Wu, J., Liu, J. T., & Wang, X. (2012). "Sediment trapping of turbidity maxima in the Changjiang Estuary". *Marine Geology*, 303, 14-25.

- Yadav, A. S., Gururaja, K. V., Karthik, B., Rao, G. R., Mukri, V., Chandran, S. M. D., & Ramchandra, T. V. (2008). "Ecological Status of Kali River Flood Plain". *ENVIS Technical Report*.

- Yang, S. L., Milliman, J. D., Li, P., & Xu, K. (2011). "50,000 dams later: erosion of the Yangtze River and its delta". *Global and Planetary Change*, 75(1), 14-20.

- Yang, S. L., Zhang, J., & Xu, X. J. (2007). "Influence of the Three Gorges Dam on downstream delivery of sediment and its environmental implications, Yangtze River". *Geophysical Research Letters*, 34(10).

- Yang, S. L., Zhang, J., Zhu, J., Smith, J. P., Dai, S. B., Gao, A., & Li, P. (2005). "Impact of dams on Yangtze River sediment supply to the sea and delta intertidal wetland response". *Journal of Geophysical Research: Earth Surface*, 110(F3).

- Yang, X., & Lu, X. X. (2014). "Estimate of cumulative sediment trapping by multiple reservoirs in large river basins: An example of the Yangtze River basin". *Geomorphology*, 227, 49-59.

- Yang, Y. P., Li, Y. T., Fan, Y. Y., & Zhang, J. H. (2014). "Impact of water and sediment discharges on subaqueous delta evolution in Yangtze Estuary from 1950 to 2010". *Water Science and Engineering*, 7(3), 331-343.

- Yang, Z., de Swart, H. E., Cheng, H., Jiang, C., & Valle-Levinson, A. (2014). "Modelling lateral entrapment of suspended sediment in estuaries: The role of spatial lags in settling and M 4 tidal flow". *Continental Shelf Research*, 85, 126-142.

- Young, R. S., Pilkey, O. H., Bush, D. M., & Thieler, E. R. (1995). "A discussion of the generalized model for simulating shoreline change (GENESIS)". *Journal of Coastal Research*, 875-886.

- Yu, J., Fu, Y., Li, Y., Han, G., Wang, Y., Zhou, D., ... & Meixner, F. X. (2011). "Effects of water discharge and sediment load on evolution of modern Yellow River Delta, China, over the period from 1976 to 2009". *Biogeosciences*, 8(9), 2427-2435.

- Yunping, Y., Jinyun, D., Mingjin ZHANG, Y. L., & Wanli, L. I. U. (2015). "The synchronicity and difference in the change of suspended sediment concentration in the Yangtze River Estuary". *地理学报 (英文版*, 25(4), 399-416.

- Zamora, H. A., Nelson, S. M., Flessa, K. W., & Nomura, R. (2013). "Post-dam sediment dynamics and processes in the Colorado River estuary: Implications for habitat restoration". *Ecological engineering*, 59, 134-143.

- Zhang, S., & Mao, X. Z. (2015). "Hydrology, sediment circulation and long-term morphological changes in highly urbanized Shenzhen River estuary, China: A combined field experimental and modeling approach". *Journal of Hydrology*, 529, 1562-1577.

- Zheng, S., Guan, W., Cai, S., Wei, X., & Huang, D. (2014). "A model study of the effects of river discharges and interannual variation of winds on the plume front in winter in Pearl River Estuary". *Continental Shelf Research*, 73, 31-40.

- Zhu, L., He, Q., Shen, J., & Wang, Y. (2016). "The influence of human activities on morphodynamics and alteration of sediment source and sink in the Changjiang Estuary". *Geomorphology*, 273, 52-62.

- Thieler, E. R., Himmelstoss, E. A., Zichichi, J. L., & Ergul, A. (2009). "The Digital Shoreline Analysis System (DSAS) version 4.0-an ArcGIS® extension for calculating shoreline change (No. 2008-1278)". *US Geological Survey*.

- Kermani, S., Boutiba, M., Guendouz, M., Guettouche, M. S., & Khelfani, D. (2016). "Detection and analysis of shoreline changes using geospatial tools and automatic computation: Case of jijelian sandy coast (East Algeria)". *Ocean & coastal management*, 132, 46-58.

- Ford, M. (2013). "Shoreline changes interpreted from multi-temporal aerial photographs and high-resolution satellite images: Wotje Atoll, Marshall Islands". *Remote Sensing of Environment*, 135, 130-140.

- Lillesand, T., Kiefer, R. W., & Chipman, J. (2015). "Remote sensing and image interpretation". *John Wiley & Sons*.

- Clarke, K. C. (1986). "Advances in geographic information systems". *Computers, environment and urban systems*, 10(3-4), 175-184.

- Maliene, V., Grigonis, V., Palevičius, V., & Griffiths, S. (2011). "Geographic information system: Old principles with new capabilities". *Urban Design International*, 16(1), 1-6.

7   LIST OF PUBLICATIONS

Journals:

1. **Yadav, A**., Dodamani, B. M., & Dwarakish, G. S. (2018). "Shoreline analysis using Landsat-8 satellite image". *ISH Journal of Hydraulic Engineering*, 1-9. Taylor and Francis Publication.
   DOI: https://doi.org/10.1080/09715010.2018.1556569

2. **Yadav, A**., Dodamani, B. M., & Dwarakish, G. S. (2018). "Shoreline change threat to coastal zone: a case study of Karwar coast". *Climate Change*, 2(2), 18-30, DOI: https://doi.org/10.17501/2513258X.2018.2202

3. **Yadav, A**., Dodamani, B. M., & Dwarakish, G. S. (2019). "Study of Dynamic Changes Through Geoinformatics Technique: A Case Study of Karwar Coast, West Coast of India". *Lecture Notes in Civil Engineering*, 22, 185-197 (LNCE, volume 23) DOI: https://doi.org/10.1007/978-981-13-3134-3_14

4. **Yadav, A**., Dodamani, B. M., & Dwarakish, G. S. (2020). "Effect of disturbed river sediment supply on shoreline configuration: A case study". *Journal of Geological Society of India* (Under Review)

Conference:

1. **Arunkumar Yadav**, B M Dodamani and Dwarakish G.S (2016), "Review on Estimation of Longshore Sediment Transport Rate", *21st International Conference on Hydraulics, Water Resources and Coastal Engineering.* [HYDRO 2016] CWPRS, Pune, India, 8th -10th December 2016, pp 130.

2. **Arunkumar Yadav**, B M Dodamani and Dwarakish G S (2017), "Shoreline Change: A Review", *Proceedings Volume of International Conference*, ISBN: 978-93-5267-355-1, [ICGCSC-2017], MITE, Moodbidri, INDIA, 17th –18th March, 2017, pp 72-77.

3. **Arunkumar Yadav**, B M Dodamani and G. S. Dwarakish (2017). "Shoreline Analysis Using Landsat- 8 Satellite Image. *22nd International Conference on Hydraulics, Water Resources and Coastal Engineering (HYDRO-2017*

International Conference), L. D. College of Engineering Ahmedabad, India. December 21st-23rd, 2017.

4. **Arunkumar Yadav**, B M Dodamani and G. S. Dwarakish (2018). "Shoreline change threat to coastal zone: A case study of Karwar coast". *The 2nd International Conference on Climate change (ICCC 2018), Sri Lanka.* Feb 18th-19th 2018. **(Awarded Best sessions Paper).**

5. **Arunkumar Yadav**, B M Dodamani and G S Dwarakish (2018). "Study of Dynamic Changes through Geoinformatics Technique: A case study of Karwar Coast, West Coast of India". *Springer Proceeding, 4th International Conference in Ocean Engineering (ICOE 2018),* 18th – 21st February, 2018 | Chennai, India.

6. **Arunkumar Yadav**, Athira, K., Dodamani, B. M., & Dwarakish, G. S. (2019). "Impacts of dams on sediment yield and coastal processes using SWAT and DSAS tools". *Proceedings of 9th International Conference on Civil Engineering Trends and Challenges for Sustainability (CTCS 2019)* held at NMAMIT, Nitte, on May 23 & 24, 2019.

7. **Arunkumar Yadav**, B M Dodamani and G S Dwarakish (2019). "Estuary Change Analysis Using Landsat Satellite Imagery: A Case Study Of Kali River Estuary, West Coast of India. *24th International Conference on Hydraulics, Water Resources and Coastal Engineering (HYDRO-2017 International Conference), (Paper Accepted).* To be held on 18-20, December, 2019, organized by University College of Engineering, OU Hyderabad, TS, India.

8 BIO-DATA

Name	**Mr. ARUNKUMAR YADAV**	
Register Number	**AM15F03155092**	
Date Of Birth	**18/08/1988**	
Father's Name	**Tukaram L Yadav**	
Address	**S/O T L Yadav** **#554, Ravindra Nagar,** **Behind Maruti Temple,** **Mundagoad Road,** **Yellapur Taluk,** **Uttara Kannada Dist-** **581359**	
Mother Tongue	**Kannada**	
Phone	**09980815739, 09923940077**	
Email	**atyyadav@gmail.Com**	

PUBLICATION DETAILS

Papers Published	Under Review	Conference	Workshops/ Symposium	Awards and Recognitions
3	1	7	10	1. MHRD Scholarship for perusing Ph.D. 2. Sessions Best paper award at ICCC 2018, Sri Lanka.

I declare that the above information is true and correct to the best of my knowledge.

(ARUNKUMAR YADAV)